Twinning excellence on organic soil amendments effect on nutrient and contaminant dynamics in the subsurface

TwinSubDyn

Deliverable D1.3 2nd Summary report on mobility

Written by the TwinSubDyn project consortium

N°	Short	Beneficiary	Role
1	UNSPMF	University of Novi Sad Faculty of Sciences	CO
2	UNIVIE	University of Vienna	BEN
3	FZJ	Forschungszentrum Jülich	BEN
4	MLU	Martin-Luther-Universität Halle-Wittenberg	BEN
5	CSIC	Spanish National Research Council	BEN

Funded by the European Union. Views and opinions expressed are however those of the author(s) only and do not necessarily reflect those of the European Union or European Research Executive Agency (REA). Neither the European Union nor the granting authority can be held responsible for them. Grant agreement No. 101059546.

Place and Date: Novi Sad 31.04.2025.

General Information

Project:	TwinSubDyn
GA Number:	101059546
Call identifier:	Twinning Western Balkans HORIZON-WIDERA-2021-ACCESS-02
Topic:	HORIZON-WIDERA-2021-ACCESS-02-01
Start date of project:	01/08/2022
Duration:	36 months
Work Package:	WP1
Type:	Deliverable
Number:	D1.3
Title:	2nd summary report on mobility
Due Date:	31/05/2025
Prepared by:	Spanish National Research Council (CSIC)
Responsible Person/s:	Heike Knicker
Dissemination Level:	Public

Dissemination Level		
PU	Public	**x**
SEN	Sensitive — limited under the conditions of the Grant Agreement	

Version History				
Version number	Date	Reasons for release	Responsible	Comments
1.0	22.04.2025.	Deliverable	Marijana Kragulj Isakovski	Drafting deliverable

Contents

EXECUTIVE SUMMARY 4

INTRODUCTION 4

REPORTS ON TRAINING ACTIVITIES 6

Task 1.1 (leader UNSPMF) Short exchange visits (up to 1 week) between EU research institutions and UNSPMF for 9 QR/RR from UNSPMF. 6

Task 1.2 Short-term scientific visits and stays in EU research institutions for researchers (leader CSIC). 8

Task 1.3 Hosting at least 10 high-level experts/scientists from abroad in research themes of interest to UNSPMF (leader UNSPMF)..... 10

CONCLUSION AND OUTLOOK 13

ACKNOWLEDGEMENTS 13

List of Annexes: 14

ANNEX I: Agendas and corresponding attendance list for completed one-week visits 14

ANNEX II: Mobility Reports for all UNSPMF researchers 14

ANNEX III: Agendas and corresponding attendance list for completed training sessions provided by experts from EU partner institutions at UNSPMF. 14

EXECUTIVE SUMMARY

Deliverable 1.3 documents the full scope of training activities carried out within the **TwinSubDyn** project under **Work Package 1 (WP1)**, specifically covering Tasks 1.1, 1.2, and 1.3. A comprehensive **Mobility and Training Plan** was developed and submitted in **November 2022**, tailored to meet the strategic development needs of **UNSPMF** researchers and staff. The overarching goal was to promote networking excellence and facilitate knowledge transfer between UNSPMF and its EU partners – **UNIVIE**, **FZJ**, **MLU**, and **CSIC**.

The training program was implemented through a combination of short-term scientific exchanges (STSEs), seminars, and on-site training, structured to include:

- **One-week visits** by UNSPMF-qualified researchers to EU partner institutions: **13 UNSPMF researchers visits completed**, exceeding the original target of 9.
- **Short-term staff exchanges (1–6 months)** for UNSPMF researchers (ESR, RR, QR) at EU partner facilities: **all 21 planned exchanges successfully completed**.
- **Hosting of international experts** at UNSPMF for seminars, short courses, and experimental training (1–2 weeks): **11 top researchers** from partner institutions visited UNSPMF, surpassing the initial goal of 10.

The **Steering Committee** closely monitored all mobility activities to ensure timely implementation and accurate reporting. Participating researchers were required to submit comprehensive mobility reports outlining the skills acquired and techniques learned. Supporting materials, including training presentation from UNSPMF-hosted events, are available via the **TwinSubDyn project knowledge hub**, supporting wider dissemination and future reuse.

INTRODUCTION

The **TwinSubDyn** project aims to strengthen scientific collaboration and capacity building between **UNSPMF** and four leading European research institutions – **UNIVIE, FZJ, MLU, and CSIC**—with a shared focus on the environmental and hydrogeochemical effects of **organic soil amendments (OSA)**. To achieve these objectives, the project established a robust framework for training and mobility over a **30-month implementation period.** This framework includes several key mobility components:

- **Task 1.1**: One-week visits by UNSPMF researchers to partner laboratories for direct knowledge exchange and skill development.
- **Task 1.2**: Structured **short-term staff exchanges (STSE)** ranging from 1 to 6 months, targeting early-stage (ESR), recognized (RR), and qualified researchers (QR).
- **Task 1.3**: Intensive training sessions delivered by EU partners at UNSPMF, focused on advanced techniques and experimental methodologies.

The implementation status of these activities is summarized in **Table 1** which reflects only **training exchanges conducted during the second half of the project (PM18–PM33)**, beyond what was reported in the first Mobility Report.

Table 1: Overview of realized mobilities within the second half of the project (PM18-PM33).

Activity	No reserhers participated in mobilities – requered	No reserhers participated in mobilities – realized	Means of verification
Short visits of **UNSPMF** qualified **researchers to EU partnering institutions** (1 week) (PM1-34) (Task 1.1)	9	13	Photos, attendance list, Agendas
Short-term staff exchanges (STSE) for training of UNSPMF experienced **researchers**, post-doctoral and early-stage researchers at EU-partner organization facilities at EU partnering institutions (1-6 months) (PM1-30) (Task 1.2)	21	21	Photos, mobility reports, obtained training materials and research data
Hosting a minimum of 10 scientists to deliver seminars, conduct short courses, train researchers in experimental techniques at UNSPMF (1-2 weeks) (PM1-PM33) (Task 1.3)	10	11	Photos, training materials, agenda, attendance list, open accessibility on TwinSubDyn knowledge platform

REPORTS ON TRAINING ACTIVITIES

Task 1.1 (leader UNSPMF) Short exchange visits (up to 1 week) between EU research institutions and UNSPMF for 9 QR/RR from UNSPMF.

Over the course of the TwinSubDyn project, a total of **13 short-term exchange visits** by **UNSPMF researchers**, each lasting approximately **one week**, were successfully scheduled to strengthen collaboration between UNSPMF and its European partner institutions. During the **second half of the project**, three one-week visits were hosted by **UNIVIE**, **MLU**, and **FZJ**. These exchanges were aligned with major project milestones such as **Consortium Meetings (CM)** and **Steering Committee Meetings (SCM)**, as well as the direct implementation of research activities.

These short visits served as crucial opportunities for advancing scientific dialogue, fostering hands-on collaboration, and exploring synergies across institutions. A detailed overview of all completed one-week visits for the second half of the projects, including hosting institutions and participating researchers – is presented in **Table 2**.

Table 2: Completed one-week exchange visits for the second half of the project.

Month /Year	Host	Paricipants from EU or UNSPMF	Actions
17 April 2024	UNIVIE	Snežana Maletić Srđan Rončević Marijana Kragulj Isakovski Tamara Apostolović Heike Knicker, online and Álvaro Fernando García Rodríguez Bruno Glaser Roland Bol and Lutz Weihermüller Thilo Hofmann and Thorsten Hüffer	Consortium and SC meetings
23-24 October 2024	MLU	Snežana Maletić Srđan Rončević Marijana Kragulj Isakovski Heike Knicker Álvaro Fernando García Rodríguez Bruno Glaser Arthur Gross Lutz Weihermüller Thorsten Hüffer	Consortium and SC meetings
25-26 February 2025	FZJ, Bonn	Snežana Maletić	

Srđan Rončević
Heike Knicker
Álvaro Fernando García Rodríguez
Bruno Glaser
Arthur Gross
Lutz Weihermüller
Roland Bol
Thorsten Hüffer

In the **first half of the project**, three CM/SCM meetings were hosted two at **UNSPMF** and **CSIC-IRNAS**, while in the **second half**, three additional meetings took place at **UNIVIE**, **MLU**, and **FZJ**. These meetings covered key topics such as the planning of remaining mobilities, manuscript development, preparation of new research proposals, and organization of the upcoming **Summer School**. In conjunction with these events, participants toured partner laboratories and engaged in discussions regarding different analytical techniques, equipment, and instrumentation setups (**see Figure 1**).

In total, **12 UNSPMF researchers** participated in these one-week visits to partner institutions. The core team typically included **Snežana Maletić**, **Srđan Rončević**, **Marijana Kragulj Isakovski**, and **Tamara Apostolović**, who represented UNSPMF and presented updates on ongoing project activities. Full agendas and attendance records for these meetings are provided in **Annex I**. The **next and final consortium meeting** is scheduled to take place in **Novi Sad during the Summer School in June 2025**.

Figure 1: The TwinSubDyn consortium meeting and labs tours during a visit: UNIVIE (upper), MLU (in the middle) and FZJ, Bonne (down)

Task 1.2 Short-term scientific visits and stays in EU research institutions for researchers (leader CSIC).

In alignment with **Deliverable D1.1: Mobility and Training Plan**, submitted on 30 November 2022, all planned training activities and researcher mobilities for the 34-month project duration were successfully implemented. These activities were fundamental to strengthening UNSPMF's research capacity and ensuring full engagement with EU partner expertise. The timing, locations, and specific focus of each training session and mobility were continuously adapted to reflect evolving project needs, while remaining consistent with the framework set out in D1.1. As of now, all planned visits and exchanges outlined in the original plan have been fully executed

Table 3: Overview of all 6-month STSE and up to 1-month training sessions at EU institutions realized within second half of the project

No	Place/subtask	Researcher	Time	Status	Mean of verification
			6-month STSE		
1.	UNIVIE/1.2.7	T. Apostolović	2 November 2023 to 30 April 2024	DONE	Photos, Mobility report (Annex II)
2.	CSIC/1.2.2	M. Šolić	1 April 2024 to 30 September 2024	DONE	Photos, Mobility report (Annex II)
3.	FZJ/1.2.5	S. Tenodi	2 October 2024 to 28 March 2025	DONE	Photos, Mobility report (Annex II)
			1-month visits		
1.	FZJ/1.2.4	S. Maletić	13 January 2025 to 31 January 2025	DONE	Photos, Mobility report (Annex II)
2.	FZJ/1.2.5	T. Apostolović	13 January 2025 to 31 January 2025	DONE	Photos, Mobility report (Annex II)
3.	MLU/1.2.3	S. Maletić	1 July to 28 July 2024	DONE	Photos, Mobility report (Annex II)
4.	UNIVIE/1.2.7	M. Kragulj Isakovski	7 July 2024 to 27 July 2024	DONE	Photos, Mobility report (Annex II)

A detailed overview of the long-term (6-month) and short-term (up to 1-month) STSEs conducted during the second half of the project is presented in **Table 3** and elaborated further in **Annex II**. These include three additional 6-month exchanges, and four 1-month visits carried out within the scope of Tasks 1.2.2 to 1.2.7. Each exchange focused on specialized training aligned with partner expertise, contributing directly to the researchers' technical development and the project's scientific goals.

Comprehensive **Mobility Reports** have been submitted by each participating researcher, detailing the scope of their training, techniques acquired, and skills developed. These reports are supplemented with photographic documentation and in-depth descriptions and are compiled in **Annex II**. The research outcomes from these mobilities have been integrated into **Deliverable D3.2: Final Research Report**, with several results already published or in the process of publication, highlighting the tangible scientific contributions generated through these collaborative exchanges.

Task 1.3 Hosting at least 10 high-level experts/scientists from abroad in research themes of interest to UNSPMF (leader UNSPMF).

During the previously reported period, ten scientists were hosted UNSPMF to deliver seminars, provide training in experimental techniques, and collaborate on designing research experiments. These visits significantly contributed to capacity building at the institution. All training materials, including PowerPoint presentations, have been made available on the TwinSubDyn Knowledge Hub under the "HUB/Education Resources" section: https://knowledge-hub.pmf.uns.ac.rs/course/view.php?id=3.

Subtask 1.3.4 (leader FZJ) Two-week visits (PM29) of QR/RR from FZJ to deliver training on modelling of nutrient and element cycling, colloid and nanoparticle transport in the unsaturated zone.

Among the various trainings conducted, the only one delivered in the second half of the project period was focused specifically on soil hydrology modelling, including nutrient and element cycling. This training was part of Subtask 1.3.4 and was led by Dr. Lutz Weihermüller. The course, titled *"Course on Soil Hydrology Modelling,"* was delivered in two parts (Table 4, Figure 2). The first part was held online on 26 June 2024, serving as an introductory session and incorporating feedback gathered from student questionnaires. The second part took place onsite at UNSPMF from 9 to 13 September 2024 and spanned five intensive training days.

Table 4: Training Activities Conducted at UNSPMF and Participant Types in the second mobility period

No	Institution Subtask	Speaker	Time	No of participants per day	Audience (estimated)
1	FZJ 1.3.4	Lutz WEIHERMÜLLER	Online introduction 26 June 2024; 9 to 13 September 2024	13+11+10+10+9+ 1 (online)	UNSPMF, FZJ PhD: 2 Researchers: 1 Scientistists: 2 Teaching Assistance: 2 Prof: 6

The onsite training covered a wide range of key topics, including principles of water content measurements, soil hydraulic characterization, soil hydraulic functions and parameters, capillarity

and water potential, and water movement in both saturated and unsaturated zones. Additionally, the course addressed principles of solute transport in the unsaturated zone and included practical applications to real-world scenarios. Each training session combined theoretical instruction with hands-on computer-based exercises, followed by in-depth discussions on the results and their implications.

Figure 2: Training on Soil Hydraolic Modeling at UNSPMF

To ensure long-term accessibility and maximize the impact of the training, all lecture materials have been uploaded to the TwinSubDyn Knowledge Hub. Interested participants and future users can access the full course content and supporting documents at the following links: https://knowledge-hub.pmf.uns.ac.rs/course/view.php?id=3.

The majority of participants in the training course were affiliated with the UNSPMF. Additionally, two participants joined online from FZJ. The course was organized in a hybrid format, combining both onsite and online participation to increase accessibility and outreach. However, due to incomplete data from the online attendance lists, only onsite participants were included in the analysis. The composition of the onsite audience is illustrated in Figure 3.

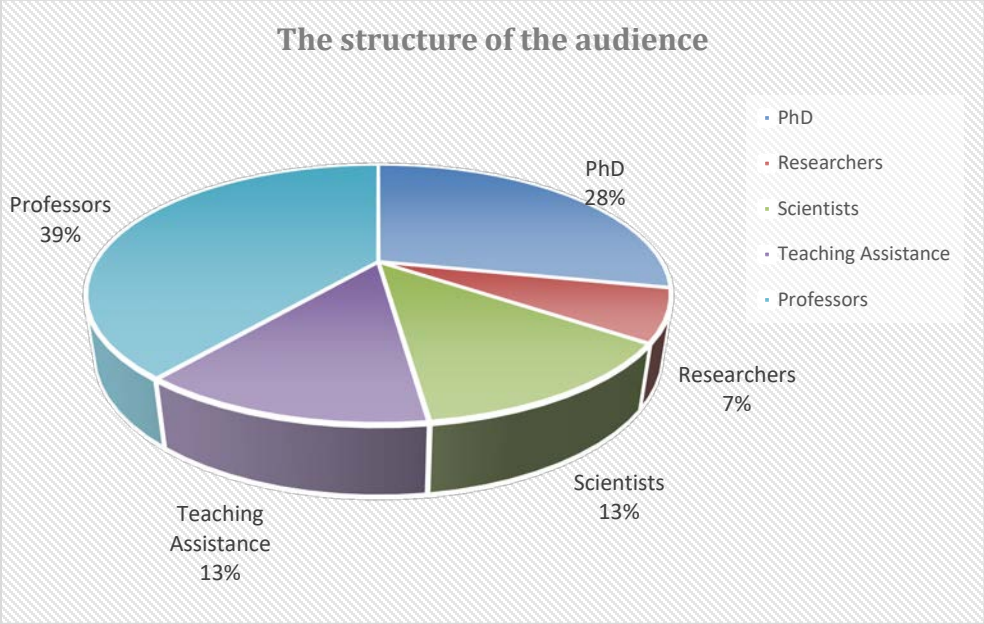

Figure 3: The audiance of the structure

Based on the attendance records, the participant group consisted predominantly of professors (39%) and PhD students (28%), followed by teaching assistants (13%), scientists (13%), and researchers (7%). This academic-oriented distribution aligns with the primary objective of the training– to build modelling expertise in soil hydraulic properties and enhance theoretical understanding among researchers and teaching staff. The strong presence of academic staff and early-career researchers highlights the course's relevance to the institutional goals of strengthening research capacity and promoting knowledge transfer. Detailed agendas and attendance records for each training session are provided in Annex III.

CONCLUSION AND OUTLOOK

All **eight planned six-month STSEs** have been **successfully completed**, providing UNSPMF researchers with in-depth training on the effects of **OSA** on **carbon, nutrient, and contaminant dynamics** in soils and subsurface environments. These extended mobilities allowed researchers to gain expertise in advanced experimental methodologies and analytical techniques used for studying OSA impacts.

In addition, **eleven one-month training visits** were carried out by PM33 across partner institutions: **three at FZJ**, **two at MLU**, **four at UNIVIE**, and **two at CSIC**. These visits specifically targeted **Qualified Researchers (QR)** and were designed to enhance their technical capabilities in line with project objectives.

Furthermore, **UNSPMF hosted 11 distinguished researchers** from EU partner institutions who delivered training sessions, seminars, and hands-on courses on various TwinSubDyn-relevant topics. The knowledge and findings generated through these collaborative activities are being disseminated via peer-reviewed scientific publications. Several manuscripts are already published or under review, fulfilling the project's dissemination and impact goals.

ACKNOWLEDGEMENTS

Funded by the European Union. Views and opinions expressed are however those of the author(s) only and do not necessarily reflect those of the European Union or European Research Executive Agency (REA). Neither the European Union nor the granting authority can be held responsible for them. Grant agreement No. 101059546.

List of Annexes:

ANNEX I: Agendas and corresponding attendance list for completed one-week visits

ANNEX II: Mobility Reports for all UNSPMF researchers

ANNEX III: Agendas and corresponding attendance list for completed training sessions provided by experts from EU partner institutions at UNSPMF

ANNEX I

AGENDA

STEERING COMMITE and CONSORTIUM MEETING

Twinning excellence on organic soil amendments effect on nutrient and contaminant dynamics in the subsurface – TwinSubDyn

DAY 1.	**17.04.2024.**	
13:00 – 13:15	Meet & greet	
Work packages – WP1		
13:15 – 13:30	Project review report – recommendations for second period	Snežana Maletić
Work packages – WP2 (activities for second period)		
13:30 – 14:00	Summer school organization - Task 2.2	Snežana Maletić
	Suggestion for summer school program	All partners (please prepare some suggestion for this, requirements from GA*)
	Potential invited speakers (we need 10)	
	Potential participants	
	Potentials for EGU funding for training schools and conference series	Heike Knicker
14:00 – 14:30	Science and Innovation Strategy Task 2.5- next steps	Srđan Rončević
Work packages – WP4 (activities for next period)		
14:30 – 15:30	Publication strategy - plan and requirements (publication plan see table**)	Snežana Maletić
	Status of the planned papers 1, 2, 3	Thorsten Hüffer
	Status of the planned papers 4, 5, 6, 7, 8, 9	Snežana Maletić
	Status of the planned papers 10, 11	Roland Bol and Lutz Weihermüller
	Status of the planned papers 12, 14, 15	Bruno Glaser
	Status of the planned papers 13 (divided in 2 papers)	Heike Knicker, Alvaro Garcia, Tamara Apostolovic
15:30 – 15:45	Dissemination activities needed for fulfillment of the GA by the end of the project (social networks, website, hub, events etc)	Marijana Kragulj Isakovski
15:45 - 16:30	Coffee break	
	Institutional tour	Thorsten Hüffer
Work package – WP3 (activities for next period)		
16:30 – 17:30	Progress and activities needed for finalization of the tasks 3.1; 3.3.2; 3.4.4	Marijana Kragulj Isakovski

Funded by the European Union. Views and opinions expressed are however those of the author(s) only and do not necessarily reflect those of the European Union or European Research Executive Agency (REA). Neither the European Union nor the granting authority can be held responsible for them. Grant agreement No. 101059546.

	Progress and activities needed for finalization of the tasks 3.2.1	Heike Knicker
	Progress and activities needed for finalization of the tasks 3.2.2	Bruno Glaser
	Progress and activities needed for finalization of the tasks 3.3.1; 3.6.1	Roland Bol, Lutz Weihermüller
	Progress and activities needed for finalization of the tasks 3.4.1; 3.4.2; 3.4.3; 3.4.5; 3.6.2	Thorsten Huffer
Work package -WP1 (activities for next period)		
17:30 – 17:50	Activities needed for fulfillment of the GA and finalization tasks 1.1; 1.2; 1.3	Marijana Kragulj Isakovski
	Activities needed for fulfillment of the GA and finalization tasks 1.4 (could be discussed during the administrative meetings organized in Tuesday with G. Vlahovic, I. Pejović and S. Rončević)	Thorsten Hüffer
17:50 – 18:30	Forthcoming call for proposal (potential calls given below***)	Snežana Maletić
20:00	Social event – diner	

*Requirements for Summer school from GA

- Scientific Committee (the base of the Scientific Committee will be the Steering Committee with top scientists from EU partnering organizations, as well as UNSPMF qualified researchers) – Done, could be extended with researchers outside the consortium.
- SC responsible for defining the main topics, and later the program of the conference.
- SC will be responsible for the selection of 2-3 keynote lecturers and at least 10 invited speakers and preparation of the summer school program.
- Organizing Committee TwinSubDyn project researchers and including young TwinSubDyn project researchers and representatives of the UNSPMF administrative staff) - responsible for the logistics of the summer school organization. - Done
- The summer school is planned to host at least 50 participants from EU and WBC

**Publication plan – need 8 papers by the end of the project

	working title	**experimental period**	**institution lead**
1.	Leaching of phthalates from PVC in OSA extracts	2023	UniVie
2.	Screening OSA leachates for plastic associated pollutants	2023	UniVie
3.	Estimating the relevance of organic soil amendment affected colloids and nano-particles for facilitated transport of hydrophobic organic contaminants in porous media	2023/2024	UniVie
4.	Chlorinated phenols phate in different soil layer	2023	UNSPMF/UNIVIE

Funded by the European Union. Views and opinions expressed are however those of the author(s) only and do not necessarily reflect those of the European Union or European Research Executive Agency (REA). Neither the European Union nor the granting authority can be held responsible for them. Grant agreement No. 101059546.

5.	Organophosphorous pesticide fate in presence of hydrochar and biochar	2024	UNSPMF/CSIC
6.	OSA application in soil rewiew	2024	UNSPMF/ALL
7.	Meta-analysis of biosolid application effects on toxic element concentration in soil and plants	2023	UNSPMF/MLU
8.	Meta-Analysis of pesticide degradation in persulfate activated by biochar system	2023	UNSPMF/MLU
9.	Ciprodynil and Cipemetryn fate in soil -LYS experiment	2024	FZJ/UNSPMF
10.	Heavy metal leaching out of soils amended with bichar and compast -LYS experiment	2024	FZJ/UNSPMF
11.	Assessing the effects of acidified manure application on the phytoextractability of heavy metals in rapeseed and its potential effects on dissolved and colloidally mediated heavy metal losses.	2023/2024	FZJ/UNSPMF
12.	Assessment of long-term biochar degradation under field conditions using black carbon metabolites	2023	MLU
13.	Aged biochar yield effects	2023	MLU/CSIC
14.	Carbon sequestration potential of biochar amendments and biochar stability in agricultural soils	2023	MLU
15.	Biochar transport in soil - Evidence from four long-term field experiments in Germany	2023/2024	MLU

***Forthcoming calls

HORIZON-MSCA-2024-SE-01-01 MSCA Staff Exchanges 2024	10 Oct 2024
HORIZON-MSCA-2024-DN-01-01 MSCA Doctoral Networks 2024	29 May 2024

Other calls?

Funded by the European Union. Views and opinions expressed are however those of the author(s) only and do not necessarily reflect those of the European Union or European Research Executive Agency (REA). Neither the European Union nor the granting authority can be held responsible for them. Grant agreement No. 101059546.

Twin SoS Dyn Meeting 17.9.24

Thilo Hofmann	UniVie	
Bruno Glaser	MLU	
TAMARA APOSTOLOVIĆ	UNSPMF	
ALVARO GARCIA	CSIC	
MARIJANA KRAOUS-ISAKOVSKI	UNSPMF	
SRDAN RONČEVIĆ	UNSPMF	
ROLAND BOL	FZJ	
Lutz Weihermüller	FZJ	
THORSTEN HÜFFER	UVIE	
SNEŽANA MALETIĆ	UNSPMF	

AGENDA

STEERING COMMITE and CONSORTIUM MEETING

Twinning excellence on organic soil amendments effect on nutrient and contaminant dynamics in the subsurface – TwinSubDyn

DAY 1.	**23.10.2024.**	
13:00 – 13:15	Meet & greet	
Work packages – WP2 (activities for second period)		
13:15 – 14:30	Summer school organization - Task 2.2 (requirements from GA*)	Snežana Maletić
	Summer school program, organization status and next steps	Snežana Maletić, all partners
	Keynote and invited speakers (target 10, current 6, 4 to be selected from participants/ESR)	
	Potential participants (target 50 from EU, sending announcements to potential participants)	
	Potentials grants for travel for ESR participants, EGU, IHSS funding for training schools and conference series	Heike Knicker
14:30 – 15:15	Science and Innovation Strategy Task 2.5- status and next steps for finalization of the task	Srđan Rončević
15:15 – 16:00	Coffee break	
	Institutional tour	Arthur Gross
Work packages – WP1 and 4 (status, and needed activities to fulfill requirements from GA)		
16:00 – 17:15	Publication strategy - plan and requirements (prepare few slides to show status/progress, if possible, include information about planned journal, journal rank and IF, **see table with planned publications)	
	Status of the planned papers 1, 2, 3, 4	Thorsten Hüffer
	Status of the planned papers 5-11	Snežana Maletić
	Status of the planned papers 13, 14, 15	Roland Bol and Lutz Weihermüller
	Status of the planned papers 12, 16-19	Bruno Glaser
	Status of the planned papers 20	Heike Knicker, Alvaro Garcia, Tamara Apostolovic

Funded by the European Union. Views and opinions expressed are however those of the author(s) only and do not necessarily reflect those of the European Union or European Research Executive Agency (REA). Neither the European Union nor the granting authority can be held responsible for them. Grant agreement No. 101059546.

17:15 – 17:30	Dissemination activities needed for fulfillment of the GA by the end of the project (social networks, website, hub, events etc)	Marijana Kragulj Isakovski
17:30 – 18:00	Activities needed for fulfillment of the GA and finalization tasks 1.1; 1.2; 1.3, 1.4	Marijana Kragulj Isakovski
	Activities needed for fulfillment of the GA and finalization tasks 1.4 (media training)	Thorsten Hüffer
19:00	Social event – diner	
DAY 2	**24.10.2024.**	
Work package – WP3 (activities for finalization of the task -*please prepare few slides, task end April 2025- please check D3.1 and GA, everything what is not given in the D3.1, and it is required by GA should be added to the D3.2 – some indication are included**)*		
09:00 – 10:45	Progress and activities needed for finalization of the tasks 3.1; 3.3.2; 3.4.4 (final results for characterization of materials, cyprodinil and cypermethrin sorption results, nutrients leaching results)	Marijana Kragulj Isakovski
	Progress and activities needed for finalization of the tasks 3.2.1 (Tamara's secondment -respirometry data, FTIR, BET.., Marko's all experimental results)	Heike Knicker
	Progress and activities needed for finalization of the tasks 3.2.2 (Marko's secondment – BPCA measurement.., Snezana's visit BPCA and isotopic composition of bulk samples from LYS experiment)	Bruno Glaser
	Progress and activities needed for finalization of the tasks 3.3.1; 3.6.1 (all Novi Sad and Julich data from Lysimeters experiments – only examples are given in D3.1).	Lutz Weihermüller, Roland Bol
	Progress and activities needed for finalization of the tasks 3.4.1; 3.4.2; 3.4.3; 3.4.5; 3.6.2 (Sanja's secondment results, Irina's results for revers chromatography – only examples are given in D3.1, Tamara's secondment all results)	Thorsten Hüffer
10:45 – 11:00	Coffee break	
Work package -WP5 (project management -*important information for the final period**)*		
11:00 – 12:00	External reviewer recommendation status of realisation Project outcomes defined in GA vs achieved Project deliverable status Project financial monitoring	Snežana Maletić
	Call for proposal - HORIZON-MSCA-2024-SE-01-01 MSCA Staff Exchanges 2024	
12:00	Lunch/End of meeting	

Funded by the European Union. Views and opinions expressed are however those of the author(s) only and do not necessarily reflect those of the European Union or European Research Executive Agency (REA). Neither the European Union nor the granting authority can be held responsible for them. Grant agreement No. 101059546.

*Requirements for Summer school from GA

- Scientific Committee (the base of the Scientific Committee will be the Steering Committee with top scientists from EU partnering organizations, as well as UNSPMF qualified researchers) – Done, could be extended with researchers outside the consortium.
- SC responsible for defining the main topics, and later the program of the conference.
- SC will be responsible for the selection of 2-3 keynote lecturers and at least 10 invited speakers and preparation of the summer school program.
- Organizing Committee TwinSubDyn project researchers and including young TwinSubDyn project researchers and representatives of the UNSPMF administrative staff) - responsible for the logistics of the summer school organization. - Done
- The summer school is planned to host at least 50 participants from EU and WBC

**Publication plan – need 8 papers by the end of the project

	Working/final title	**experimental period**	**institution lead/included** (person involved)
1.	Leaching of phthalates from PVC in OSA extracts -	End 2024	**UniVie/UNSPMF** (Sanja, Aleksandra, Charlot, Thorsten, Snezana)
2.	Critical review of the role of micro- and nanoplastics as transport vector for organic contaminants in the environment	2024	**UniVie/UNSPPMF** (Charlot,Thorsten, Thilo, Snezana) - submitted
3.	Chlorinated phenols phate in different soil layer	End 2024	**UNSPMF** (Marijana, Snezana, Tamara)
4.	Organophosphorus pesticide fate in presence of hydrochar and biochar	2024	**UNSPMF/CSIC** – Published
5.	The efficiency of the hard wood origin biochar addition on the PAHs bioavailability and stability in sediment	2023	**UNSPMF** -published (not joint paper)
6.	Environmental Restoration of Contaminated Sediment and Soils: The Role of Organic Amendments in PAH Remediation		**UNSPMF** -published (not joint paper)
7.	Assessing Organic Amendment Capacity To Reduce Trifluralin Bioavailability	End 2024	**UNSPMF** -submitted revision (not joint paper)
8.	Meta-Analysis of pesticide degradation in persulfate activated by biochar system	2024	**UNSPMF/MLU**-(Jelena M, Bruno, Arthur, Snezana), published
9.	Heavy metal leaching out of soils amended with sediment, bichar and compost -LYS experiment	End 2024	**FZJ/UNSPMF** (Nina, Jelena, Jens, Lutz, Roland, Snezana)
10.	Assessing the effects of acidified manure application on the phytoextractability of heavy metals in rapeseed and its potential effects on dissolved and colloidally mediated heavy metal losses.	2024/2025	**FZJ/UNSPMF** (Jens, Nina, Jelena B., Lutz, Roland, Snezana)
11.	Assessment of the hydraulic properties of soils amended with sediment, bichar and compost -LYS experiment	End 2024	**FZJ/UNSPMF** (Slaven, Lutz, Roland, Snezana)
12.	Carbon sequestration potential of biochar amendments and biochar stability in agricultural soils	2024	**MLU** (Arthur, Bruno) – submitted, not joint paper published
13.	Evaluating the Influence of Aging on Biochar-Enhanced Soil: Impacts on Soil Health and Stability	End 2024	**MLU-CSIC/UNCPMF** (Arthur, Tamara, Bruno, Heike, Snezana...)
14.	Aged biochar yield effects	End 2024	**CSIC/MLU/UNSPMF** (Alvaro, Heike, Tamara, Snezana…….)
OTHER SUGGESTION			
15.	Aged biochar yield effects - Marko experiments at CSIC		**CSIC/MLU/UNSPMF**
16.	Biochar vertical transport using black carbon metabolites – LYS experiment		**MLU/FZJ/UNSPMF**
17.	Synthesis paper from WP3 – suggested by the project external reviewer		**ALL**

Funded by the European Union. Views and opinions expressed are however those of the author(s) only and do not necessarily reflect those of the European Union or European Research Executive Agency (REA). Neither the European Union nor the granting authority can be held responsible for them. Grant agreement No. 101059546.

ATTENDANCE LIST
STEERING COMMITE and CONSORTIUM MEETING

Day 1 23. Oct. 2024.

Twinning excellence on organic soil amendments effect on nutrient and contaminant dynamics in the subsurface – TwinSubDyn (Grant agreement No 101059546)

No	Attendee name	Institution name	e-mil	Signature
1	SNEZANA MANDIC	UNSPMF	SNEZANA.MANDIC@DGH.UNS.AC.RS	
2	MARIJANA KRAGULJAC	UNSPMF	MARIJANA.KRAGULJAC@DGH.UNS.AC.RS	
3	SRDJAN RONCEVIC	UNSPMF	SRDJAN.RONCEVIC@DGH.UNS.AC.RS	
4	Bruno Glaser	MLU / IAEW	bruno.glaser@landw.uni-halle.de	
5	Arthur Gross	MLU	arthur.gross@landw.uni-halle.de	
6	Dirk Müller-Lux	FZJ	d.mueller-lux@fz-juelich.de	
7	Alvaro Garcia	CSIC	alvaro.garcia.r@csic.es	
8	KNICKER HEIKE	CSIC	heknicker@ig.csic.es	
9	HÜFFER Hanna	uni wien	hanna.hueffer@univie.ac.at	
10				
11				
12				
13				
14				
15				
16				
17				
18				
19				
20				
21				

Funded by the European Union. Views and opinions expressed are however those of the author(s) only and do not necessarily reflect those of the European Union or European Research Executive Agency (REA). Neither the European Union nor the granting authority can be held responsible for them. Grant agreement No. 101059546.

ATTENDANCE LIST
STEERING COMMITE and CONSORTIUM MEETING

Day 2 24. Oct. 2024.

Twinning excellence on organic soil amendments effect on nutrient and contaminant dynamics in the subsurface – TwinSubDyn (Grant agreement No 101059546)

No	Attendee name	Institution name	e-mil	Signature
1	Arthur Gross	MLU	arthur.gross@landw.uni-halle.de	
2	Heike Knicker	CSIC	hc knicker@ig.csic.es	
3	Alvaro Garcia	CSIC	alvaro.garcia@csic.es	
4	SRĐAN RAŠČEVIĆ	UNSPMF	srdjan.rascevic@dbe.uns.ac.rs	
5	MARIANA L. HARDGREY	UNIPMR	mariana.hardgrey@dii.uns.ac.rs	
6	SNEŽANA MAĐENIĆ	UNSPMF	snezana.madjenic@df.uns.ac.rs	
7	HÜFFER, Thorsten	UNIVIE	thorsten.hueffer@univie.ac.at	
8	Bruno Glaser	MLU/IAEW	bruno.glaser@landw.uni-halle.de	
9	Lutz Weihermüller	FZJ	l.weihermueller@fz-juelich.de	
10				
11				
12				
13				
14				
15				
16				
17				
18				
19				
20				
21				

Funded by the European Union. Views and opinions expressed are however those of the author(s) only and do not necessarily reflect those of the European Union or European Research Executive Agency (REA). Neither the European Union nor the granting authority can be held responsible for them. Grant agreement No. 101059546.

STEERING COMMITE and CONSORTIUM MEETING

Twinning excellence on organic soil amendments effect on nutrient and contaminant dynamics in the subsurface – TwinSubDyn

DAY 1.	**25.02.2025.**	
13:00 – 13:15	Meet & greet	
Work packages – WP2 (activities for second period)		
13:15 – 18:00	Summer school organization - Task 2.2 (requirements from GA*): • Program finalization (selection submitted abstract for oral or poster based on the Scientific board inputs, division of the abstracts within the specific sessions…) • decision for travel grants from EGU and UNSPMF_TSD • Other Technical preparations	All partners
19:00	Social event – diner	
DAY 2	**26.02.2025.**	
Work packages – WP4 (status, and needed activities to fulfill requirements from GA)		
09:00 – 9:45	Publication strategy - plan and requirements (prepare few slides to show status/progress, if possible, include information about planned journal, journal rank and IF, **see table with planned publications)	All partners
09:45 – 10:00	Dissemination activities needed for fulfillment of the GA by the end of the project	S. Meletic
Work packages – WP1 and WP2 (status, and needed activities to fulfill requirements from GA)		
10:00 – 10:15	Activities needed for fulfillment of the GA and finalization tasks 1.1; 1.2; 1.3, 1.4 (media training)	Snežana Maletić and Thorsten Hüffer
10:15 – 10:45	Science and Innovation Strategy Task 2.5- status and next steps for finalization of the task	Srđan Rončević
Work package – WP3 (activities for finalization of the task -*please prepare few slides, task end April 2025- please check D3.1 and GA, everything what is not given in the D3.1, and it is required by GA should be added to the D3.2 – some indications are included****)***		
10:45 – 11:45	Deliverable D3.2 status and needed inputs Progress and activities needed for finalization of the tasks 3.1; 3.3.2; 3.4.4 (final results for characterization of materials, cyprodinil and cypermethrin sorption results, nutrients leaching results)	Thorsten Hüffer Snežana Maletić

Funded by the European Union. Views and opinions expressed are however those of the author(s) only and do not necessarily reflect those of the European Union or European Research Executive Agency (REA). Neither the European Union nor the granting authority can be held responsible for them. Grant agreement No. 101059546.

	Progress and activities needed for finalization of the tasks 3.2.1 (Tamara's secondment -respirometry data, FTIR, BET.., Marko's all experimental results)	Heike Knicker
	Progress and activities needed for finalization of the tasks 3.2.2 (Marko's secondment – BPCA measurement.., Snezana's visit BPCA and isotopic composition of bulk samples from LYS experiment)	Bruno Glaser
	Progress and activities needed for finalization of the tasks 3.3.1; 3.6.1 (all Novi Sad and Julich data from Lysimeters experiments – only examples are given in D3.1).	Lutz Weihermüller, Roland Bol
	Progress and activities needed for finalization of the tasks 3.4.1; 3.4.2; 3.4.3; 3.4.5; 3.6.2 (Sanja's secondment results, Irina's results for revers chromatography – only examples are given in D3.1, Tamara's secondment all results)	Thorsten Hüffer
Work package -WP5 (project management -*important information for the final period****)***		
11:45 – 12:45	Project outcomes defined in GA vs achieved Project deliverable status Project financial monitoring	Snežana Maletić
13:00	Lunch/End of meeting	

*Requirements for Summer school from GA

- Scientific Committee (the base of the Scientific Committee will be the Steering Committee with top scientists from EU partnering organizations, as well as UNSPMF qualified researchers) – Done, could be extended with researchers outside the consortium.
- SC responsible for defining the main topics, and later the program of the conference.
- SC will be responsible for the selection of 2-3 keynote lecturers and at least 10 invited speakers and preparation of the summer school program.
- Organizing Committee TwinSubDyn project researchers and including young TwinSubDyn project researchers and representatives of the UNSPMF administrative staff) - responsible for the logistics of the summer school organization. - Done
- The summer school is planned to host at least 50 participants from EU and WBC

**Publication plan – need 8 papers by the end of the project

	Working/final title	experimental period	institution lead/included (person involved)
1.	Leaching of phthalates from PVC in OSA extracts	2025	**UniVie/UNSPMF** (Sanja, Aleksandra, Charlot, Thorsten, Snezana)
2.	Critical review of the role of micro- and nanoplastics as transport vector for organic contaminants in the environment	2024	**UniVie/UNSPPMF** (Charlot,Thorsten, Thilo, Snezana) – submitted, under revision
3.	Chlorinated phenols phate in different soil layer	2025	**UNSPMF** (Marijana, Snezana, Tamara, Jelena, Lutz) **UNSPMF** -submitted, under revision
4.	Organophosphorus pesticide fate in presence of hydrochar and biochar	2024	**UNSPMF/CSIC** – Published

Funded by the European Union. Views and opinions expressed are however those of the author(s) only and do not necessarily reflect those of the European Union or European Research Executive Agency (REA). Neither the European Union nor the granting authority can be held responsible for them. Grant agreement No. 101059546.

5.	Microplastic in OSA – review	2025	**UNSPMF/UniVie** (Aleksandra, Sanja, Charlot, Thorsten)
6.	The efficiency of the hard wood origin biochar addition on the PAHs bioavailability and stability in sediment	2023	**UNSPMF** -published (not joint paper)
7.	Environmental Restoration of Contaminated Sediment and Soils: The Role of Organic Amendments in PAH Remediation		**UNSPMF** -published (not joint paper)
8.	Assessing Organic Amendment Capacity to Reduce Trifluralin Bioavailability	2025	**UNSPMF** -submitted, under revision
9.	Meta-Analysis of pesticide degradation in persulfate activated by biochar system	2024	**UNSPMF/MLU**-(Jelena M, Bruno, Arthur, Snezana), published
10.	Heavy metal leaching out of soils amended with sediment, biochar and compost -LYS experiment	2025	**FZJ/UNSPMF** (Nina, Jelena, Jens, Lutz, Roland, Snezana)
11.	Assessment of the hydraulic properties of soils amended with sediment, biochar and compost -LYS experiment	2025	**FZJ/UNSPMF** (Slaven, Lutz, Roland, Snezana) - Drafted
12.	Carbon sequestration potential of biochar amendments and biochar stability in agricultural soils	2024	**MLU** (Arthur, Bruno) – submitted, not joint paper published – Published
13.	Impact of biochar aging on soil physicochemical properties	2024	**MLU-CSIC/UNCPMF** (Arthur, Tamara, Bruno, Heike, Snezana…) - Published
14.	The relevance of metabolization effects for the dissipation of biochar – evidence from a long-term field experiment		**MLU** (Arthur, Bruno, Tobias, Marko, Snezana) – Drafted
15.	Aged biochar yield effects	End 2024	**CSIC/MLU/UNSPMF** (Alvaro, Heike, Tamara, Snezana…….)
OTHER SUGGESTION			
16.	Biochar vertical transport using black carbon metabolites – LYS experiment		**MLU/FZJ/UNSPMF**
17.	Synthesis paper from WP3 – suggested by the project external reviewer		**ALL, suggested on the review meeting by external expert.**

Funded by the European Union. Views and opinions expressed are however those of the author(s) only and do not necessarily reflect those of the European Union or European Research Executive Agency (REA). Neither the European Union nor the granting authority can be held responsible for them. Grant agreement No. 101059546.

TwinSubDyn

Funded by the European Union

ATTENDANCE LIST
STEERING COMMITE and CONSORTIUM MEETING

Day 1 25. Feb. 2025.
Twinning excellence on organic soil amendments effect on nutrient and contaminant dynamics in the subsurface – TwinSubDyn (Grant agreement No 101059546)

No	Attendee name	Institution name	e-mil	Signature
1	Wulfram Müller Lutz	FZJ	[illegible]	
2	Hüffer, Thorsten	UNIVIE	[illegible]	
3	Rončević Srđan	UNSPMF	srdjan.roncevic@dh.uns.ac.rs	
4	Grob, Arthur	MLU	[illegible]	
5	Glaser, Bruno	MLU	[illegible]	
6	Bol, ROLAND	FZJ	[illegible]	
7	Alvaro Garcia	CSIC	r.bol@fz-juelich.de	
8	Heike Knicker	CSIC	alvaro.garcia@csic.es	
9	Snežana Maletić	UNSPMF	hknicker@csic.es	
10			SNEZANA.MALETIC@DGH.UNS.AC.RS	
11				
12				
13				
14				
15				
16				
17				
18				
19				
20				
21				

Funded by the European Union. Views and opinions expressed are however those of the author(s) only and do not necessarily reflect those of the European Union or European Research Executive Agency (REA). Neither the European Union nor the granting authority can be held responsible for them. Grant agreement No. 101059546.

TwinSubDyn

Funded by the European Union

ATTENDANCE LIST
STEERING COMMITE and CONSORTIUM MEETING

Day 2 26. Feb. 2025.

Twinning excellence on organic soil amendments effect on nutrient and contaminant dynamics in the subsurface – TwinSubDyn (Grant agreement No 101059546)

No	Attendee name	Institution name	e-mil	Signature
1	Lutz Weihermüller	FZJ	l.weilermueller@fz-juelich.de	L. Wei
2	Thorsten Hüttel	UMWE	thorsten.huettel@umwelt.ac.at	T. H
3	RONČEVIĆ SRĐAN	UNSPMF	srdjan.roncevic@dh.uns.ac.rs	
4	Heike Knicker	CSIC	heknicker@ig.csic.es	
5	Alvaro García	CSIC	alvaro.garcia.s@ecs.ic.es	
6	Arthur Gmp	MLU	[illegible]	
7	Bruno Glaser	MLU	bruno.glaser@landw.uni-halle.de	
8	SNEŽANA MAĆEJIĆ	UNSPMF	snezana.macejic@pmf.uns.ac.rs	S. Mac
9	ROLAND BOL	FZJ	r.bol@fz-juelich.de	R.B.
10				
11				
12				
13				
14				
15				
16				
17				
18				
19				
20				
21				

Funded by the European Union. Views and opinions expressed are however those of the author(s) only and do not necessarily reflect those of the European Union or European Research Executive Agency (REA). Neither the European Union nor the granting authority can be held responsible for them. Grant agreement No. 101059546.

ANNEX II

MOBILITY REPORT - 6-months secondment at University of Vienna, Austria

Researcher: Dr. Tamara Apostolović, UNSPMF

Assigned supervisor: Dr. Thorsten Hüffer, UNIVIE

Duration of the visit: 02.11.2023. - 30.04.2024.

Executive Summary

The 6-months visit to the University of Vienna (UNIVIE) had two main focuses: (I) characterization of untreated and biochar-treated soil dissolved organic matter (DOM), and (II) determining the particle size distribution of different soils and organic soil amendments (OSA).

1. DOM was characterized for soils sampled at an experimental field near Bayreuth, Germany, established in 2010, by project partners at the Martin-Luther-University Halle-Wittenberg, Germany. These soils were used to grow lettuce in a pot experiment carried out at the Institute for Natural Resources and Agrobiology (Instituto de Recursos Naturales y Agrobiología de Sevilla, IRNAS) of the Spanish National Research Council (Consejo Superior de Investigaciones Científicas, CSIC) in Seville, Spain. Composite samples of each soil variant at the beginning and end of the pot experiments were freeze-dried and sent to Vienna for DOM characterization. After extraction in MiliQ water, DOM was analyzed using a total organic carbon (TOC) analyzer, UV/Vis spectrophotometry, single point and scanning fluorescence spectroscopy, and dynamic light scattering analysis (DLS). Solid sample analysis was also carried out, namely X-ray diffraction (XRD) and Electron paramagnetic resonance spectroscopy (EPR).
2. Soils and organic soil amendments were characterized to obtain data for transport modelling. Three soils and six OSA samples were extracted with MiliQ water and the aqueous phase was analyzed for particle concentration (turbidity) and particle size distribution (DLS). In addition, members of the UNSPMF team attended a course on modelling colloid-facilitated transport through porous media. The obtained results, together with literature data for specific pollutants will be used to model pesticide and tire additive transport in amended soils with the aim of assessing the risk of colloid-facilitated transport of these compounds through the soil.

Introduction

Background

Composite samples of three treatment variants from the experimental field near Bayreuth, Germany were used: Control soil (untreated Cambisol used as a reference soil), ABC-soil (soil treated with 31.5 t/ha biochar in 2010 - aged biochar treated soil), and CCBC-soil (soil treated with co-composted biochar in the ratio 31.5 t/ha biochar and 70 t/ha compost in 2010 - aged co-composted biochar treated soil). In addition, a fourth variant of soil (FBC-soil) was prepared by treating control soil with fresh biochar (the same biochar and dose used for biochar treatment in 2010 - fresh biochar-treated soil). After taking samples for soil characterization at the beginning of the pot experiment at IRNAS (0DAS (days after sawing)), the composite soil samples were divided into six pots per treatment (24 pots in total). Lettuce seeds were sown, and grown for 60 days, maintaining moderate irrigation conditions by keeping the water content at around 60% of water holding capacity. At the end of the experiment (60DAS), composite samples from the 6 posts for each soil variant were taken. All samples (0DAS and 60DAS) were homogenized and freeze-dried, and taken to Vienna for dissolved organic matter (DOM) characterization.

Scope of the secondment

The six-month secondment at the Department of Environmental Geosciences at the University of Vienna (UNIVIE) focused on two key research areas: (1) the characterization of untreated and biochar-treated soil DOM, and (2) the determination of particle size distribution in various soils and organic soil amendments (OSA). The DOM analysis involved freeze-dried soil samples from an experimental field in Bayreuth, Germany, which were processed using advanced spectroscopic and analytical techniques. Additionally, soils and OSA were assessed for particle concentration and size distribution to support transport modeling aimed at evaluating the risk of colloid-facilitated transport of pollutants in amended soils.

Methods

Soil characterization

Soils sampled at the MLU experimental field in Germany, and used in the pot experiments at CSIC/IRNAS in Spain were characterized at UNIVIE for DOM properties, as well as crystal

structure and free-radicals content. Soil samples analyzed are listed in Table 1., and the specific analyses carried out are given in Figure 1.

Table 1. Soil samples analyzed at UNIVIE

Label	Soil	Description
Control soil, 0DAS Control soil, 60DAS	Control soil	Untreated Cambisol used as a reference soil
ABC-soil, 0DAS ABC-soil, 60DAS	Aged BC treated soil	Cambisol treated with 31.5 t/ha BC in 2010
CCBC-soil, 0DAS CCBC-soil, 60DAS	Aged co-composted BC treated soil	Cambisol treated with co-composted BC in the ratio 31.5 t/ha BC and 70 t/ha compost material in 2010
FBC-soil, 0DAS FBC-soil, 60DAS	Fresh BC treated soil	Cambisol treated with 31.5 t/ha BC in 2023

BC - biochar, DAS - days after sawing

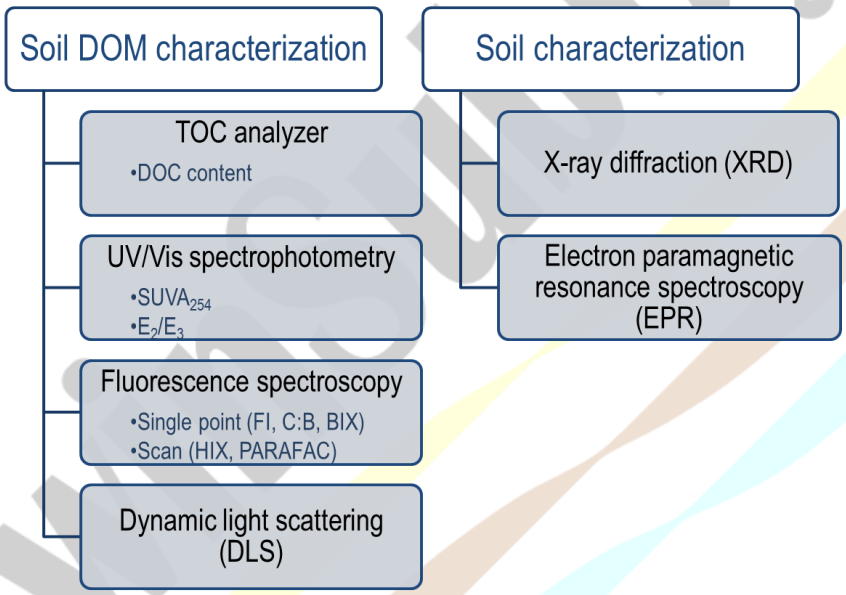

Figure 1. Soil analysis carried out at UNIVIE

Soil dissolved organic matter characterization

Extraction. DOM of the soils was extracted from the solid, freeze-dried soil samples by the following procedure (Figure 2): Around 4 g of soil was weighed on an analytical scale into 50 mL centrifuge tubes, and 40 mL of MiliQ distilled water was added (1:10, w/w). Samples were mixed on a horizontal shaker for 24 hours at 125 rpm. Mixing was carried out in the dark (the tubes

were covered with Al-foil) to avoid exposure to sunlight. After 24 hours, samples were centrifuged for 30 min at 10.000 x g to separate the solid fraction. Supernatants were filtered through sterile 0.22 µm PES filters into glass vials. The samples were kept in a refrigerator, covered with Al-foil until analysis.

Figure 2. DOM extraction from soil

DOC content. The TOC-L (Shimadzu) instrument measures the amount of total carbon (TC), inorganic carbon (IC), and total organic carbon (TOC) in a liquid sample. The dissolved organic carbon (DOC) content was measured by filtering the extract through a 0.22 µm filter membrane, to eliminate any particulate matter. TOC or DOC concentrations are measured by direct measurement, called the non-purgeable organic carbon (NPOC) method. By using the NPOC method, the samples are acidified to pH<2 using hydrochloric acid (HCl). This can be done automatically or manually during sample preparation. Then, the sample is automatically sparged by the carrier gas (synthetic air) for 150 seconds. The sparging causes the inorganic carbon (IC) to transform into CO_2, which is then released from the sample. Sparging can take place in a 5

mL syringe installed in the instrument or by an external sparging option. The remaining organic fraction (NPOC) is detected by catalytic combustion oxidation with an NDIR-detector. Sample preparation and DOC measurement are shown in Figure 3.

Figure 3. Dissolved organic carbon content measurement

UV/Vis spectrophotometry. The Lambda 35 (PerkinElmer) is a versatile spectrophotometer operating in the ultraviolet (UV) and visible (Vis) spectral ranges. The spectrophotometer features a double-beam and an all-reflecting system. UV/Vis spectrophotometry is used to obtain the absorbance spectra of a compound in solution. What is being observed spectroscopically is the absorbance of light energy or electromagnetic radiation, which excites electrons from the ground state to the first singlet excited state of the compound or material. The UV/Vis region relates to a wavelength range of 800 nm to 200 nm. The Beer-Lambert Law ($A = abc$) is the principle behind absorbance spectroscopy. For a single wavelength, A is absorbance (unitless), a is the molar absorptivity of the compound or molecule in solution (M^{-1} cm^{-1}), b is the path length of the cuvette or sample holder (usually 1 cm), and c is the concentration of the solution. UV/Vis spectroscopic data can give qualitative and quantitative information of a given compound or molecule. Irrespective of whether quantitative or qualitative information is required it is important to use a reference cell to zero the instrument for the solvent the compound is in.

To determine the aromaticity of the DOM extracts, the UV absorbance was measured at 254 nm wavelength, in a 10 mm quartz cuvette. Specific UV absorbance ($SUVA_{254}$) values were calculated by dividing the absorbance at 254 nm by the DOC concentration ($SUVA_{254} = 100 * A_{254}$ / DOC). As a further indicator of aromaticity, the ratio between the specific UV absorbance at 250 nm (E_2) to that of 365 nm (E_3) was calculated. E_2/E_3 negatively correlates to the aromaticity of the DOM. Sample analysis on the UV/Vis spectrophotometer is shown in Figure 4.

Figure 4. UV/Vis spectrophotometric analysis

Fluorescence spectroscopy. Fluorescence measurements were obtained using a FluoroMax-4 spectrometer (Horiba) (Figure 5). Samples were analyzed in a 10 mm mirrored glass cuvette.

Figure 5. Fluorescence measurements

Before measurement, the excitation- and emission-monochromator calibration checks were performed. The excitation-monochromator calibration check verifies the wavelength calibration of the excitation monochromator, using the reference photodiode located before the sample compartment. It is an excitation scan of the xenon lamp's output (200-600 nm excitation spectra at the emission wavelength 350 nm). The emission-monochromator calibration check verifies the wavelength calibration of the emission monochromator with the emission photomultiplier tube. It is an emission scan of the Raman-scatter band of water (365-450 nm emission spectra at the excitation wavelength 350 nm) in right-angle mode. This check should be performed with a MQ grade water sample. The calibration check is shown in Figure 6.

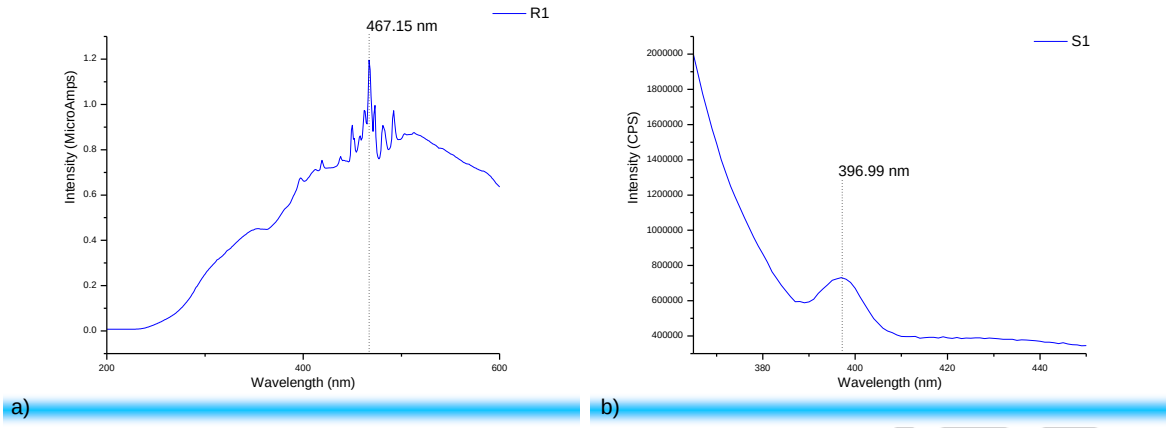

Figure 6. Calibration check for a) excitation-monochromator and b) emission-monochromator

Single-point fluorescence measurements were carried out at the following excitation (ex.) / emission (em.) wavelength pairs: ex.370/em.470 nm, ex.370/em.520 nm, ex.340/em.440 nm (peak C), ex.275/em.305 nm (peak B), ex.310/em.380 nm and ex.310/em.430 nm. The fluorescence index (FI) was calculated as the ratio between the emission intensity at 470 nm and 520 nm, obtained at an excitation wavelength of 370 nm. Measurements included peak C and peak B, corresponding to the maximum fluorescence intensities of humic-like substances and tyrosine/protein-like substances, respectively. FI inversely correlates with both the degree of humification and the aromatic carbon content, and the C:B ratio describes the ratio of humic-like fluorophores to tyrosine-like fluorophores. The C:B ratio is used as a supporting indicator to predict aromaticity. The biological index (BIX) was calculated as the ratio between the emission intensity at 380 and 430 nm, obtained at an excitation wavelength of 310 nm. BIX assess the presence of recently produced autochthonous (in situ) biological or microbial activity in environmental samples, particularly DOM.

To determine the humification index (HIX), emission scans were also analyzed, at excitation wavelength 254 nm and two emission ranges: 300-345 nm and 435-480 nm. HIX was determined as the integrated fluorescence intensity over a specific range of emission wavelengths: HIX = I(435-480 nm) / I(300-345 nm) when excited at a wavelength of 254 nm. The fluorescence intensity in the higher wavelength range (435-480 nm) is associated with more humified, complex organic matter, whereas the intensity in the lower range (300-345 nm) is associated with simpler, less humified compounds. HIX calculated from the fluorescence emission spectra of DOM provides insights into the degree of humification, which in turn reflects the age, origin, and degradation state of the organic matter.

In addition, 3D spectral analysis was carried out to obtain fluorescence excitation-emission matrices (EEMs) of DOM. These spectra were used to perform parallel factor analysis (PARAFAC) to gain spectral profiles to identify fluorophores present in DOM, determine their relative abundance and use the results to obtain environmental insight into the source and fate of DOM. As a reference, river sediment natural organic matter (NOM) was analyzed. An example of an EEM is shown in Figure 7.

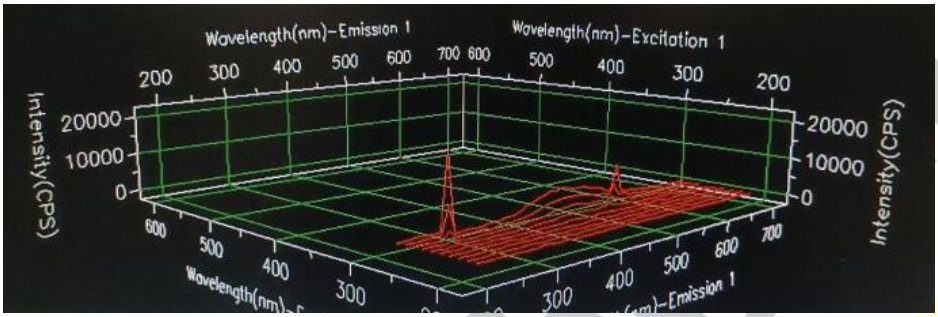

Figure 7. Example of an excitation-emission matrix

Dynamic light scattering (DLS). The Litesizer 500 (Anton Paar) uses dynamic (DLS) and electrophoretic light scattering (ELS) for measuring particle size distributions and zeta potentials of finely dispersed suspensions and emulsions. It can also determine the transmittance and refractive index of liquid samples. DLS measures the Brownian motion of particles in a liquid. This motion causes fluctuations in the intensity of scattered light when a laser is shone on the sample. By analyzing these fluctuations, the DLS technique can determine the hydrodynamic diameter of the particles, which is the size of the particle along with the layer of solvent molecules attached to it. A key step of sample preparation for DLS analysis is ensuring the sample is well-dispersed in the solvent, as large aggregates or air bubbles may interfere with measurements. The sample is placed into an appropriate cuvette (sample volume should be between 0.85 and 3 mL), and the cuvette is inserted into the sample holder of the instrument. During measurements, the laser beam is directed at the sample, and the light scattered by the particles is collected by the detector. The correlator measures the fluctuations in the intensity of scattered light over time, which reflects the movement of particles. The correlation function is created by comparing the intensity of the scattered light at different time points. This function provides insights into how fast the particles diffuse in the solvent. The Litesizer software uses the measured diffusion coefficient (related to Brownian motion) to calculate the hydrodynamic diameter (D_h) of particles using the Stokes-Einstein equation:

$$D_h = \frac{k_B T}{3\pi\eta D}$$

where:

- k_B is the Boltzmann constant (J K^{-1}),
- T is the absolute temperature (K),
- η is the viscosity of the solvent (Pa s), and
- D is the diffusion coefficient of the particles (m^2 s^{-1}).

The DLS method indicates the relative frequency of particles of different sizes in the sample. The measurement of particle size distribution using the Litesizer 500 instrument is shown in Figure 8.

Figure 8. DLS analysis using Litesizer 500

Soil analysis

Soil samples were analyzed using X-ray diffraction (XRD) and electron paramagnetic resonance spectroscopy (EPR). Prior to these measurements, previously homogenized, and manually ground solid soil samples were additionally milled to a fine powder (Figure 9).

Figure 9. Sample preparation for X-ray diffraction analysis and electron paramagnetic resonance spectroscopic analysis

X-ray diffraction (XRD). The Rigaku Miniflex 600 XRD was used to determine the mineralogical composition of soils (Figure 10) by analyzing the interactions between the X-rays and the crystal structures of soil minerals. When X-rays are directed at a soil sample, they are diffracted by the crystal lattice planes, creating a pattern of peaks that are unique to each mineral. Analyzing diffraction patterns, the minerals present in the soil can be identified and quantified. XRD is significant because it provides precise, non-destructive identification of minerals, which is crucial for understanding soil properties such as texture, nutrient availability, and reactivity. It is especially useful for studying clay minerals, which strongly influence soil behavior, water retention, and fertility. Understanding the mineralogical composition of soils through XRD helps in fields like agriculture, environmental remediation, and geotechnical engineering.

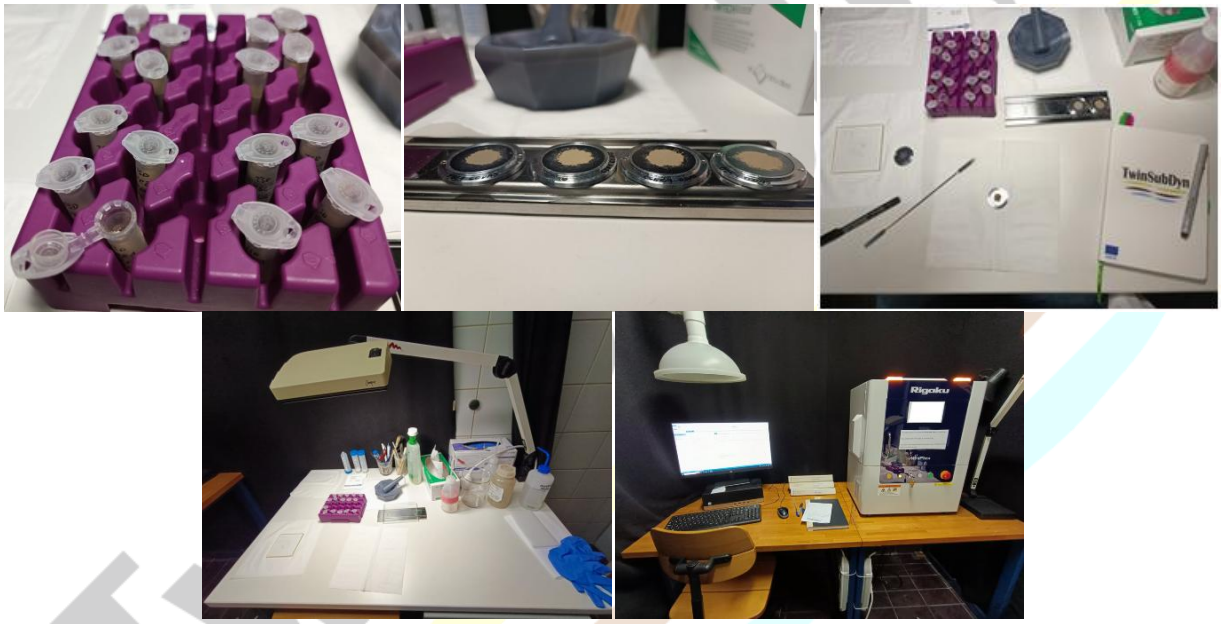

Figure 10. X-ray diffraction

Electron paramagnetic resonance spectroscopy (EPR). Free radicals were measured using the Bruker Elexsys-II E500 EPR spectrometer (Bruker BioSpin GmbH) (Figure 11). The EPR analysis is a technique used to detect unpaired electrons in a sample. In soil analysis, EPR provides valuable insight into the paramagnetic species present, such as transition metals, free radicals, and defects in mineral structure. Soil samples milled to a fine powder are packed into 100 µl quartz EPR sample tubes (quartz is transparent to microwaves and does not interfere with the signal). The tube was placed into a high-sensitivity resonator (Bruker ER 4122SHQE).

A strong, static magnetic field is applied to the sample, causing the magnetic moments of the unpaired electrons to align. Simultaneously, the sample is irradiated with microwaves at a specific frequency (commonly in the X-band, around 9.5 GHz). When the energy from the microwaves matches the energy difference between the electron's spin states (determined by the magnetic field strength), resonance occurs, and the unpaired electrons absorb microwave energy. The system detects this energy absorption and produces a characteristic EPR spectrum.

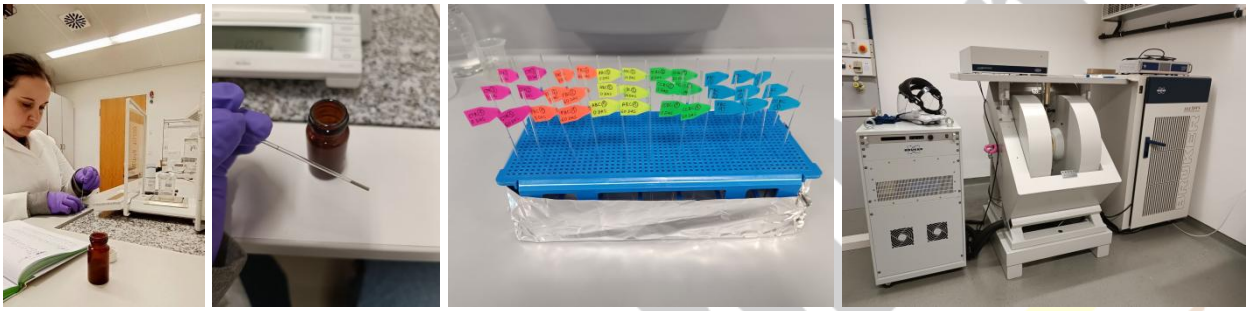

Figure 11. Analysis of free-radicals in soil

OSA characterization

The second research area of the 6-month visit to UNIVIE focused on organic soil amendments (OSA) characterization for colloid content and size distribution. The following OSAs and soils were analyzed: Danube alluvial sediment, Itebej sediment, Bayreuth soil, biochar, cow manure, Wien compost, Pixendorf compost, Subotica compost and Subotica sludge. Samples were prepared using a similar procedure as the DOM extraction (Figure 12): Around 2 g of OSA was weighed on an analytical scale into 50 mL centrifuge tubes, and 20 mL of MiliQ distilled water was added (1:10, w/w). Samples were mixed on a horizontal shaker for 24 hours at 125 rpm. Mixing was carried out in the dark (the tubes were covered with Al-foil) to avoid exposure to sunlight. After 24 h, samples were centrifuged for 30 min at 10.000 x g to separate the solid fraction. Supernatants were carefully decanted into glass vials. The samples were kept in a refrigerator, and covered with Al-foil until analysis. The content of colloids in the OSA and soil extracts was determined by turbidimetry, using the TurbiScan Formulaction (Figure 13), and then DLS analysis was carried out as previously described (Figure 14).

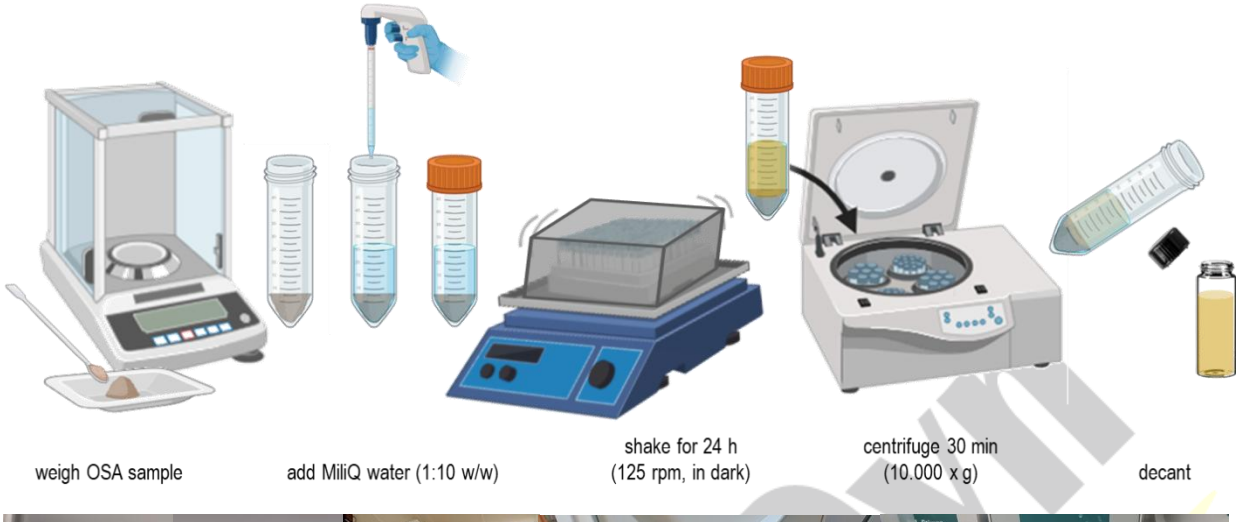

Figure 12. Extraction of organic soil amendments

Figure 13. Turbidimetric measurements

Figure 14. DLS analysis of organic soil amendments and soils

Results and Discussion

Characterization of dissolved organic matter in soil

Results of DOC measurement are shown in Figure 15. Aged biochar-treated soils (ABC-soil and CCBC-soil) have slightly higher DOC content in comparison to the control soil. The difference in DOC may stem from biochar aging, given that the biochar in the two soils, treated in 2010, may have undergone weathering and microbial colonization[1]. The aged biochars may act as sources of labile organic compounds, contributing to DOC in the soils, leading to the observed higher DOC levels compared to the control.

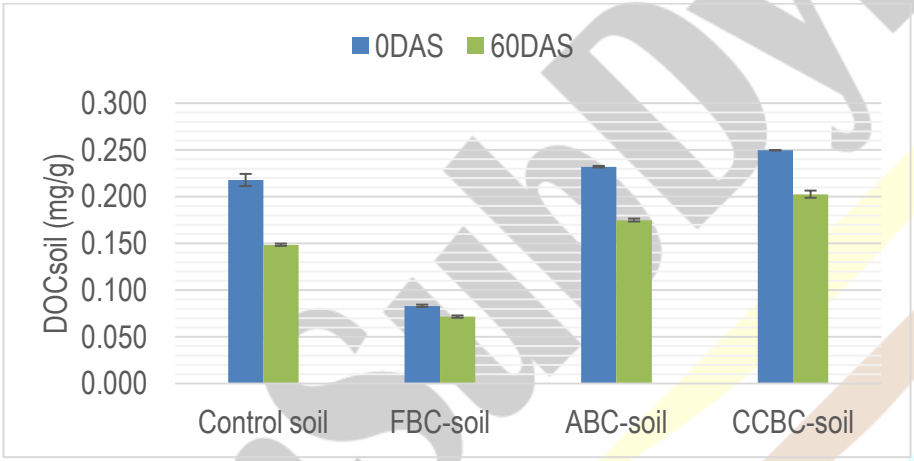

Figure 15. DOC content of soils

DOC content of the freshly amended soil (FBC-soil) is lower than that of the control soil, and both aged biochar-treated soils. This is in contrast to the results from TOC analysis, measured in Spain (Figure 16, left), where we found that TOC content was highest in the freshly amended soil. This can be explained by the strong sorption capacity of fresh biochar, binding organic compounds including DOC, effectively reducing the mobility of organic carbon in the soil solution. This explanation is supported by the fact that DOC content shows a high negative correlation to the specific surface area (SSA) of the soils, with R2>0.92 (Figure 16, right). Soils with higher SSA have more available active places for interactions and tend to have higher capacities for the sorption of organic molecules, therefore, the significant increase in SSA with

[1] Williams, E.K., Jones, D.L., Sanders, H.R. et al. Effects of 7 years of field weathering on biochar recalcitrance and solubility. Biochar 1, 237–248 (2019). https://doi.org/10.1007/s42773-019-00026-1

the addition of fresh biochar may cause an increased sorption capacity of the FBC-soil, reducing DOC present in the soil solution.

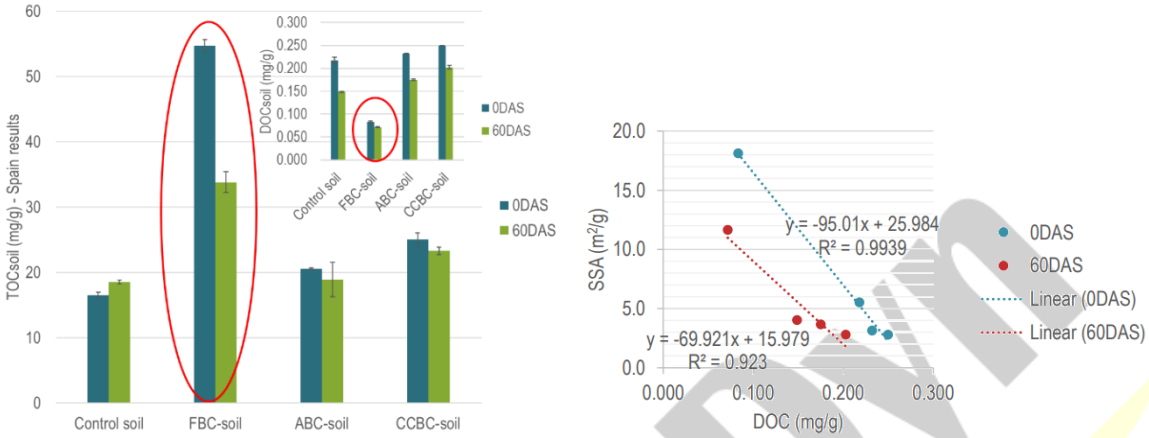

Figure 16. Comparison of DOC and TOC content of the analyzed soils (left) and correlation of DOC with specific surface area of the soils (right)

For all four soils, DOC decreased over time of the pot experiment (0DAS and 60DAS in Figure 15). The decrease in DOC for all soil samples is caused by decomposition and stabilization of organic matter, as well as plant uptake[2]. At the beginning of the experiment (0DAS), more labile carbon was present, but as the experiment progresses, the readily available DOC is consumed by microbial activity, leading to a lower concentration in the soil solution at the end of the pot experiment (60DAS).

UV/Vis spectrophotometry was used to measure the specific UV absorption at 254 nm, 250 nm and 365 nm to determine the $SUVA_{254}$ value and E_2/E_3 ratio for each soil (Figure 17). $SUVA_{254}$ values were similar for the control soil, and both aged biochar-treated soils (ABC-soil and CCBC-soil), and were between 3-4, suggesting a moderate level of aromaticity in the DOM, with similar trends between these soils[3]. A slight increase in $SUVA_{254}$ was observed at the end of the pot experiment, indicating that microbial activity mostly affects more labile, easily decomposed DOM, whereas more aromatic and potentially recalcitrant organic compounds remained in the soil after the experiment. For the FBC-soil, $SUVA_{254}$ was significantly lower than the other soils

[2] Ren, T., Ukalska-Jaruga, A., Smreczak, B., Cai, A. Dissolved organic carbon in cropland soils: A global meta-analysis of management effects. Agriculture, Ecosystems and Environment, 371 (2024) 109080. doi:10.1016/j.agee.2024.109080

[3] Korak, J.A., McKay, G. Critical review of fluorescence and absorbance measurements as surrogates for the molecular weight and aromaticity of dissolved organic matter. Environmental Science: Processes & Impacts, 26, 1663-1702 (2024) https://doi.org/10.1039/D4EM00183D

at the beginning of the experiment (around 2), suggesting that the DOM is more aliphatic and labile. Results of solid state nuclear magnetic resonance (NMR, measurements carried out at CSIC, Spain) indicate that the addition of fresh biochar into the soil, significantly increases the aromatic fraction of organic carbon (Figure 18). The subsequent decrease in DOM aromaticity could suggest that the aromatic compounds in the soil solution interact with the Aryl C fraction and are immobilized on the biochar particles.

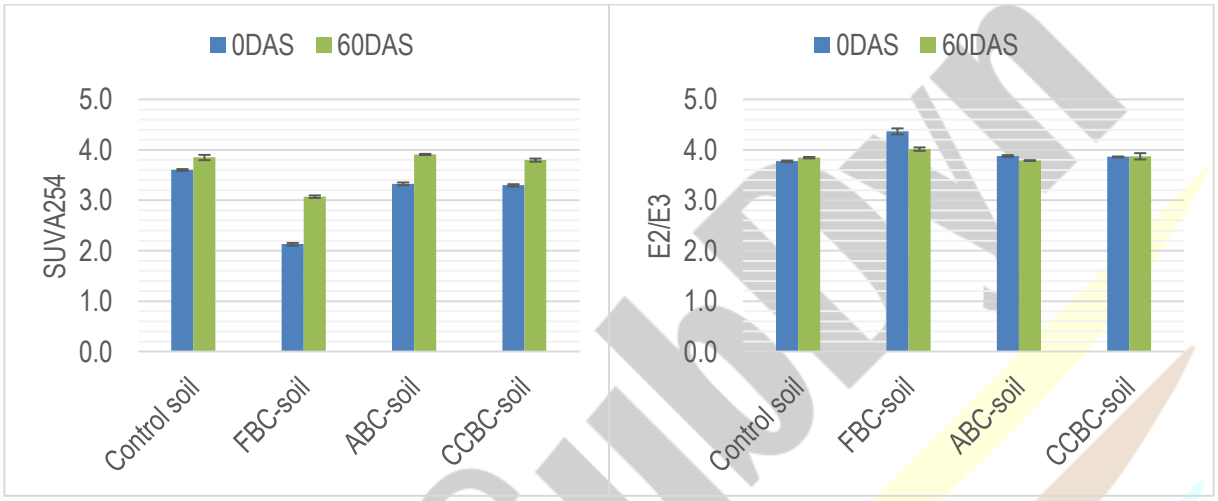

Figure 17. $SUVA_{254}$ and E_2/E_3 ratios of the untreated and biochar-treated soils

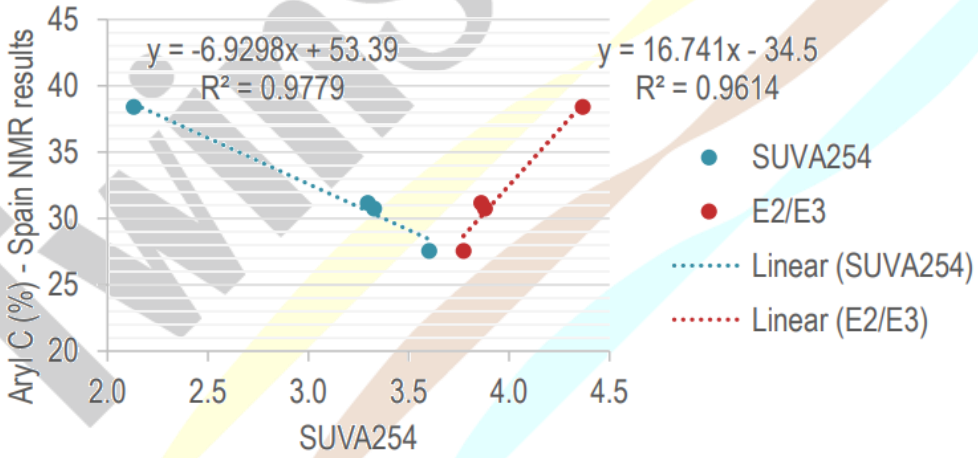

Figure 17. Correlation of $SUVA_{254}$ and E_2/E_3 ratios to the relative abundance of Aryl C (determined by solid state NMR)

The consistent E_2/E_3 ratio around 3.8 for the control soil, ABC-soil and CCBC-soil, both at the beginning and at the end of the pot experiment, suggests that the DOM in these soils is

relatively stable in molecular weight, with little change during the experiment. E_2/E_3 ratios around 3-5 indicate DOM composed of a mix of higher molecular weight and more humified organic compounds[4]. For the FBC-soil, the higher E_2/E_3 ratio at the beginning of the experiment (around 4.4) suggests that the DOM in the fresh biochar-treated soil initially consisted of smaller molecular weight compounds, which are more labile and easily decomposed. The decrease to around 4 by the end of the experiment reflects a shift towards larger molecular weight compounds, resulting from microbial degradation of simpler, smaller molecules. This indicates that fresh biochar introduces more labile organic matter initially, while stabilized aged biochar leads to a more consistent DOM profile over time.

The FI, C:B ratio, BIX, and HIX of the soils (Figure 18) show distinct patterns reflecting differences in organic matter dynamics and microbial activity in the four soils, particularly when observing the aging process of the added biochar. The high FI observed for the FBC-soil suggests a predominance of microbial-derived organic matter, typical of fresh biochar treatments due to the initial presence of more labile, easily decomposable organic compounds. These compounds may encourage microbial activity early on, leading to the higher fluorescence signal. Slightly lower FI values for the other three soils, that do not vary between treatments, reflect more stable DOM with higher aromaticity and less microbial influence compared to fresh biochar. The FI remaining constant throughout the experiment suggests that the organic matter quality in these soils is relatively stable.

The C:B ratio, indicative of the humic-like to protein-like fluorophores in DOM, showed more variance than FI. During the pot experiment, C:B decreased in control soil from 140 to 105, indicating a decline in microbial biomass relative to total carbon, which might reflect organic matter decomposition during the experiment. In contrast, the ABC-soil maintained a relatively stable C:B ratio, suggesting that the biochar-supported microbial community persisted without significant organic matter depletion[5]. In the CCBC-soil, C:B increased from 150 to 180 during the experiment, which could be an indicator of microbial biomass buildup, likely due to improved nutrient availability or the slow release of organic matter from the co-composted biochar,

[4] Yue Y, Xu L, Li G, Gao X, Ma H. Characterization of Dissolved Organic Matter Released from Aged Biochar: A Comparative Study of Two Feedstocks and Multiple Aging Approaches. Molecules. 28(11):4558 (2023). 10.3390/molecules28114558

[5] Zhang P, Huang P, Xu X, Sun H, Jiang B, Liao Y. Spectroscopic and molecular characterization of biochar-derived dissolved organic matter and the associations with soil microbial responses. Science of the Total Environment, (2020) 708, 134619, 10.1016/j.scitotenv.2019.134619

enhancing microbial activity. On the other hand, FBC-soil had a significantly lower C:B ratio, about 30 and 35 at the beginning and at the end of the experiment, respectively. This indicates that fresh biochar initially may promote microbial growth, but due to limited bioavailable carbon relative to microbial biomass after the rapid consumption of the available organic carbon, the microbial activity decreases over time.

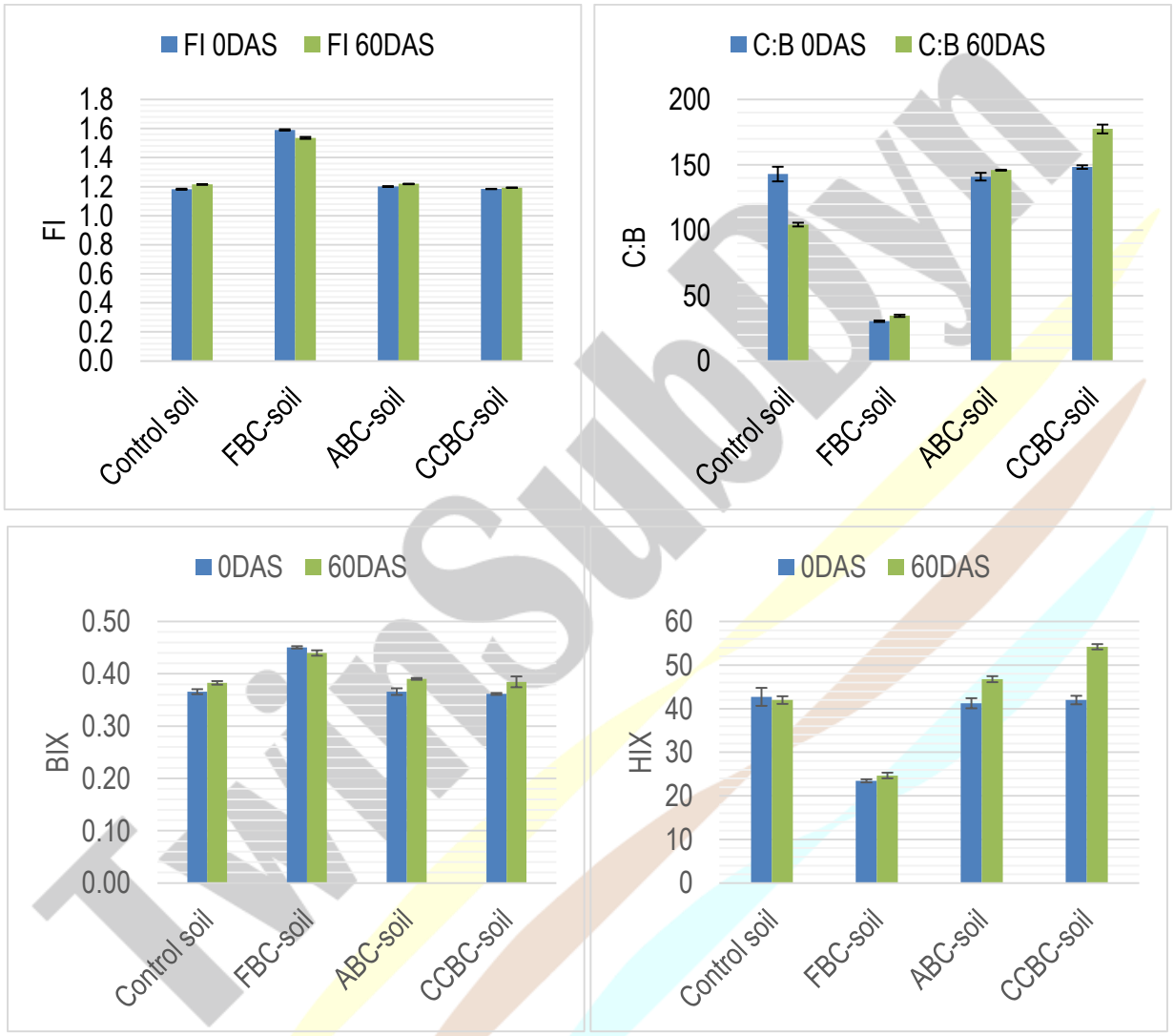

Figure 18. Fluorescent index (FI), C:B ratio, biological index (BIX), and humification index (HIX) of the soils

The BIX provides insight into the biological activity and freshness of the DOM in soil. Higher values indicate a greater contribution of microbial-derived, labile organic matter, while lower

values suggest a dominance of older, more stable organic matter[6]. Control soils, ABC-soil, and CCBC-soil all exhibited similar BIX with a slight increase during the experiment. These results indicate a balanced microbial activity and organic matter stabilization, with a more active microbial community towards the end of the experiment. The higher BIX of the FBC-soil at the beginning reflects the initial boost in microbial activity caused by the fresh biochar's labile organic matter. The slight decrease by the end of the experiment may indicate a reduction in available organic substrates, causing a decline in microbial efficiency or activity.

The HIX of soil DOM is used to assess the degree of humification, or the extent to which organic matter has been decomposed and transformed into more complex, recalcitrant compounds[7]. Humification is a key process in the formation of stable organic matter in soils. The stable HIX of the control soil throughout the duration of the experiment shows that the humification state of organic matter in the control soil remains largely unchanged, suggesting that organic matter is not undergoing significant transformation during the experiment. On the other hand, the increase in HIX of the ABC-soil and CCBC-soil at the end of the experiment suggests enhanced humification processes, likely the result of gradual organic matter release from the biochar, then further decomposition and incorporation into stable, humified organic matter. The co-composted biochar shows a more pronounced increase in HIX, possibly due to its already partially decomposed nature, facilitating faster humification. For the FBC-soil, a much lower HIX was observed, indicating that the addition of fresh biochar introduces less humified, more labile organic matter, which then decomposes more easily. This could mean that the organic matter in the FBC-soil is in the earlier stage of decomposition, with lower aromaticity and stability, which is in accordance with the $SUVA_{254}$ results.

An EEM of a river sediment natural organic matter (NOM) was analyzed as a reference material, and is presented in Figure 19. The EEMs of the four soils (control soil, FBC-soil, ABC-soil, and CCBC-soil) at the beginning (0DAS) and at the end of the pot experiment (60DAS) are shown in Figure 20. These fluorescence 3D spectra will be analyzed by PARAFAC analysis to

[6] Kracmarova-Farren, M., Alexova, E., Kodatova, A. et al. Biochar-induced changes in soil microbial communities: a comparison of two feedstocks and pyrolysis temperatures. Environmental Microbiome 19, 87 (2024). https://doi.org/10.1186/s40793-024-00631-z

[7] Fan J, Duan T, Zou L, Sun J. Characteristics of dissolved organic matter composition in biochar: Effects of feedstocks and pyrolysis temperatures. Environ Sci Pollut Res Int. (2023), 30(36):85139-85153. 10.1007/s11356-023-28431-x

gain spectral profiles to identify fluorophores present in DOM, determine their relative abundance and use the results to obtain environmental insight into the source and fate of DOM.

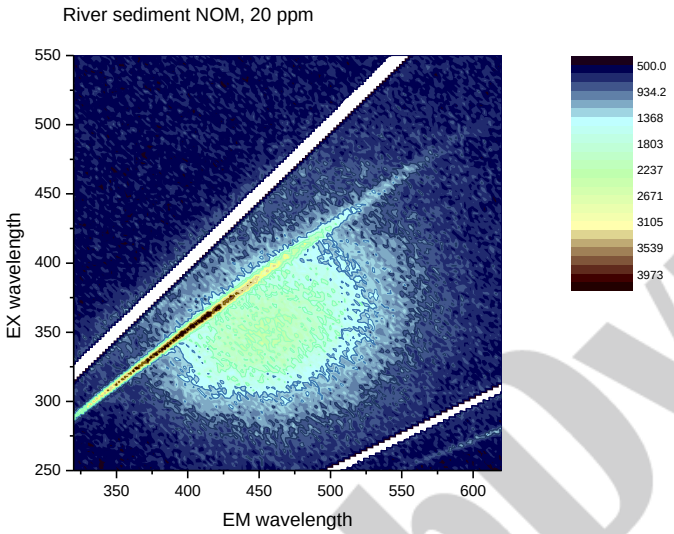

Figure 19. An EEM of a reference material - river sediment NOM (20 ppm)

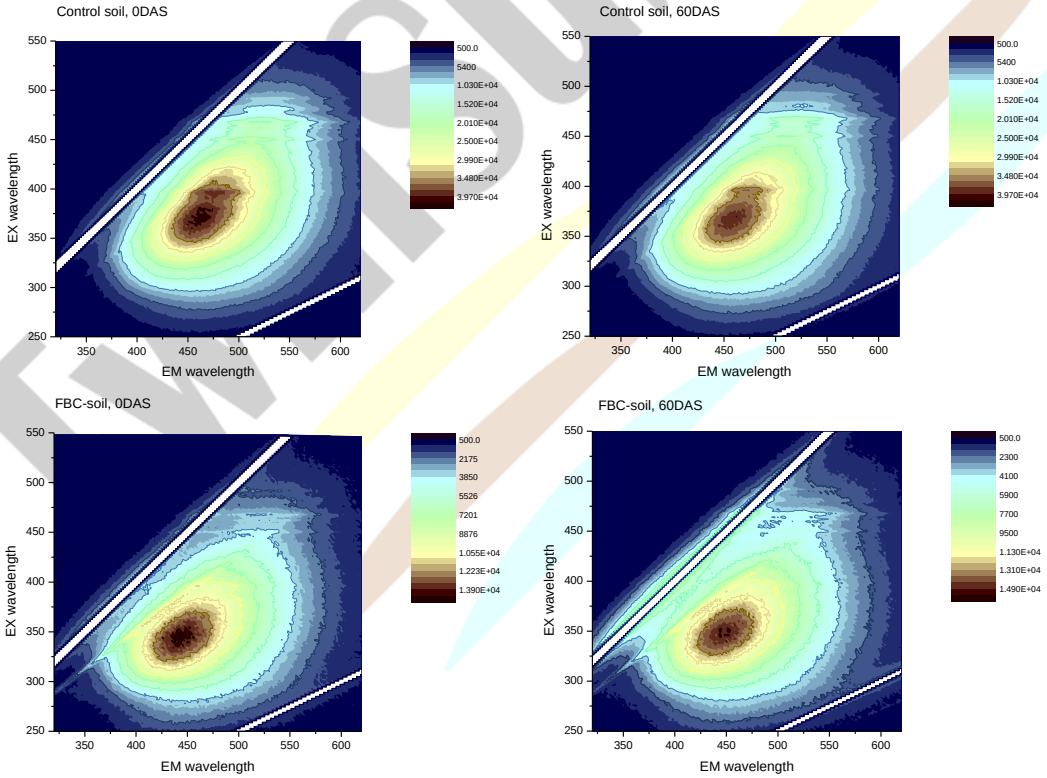

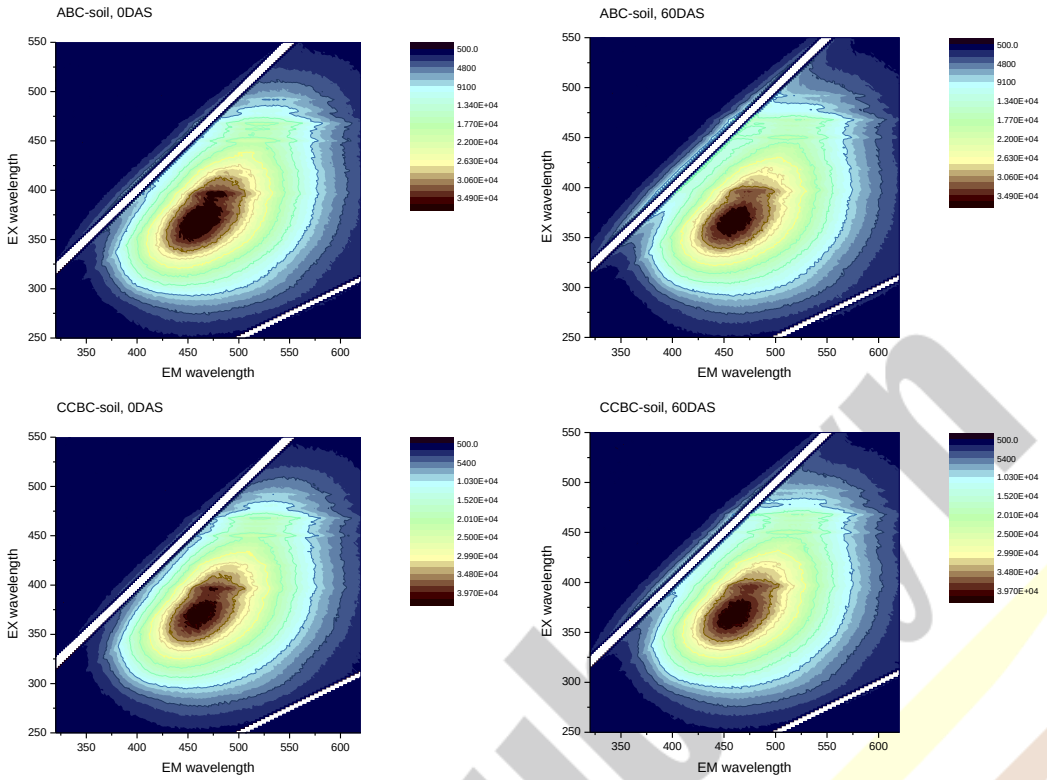

Figure 20. EEMs of untreated and biochar treated soils

Particle size distribution of the control soil and the biochar treated soils was analyzed using DLS. Result are shown in Figure 21 together with hydrodynamic diameters for each soil.

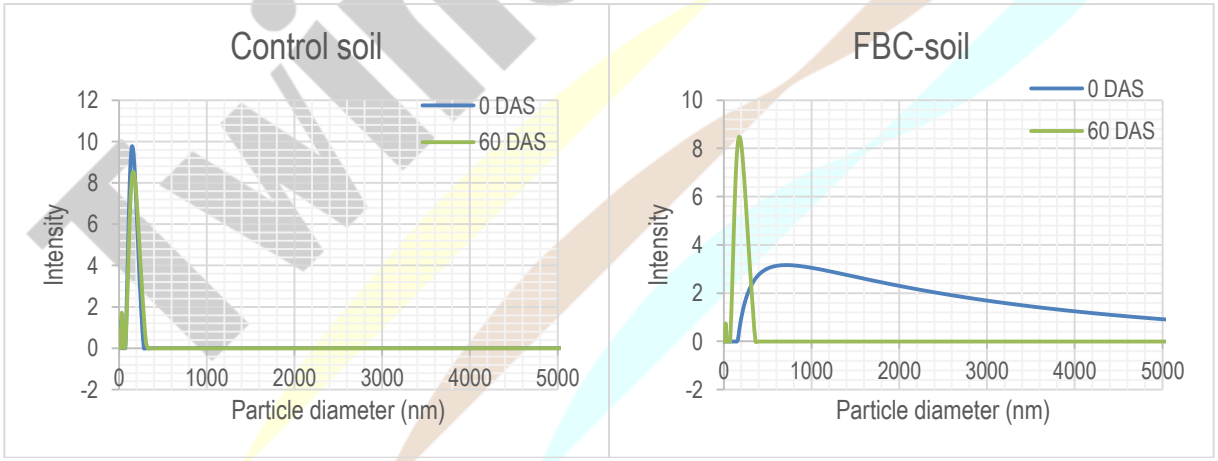

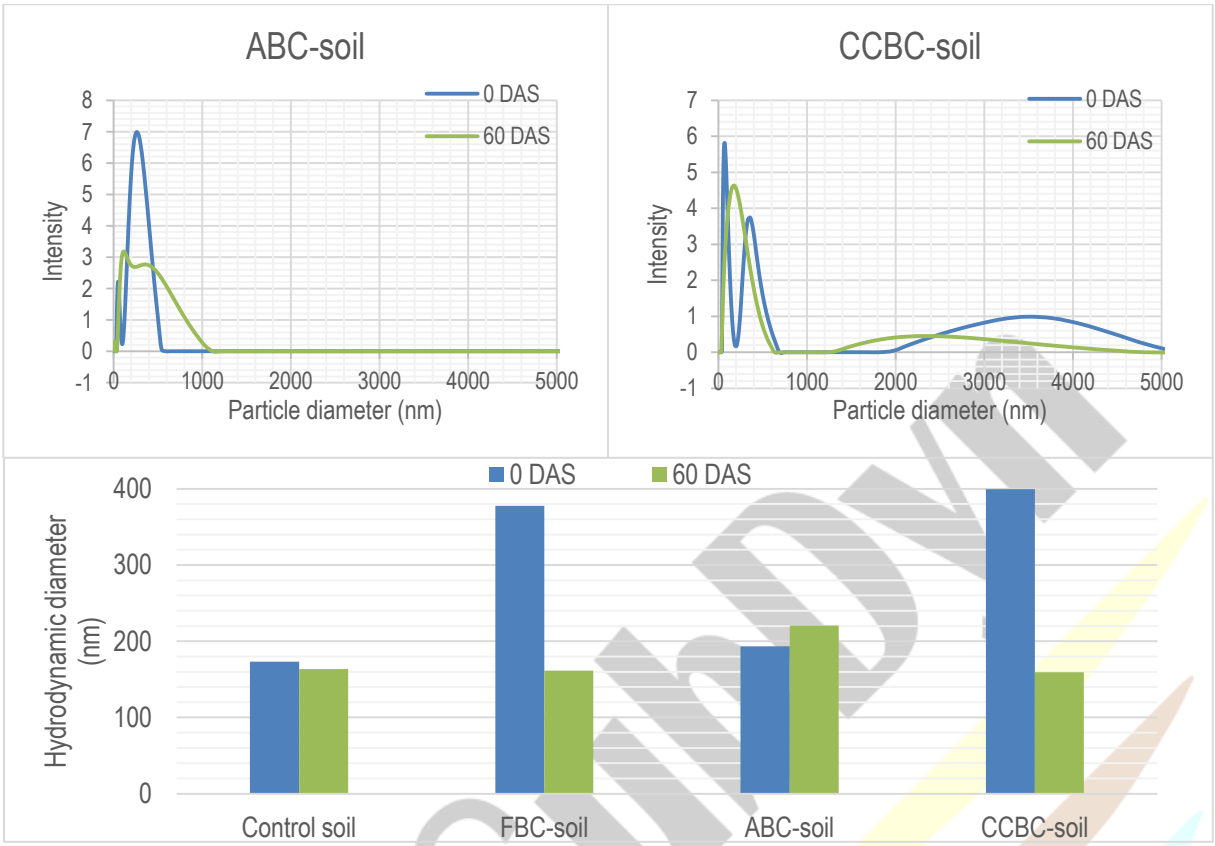

Figure 21. Particle size distribution and hydrodynamic diameters of the untreated and biochar-treated soils

Free-radicals content was determined by EPR for the untreated and biochar-treated soils, as well as the fresh (FBC), aged (ABC) and co-composted biochar (CCBC). Results are shown in Figure 22. The EPR analysis indicates marked differences in free radical content between soils treated with biochar and the untreated control, as well as significant variations among the different types of biochar utilized[8]. The control soil maintained a stable free radical content of approximately 15 mmol/g throughout the duration of the experiment, suggesting limited oxidative activity or turnover of organic matter. In contrast, the soils treated with biochar exhibited substantially elevated free radical concentrations, indicative of the reactive surface properties inherent to biochar. Among the various treatments, the fresh biochar-amended soil (FBC-soil) exhibited the highest initial free radical content at 55 mmol/g, which subsequently decreased to 48 mmol/g by the conclusion of the experiment. This decline implies a degree of

[8] Zhang, X.; Saul, N.; Lieke, T.; Chen, Y.; Wu, M.; Pan, B.; Steinberg, C.E.W. Biochar Extracts Can Modulate the Toxicity of Persistent Free Radicals in the Nematode Caenorhabditis elegans. Appl. Biosci. 2023, 2, 71-83. https://doi.org/10.3390/applbiosci2010007

stabilization of the biochar, likely resulting from interactions with soil organic matter and microbial activity. Nonetheless, the elevated initial levels highlight the high reactivity of fresh biochar immediately following its application. The aged biochar-treated soil (ABC-soil), which was treated in 2010, displayed a significantly lower free radical content of 27 mmol/g, remaining stable throughout the experiment. This stability suggests that the biochar has undergone considerable stabilization over time, resulting in reduced interaction between its reactive surfaces and the surrounding soil environment. Similarly, the co-composted biochar soil (CCBC-soil) began with a high free radical content of 52 mmol/g, which decreased to 44 mmol/g, indicating ongoing but reduced reactivity compared to the freshly amended FBC-soil.

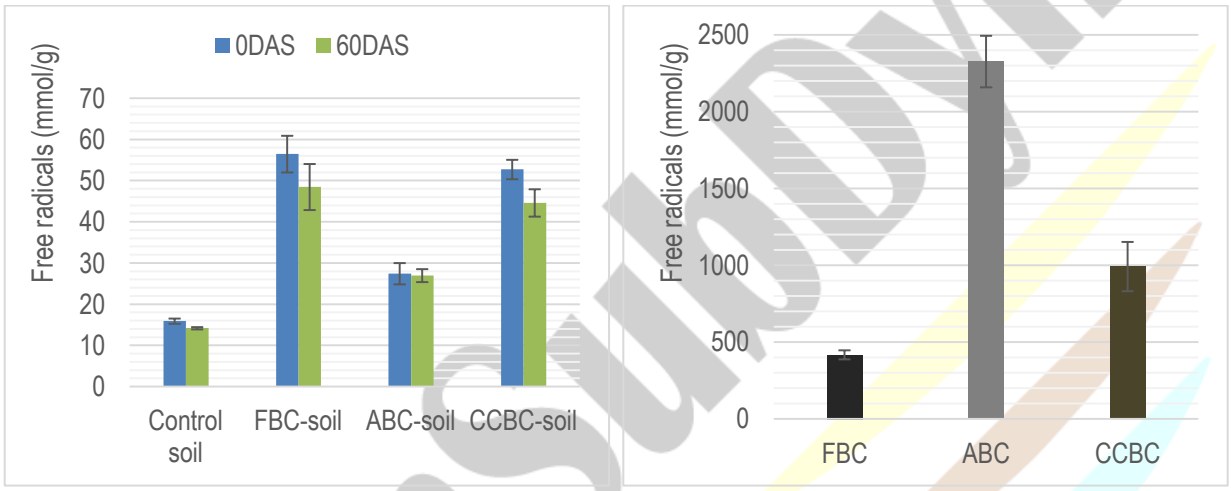

Figure 22. Free-radical content in untreated and biochar-treated soils (left) and fresh, aged and co-composted biochar (right)

The elevated free-radical concentrations observed in the biochar materials themselves (400 mmol/g for FBC, 2250 mmol/g for ABC, and 1000 mmol/g for CCBC) underscore the inherently reactive characteristics of biochars, particularly those that are aged, which tend to accumulate free radicals over time through environmental interactions. The exceptionally high levels recorded for ABC (2250 mmol/g) may be attributed to extended exposure to environmental factors, potentially enhancing its oxidative capacity[9]. XRD gave very similar spectra for all soil samples (Figure 23). Further software analysis will be performed to identify chemical structures present in the soils.

[9] Rashid MS, Liu G, Yousaf B, Hamid Y, Rehman A, Arif M, Ahmed R, Ashraf A, Song Y. A critical review on biochar-assisted free radicals mediated redox reactions influencing transformation of potentially toxic metals: Occurrence, formation, and environmental applications. Environmental Pollution, 2022, 15;315:120335. 10.1016/j.envpol.2022.120335

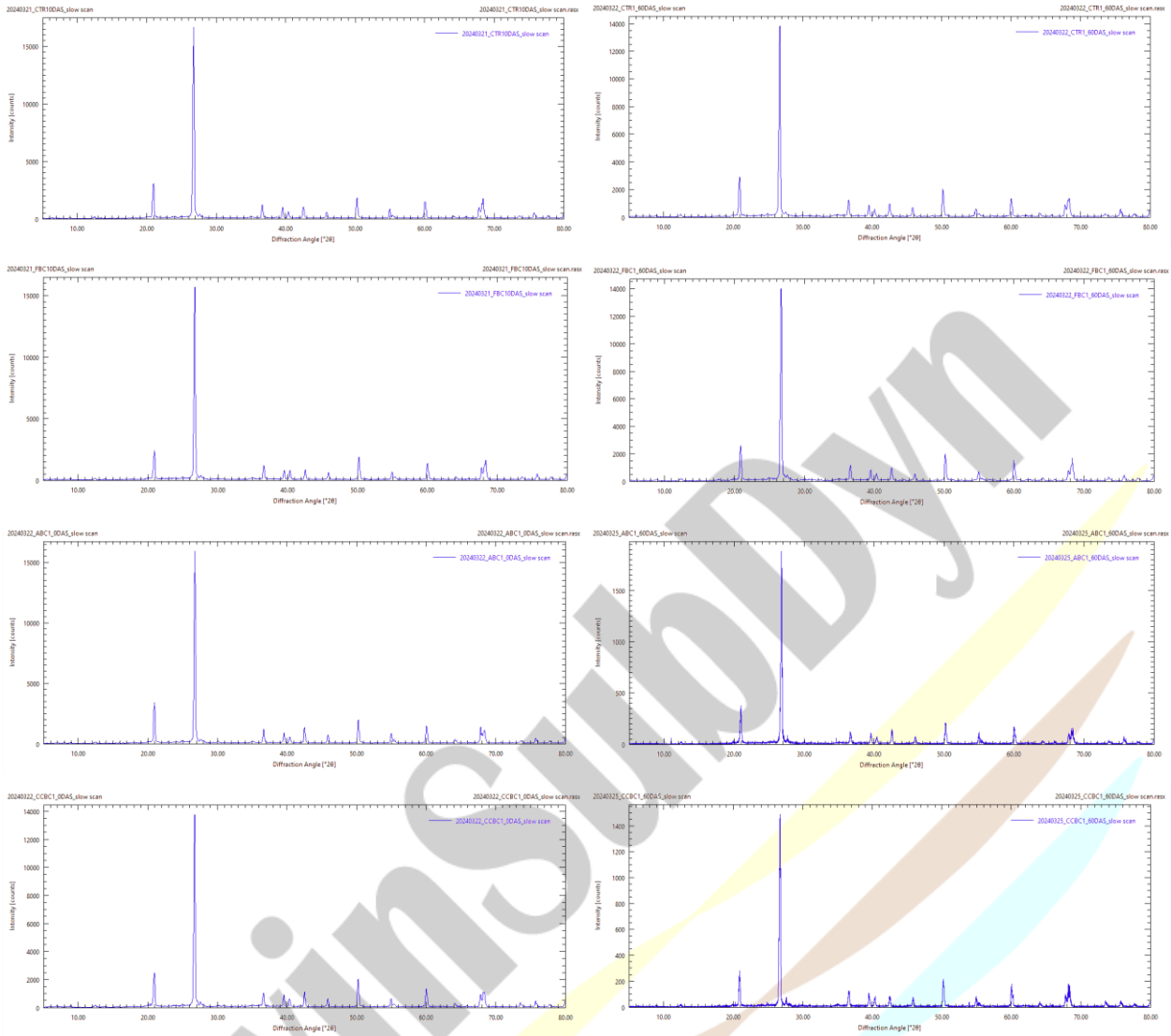

Figure 23. X-ray diffraction spectra of untreated and biochar-treated soils

Organic soil amendments and soil characterization

Several different organic soil amendments (biochar, cow manure, 3 composts and one sludge) as well as three different soils (Danube alluvial sediment, Itebej sediment and Bayreuth soil) were prepared for turbidity and DLS measurements to determine the content of colloids and their size distribution in these samples. TOC of the extracts revealed distinct differences among various soil types and organic amendments (Figure 24). The Danube alluvial soil, which has high sand content is characterized by a very low TOC concentration, demonstrates a low organic matter content, which is typical for this soil type. In contrast, the river sediment from Itebej and the Cambisol from Bayreuth exhibit higher TOC levels, measuring around 10 mg/L

and 30 mg/L, respectively, suggesting a greater presence of organic material. Composts and manure show significantly higher TOC values, with composts ranging from 140 to 355 mg/L and cow manure around 315 mg/L, underscoring their substantial organic matter content. The TOC level in active sludge (about 225 mg/L), reflects its organic-rich nature resulting from wastewater treatment processes. Biochar presents a moderate TOC value of 30 mg/L, which is consistent with its stable carbon structure.

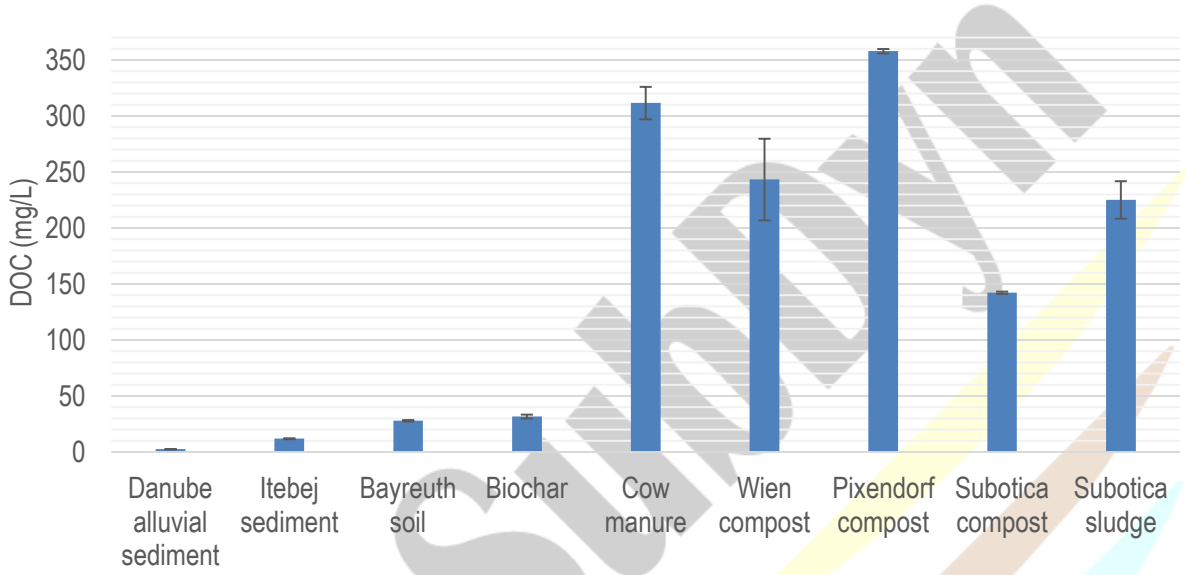

Figure 24. TOC of the soils and OSAs prepared for colloid analysis

The turbidity measurements reveal varying levels of suspended particles and colloids across the samples (Figure 25). Itebej sediment, with less than 20 NTU, shows relatively low turbidity, suggesting fewer suspended solids. Bayreuth soil, Subotica compost (around 40 NTU each), and the Danube alluvial sediment (45 NTU) have slightly higher but still moderate turbidity, indicative of moderate particulate matter. Biochar (60 NTU) shows more suspended particles, likely due to its porous structure releasing fine particles during extraction. The compost samples differ significantly, with Wien compost (80 NTU) showing moderate turbidity, while Pixendorf compost (140 NTU) has much higher values, likely due to different stages of composting and particle size. The much higher turbidity in cow manure (560 NTU) and especially in sludge (1680 NTU) is consistent with their high organic and particulate content, reflecting significant suspended matter, especially in sludge, which is rich in microbial biomass and organic particulates from wastewater treatment.

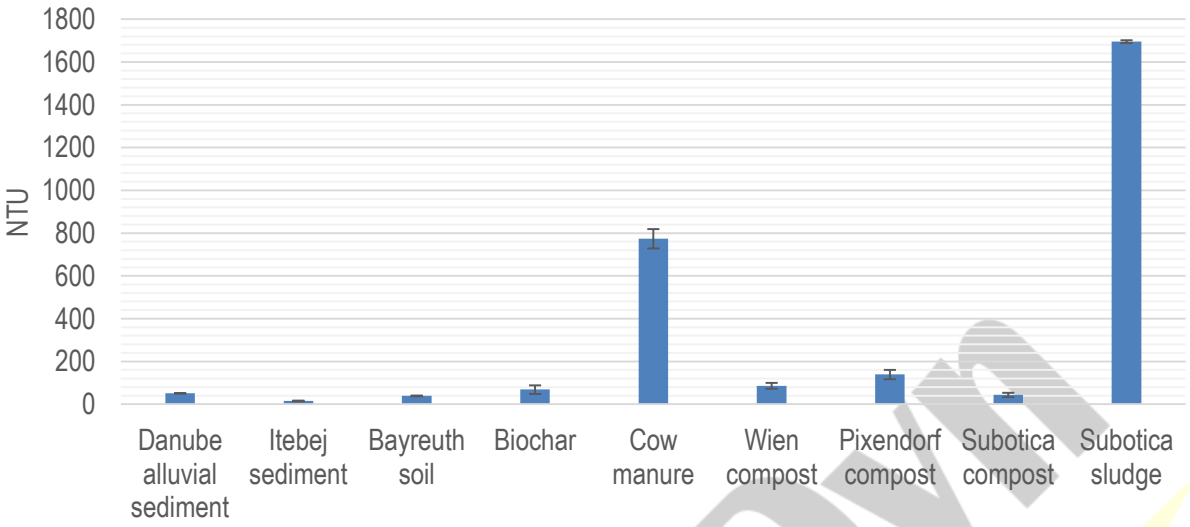

Figure 25. Turbidity of soils and OSA extracts

Hydrodynamic diameters and particle size distribution data were obtained by DLS analysis of the soil and OSA extracts (Figures 26 and 27).

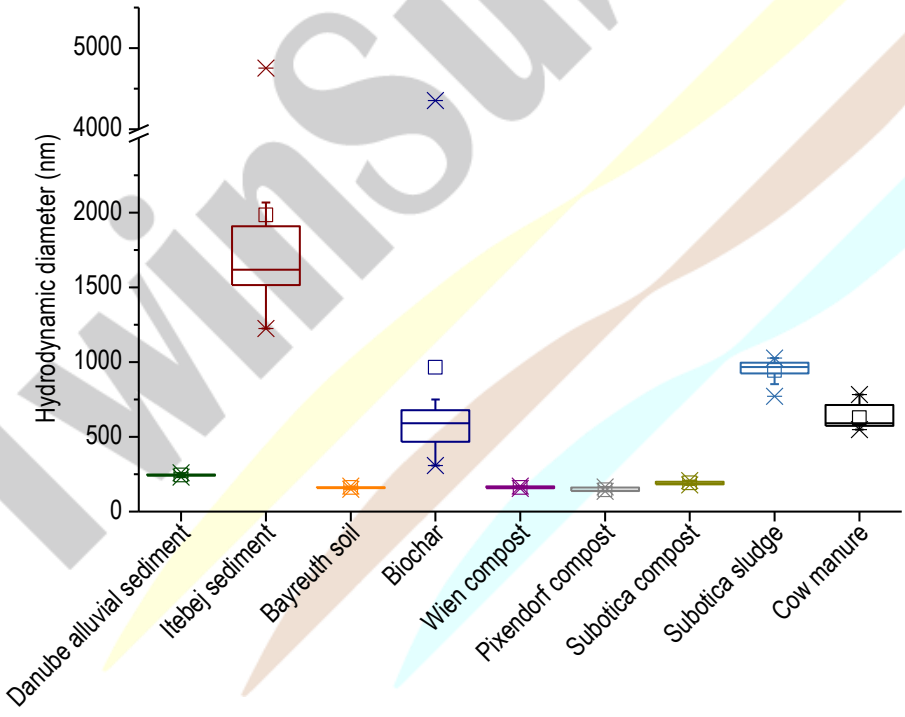

Figure 26. Hydrodynamic diameters of soils and OSA, obtained by DLS analysis

Figure 27. Particle size distribution of soils and OSAs

These results together with literature data on organic contaminants such as pesticides and tire additives (e.g., K_{ow}, K_{oc}) will build the dataset necessary for modeling the colloid-facilitated transport of pollution through soil columns. Modelling the colloid-facilitated transport of pesticides and other organic contaminants in soil can give insight into the mobility and fate of pollutants in soils, and subsequently help assess the risk of groundwater and surface water contamination and human exposure to potentially toxic compounds.

Modelling course

Team members from the UNSPMF group attended a modelling course on colloid transport titled “Nanotechnologies for the remediation of contaminated sites (with principles of numerical transport in porous media)“ (Figure 28).

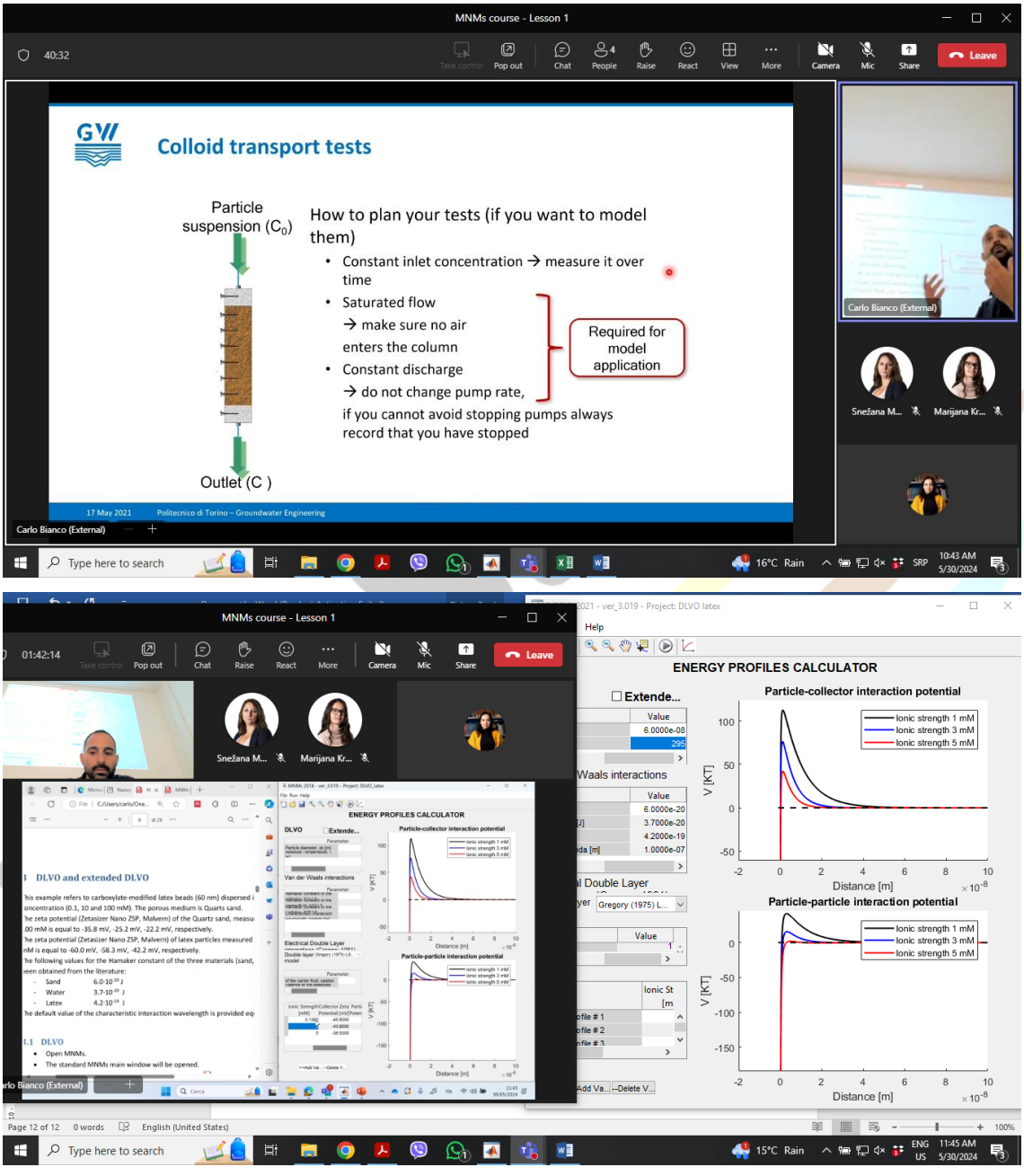

Figure 28. Members of UNSPMF team attending the modelling course

The course covered the following topics:

- Introduction to nanoparticles in the environment, nanoremediation and environmental application of engineered nanomaterials. Flow in porous media.
- Particle transport in porous media at the nano- and micro-scale: surface and hydrodynamic forces, attachment efficiency and single collector efficiency.
- Solute transport in porous media: mechanisms and governing equations
- Numerical methods for the solution of NP transport equations in 1D geometries: theoretical concepts and application
- Particle transport in porous media at the macroscale: mass transport equations, colloid/porous medium interaction mechanisms (equilibrium and nonequilibrium interactions, reversible and irreversible reten tion).
- Particle transport in porous media: porous medium clogging and transport of unstable colloidal suspensions.
- PRACTICAL: MNMs tutorial and practical use
- PRACTICAL: Guided project on the application of the proposed numerical methods to solve basic problems of solute reactive transport
- PRACTICAL: Guided project on the application of the proposed numerical methods to solve basic problems of solute reactive transport
- Nanoparticles for groundwater remediation: reactivity, colloidal stability, functionalization, coating and injection strategies.

Modeling of pesticide transport in unamended and amended soil

For the modeling of colloid-facilitated transport in unamended and amended soil, it was necessary to select the soil and contaminants to include in the investigation. For the soil, the Bayreuth soil was selected, as it is agricultural soil. Further, pesticides listed in Annex 1 of the EU Directive 2013/39/EU[10] "List of priority substances in the field of water policy" are given in Table 2, along with their octanol-water (logKow) and organic carbon-water partitioning coefficients (Koc). Based on these two coefficients, two pesticides were selected, cypermethrin

[10] European Parliament and Council of the European Union. (2013). Directive 2013/39/EU of the European Parliament and of the Council of 12 August 2013 amending Directives 2000/60/EC and 2008/105/EC as regards priority substances in the field of water policy. Official Journal of the European Union, L226, 1–17

as the most hydrophobic, and thus least mobile and least likely to leach into grounwaters, and dichlorvos, with the lowest logKow values, indicating high water solubility and mobility, thus posing the highest risk of contamination to groundwaters. Based on Koc values and soil and OSA properties, soil-solution (Kd) and colloid-solution partitioning coefficients (K_d^{coll}), as well as attachment (k_a) and detachment (k_d) rates of the pesticide to the solid particles were estimated (Table 3).

Table 2. Pesticides listed in Annex 1 "List of priority substances in the field of water policy" of the EUDirective 2013/39/EU

Compound	logKow[11]	Koc* (L/kg)	Compound	logKow*	Koc** (L/kg)
Alachlor	3.52	2.04	1,2,3-trichlorobenzene	4.05	6.92
Atrazine	2.61	0.25	Chloroform	1.97	0.06
Chlorfenvinphos	3.81	3.98	Trifluralin	5.34	134.90
Chlorpyrifos	4.96	56.23	Dicofol	5.02	64.57
Diuron	2.68	0.30	Quinoxyfen	4.66	28.18
alpha-Endosulfan	3.83	4.17	Aclonifen	4.04	6.76
beta-Endosulfan	3.62	2.57	Bifenox	4.48	18.62
Hexachlorobenzene	5.73	331.13	Cypermethrin	6.60	2454.71
Isoproturon	2.87	0.46	Dichlorvos	1.43	0.02
Pentachlorobenzene	5.18	93.33	Heptachlor	6.10	776.25
Pentachlorophenol	5.12	81.28	Heptachlor epoxide	5.40	154.88
Simazine	2.18	0.09	Terbutryn	3.74	3.39

*calculated from logKow values, logKoc=logKow-0.21[12] (Watanabe et al., 1985)

Table 3. Soil, OSA and pesticide properties used in the modeling of pesticide transport

		Soil (bulk)	Biochar	Colloid fraction: Cow manure	Wien compost	Pixendorf compost	Subotica compost	Subotica sludge
	foc	0.016	0.31	0.27	0.56	0.51	0.65	0.11
	Mean particle diameter (m)	3.10E-04	5.44E-06	6.29E-06	1.61E-06	1.46E-06	1.92E-06	9.44E-06
	Porosity	0.472	/	/	/	/	/	/
	Water content %	0.38	/	/	/	/	/	/
	Sat. Hydr. Cond. cm/s	0.0535	/	/	/	/	/	/
	Collision efficiency (α)	/	0.05	0.225	0.155	0.155	0.155	0.25
	K_d^{col} (m^3/kg)	3.65E-04	5.14E-03	4.45E-03	9.35E-03	8.54E-03	1.08E-02	1.84E-03
Dichlovos	**k_a (1/s)**	3.65E-07	6.76E-04	2.64E-03	3.81E-03	3.48E-03	4.40E-03	1.21E-03
	k_d (1/s)	1.00E-03	7.60E+00	1.69E+00	2.45E+00	2.45E+00	2.45E+00	1.52E+00
	K_d^{col} (m^3/kg)	1.12E+05	7.60E+02	6.59E+02	1.38E+03	1.26E+03	1.60E+03	2.72E+02
Cypermethrin	**k_a (1/s)**	1.12E-01	1.00E+02	3.90E+02	5.64E+02	5.15E+02	6.51E+02	1.79E+02
	k_d (1/s)	1.00E-06	7.60E+00	1.69E+00	2.45E+00	2.45E+00	2.45E+00	1.52E+00

[11] https://pubchem.ncbi.nlm.nih.gov/

[12] Watanabe, N., Sato, E., Ose, Y. Adsorption and desorption of polydimethylsiloxane, PCBS, cadmium nitrate, copper sulfate, nickel sulfate and zinc nitrate by river surface sediments. Science of The Total Environment, (1985), 41(2), 153-161.

The obtained breakthrough curves (BTC) simulating dichlorvos and cypermethrin transport through the unamended soil showed drastic differences in breakthrough times (Figure 29). Dichlorvos (an organophosphate insecticide) is highly water-soluble (approx. >8,000 mg/L), low in sorption affinity, and relatively non-persistent in soils. These traits allow it to move quickly through the soil profile, resulting in a sharp breakthrough after less than 1 hour. This behavior makes dichlorvos prone to leaching, especially in sandy or low-organic-matter soils[13]. On the other hand, the breakthrough time of cypermethrin was close to 5 years. This is a pesticide with a very low water solubility (~0.004 mg/L) and high affinity for soil organic matter. It binds strongly to soil particles and organic carbon, leading to extremely delayed breakthrough and limited vertical movement[14] (Xu et al., 2008; Gan et al., 2005). Its apparent 5-year delay suggests near-complete retardation in the soil column under the modeled conditions.

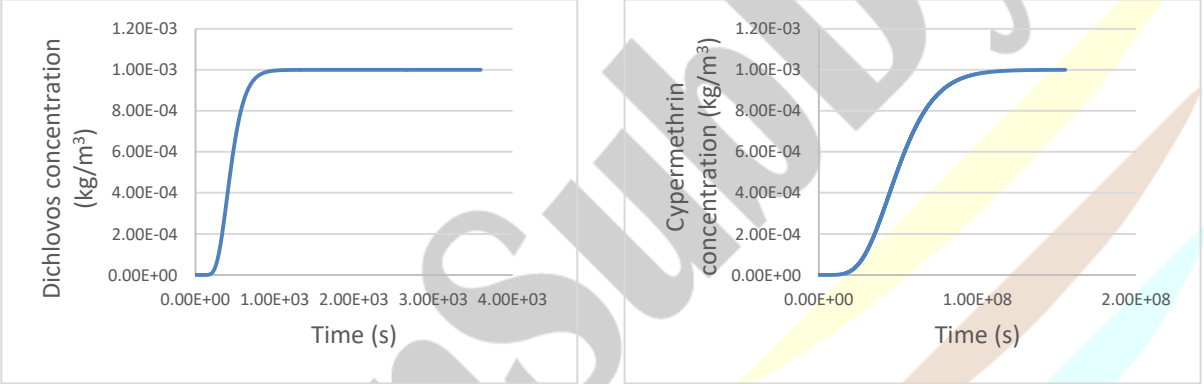

Figure 29. Breakthrough curves of dichlorvos and cypermenthrin in the unamended soil

Despite stark differences in pesticide mobility, adding six organic soil amendments (biochar, cow manure, three composts, and sewage sludge) had no notable effect on the breakthrough curves of dichlorvos or cypermethrin (Figures 30 and 31). Dichlorvos remained highly mobile, with no delay or reduction in peak concentrations, while cypermethrin, already strongly retained, showed no further retention. Possible reasons include low amendment rates (likely below the >5% threshold for meaningful sorption changes), limited contact time before pesticide application, and the dominant role of pesticide properties - high mobility for dichlorvos and strong sorption for cypermethrin - in determining transport behavior.

[13] Gao, J. P., Maguhn, J., Spitzauer, P., & Kettrup, A. Sorption of pesticides in the sediment of the Teufelsweiher pond. Science of the Total Environment, (1998), 220(1), 45–57.
[14] Xu, T., Wang, J., Lu, M., & Li, X. Sorption and degradation of cypermethrin in soils and sediment. Journal of Environmental Sciences, (2008), 20(4), 464–469.

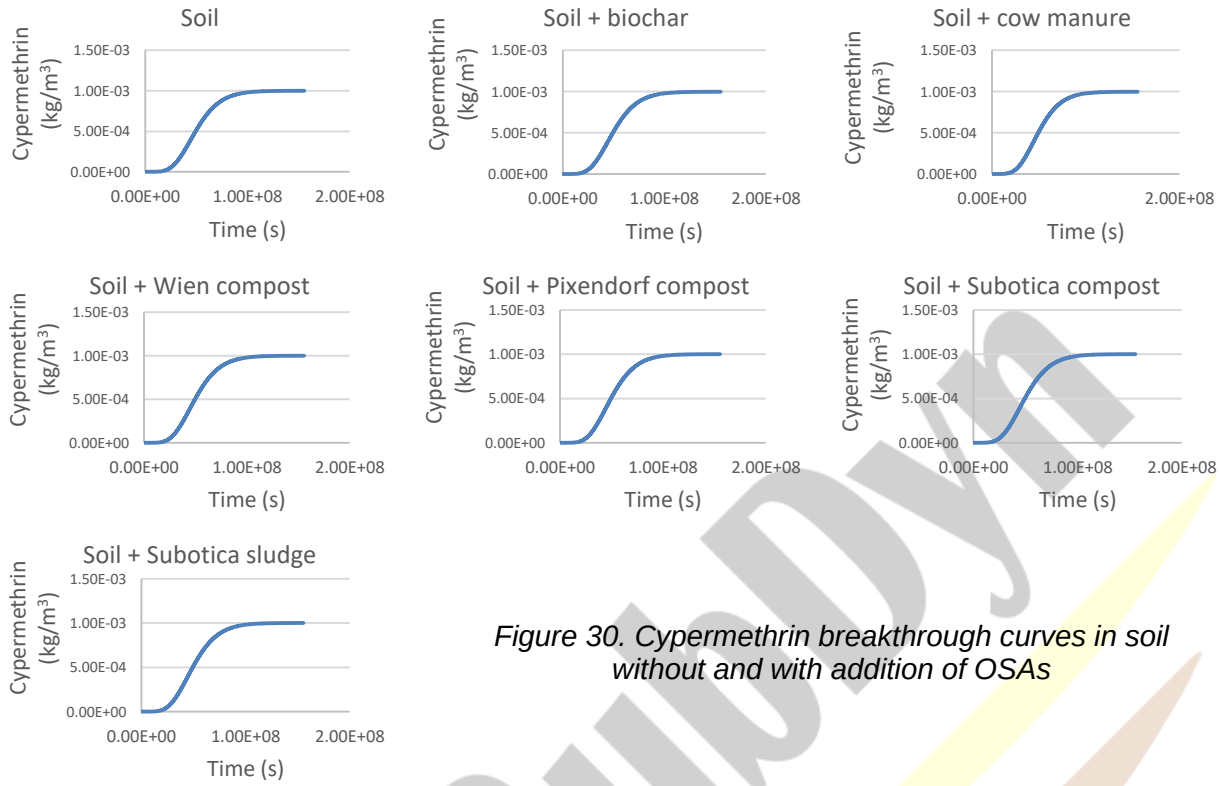

Figure 30. Cypermethrin breakthrough curves in soil without and with addition of OSAs

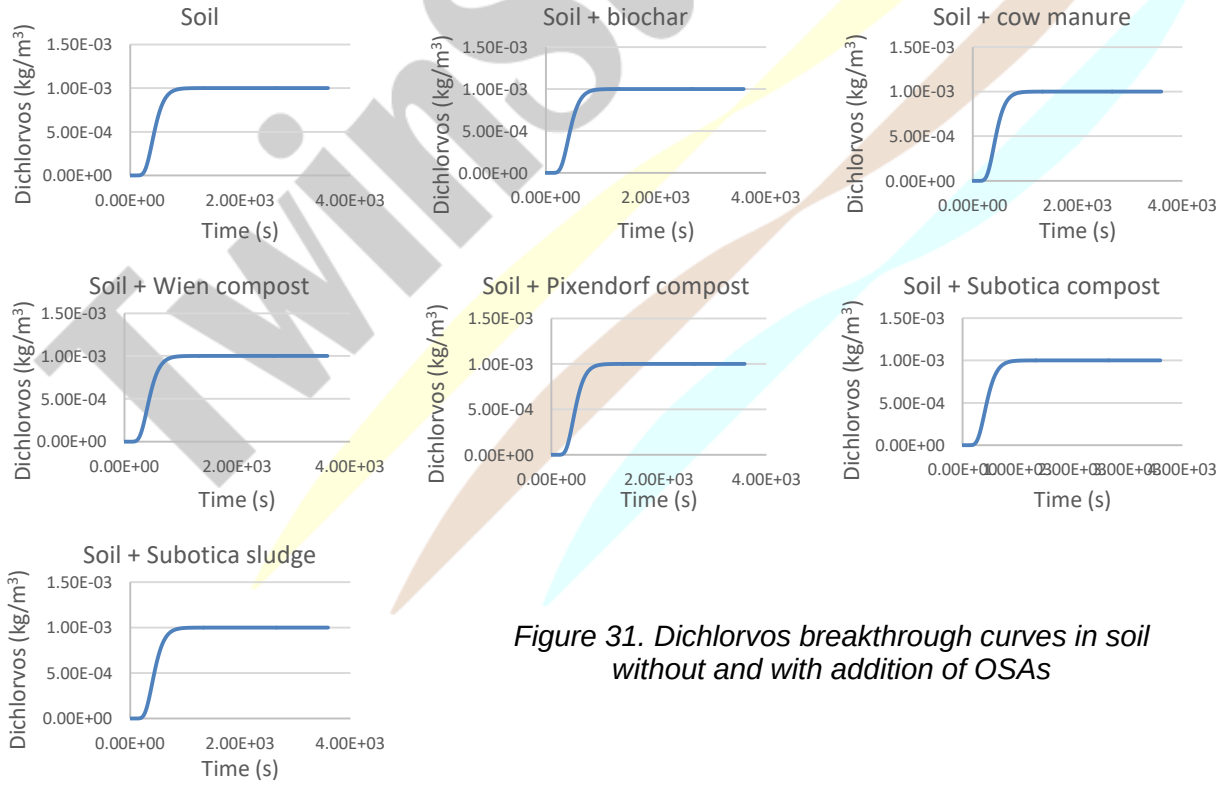

Figure 31. Dichlorvos breakthrough curves in soil without and with addition of OSAs

Impact on your project

The six-month visit to the University of Vienna significantly advanced the project by providing comprehensive insights into DOM properties and particle dynamics in biochar-treated soils. The in-depth DOM characterization, utilizing both techniques already in use at UNSPMF like TOC analysis, UV/Vis spectrophotometry, but also some newer and more advanced techniques such as fluorescence spectroscopy, DLS and EPR, enabled a thorough understanding of organic matter transformations in untreated soil, fresh and aged biochar-treated soil, and co-composted biochar treated soil. These data are critical for assessing biochar's long-term impact on soil organic matter dynamics and its implications for soil fertility and carbon sequestration.

The determination of particle size distribution and turbidity in soils and OSA provided essential data for modeling colloid-facilitated transport. This modeling will help predict the movement of pollutants, including pesticides and tire additives, through amended soils, which is crucial for environmental risk assessments. The knowledge gained from the particle analysis and colloid transport modeling course attended by UNSPMF team members will support the project's goal of evaluating the potential risks of contaminant migration in biochar-amended soils, ultimately contributing to safer agricultural practices and improved soil management strategies.

Subtask 1.2.2: 6-month secondment for an ESR/RR at CSIC, focused on investigating the impact of different organic amendments on the soil-plant system behavior, with a particular emphasis on nitrogen dynamics within it

MOBILITY REPORT

Researcher: Dr. Marko Šolić, UNSPMF

Assigned supervisor: Prof. Dr. Heike Knicker, CSIC

Duration of the visit: 01.04.2024. - 30.09.2024.

Executive Summary

The six-month research stay at the Spanish National Research Council (Consejo Superior de Investigaciones Científicas, CSIC) was aimed at training a UNSPMF researcher in the design and implementation of pot experiment, as well as in acquiring expertise in techniques for characterizing both the tested soils and cultivated plants. The overarching goal was to evaluate the impact of different types of biochar (BC) on the systems of interest, particularly focusing on the fate and movement of nitrogen within it.

This objective was realized through the development of a specific pot experiment conducted under controlled greenhouse conditions. The experiment consisted of eight treatment variants (including untreated soil, and soil treated with fresh, aged, and co-composted BC), divided into two series. Only one series included the application of commercial NPK fertilizer, while both were enriched with the nitrogen isotope ^{15}N.

Throughout various stages of the experiment, the following analyses were conducted on the soil: water holding capacity, pH value, electrical conductivity, content of organic matter and carbon (including NMR characterization), total and/or available macro- and micronutrient content, microbial activity, and stable nitrogen isotope ratios.

Upon completion of the pot experiment, biomass from green lettuce (used as the test plant) was collected and analyzed for yield, macro- and micronutrient content (total and/or available), plant health status (chlorophyll content and photosynthetic efficiency), and stable nitrogen isotope ratio.

In addition to the experimental activities, the training also included participation in a seminar on the theoretical background and application of the solid state NMR technique, delivered by Prof. Dr. Heike Knicker.

Introduction

1. Background

The soils used in the pot experiment conducted during this six-month training originate from the experimental field near Bayreuth, Germany, established in 2010. These soils were sampled for the purposes of the six-month training of Dr. Tamara Apostolović (conducted as part of the TwinSubDyn project) and included three out of the ten treatment variants examined in the afore-mentioned field: control (untreated soil used as reference soil), K_31.5 (soil treated with 31.5 t/ha BC), and BGK31.5/70 (soil treated with co-composted BC in a ratio of 31.5 t/ha BC and 70 t/ha compost material). An additional fourth treatment variant was introduced, involving the enrichment of the control soil with fresh biochar of the same origin and in an identical dose as applied during the 2010 experiment.

After the completion of Dr. Tamara Apostolović's pot experiment, which lasted 60 days, the specified soils were stored and, after approximately one year, were used in pot experiments conducted during the training described in this mobility report (see **Photos 1 to 3**).

Photos 1 to 3. Sampling of the experimental field near Bayreuth, Germany, and stored soil samples used in the pot experiment covered in this mobility report

Experimental setup: The experimental setup consisted of two series of soil samples, each incorporating four previously described treatment variants: control, "fresh" BC (mixed with soil for one year), aged BC, and co-composted BC. To ensure reliability, all experiments were performed in triplicate, totaling 12 pots per series. In one of the two series, prior to sowing, the soil was

amended with commercial NPK fertilizer at a rate equivalent to 85 kg/ha of nitrogen. The amendment process involved extracting the topsoil layer from each of the 12 pots, homogenizing it with powdered NPK, and returning the treated soil to its respective pots (with the exception of water holding capacity analysis, all soil characterization experiments were conducted after the application of NPK). Following soil preparation, seeds of *Lactuca sativa* L. var. (green lettuce) were sown. Upon germination, an N-15 solution was applied to each of the 24 pots at a concentration corresponding to 1% of the initially applied nitrogen dose. The growth of green lettuce was monitored over a 60-day period. To maintain consistent growing conditions, irrigation was regulated to ensure that the soil moisture content remained at 60% of the soil's water holding capacity (see **Scheme 1** and **Photos 4 to 12**).

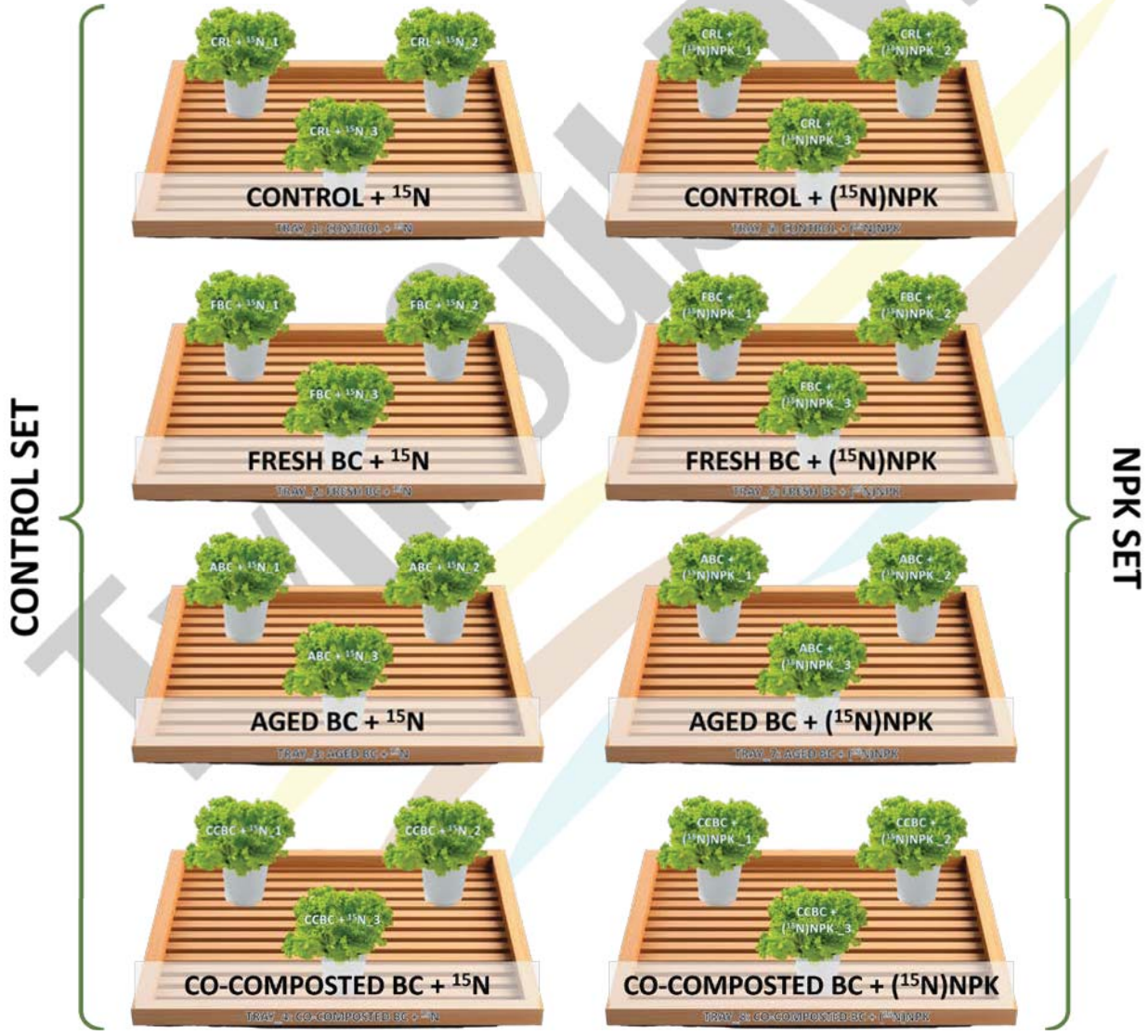

Scheme 1. Schematic representation of the experimental design

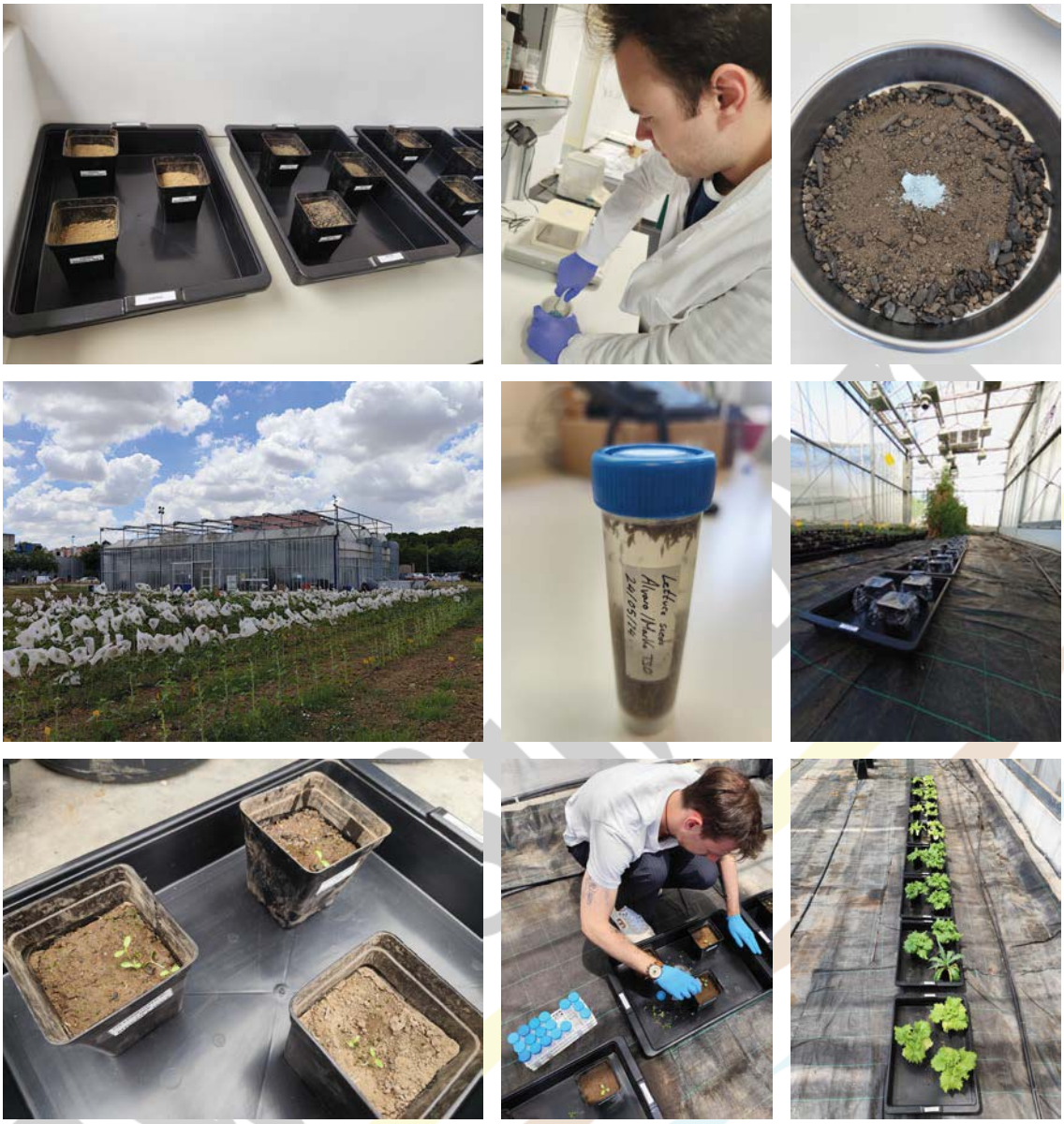

Photos 4 to 12 (from left to right). Different phases in setting up the pot experiment

2. Scope of the secondment

The scope of this secondment was the transfer of knowledge in the field of designing and conducting pot experiments, as well as the application of characterization techniques relevant for monitoring changes within the studied soil–plant systems. In addition to their effects on various parameters reflecting soil quality and plant growth and development, special emphasis was placed on studying how the presence of different types of BC (fresh, aged, and co-composted) in soil influences nitrogen dynamics within the soil–plant system.

This was achieved through the implementation of a 60-day pot experiment conducted under greenhouse conditions, which involved the selective treatment of tested variants with commercial NPK fertilizer, as well as nitrogen isotope (^{15}N) labeling. Prior to the experiment, or upon its completion, the following analyses were carried out on the soil and/or lettuce (used as a test plant), depending on the parameter: water holding capacity, pH value, electrical conductivity, content of organic matter and carbon (including NMR characterization), total and/or available macro- and micronutrient content, microbial activity, stable nitrogen isotope ratio, biomass yield, and plant health status.

Content

1. Methods

1.1. Water Holding Capacity (WHC)

Materials: 1 set “flask + funnel + filter (Whatman 2)” and 1 beaker per sample, distilled water, notebook, pen, and marker (see **Photos 13 and 14**).

Procedure:

1. Mark/label and weigh each set (“flask + funnel + filter”), with both a dry filter and a humid filter;
2. Weigh 2 g of sample and record the weight (“flask + funnel + humid filter + dry sample”);
3. Add an excess amount of distilled water (~10 mL) to saturate the sample;
4. Leave the setup for 2 hours (with the “filter + funnel + sample” on the beaker);
5. After 2 hours, weigh the “flask + funnel + humid filter + humid sample”;
6. Calculate the wet weight of the sample, considering the weight of the funnel and filter paper. The difference in weight between the wet sample (after 2 hours) and the dry sample represents the amount of water the sample can retain (WHC). WHC is expressed as:

$$WHC\ (\%) = \frac{weight\ of\ water\ retained\ by\ the\ sample}{initial\ weight\ of\ the\ sample} \times 100$$

Photos 13 and 14. Laboratory analysis of soil water holding capacity

1.2. pH and Electrical Conductivity (EC)

Materials: 1 centrifuge tube per sample (30 mL), 1 test tube per sample (Ø ~16 mm, small), rotator, filter-blotting paper, funnels, clock/timer, notebook, pen, and marker (see **Photos 15 to 18**).

Procedure:

1. Label the tubes and weigh 1 g of soil;
2. Add 10 mL of milli-Q/elix water (type II distilled water);
3. Shake in the rotator for 2 hours;
4. Let the sample sit for 30 minutes;
5. Measure the pH (clean the electrode with distilled water and dry it between each measurement);
6. After the pH measurement, filter the supernatant into a test tube (since part of the water remains retained in the “sample + filter”, the volume of the filtrate is small, and the electrode must be well immersed);
7. Directly measure EC in the filtrate;
8. The soil collected on the filter can be dried (< 40ºC) and reused for other analyses.

NOTE: Before starting the protocol, ensure that the pH meter is properly prepared. Allow it to stabilize after pre-ignition, calibrate it, and verify the pH of the water to be used.

Photos 15 to 18. Laboratory analysis of soil pH and electrical conductivity

1.3. Total Organic Carbon (TOC) and Total Nitrogen (TN) Content in Soil and Plants

The determination of TOC and TN content in soil and plants is a crucial step in assessing soil health, nutrient availability, and environmental impact. This analysis is commonly conducted using a TOC analyzer, which offers a modern, efficient, and highly accurate method for determining the TOC and TN content in samples. These analyzers are widely employed in environmental, agricultural, and soil science laboratories due to their precision and ease of use.

In the TOC analyzer, the sample – typically dried and ground (see **Photos 19 to 24**) – is introduced into a combustion chamber, where it is subjected to high temperatures, generally between 680–720ºC. During the combustion process, all the carbon present in the sample is oxidized to form carbon dioxide (CO_2). The CO_2 is then measured using an infrared (IR) detector, which quantifies the concentration of the gas released, allowing for the precise calculation of the TOC content.

In many advanced TOC analyzers, a TN module is included. This allows the same combustion process used for carbon analysis to be adapted for nitrogen measurements. During combustion, nitrogen in the sample is converted into nitrogen oxides (NO_X). The released NO_X gases are then chemically reduced to form nitric oxide (NO), which is subsequently measured using a chemiluminescence detector. This method provides accurate and reliable results for TN content in the sample.

Accurate TOC and TN measurements provide valuable insights into soil fertility, carbon sequestration, and the overall health of ecosystems. For example, TOC measurements help in understanding the amount of organic material available for soil microorganisms, while TN content is essential for evaluating nutrient availability and soil nitrogen status, which is critical for optimizing agricultural practices.

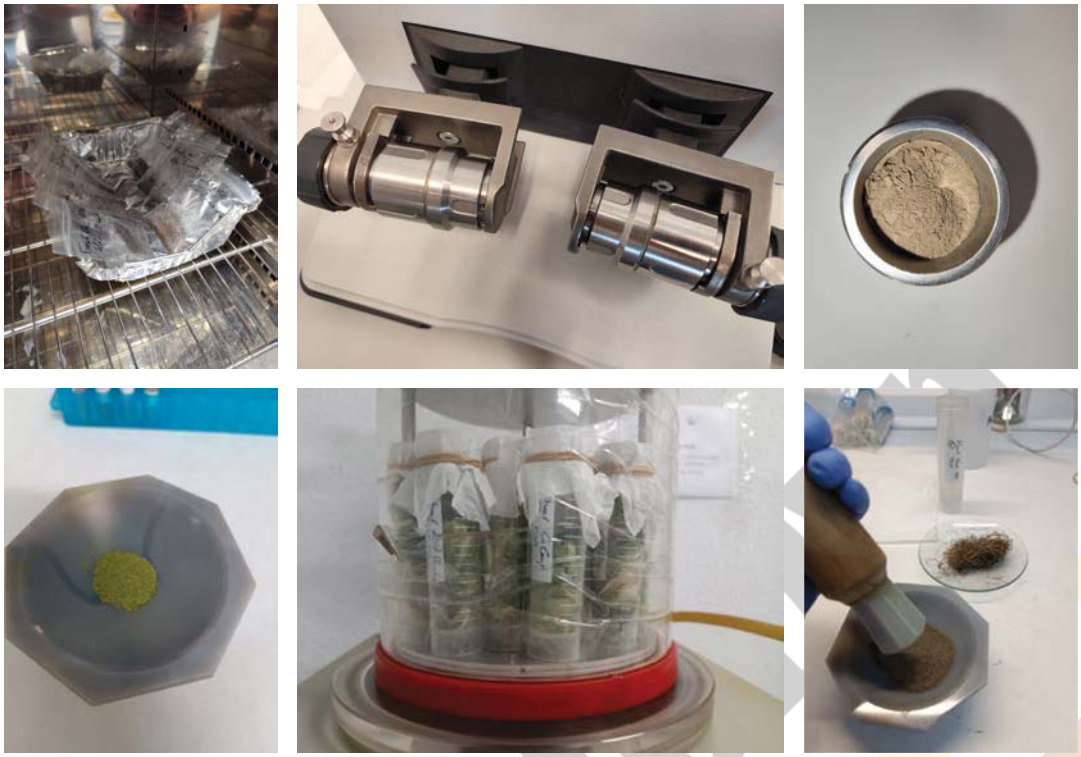

Photos 19 to 24 (from left to right). Laboratory preparation of soil and plant material samples for the determination of total organic carbon and total nitrogen content

NOTE: This activity involved the preparation of soil and plant material, while the analysis of TOC and TN content was performed by the Institute of Natural Resources and Agrobiology of Seville (IRNAS) as a service.

1.4. Ammonium and Nitrate Contents in Soil and Plants

The majority of nitrogen in soil is in an organic form, which is unavailable to plants. The inorganic (mineral) nitrogen forms available for plant uptake are nitrate and ammonium ions, which can be extracted using a potassium chloride (KCl) solution and analyzed with a spectrophotometer.

KCl extraction:

a) Materials:

- 50 mL Falcon tubes, a shaker, funnels, and Whatman 2V filter paper.

b) Reagents:

- 1 M KCl solution: Dissolve 74.56 g of KCl in 600 mL of milli-Q/elix water, then dilute to 1000 mL.

c) Procedure:

- Weigh 1 g of dry soil into the 50 mL Falcon tubes and add 10 mL of KCl solution;
- Shake for 1 hour at 180 rpm;
- Centrifuge the samples for 5 minutes at 4000 rpm, then filter through Whatman 2V filter paper;
- Measure immediately or store in the refrigerator at -18ºC.

Measurement of ammonium (based on DIN 38406/5):

For the determination of NH_4-N content in soil, the Nessler method is used.

a) Reagents:

- Stock solution: Dissolve 4.719 g of dry ammonium sulfate ($(NH4)_2SO_4$) in 400 mL of milli-Q/elix water in a 1 L flask, then dilute to 1000 mL (1000 mg/L NH_4-N stock solution). Maximum storage time: 1 week;
- Indicator solution: Dissolve 4 g of sodium salicylate ($C_7H_5O_3Na$) and 0.1 g of sodium nitroprusside ($Na_2[Fe(CN)_5NO]\cdot 2H_2O$) in 60 mL of milli-Q/elix water and dilute to 100 mL. Store in the dark. Maximum storage time: 1 week;
- Buffer solution: Dissolve 1.48 g of sodium hydroxide (NaOH), 4.98 g of monohydrogen phosphate, and 5 mL of hypochlorite solution (5% available chloride) in milli-Q/elix water, then dilute to 1000 mL. **Note:** exothermic reaction. Prepare on the day of use;
- EDTA 6% solution: Dissolve 3 g of disodium diacid ethylenediaminetetraacetate (EDTA) in 50 mL of milli-Q/elix water. Maximum storage time: 1 month in the refrigerator.

b) Calibration:

- From the stock solution, prepare working solutions (1, 10, and 100 mg/L);
- Pipette an appropriate amount of working solutions into the microplate to prepare calibration standards with concentrations ranging from 0.0 to 2.0 ppm NH_4-N. Make up the volume with milli-Q/elix water. Standards should be prepared fresh each measurement day, immediately before use.

c) Procedure:

- In a microplate, add 50 µL of soil extract. Then add 10 µL of EDTA solution, 60 µL of indicator solution, 100 µL of milli-Q/elix water, and 30 µL of buffer solution;
- Shake for 1 minute, then incubate for 30 minutes at 37ºC;
- Wait for 5 minutes;

- Measure absorbance at 667 nm;
- For the blank, measure 50 µL of extraction solution (1 M KCl) instead of the sample;
- For calibration points, measure 50 µL of 1 M KCl, then add an appropriate volume of working standards to the microplate and make up to 100 µL with milli-Q/elix water.

Measurement of nitrates:

a) Reagents:

- Copper sulfate solution (Sol. 1): Dissolve 0.5 g of $CuSO_4 \cdot 5H_2O$ in 40 mL of milli-Q/elix water and dilute to 50 mL;
- Zinc sulfate solution (Sol. 2): Dissolve 0.5 g of $ZnSO_4 \cdot 7H_2O$ in 40 mL of milli-Q/elix water and dilute to 50 mL;
- Catalyst solution: Dissolve 0.5 g of NaOH (lentils) in 40 mL of milli-Q/elix water, add 0.4 mL of 50% orthophosphoric acid (H_3PO_4), and dilute to 50 mL with milli-Q/elix water;
- Hydrazine sulfate solution: Add 0.5 mL of Sol. 1, 0.5 mL of Sol. 2, and 0.1 g of hydrazine sulfate ($N_2H_6SO_4$) to 40 mL of milli-Q/elix water, then dilute to 50 mL;
- SNEDD coloring solution: Dissolve 0.5 g of sulfanilamide ($C_6H_8N_2O_2S$) in 40 mL of milli-Q/elix water (heat if necessary), add 0.025 g of N-(1-naphthyl) ethylenediamine ($C_{12}H_{14}N_2$), and 10 mL of 50% H_3PO_4. Dilute to 50 mL;
- Stock solution, 1000 ppm N-NO_3: Dissolve 1.0804 g of KNO_3 in milli-Q/elix water and dilute to 250 mL.

Procedure:

- In a microplate, measure 30 µL of sample (extract) or 40 µL of 1 M KCl;
- For blanks and calibration standards only, add 20 µL of KCl;
- Add 60 µL of the catalyst solution and agitate;
- Add 20 µL of hydrazine sulfate solution and agitate;
- Cover the plate with parafilm and agitate for 30 seconds;
- Place in the incubator at 37ºC for 20 minutes;
- Add 60 µL of SNEDD solution and agitate;
- Add 80 µL of Elix water to the samples, or 50 µL to the calibration standards and blanks;
- Measure the N-NO_3 content on the spectrophotometer at 540 nm.

NOTE: The analysis of these parameters has not yet been carried out due to time constraints. In the upcoming period, it will be conducted according to the procedures outlined here.

1.5. Nitrogen Isotope Ratio in Soils and Plants

The application of N-15 stable isotope labeling is a well-established method in environmental and agricultural research for investigating nitrogen dynamics. By enabling the precise tracking of nitrogen sources and transformations, N-15 labeling provides valuable insights into processes such as nitrogen uptake by plants, retention in soil, and potential losses through leaching or volatilization.

To assess these processes, isotopic analyses were conducted on plant and soil samples collected after the harvest of plant material, according to the following procedure. Subsamples of powdered materials (see **Photos 19 to 24**) were weighed to the nearest µg and placed into tin capsules for stable isotope analysis of nitrogen ($\delta^{15}N$). Subsequently, the samples were combusted at 1020ºC using a continuous flow isotope-ratio mass spectrometry system, consisting of a Flash HT Plus elemental analyzer coupled to a Delta-V Advantage isotope ratio mass spectrometer via a CONFLO IV interface (Thermo Fisher Scientific, Bremen, Germany). The isotopic composition is reported in the conventional delta (δ) per mil notation (‰), relative to atmospheric N_2.

Analytical precision was ensured through replicate assays of standards routinely inserted within the sampling sequence. The measurement error for $\delta^{15}N$ was ±0.2‰. The standards used for calibration included IAEA-600 (caffeine, international standard) and internal standards: LIE-P-22 (casein), LIE-BB (whale baleen), and LIE-PA (feathers of Razorbill). These laboratory standards were calibrated with international standards supplied by the International Atomic Energy Agency (IAEA, Vienna).

NOTE: Isotopic analyses were carried out at the Laboratorio de Isótopos Estables (LIE-EBD) of the Estación Biológica de Doñana, Spain. At this stage, only the $\delta^{15}N$ analysis has been conducted on soil samples. However, due to the nitrogen enrichment in the plant material exceeding optimal levels for analysis, the $\delta^{15}N$ analyses for roots and shoots have not yet been performed. To address this, the samples have been sent to Martin Luther University in Halle-Wittenberg, Germany, where they will undergo further analysis to determine the $\delta^{15}N$ values for these plant tissues.

1.6. Micro- and Macronutrient Content in Soil and Plants

Inductively Coupled Plasma-Optical Emission Spectrometry (ICP-OES) is a highly sensitive and precise analytical technique used to measure both micro- and macronutrients in soil and plant materials. Widely employed in soil and environmental analysis, ICP-OES is known for its ability

to detect a broad range of elements, providing valuable insights into the elemental composition of both soils and plants.

For successful analysis with ICP-OES, both soil and plant samples must first be dried and ground into a fine powder to ensure homogeneity (see **Photos 19 to 24**). This step is critical for minimizing any matrix interference and ensuring that the results are representative of the entire sample. Depending on the nature of the material and the elements of interest, a digestion step may be required to solubilize the nutrients.

Common digestion methods involve using strong acids such as nitric acid (HNO_3), perchloric acid ($HClO_4$), or hydrochloric acid (HCl). These acids help break down the sample matrix, releasing the elements into solution. For more complex samples, a combination of acids, such as HNO_3 and HCl may be used, which enhances the solubility of elements. Once digestion is complete, the solution is introduced to the ICP-OES for elemental detection and quantification.

NOTE: This activity involved the grinding and drying of soil and plant material, while the ICP-OES analysis of micro- and macronutrients was performed by the Institute of Natural Resources and Agrobiology of Seville (IRNAS) as a service.

1.7. Soluble Phosphorus in Soil

The determination of available phosphorus (P) in soil is an important aspect of soil fertility analysis, as it helps evaluate the P supply for plant growth. One commonly used method for assessing available P is the Olsen extraction method, which is particularly effective for soils with neutral to slightly alkaline pH.

This method involves extracting P from soil using a 0.5 M sodium bicarbonate ($NaHCO_3$) solution at a pH of ~8.5. The extracting solution helps dissolve a portion of the P bound to soil particles, making it available for quantification, typically carried out using spectrophotometry. The Olsen method is particularly useful for soils rich in calcium phosphate ($Ca_3(PO4)_2$), where phosphorus can be released into the solution under alkaline conditions.

Since P forms insoluble compounds with various cations, the concentration of P in the soil solution at any given time is usually quite low. Plants typically absorb P only from this soil solution, and the amount of soluble P must be continually replenished through processes like dissolution and diffusion. The factors involved in this renewal include the amount of P that can be solubilized, the degree of solubility, and the speed of diffusion from the solid surface to the plant root. An extraction of P can roughly measure the first two factors but not the third, making subsequent field

calibration necessary for the analysis to be truly useful. The types of P compounds present and other chemical properties of the soil determine the characteristics of the extractant used.

NOTE: This activity involved the grinding and drying of soil samples (see **Photos 19 to 21**), while the Olsen extraction and phosphorus quantification were performed by the Institute of Natural Resources and Agrobiology of Seville (IRNAS) as a service. The complete procedure is available in the mobility report of Dr. Tamara Apostolović.

1.8. Soil Micro-Respiration

Preparation of reagents, detection plates, and samples: Two separate solutions need to be prepared – **(a)** a stock solution of the indicator and **(b)** an agar solution. The final combination of these two solutions should yield a concentration of 1% purified agar, with a 1:2 ratio of agar to indicator solutions.

NOTE: Preparing 150 mL of the agar/indicator mixture will make 7 to 8 plates. It is advisable to prepare a few extra plates to account for any unforeseen needs.

a) Preparation method for indicator stock solution: Dissolve the ingredients listed in **Table 1** in 900 mL of milli-Q/elix water with stirring and heating (below 65ºC).

Table 1. Composition and final concentration of the indicator solution

	Amount dissolved in deionized water	Final detection plate concentration
Indicator solution	in 1000 mL:	
Cresol red	18.75 mg	12.5 µg mL^{-1}
Potassium chloride (KCl)	16.77 g	150 mM
Sodium bicarbonate ($NaHCO_3$)	0.315 g	2.5 mM

Once dissolved, transfer the solution to a 1000 mL volumetric flask and bring it to volume. After reaching the final volume, transfer the solution to a bottle and store it at 4ºC (for up to6 months).

NOTE: Cresol red is yellow in solution and turns pink when $NaHCO_3$ is added. Do not heat or autoclave the indicator solution above 65ºC.

b) Preparation methods for detection plates: Prepare a 3% purified agar solution in milli-Q/elix water (3 g per 100 mL) and dissolve by autoclaving at 121ºC for 20 minutes (microwaving is also an option). Ensure that the volume remains constant during heating. After autoclaving, allow the agar solution to rest in a water bath until it reaches 60ºC.

NOTE: Autoclaving ensures the agar is properly dissolved, but it is not for sterilization.

Next, calculate the amount of indicator solution required to achieve a 1:2 agar-to-indicator ratio. Add the calculated volume to the agar solution and carefully heat the mixture in a water bath to 60ºC.

Example:

50 mL milli-Q/elix water
1.5 g agarose
100 mL indicator solution
} *For 7-8 microplates (150 µL per well)*

Microwave 50 mL of water with 1.5 g of agarose, then add 100 mL of indicator solution (which should be pre-heated to 60ºC).

Once both solutions have reached the desired temperatures, mix them in a beaker and stir, maintaining a temperature close to 60ºC. Using a multichannel pipette, dispense 150 µL aliquots into each well, ensuring the solution does not cool to prevent the agar from solidifying. Discard the first two aliquots into the beaker to pre-warm the tips. It is important to avoid the formation of bubbles during pipetting.

NOTE: Warm the tips before use. When dispensing, keep the pipette upright (not tilted). Insert the tips into the wells so that when the agar mixture is dispensed, it rises up the end of the tips (immersing them in the agar mixture). This helps reduce bubbles and ensures the tip is “clean” when dispensing into the next well.

After completing the plates, store them in the dark at room temperature in a desiccator with soda lime (CO_2 absorbent) and a glass of water to prevent moisture loss. Leave the plates uncovered for 2-3 days to equilibrate. After this period, cover each plate with Parafilm if they are not going to be used within the next few hours (see **Photos 25 and 26**).

Photos 25 and 26. Plates stored for future application and regeneration after application

If sample loading is about to begin, first read the plate at 570 nm in the spectrophotometer. This will provide the absorbance results at T_0 (blank values).

Sample loading method for Microresp Kit: Before loading the samples, determine whether the material is fresh or lyophilized. If the material is fresh (recently sampled or frozen) and its moisture content is known, proceed directly with sample loading. If the samples are lyophilized, they must first be rehydrated to a known moisture content and left at 25ºC for 2-3 days with a CO_2 absorbent.

Considering that the experiments conducted as part of this training involved lyophilized soil samples, these were rehydrated following the procedure outlined above, which included measuring 2 g of the sample and adjusting the WHC of the soil to 60% (see **Photos 27 to 29**).

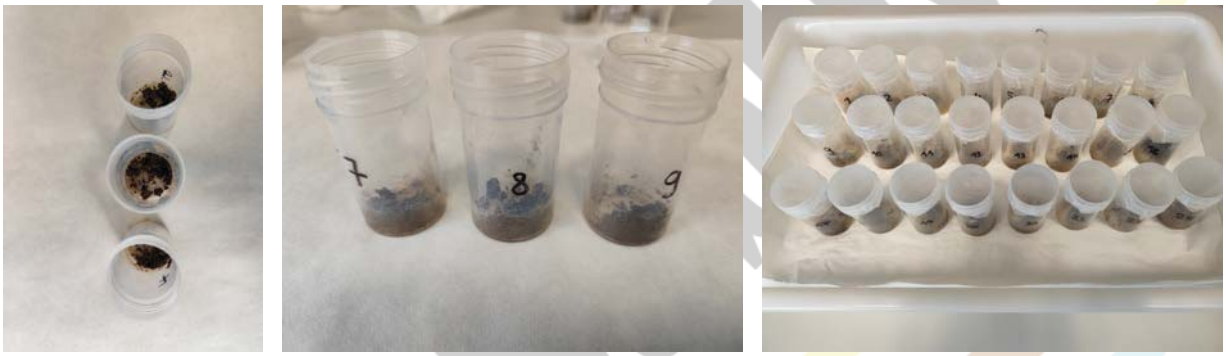

Photos 27 to 29. Rehydration and incubation of lyophilized soil samples

Insert the transparent plastic sheet into the device and place the filling piece on top of the plate. As you load the wells, slide the sheet to prevent spillage into other wells. The alternative method involves sealing the filled wells or those not currently being filled with adhesive tape. Load by columns, and do not overfill (see **Photos 30 and 31**). To determine the amount of soil added, follow these steps:

1. Weigh the empty plate;
2. Fill the column (or well) with soil;
3. Weigh the filled plate (column or well);
4. Calculate the grams of soil per well.

It is essential to know the moisture values of the various soil samples beforehand to determine the exact amount of soil added to each well.

NOTE: Do not force or press the soil into the filling device. Do not use the first or last columns of the plate; instead, tape them during loading. After each load, cover the wells with tape.

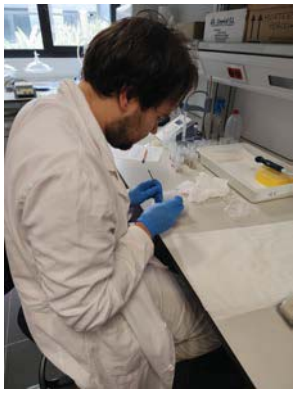
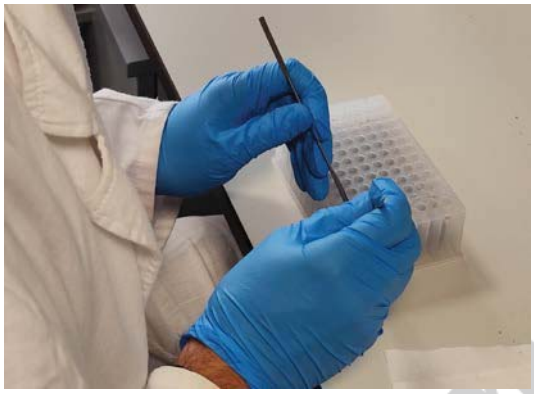

Photos 30 and 31. Loading the Microresp plate with soil samples

Once these steps are completed, place the blue silicone sheet over the wells, fit the detection plate, and seal the system with the aluminum device to create a vacuum (see **Photos 32 to 34**). Incubate in the dark at 25ºC for 24 hours. Read the plate at 570 nm in the spectrophotometer after 6 hours and again after 24 hours of incubation.

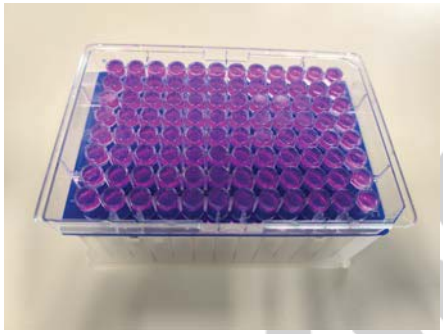


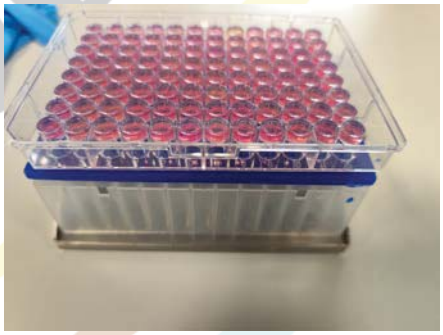

Photos 32 to 34. Setup of the detection plate and vacuum sealing for incubation, and opening after 6 hours for spectrophotometric reading

NOTE: As previously noted, before fitting the detection plate, it is essential to read it in the spectrophotometer at 570 nm to obtain the T_0 value for each well. Additionally, ensure that the variation between wells does not exceed 5% to maintain uniform initial conditions.

Normalization of absorbance data: To normalize the absorbance data at T_{xh} (6 or 24 hours), each reading should be divided by the T_0 reading and multiplied by the average of the T_0 readings:

$$A_{T_{xh}} = \frac{Abs_{T_{xh}}}{Abs_{T_0}} \times \overline{Abs_{T_0}}$$

This ensures that the absorbance values are normalized relative to the initial T_0 readings.

CO_2 percentage calculation: The following formula converts the normalized T_{xh} data into $\%CO_2$:

$$\%CO_2 = \frac{A + B}{1 + D \times A_{T_{xh}}}$$

Where: A = -0.2265, B = -1.606, and D = -6.771. This formula fits a rectangular hyperbolic curve.

CO_2 production ratio: The CO_2 production ratio is calculated by converting the CO_2 percentage value at T_{xh} into µg/g/h CO_2-C using gas constants, incubation temperature (T in ºC), headspace volume (Vol in µL) in the well (usually 945 µL), fresh weight (fwt) of soil per well (g), incubation time (hours), and dry weight percentage (dwt) of the soil. The CO_2 ratio (µg CO_2-C/g/h) is calculated using the following formula:

$$CO_2\ ratio = \frac{\left(\frac{(\%CO_2/100) \times vol \times (44/22.4) \times (12/44) \times (273/(273+T))}{soil\ fwt \times (soil\ \%\ dwt/100)}\right)}{T_{xh}}$$

NOTE: The headspace volume is typically 945 µL for the standard setup. Adjust according to the manufacturer specifications for the microplate and deep-well plate.

Substrate preparation for incubation: Substrates should be prepared at a rate of 30 mg per gram of water in the soil/sample. To load each well, add 25 µL of the prepared substrate solution. Follow these steps to determine the concentration of the carbon source to add:

1. Determine the weight of soil per well: Weigh all the soil added (biological replicates or treatments) and divide by the number of loaded wells to get the average weight of soil per well;
2. Determine the moisture content: The moisture content of the loaded soil must be known. For example, if the soil moisture is 25%, it contains 0.25 g of H_2O per gram of soil/sample;
3. Calculate the substrate requirement: Using an example of soil with 0.30 g per well:
   - Moisture content: 0.30g x 0.25 = 0.075 g of H_2O per well;
   - Substrate requirement: 0.075 g x 30 mg = 2.25 mg of substrate per well;
   - To prepare a 25 mL stock solution, dissolve 2.25 g of substrate in 25 mL of water.

Commonly used substrates: L-alanine, D-(+)-galactose, N-acetylglucosamine, L-(+)-arabinose, D-(+)-glucose, oxalic acid, L-arginine, γ-aminobutyric acid, protocatechuic acid, citric acid, α-ketoglutaric acid, D-(+)-trehalose, L-cysteine HCl, L-lysine HCl, D-(-)-fructose, L-malic acid.

For the purposes of the experiments conducted as part of this training, D-(+)-glucose and N-acetylglucosamine were used as substrates.

NOTE: Depending on soil pH (e.g., less acidic), the amount of L-Arginine may need to be adjusted to 7.5 mg per g of soil water. Substrates can be stored at 4ºC for up to 2 weeks.

Example of substrate calculation for incubation: If the soil has been watered to 60% of its original WHC, where the original WHC is 33.80%, follow these steps:

1. Calculate water retention capacity: The soil will have a water retention capacity of 0.338 x 0.60 = 0.203 g of H_2O per gram of soil;
2. Determine total or fresh weight of soil: 1 g of soil at this WHC will have a total fresh weight of 1.203 g (0.203 g of H_2O + 1 g of soil), which corresponds to a soil moisture of 16.9% (0.203 / 1.203 = 0.169);
3. Calculate the amount of water in the soil per well: If the fresh weight per well is 0.5 g, then each well contains 0.5 g x 0.169 = 0.085 g of H_2O;
4. Determine substrate requirement: If the substrate requirement is 30 mg per g of H_2O, the substrate required for a 25 µL aliquot is: 0.085 g x 30mg = 2.55 mg;
5. Prepare substrate solution: Therefore, to prepare a 25 mL stock solution, dissolve 2.55 g of substrate in 25 mL of H_2O.

1.9. Solid State Nuclear Magnetic Resonance (NMR)

Preparation of soil samples for NMR analysis: To analyze the soil samples using NMR, they were subjected to demineralization with hydrofluoric acid (HF).

a) Objectives:

1. Eliminate the mineral fraction and paramagnetic elements (Fe, Al) to minimize interferences in the NMR analysis;
2. Concentrate the organic matter.

b) Reagents:

1. Hydrochloric acid 1M (HCl):
   – To prepare 1 L of HCl solution: measure 84 mL of HCl (37% purity) and dilute to 1 L with water.
2. Hydrofluoric acid 10% (HF): To prepare 1 L of HF solution:
   – If using 48% purity HF, measure 208 mL and dilute to 1 L with distilled water;
   – If using 40% purity HF, measure 250 mL and dilute to 1 L with distilled water.

c) Procedure:

1. Removal of particulate organic matter (POM) in cases of high content:
   – Weigh:

- Record the weight of the centrifuge tube with the lid (the sample may remain on the lid);
- Tare and record the weight of the sample (in g): 10-20 g (or less, depending on C content; e.g., 5 g).

– Add 40 mL (or 20 mL) of distilled water and shake the tube;
– Centrifuge the tube (previously tared) at 3000 rpm for 10 minutes;
– Collect the organic matter in suspension into a previously tared beaker by filtration (ensure not to drag the sample from the bottom of the beaker).

2. Treatment with HCl (1 M) in cases where the sample contains carbonates ($CaCO_3$) to prevent the precipitation of calcium fluoride (CaF_2) from HF, which may increase the weight of the sample:
   – Add 40 mL (or 20 mL) of 1 M HCl (do not cover the tube completely, since gases are generated);
   – Shake slightly and leave the solution to react/settle;
   – Centrifuge the tube at 3000 rpm for 10 minutes;
   – Remove the supernatant (re-add HCl as necessary);
   – Wash with distilled water several times to remove excess HCl (until the pH is approximately neutral).
3. Treatment with 10% HF in cases requiring demineralization (use appropriate protective equipment and proceed with extreme caution; see **Photos 35 to 37**):
   – Add 40 mL (or 20 mL) of 10% HF to the sample remaining in the tube;
   – Shake the sample for 2 hours at 250 rpm;
   – Centrifuge the tube at 3000 rpm for 10 minutes;
   – Carefully remove the supernatant from the tube. Repeat the previous steps, including this one, for a total of four cycles;
   – Add 50 mL (or 20 mL) of distilled water, shake, centrifuge, and carefully remove the supernatant (repeat washing until the pH reaches 5–6);
   – Freeze the sample and lyophilize;
   – After lyophilization, weigh the tube with the sample (including the lid and any remaining sample) to determine the organic matter content resistant to acid treatment.



Photos 35 to 37. Treatment of soil samples with hydrofluoric acid and subsequent separation of organic matter

NOTES:

- Before starting work, place the no-entry sign on the laboratory door. Retrieve the gluconate ointment (stored in the fridge) and the emergency kit materials (HF safety sheet, emergency sheet, powders, red gloves, spare face shield), and place them on the entrance table. Notify the rest of the group before beginning work with HF;
- Always wear a lab coat, HF-specific gloves over standard laboratory gloves (never latex), and a face protection mask;
- Avoid touching anything outside the designated work area while wearing gloves, as they may be contaminated with HF;
- Do not use glass containers, as HF attacks silica;
- The values in parentheses correspond to a sample size of 5 g;
- Consider reagent purity when calculating the required amount of reagent;
- Ensure all equipment is in proper working condition before use;
- After finishing work, clean all used materials (including gloves and the inside of the centrifuge) and disinfect surfaces (such as the table, scale, and cabinet covers). Finally, return the emergency kit materials to their designated storage.

Lyophilization operating instructions:

NOTES:

- Always wear a face shield while operating the machine;
- Ensure the air-conditioning is ON when the machine is in operation (set to 22ºC);
- If preparation takes too long, return the samples to the freezer to prevent thawing.

Procedure:

1. Switching on the machine:
   - Check the oil level in the vacuum pump;
   - Insert the plug into the drain valve;
   - Turn on the machine by switching the main power to “ON”;
   - The refrigeration system will start, cooling down the condenser;
   - Place the frozen samples onto the holder;
   - Position the cylinder and secure the top with the valves in place;
   - After startup, the controller display will appear as follows:

2. Starting a program (see **Photos 38 and 39**):
   - Select the program button for the appropriate program (P1);

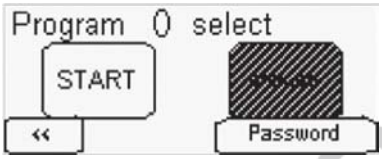

   - Press the START button;

   NOTE: Before starting the program, ensure the following:
   - The cleanliness and correct fitting of all gaskets;
   - The drain valve on the right closure;
   - The position of the rubber valves and the oil level in the vacuum pump.
   - Once all hand valves are closed, press the START button. The following screen will appear:

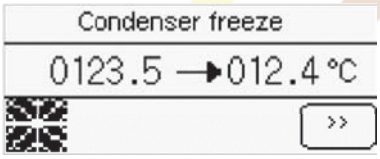

   NOTE: It might be necessary to apply light pressure to the cylinder or between the cylinder and the top for the pressure to start dropping.

- When the pressure reaches between 0.5 and 5 mbar, turn the switch on the vacuum pump from position II to position 0;
- Once the condenser reaches the set value, the first drying stage will begin. The device will then cool further down to the lowest possible temperature;

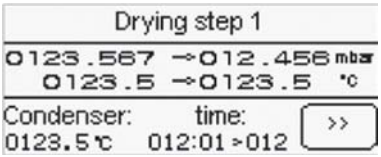

- During the drying process, the pressure and temperature will reach the set points;
- When the set time for the first drying stage is reached, proceed to the second drying stage;

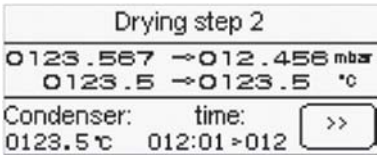

- Once the set time for the second drying stage is reached, proceed to the third drying stage;

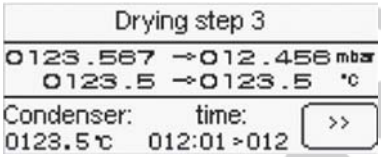

- After the third drying stage, the following screen will appear:

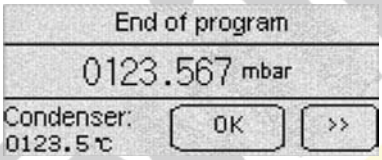

Photos 38 and 39. Initiating the lyophilization process for soil samples

3. Switching off the machine:
   - The chamber pressure and temperature will continue to be regulated to the last set values;
   - Press the “OK” button to finish the program and turn off the vacuum pump;
   - Turn off the machine by pressing the OFF button;
   - Ventilate the chamber by partially opening one of the valves (preferably one facing away from you);
   - Once the pressure is equalized, remove the top and the cylinder;
   - Retrieve your samples;
   - Clean any excess water from the top and replace the cylinder and valve top on the machine;
   - Remove the plug from the drain valve;
   - Turn the switch on the vacuum pump back to position II;
   - If the program needs to be stopped before completion, press the right arrow key, then press the “STOP” button.

Sample analysis:

- The rotor is filled with the ground sample using the support and stick to push it in. Only the hole for the plug should remain free. A black half-stripe is drawn below with a permanent marker;
- When removing the previous sample, the speed must be gradually decreased;
- The sample should always be inserted with the stopper facing up;
- For a new sample, adjusting all parameters is not necessary. Instead, a previous sample can be opened, and the spectrum can be dragged;
- “ased” → To control the parameters (this is done only for the first sample);
- “edc” → To create a new one. Change the name and title. SR: The last revision or change of probe;
- “wobb” → Tuning;
- Insert the sample;

- Go → C: 0 to 4000 Hz → 8000 Hz → 12000 Hz → 14000 Hz. N: 0 to 2000 Hz → 4000 Hz → 6000 Hz;
- Adjust tuning and matching: first, adjust the blue screw, then the yellow one (pressing NEXT on the screen on the left side of the ground may assist in the process);
- "zg" → Start measurement. Sometimes extra signals may appear (especially at 14000 Hz). Occasionally, there are echoes at the same frequency as the speed of rotation (spinning size bands). "ro" → It has to match the current operating speed;
- "ft" → Fourier transformation (converts time to frequency). For this type of experiment, there should be no negative signals → adjust to 0;
- "lb" → Line broadening. This reduces noise/background but also widens the bands;
- "efp" → To transform Acqu to Spectrum;
- "tr" → Save provisionally (to verify if the measurement is okay) → "efp";
- To end: Halt (no acquisition running) → drop to 4000 Hz → Halt (in action) → Eject.

NOTE: The analysis of the samples up to this point has not been conducted due to an instrument malfunction.

1.10. Biomass Parameters

The SPAD index, which stands for Soil-Plant Analysis Development index, is a fast and non-destructive method used to estimate the chlorophyll content in plant leaves. This index is widely utilized to evaluate the nutritional and health status of plants. Chlorophyll content is a key indicator of a plant's ability to carry out photosynthesis, and thus, its overall vitality.

In addition to measuring chlorophyll content, assessing the quantum yield of photosystem II (PSII) is essential for understanding photosynthetic efficiency and plant health (see **Photos 40 and 41**). The quantum yield of PSII represents the fraction of absorbed light energy that is used in the process of photosynthesis, specifically in the light-dependent reactions. A higher quantum yield indicates more efficient energy conversion, which is vital for plant growth and development. The most common and reliable technique for measuring PSII quantum yield is pulse amplitude modulation (PAM) fluorometry, which provides real-time data on the efficiency of photosystem II under different light conditions.

Further, plant growth and development were assessed by measuring both the fresh and dry weight of the shoots and roots (see **Photos 42 and 43**). The root/shoot ratio was calculated to

determine the allocation of resources between these two plant parts. Additionally, the leaf area of the plants was quantified using Fiji, an open-source image processing software, which allowed for accurate measurement and analysis of leaf surface area.

Photos 40 to 43. Measurement of SPAD index and quantum yield, and harvested plant material for the determination of other biomass-related parameters

2. Results

2.1. Soil Characterization

NOTES:

- Except for WHC, pH, and EC, all soil characterization experiments for the tested variants were conducted immediately after plant harvest, i.e., 60 days after sowing;
- In all treatments, except for aged BC + NPK and co-composted BC + NPK, plants had to be reseeded two weeks after the initial sowing attempt due to the absence of germination. Consequently, these plants were exposed to high temperatures for two weeks longer, starting in early July, which the available greenhouse infrastructure could not maintain at a constant set value. This significantly impacted their growth and development, causing partial wilting due to heat stress and fluctuations in soil water content (as particularly evidenced by the drop in % of WHC measured on Mondays, reflecting water loss during the weekends, shown in **Figure 1**; see also **Photos 44 to 47**). As a result, soil parameters related to plant growth, such as nutrient availability and uptake, may have been affected;
- Statistical analysis of all results was performed using two-way ANOVA (except for WHC, where one-way ANOVA was used), followed by a post-hoc Tukey test. A difference was considered statistically significant when $p < 0.05$. Different letters on the figures indicate statistically significant differences.

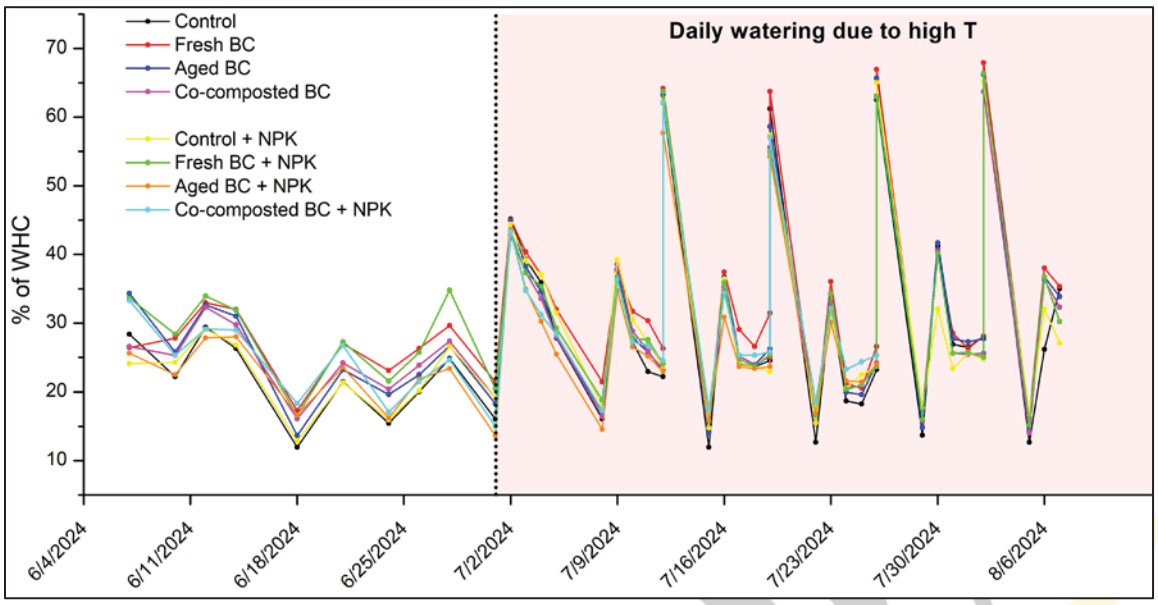

Figure 1. Periodic fluctuations in soil water content as % of WHC, targeted at 60% (up to 80% in extreme cases)

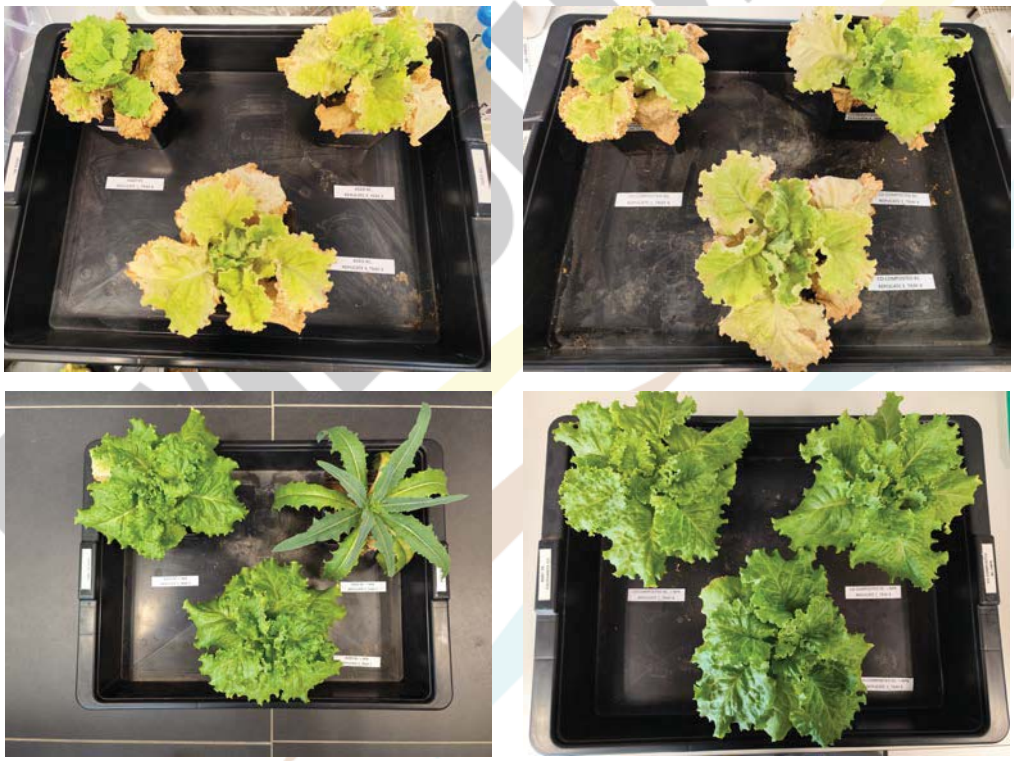

Photos 44 to 47. Condition of green lettuce plants in aged and co-composted BC treatments (first row), harvested two weeks after the corresponding NPK treatments (second row)

2.1.1. Water Holding Capacity (WHC)

The WHC of the control and three treated soils was analyzed in 6 replicates, and the results obtained are shown in **Figure 2**.

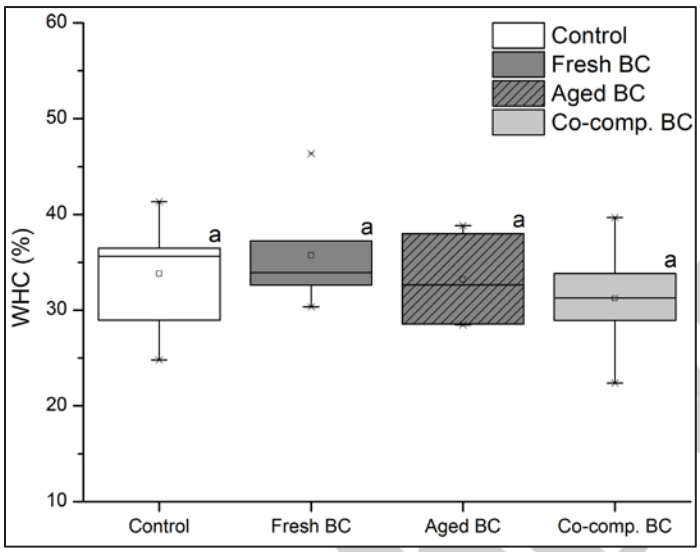

Figure 2. Water holding capacity of the four tested variants

As can be seen, the obtained results show some differences in the average WHC of the four tested variants. However, statistical analysis revealed no significant difference between the treatments.

The fresh BC treatment showed the highest average WHC value, increasing from the control soil's 33.80% to 35.74%. This suggests a potential improvement in water retention, likely due to the physical and chemical properties of fresh BC, including its highly porous structure and large surface area. These features could enhance the soil's ability to retain water by trapping it in the biochar's pores. Additionally, surface functional groups like hydroxyl (-OH) and carboxyl (-COOH) may help bind water molecules through hydrogen bonding. However, the relatively high variability (± 5.67%) observed for fresh BC indicates that the effect on WHC might be influenced by factors such as biochar particle size or uneven distribution within the soil. The lack of statistical significance suggests that these trends are not definitively supported by the data.

Aged BC showed a slight reduction in WHC (33.19 ± 4.53%), but, like fresh BC, this difference was not statistically significant. This trend could reflect expected changes due to aging, such as a reduction in surface area or the loss of certain reactive surface functional groups, making the biochar more hydrophobic and potentially less effective at retaining water.

Co-composted BC exhibited the lowest WHC value (31.23 ± 5.82%), which was lower than both the control and other biochar types. However, as with the other treatments, the difference was

not statistically significant. The reduced water retention in co-composted BC-amended soil may result from interactions during the co-composting process, which could alter the biochar's structure, reducing its porosity and water-holding capacity. Additionally, the presence of composted material could make the biochar more hydrophobic, further diminishing its ability to retain water.

2.1.2. pH and Electrical Conductivity (EC)

The pH value and EC of the soil were analyzed in each replicate of the tested variants, with each sample measured three times. The obtained results are presented in **Figures 3 and 4**.

pH: The results show noticeable differences in the average pH values across the four variants tested. Statistical analysis revealed significant differences within each treatment series (with and without NPK), except for the aged BC and co-composted BC treatments, where no significant difference was found. When comparing the corresponding treatments between the NPK and non-NPK series, a significant difference was only observed for the aged and co-composted BC variants.

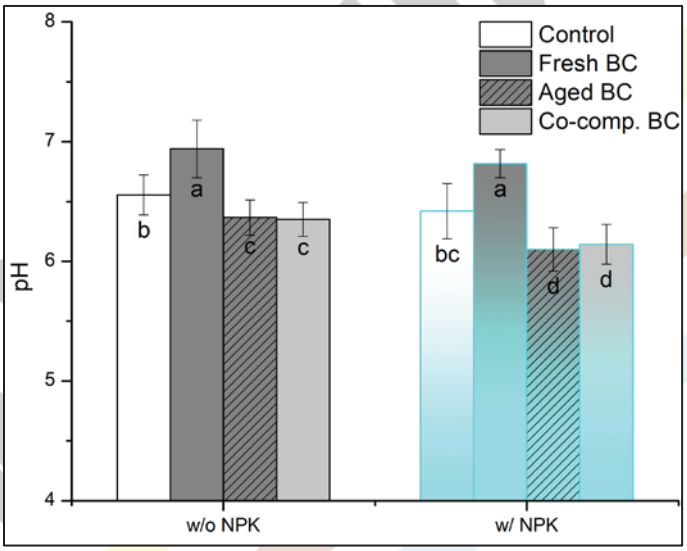

Figure 3. Soil pH values for the tested variants

The fresh BC treatment exhibited the highest pH value (6.94 ± 0.24), showing an increase compared to the control soil's pH of 6.55 ± 0.17. This suggests a liming effect, likely due to the alkaline nature of fresh BC, which may contain ash residues and basic functional groups. The porous structure of biochar, along with surface hydroxyl (-OH) and carbonate ($-CO_3^{2-}$) groups, could contribute to the pH increase by releasing alkaline substances (such as Ca cations) into the soil.

In contrast, the soil amended with aged BC showed a slightly lower pH (6.37 ± 0.15), which was comparable to the soil amended with co-composted BC (6.35 ± 0.14). The lack of a significant difference between these two treatments suggests that both aging and co-composting may lead to similar chemical changes. Over time, oxidation and microbial activity can introduce acidic functional groups like carboxyl (-COOH) and phenolic (-OH), neutralizing some of the biochar's initial alkalinity and reducing its liming effect. Moreover, environmental factors during aging or composting might lead to the leaching of soluble alkaline compounds, further lowering the pH.

The addition of NPK did not significantly affect pH values in the control and fresh BC treatments, suggesting that the buffering capacity of the control soil and the alkaline properties of fresh BC were not significantly altered by fertilization. However, a significant difference was observed in pH between the NPK and non-NPK treatments for aged and co-composted BC. This could be due to increased microbial activity stimulated by NPK, potentially accelerating processes like nitrification, which produces acidic byproducts that could lower soil pH. Additionally, interactions between biochar and NPK components might influence cation exchange dynamics, leading to slight pH modifications in the biochar-amended soils.

EC: The EC values across the tested variants show distinct trends, with significant differences observed between treatments both within each series (with and without NPK) and when comparing the corresponding treatments between the two series.

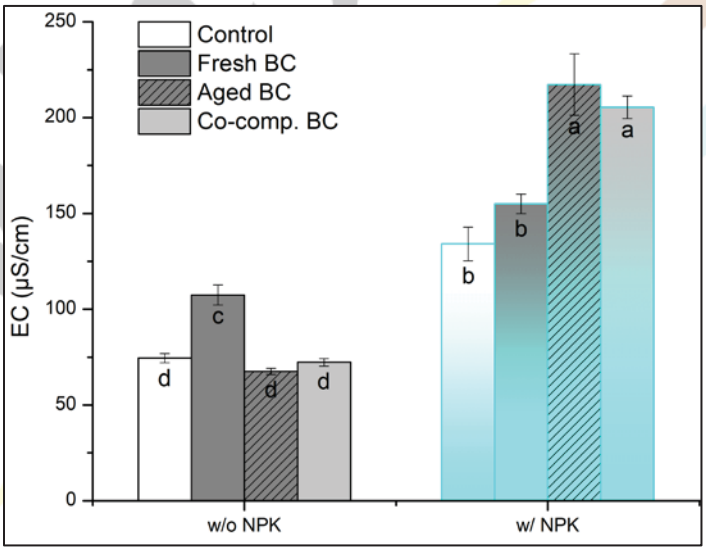

Figure 4. Soil electrical conductivity values for the tested variants

The fresh BC treatment demonstrated the highest EC value observed in the non-NPK series, with a measured value of 107.43 ± 5.17 µS/cm, significantly surpassing all other treatments in this

group. This suggests that fresh BC increases the ionic strength of the soil, likely due to the presence of soluble salts and alkaline substances (such as Ca^{2+}, Na^{+}, and K^{+}), which can leach into the soil, thereby raising its EC. The porous structure of fresh biochar could further facilitate the release of these ions into the soil solution, contributing to the increased EC.

In contrast, the aged BC and co-composted BC treatments showed lower, similar EC values (67.57 ± 1.63 µS/cm and 72.31 ± 1.94 µS/cm, respectively), with no significant difference between them. This indicates that biochar's ion-releasing capacity decreases over time due to aging or composting. These processes likely lead to a reduction in biochar's alkalinity and the solubility of salts. During aging, oxidation and microbial activity can neutralize some of the biochar's initial alkalinity, which contributes to the lower EC values observed in these treatments.

When NPK fertilizer was added, a substantial increase in EC was observed across all treatments, reflecting the contribution of the added ions from the fertilizer. Aged BC + NPK and co-composted BC + NPK showed the highest EC values (217.28 ± 16.04 µS/cm and 205.44 ± 5.92 µS/cm, respectively). These results suggest that both aged and co-composted BC facilitate the retention and release of fertilizer ions in the soil, leading to elevated ionic strength. The higher cation exchange capacity (CEC) of these biochars may enhance their ability to retain and exchange ions, increasing the EC when combined with NPK fertilizer. On the other hand, the EC of fresh BC + NPK (154.98 ± 5.09 µS/cm) was lower than that of the aged and co-composted treatments, indicating that while fresh BC increases EC due to its soluble salts, it does not interact as effectively with NPK ions. This may be attributed to the lower CEC and stability of fresh BC, which could limit its capacity to retain and release NPK ions in the soil.

Significant differences in EC were observed when comparing treatments between the two series, as expected. The addition of NPK resulted in consistently higher EC values across all treatments, reflecting the contribution of soluble salts from the fertilizer. Notably, the magnitude of increase in EC was greater in biochar-amended soils compared to control soil, indicating that biochar plays a key role in modifying soil ionic composition.

2.1.3. Soil Organic Matter (SOM), Total Organic Carbon (TOC) and Total Nitrogen (TN)

The SOM content, TOC, and TN of the soil were analyzed in each replicate of the tested variants, and the obtained results are presented in **Figures 5 and 6**.

SOM and TOC: The results demonstrate clear differences in SOM and TOC values across the four tested variants, with statistical analysis revealing significant differences within each series

(with and without NPK). Specifically, in both series, fresh BC treatment exhibited a statistically significant increase in SOM and TOC compared to the other variants, while no significant differences were observed among aged BC, co-composted BC, and control soil. When comparing corresponding variants between the NPK and non-NPK series, no statistically significant differences were found in any case.

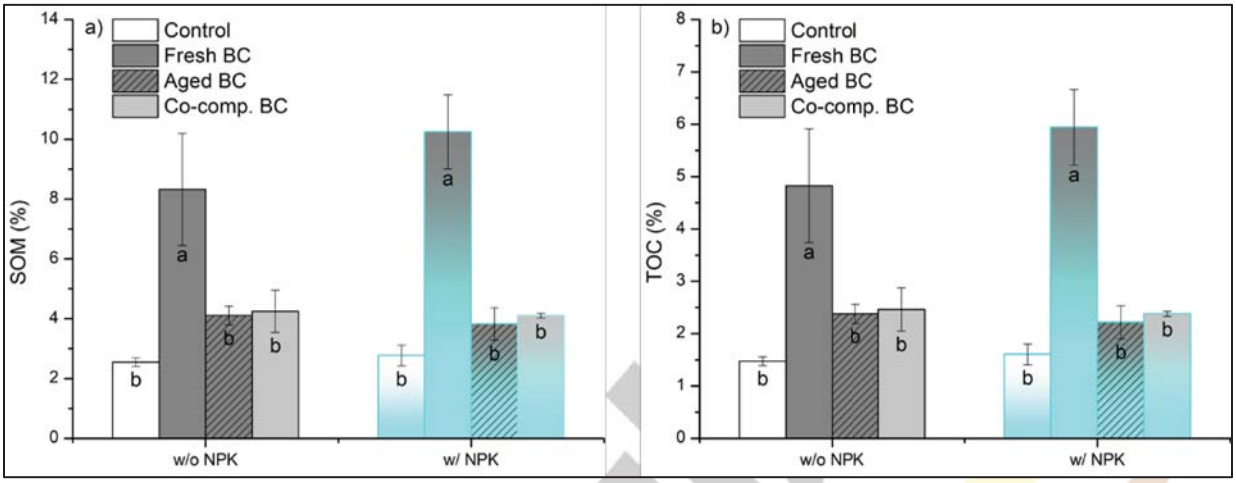

Figure 5. Soil organic matter (a) and total organic carbon (b) values for the tested variants

The fresh BC treatment recorded the highest SOM (8.32 ± 1.87%) and TOC values (4.83 ± 1.09%) in the non-NPK series, showing a substantial increase compared to the control soil (2.55 ± 0.15% SOM and 1.48 ± 0.08% TOC). This pronounced effect can be attributed to the high carbon content of fresh BC, which contains a large proportion of recalcitrant organic carbon. Fresh BC retains a high fraction of aromatic carbon structures, which are resistant to microbial decomposition and persist in the soil for extended periods.

In contrast, aged BC and co-composted BC resulted in significantly lower SOM and TOC values than fresh BC, with no significant differences between the two. The SOM values for aged BC and co-composted BC were 4.10 ± 0.31% and 4.25 ± 0.71%, respectively, while their corresponding TOC values were 2.38 ± 0.18% and 2.46 ± 0.41%. These findings suggest that the aging and composting processes lead to partial oxidation and microbial decomposition of biochar, reducing its contribution to SOM. Additionally, microbial processing during composting may result in the loss of labile carbon fractions, further explaining the reduced SOM and TOC values compared to fresh BC.

The lower SOM and TOC values in aged and co-composted BC treatments could also be partly due to the physical loss of biochar particles over time (as aged and co-composted BC were under experimental field conditions for 13 years, until sampling in 2023), with biochar particles potentially moving from the topsoil to subsoil, contributing to the declining carbon content in the topsoil.

When NPK was applied, a similar pattern was observed. Fresh BC + NPK exhibited the highest SOM (10.25 ± 1.24%) and TOC (5.94 ± 0.72%) values, significantly exceeding those of the other variants. The aged BC + NPK (3.82 ± 0.54% SOM, 2.22 ± 0.32% TOC) and co-composted BC + NPK (4.10 ± 0.08% SOM, 2.38 ± 0.05% TOC) treatments did not differ significantly from one another, nor did they significantly differ from their non-NPK counterparts. The control + NPK treatment also exhibited only a slight increase in SOM and TOC values compared to the control soil without NPK.

The absence of significant differences between the corresponding treatments in the NPK and non-NPK series suggests that inorganic fertilization does not directly influence SOM or TOC accumulation. This is consistent with the understanding that SOM dynamics are primarily driven by organic inputs rather than mineral fertilizers. While NPK enhances microbial activity and nutrient cycling, its influence on SOM and TOC appears to be negligible within the studied timeframe.

These results emphasize that biochar type is the dominant factor affecting soil organic carbon levels, with fresh BC providing the greatest increase due to its high initial carbon content. The lower values observed in aged and co-composted BC treatments suggest that chemical and microbial transformations reduce the carbon retention potential of biochar over time.

TN: The TN values exhibited minimal variation across the tested variants. In the non-NPK series, TN levels ranged from 0.14% to 0.16%, with the co-composted BC treatment yielding the highest value. A similar trend was observed in the NPK-treated series, where TN levels ranged from 0.13% to 0.17%, again with the co-composted BC + NPK treatment displaying the highest TN content. However, statistical significance was observed only between the control + NPK and co-composted BC + NPK variants. No significant differences were detected among the other variants within each series or between corresponding variants across the NPK and non-NPK series.

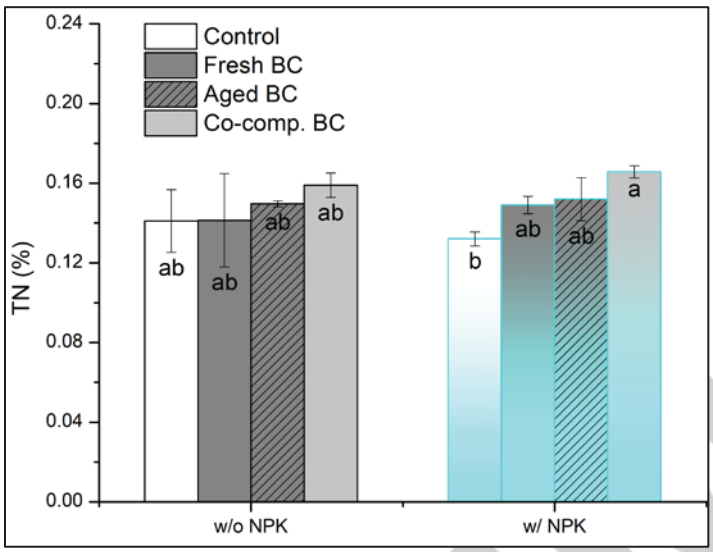

Figure 6. Soil total nitrogen values for the tested variants

The statistically significant increase in TN content in the co-composted BC + NPK treatment suggests that co-composted BC, when combined with NPK, may enhance nitrogen retention or stabilization in soil. This effect could be attributed to the composting process, which may integrate nitrogen into more stable organic fractions, reducing its susceptibility to leaching or volatilization. Additionally, co-composted BC could influence microbial activity, potentially enhancing nitrogen retention by stabilizing organic nitrogen and reducing losses, or modifying nitrogen mineralization dynamics in a way that balances inorganic nitrogen availability without depleting TN. The absence of this effect in the non-NPK series suggests that the interaction between co-composted BC and inorganic nitrogen from NPK fertilizer plays a role in the observed increase in TN.

The lack of significant differences among the remaining variants indicates that neither fresh nor aged BC substantially influenced TN content under the tested conditions. Moreover, the addition of NPK fertilizer did not significantly alter TN levels across treatments. While microbial assimilation of inorganic nitrogen from NPK could contribute to TN, the absence of a measurable increase suggests that nitrogen was either rapidly cycled, lost through leaching or volatilization, or that the experimental duration was insufficient to detect significant TN accumulation.

Overall, these findings indicate that biochar had a limited effect on TN dynamics, except for co-composted BC in the NPK-treated series, where a significant increase was observed. However, the lack of significant differences in other treatments implies that biochar's impact on TN may depend on longer experimental durations or specific soil conditions.

2.1.4. Micro- and Macronutrient Content

The amounts of micro- and macronutrients in the soil of the tested variants, each analyzed in composite samples made from three replicates, are presented in **Table 2**. The key trends identified are outlined and discussed in the following text.

Table 2. Amount of micro- and macronutrients in the tested variants

Variant [(1)]	Al	As	B	Ba	Ca	Cd	Co	Cr	Cu	Fe	K
	mg/kg										
V_1	12592	15.0	9.55	51.2	**1634**	0.27	4.47	86.4	9.00	11036	**2388**
V_2	14059	18.7	9.83	67.5	**2530**	0.25	4.69	85.4	9.16	11007	**2935**
V_3	13385	12.9	8.28	57.2	**2023**	0.17	5.02	78.5	9.22	10590	**2479**
V_4	13127	13.6	7.73	53.7	**2102**	0.18	4.69	79.7	9.14	10836	**2560**
V_1 + NPK	12466	13.3	6.74	50.5	**1557**	< 0.10	4.61	87.0	8.76	10226	**2585**
V_2 + NPK	13578	14.5	8.46	65.1	**2562**	0.39	4.60	84.3	9.04	10906	**2695**
V_3 + NPK	13431	12.8	8.51	56.2	**2103**	0.28	4.50	75.7	9.05	10538	**3320**
V_4 + NPK	14078	13.2	8.16	58.4	**2165**	0.36	4.80	78.9	9.51	13329	**3405**
Variant [(1)]	**Li**	**Mg**	**Mn**	**Na**	**Ni**	**P**	**Pb**	**S**	**Sr**	**Zn**	**/**
	mg/kg										
V_1	10.7	**1015**	436	53.2	8.13	**682**	20.4	**221**	16.3	29.0	/
V_2	11.2	**1098**	500	68.1	7.88	**721**	21.8	**243**	19.2	32.3	/
V_3	11.5	**1081**	486	51.8	7.40	**732**	21.2	**261**	18.0	32.3	/
V_4	10.9	**1070**	433	59.3	7.85	**756**	20.1	**283**	17.4	32.5	/
V_1 + NPK	10.6	**971**	424	63.7	7.16	**709**	20.8	**248**	15.9	28.2	/
V_2 + NPK	10.8	**1041**	494	64.7	7.72	**746**	24.8	**271**	18.9	30.9	/
V_3 + NPK	11.3	**1079**	476	92.5	7.32	**806**	20.5	**315**	18.2	33.0	/
V_4 + NPK	11.1	**1119**	488	95.5	8.96	**883**	23.0	**321**	18.7	36.8	/

[(1)] V_1 - Control; V_2 - Fresh BC; V_3 - Aged BC; V_4 - Co-composted BC

As can be seen, biochar amendments enhance the Ca content in soils, with soils treated with biochar consistently showing higher Ca levels compared to the control soil. This increase is particularly noticeable in the fresh BC variant, suggesting that fresh biochar helps improve the availability of Ca in the soil, likely due to its higher surface reactivity and higher initial Ca content compared to aged or co-composted biochar. Soils treated with NPK fertilizer, as expected, show higher P and K content than those amended with biochar alone, indicating that NPK enhances their availability. However, biochar amendments also increase both P and K levels compared to the control soil, and when combined with NPK fertilizer, these nutrients are further enhanced in

an additive effect. The content of Mg is lowest in the control soil, suggesting that biochar amendments help increase Mg levels. Similarly, S content appears to rise in biochar-amended soils, particularly when combined with NPK fertilizer.

Overall, biochar amendments, especially when paired with NPK fertilizer, appear to improve soil nutrient content not only by increasing nutrient levels but also by helping retain nutrients in the soil, reducing nutrient leaching while still making them available for plant uptake. The most notable increases are observed in Ca, P, K, Mg, and S, reinforcing biochar's potential role in improving soil fertility and sustainability when combined with fertilizers.

2.1.5. Soluble Phosphorus

The soluble phosphorus (P-Olsen) in the soil was analyzed in each replicate of the tested variants, and the results are presented in **Figure 7**.

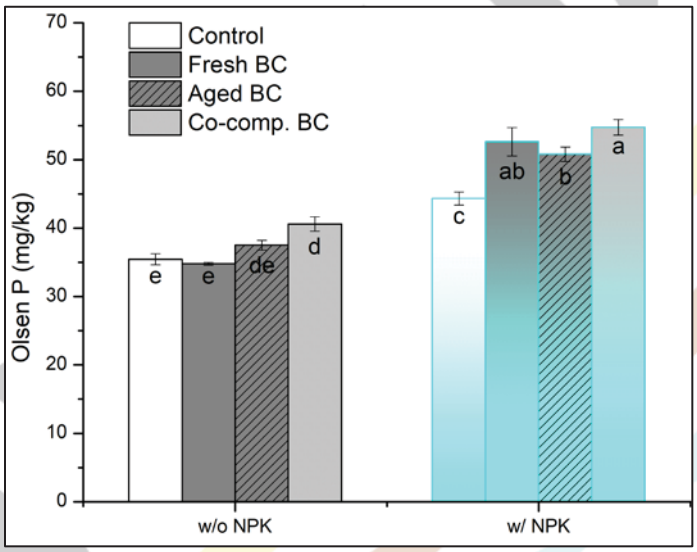

Figure 7. Soil soluble phosphorus values for the tested variants

The results demonstrate significant differences in P-Olsen values across the four tested variants, with statistical analysis revealing distinct trends within each series (with and without NPK). More specifically, in both series, the co-composted BC treatment exhibited the highest P-Olsen values, outperforming the other three variants in absolute terms. However, statistically, it outperformed the control and fresh BC in the non-NPK series but not aged BC, while in the NPK-treated series, it exceeded the control and aged BC but not fresh BC. When comparing corresponding variants between the NPK and non-NPK series, significantly higher P-Olsen concentrations were observed in the NPK-treated series than in the non-NPK series for all cases. This trend underscores the

role of NPK fertilization in enhancing phosphorus availability, likely through its impact on phosphorus cycling and interaction with biochar treatments.

In the non-NPK series, fresh BC (34.80 ± 0.20 mg/kg) recorded the lowest P-Olsen concentration, while co-composted BC (40.60 ± 1.06 mg/kg) exhibited the highest phosphorus availability. A significant difference was observed between the control and co-composted BC treatments, as well as between fresh and co-composted BC, suggesting that co-composted BC enhances phosphorus availability more effectively under non-fertilized conditions. However, no significant difference was found between co-composted BC and aged BC, indicating similar phosphorus release under non-NPK conditions. The higher availability in co-composted BC could be attributed to the organic matter incorporated during co-composting, which may improve nutrient release and retention. The microbial communities in co-composted BC may facilitate the mineralization of organic phosphorus, increasing its solubility and bioavailability. The difference between fresh and co-composted BC indicates that co-composted BC likely holds more nutrients, which might help in releasing phosphorus more effectively over time compared to fresh BC.

In the NPK-treated series, all biochar treatments resulted in significantly higher phosphorus concentrations compared to the control + NPK (44.33 ± 0.96%) variant. Once again, co-composted BC + NPK (54.73 ± 1.12%) showed the highest phosphorus concentration among the biochar treatments, indicating that biochar can enhance phosphorus dynamics even in the presence of inorganic phosphorus. However, while co-composted BC exhibited the highest absolute phosphorus availability in this series, its difference from fresh BC + NPK was not statistically significant. This suggests that fresh BC, under fertilized conditions, may retain and release phosphorus in a way that is comparably effective to co-composted BC. The positive interaction between NPK and biochar suggests that biochar may influence phosphorus cycling by altering soil pH, enhancing microbial activity, or modifying the adsorption-desorption behavior of phosphorus compounds. Furthermore, a significant difference between aged and co-composted BC was observed, suggesting that the co-composting process introduced additional nutrients or structural modifications that enhanced phosphorus availability under fertilized conditions.

These findings underscore the positive influence of NPK fertilization on phosphorus availability in soil, with biochar potentially enhancing the efficiency of phosphorus uptake from both organic and inorganic sources. The role of biochar in increasing phosphorus availability may vary depending on its type and how it interacts with soil nutrients, with co-composted biochar showing the most promise for improving phosphorus dynamics, both with and without NPK addition.

2.1.6. Nitrogen Isotope Ratio

The nitrogen isotope ratio ($\delta^{15}N$) of the soil was analyzed in each replicate of the tested variants, with two subsamples collected and measured per replicate. The obtained results are presented in **Figure 8**.

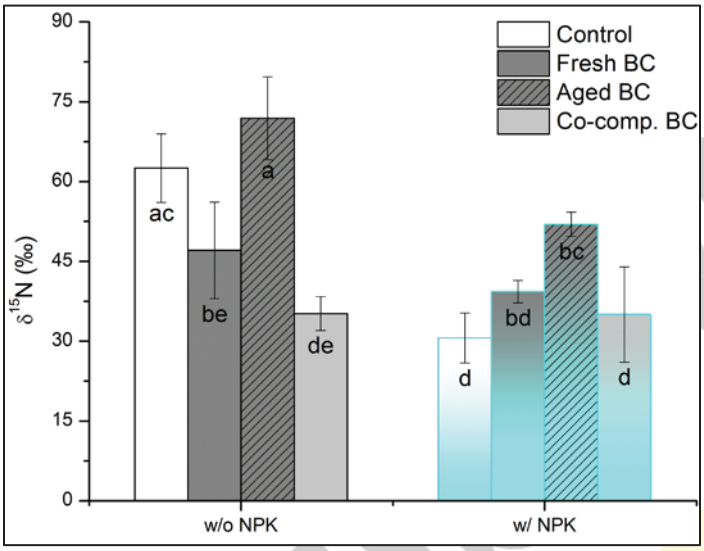

Figure 8. Soil nitrogen isotope ratio values for the tested variants

The $\delta^{15}N$ values across the tested variants demonstrate distinct patterns of nitrogen retention and uptake, with statistically significant differences observed both within each series (with and without NPK) and when comparing corresponding variants across the two fertilization regimes.

In the non-NPK series, the control soil recorded a $\delta^{15}N$ value of 62.52 ± 6.46‰, which was significantly higher than that of the fresh BC (47.07 ± 9.08‰) and co-composted BC (35.20 ± 3.19‰) treatments, but not statistically different from the aged BC (71.88 ± 7.77‰). The elevated $\delta^{15}N$ in the aged BC treatment indicates substantial retention of the ^{15}N-labeled nitrate in the soil, which may be attributed to the physicochemical properties of aged BC, such as increased surface area, oxidation, and functional groups that promote adsorption of nitrate or support microbial immobilization.The similarity between aged BC and the control further suggests limited enhancement of nitrogen assimilation relative to losses, pointing toward a soil system where labeled nitrogen remained accessible but was not effectively removed through plant uptake.

In contrast, co-composted BC exhibited the lowest $\delta^{15}N$ value in the non-fertilized series, significantly differing from both the control and aged BC. This pattern is indicative of enhanced nitrogen turnover and tracer depletion from the soil pool, likely resulting from improved nitrogen availability and uptake efficiency. The composted organic fraction may have released mineralized, unlabeled

nitrogen, promoting plant assimilation and thereby diluting the residual tracer signal. The fresh BC treatment showed an intermediate $\delta^{15}N$ value and was not significantly different from co-composted BC, suggesting partial retention and partial uptake of the tracer. This possibly reflects a combination of short-term nitrate sorption and gradual release from the biochar matrix, along with moderate plant assimilation of available nitrogen.

When NPK fertilizer was applied, all treatments exhibited a pronounced decline in $\delta^{15}N$ values, consistent with the expected dilution effect resulting from the addition of unlabeled nitrogen. Control + NPK recorded the lowest $\delta^{15}N$ (30.59 ± 4.70‰), suggesting efficient plant assimilation of available nitrate, including the ^{15}N-labeled fraction. Similarly, co-composted BC + NPK showed a comparable $\delta^{15}N$ value (35.02 ± 8.96‰), reinforcing the role of this treatment in supporting dynamic nitrogen cycling and plant uptake in the presence of mineral fertilizer. Aged BC + NPK, however, displayed the highest $\delta^{15}N$ (51.97 ± 2.30‰) in the fertilized series, and was significantly different from both control + NPK and co-composted BC + NPK. The elevated $\delta^{15}N$ in aged BC + NPK suggests that the labeled nitrate was retained within the soil, either through enhanced adsorption or microbial immobilization, and was less readily assimilated by plants. Fresh BC + NPK recorded a $\delta^{15}N$ value of 39.30 ± 2.10‰, which was not significantly different from aged BC + NPK, suggesting a similar, though less pronounced, retention effect.

When comparing the same variants across fertilization regimes, the control and aged BC variants showed significant reductions in $\delta^{15}N$ following NPK addition, consistent with the dilution of the tracer by unlabeled fertilizer N. These observations confirm that in the absence of added N, both treatments accumulated labeled nitrogen in the soil, which was partially offset when fertilizer increased the total nitrogen pool. In contrast, fresh BC and co-composted BC treatments did not exhibit significant differences in $\delta^{15}N$ between fertilized and unfertilized conditions. This stability suggests that both biochar types either buffered nitrogen transformations or maintained a consistent balance between mineralization, sorption, and plant uptake. In the case of co-composted BC, this may reflect a steady release of mineral N from the compost fraction, while in fresh BC it could be linked to short-term nitrate retention and gradual release supporting sustained uptake.

Overall, these results underscore the strong influence of biochar type and fertilization on nitrogen cycling pathways, with $\delta^{15}N$ serving as a sensitive integrative measure of plant-accessible nitrogen dynamics. Co-composted BC consistently promoted tracer depletion from soil, likely due to a combination of improved nitrogen availability and active uptake, while aged BC retained a greater proportion of ^{15}N, suggesting reduced accessibility or assimilation.

2.1.7. Microbial Respiration

Soil microbial respiration was analyzed for each replicate of the tested variants, with four sub-samples measured per replicate. This encompassed both basal respiration and respiration with D-glucose and N-acetylglucosamine as substrates at 6 h and 24 h intervals. The results are shown in **Figure 9**.

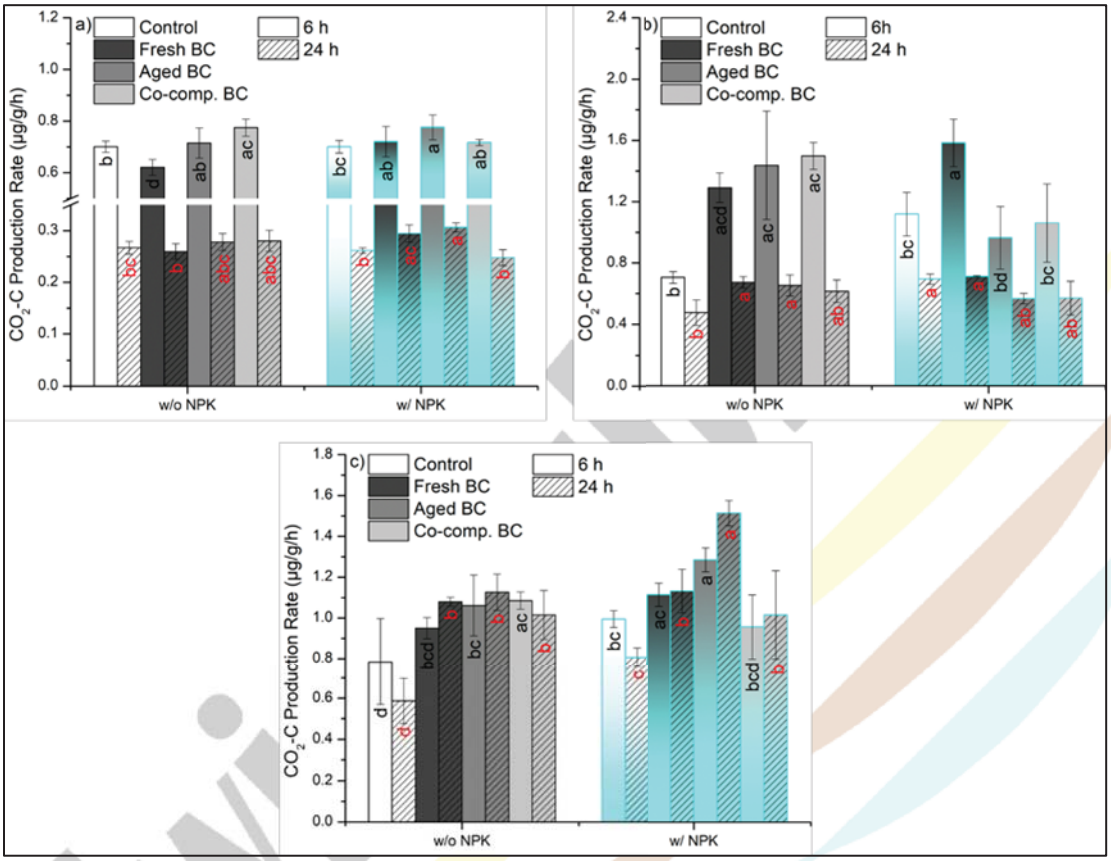

Figure 9. Basal (a), D-glucose (b), and N-acetylglucosamine (c) soil microbial respiration

Basal respiration, representing microbial activity in the presence of water alone, showed generally lower CO_2 production compared to substrate-induced respiration, as expected. In the non-NPK series, fresh BC resulted in the lowest respiration rate (0.62 ± 0.031 µg CO_2/g/h), while co-composted BC exhibited the highest rate (0.77 ± 0.033 µg CO_2/g/h). The control soil and aged BC showed intermediate, similar values. The significantly lower respiration in fresh BC-amended soil may be attributed to the adsorption of labile organic matter, limiting microbial access to easily degradable carbon sources. On the other hand, co-composted BC, having undergone microbial processing, likely provided more bioavailable organic compounds, stimulating respiration.

In the NPK-treated series, respiration rates increased in the fresh BC + NPK and aged BC + NPK treatments, with aged BC + NPK exhibiting the highest rate (0.78 ± 0.049 µg CO_2/g/h). This could imply a synergistic effect of both fresh and aged BC with nutrient availability in stimulating microbial activity. Co-composted BC + NPK showed a decrease compared to the non-NPK series, while the control + NPK variant showed similar values to the non-NPK series, indicating no substantial increase in respiration. This suggests that basal respiration was not significantly influenced by NPK alone. At 24 hours, respiration decreased across all variants, both in the NPK and non-NPK series, suggesting depletion of readily available carbon sources.

Statistical analysis revealed that, in the non-NPK series at 6 hours, significant differences were found between the control and fresh BC, as well as between fresh BC and the other two biochar treatments. Co-composted BC also differed significantly from the control but not from aged BC. Significantly lower respiration by fresh BC compared to the other variants indicates that biochar type influenced basal respiration without NPK at this time point. However, these differences diminished after 24 hours, which may suggest changes in microbial activity or adaptation to biochar properties. In the NPK series, only aged BC + NPK exhibited a significant difference compared to the control + NPK. When comparing corresponding variants between the non-NPK and NPK series, a significant difference was found only between fresh BC and fresh BC + NPK. At 24 hours, no significant differences were observed in the non-NPK series, while in the NPK series, control + NPK differed significantly from fresh BC + NPK and aged BC + NPK. Additionally, when comparing corresponding treatments between the non-NPK and NPK series at 24 hours, a significant difference was observed only between fresh BC and fresh BC + NPK.

D-glucose-induced respiration followed a different pattern, providing insights into the microbial capacity to metabolize simple carbohydrates. In the non-NPK series, all biochar treatments resulted in significantly higher respiration compared to the control soil, which recorded the lowest CO_2 production rate (0.71 ± 0.038 µg CO_2/g/h). Among the biochar treatments, co-composted BC exhibited the highest respiration (1.50 ± 0.088 µg CO_2/g/h), followed closely by aged and fresh BC. The highest respiration rate in co-composted BC treatment reinforces the hypothesis that microbial pre-conditioning of biochar increases its suitability as a microbial habitat and carbon source. These findings indicate that biochar amendments, in general, enhanced microbial capacity to metabolize simple carbohydrates, likely by increasing microbial biomass and activity.

In the NPK series, glucose-induced respiration patterns changed. Fresh BC + NPK exhibited the highest respiration (1.58 ± 0.154 µg CO_2/g/h), while aged BC + NPK (0.97 ± 0.204 µg CO_2/g/h)

and co-composted BC + NPK recorded lower values, not only in comparison to fresh BC + NPK but also in relation to their counterparts without NPK. The control + NPK variant resulted in a respiration rate higher than the control without NPK but lower than that of fresh BC + NPK. This suggests that while biochar amendments influenced microbial activity, the interaction with NPK was dependent on the biochar type, with only fresh BC + NPK showing a higher respiration rate than control + NPK. This variation could be due to nutrient addition modulating microbial preferences for different carbon sources, potentially altering microbial community composition or shifting metabolic pathways. At 24 hours, respiration rates declined across all treatments, both in NPK and non-NPK series, but remained higher than basal respiration, indicating a rapid microbial response to glucose followed by substrate depletion.

Statistical analysis showed that, in the non-NPK series at 6 hours, the control differed significantly from all biochar treatments, but no significant differences were observed among the biochar variants themselves. In the NPK series, fresh BC + NPK differed significantly from all other variants, while the remaining variants did not show significant differences between each other. When comparing corresponding variants between the non-NPK and NPK series, a significant difference was found only between aged BC and aged BC + NPK. At 24 hours, fewer significant differences were observed, with only the control differing significantly from fresh and aged BC in the non-NPK series, while no differences were found among NPK-treated variants. Regarding the comparison of corresponding variants at 24 hours, a significant difference was found only between the control and control + NPK.

N-acetylglucosamine-induced respiration, which reflects microbial metabolism of nitrogen-rich substrates and serves as an indicator of fungal and actinobacterial activity, exhibited a similar trend. In the non-NPK series, all biochar treatments showed higher respiration than the control, with aged BC (1.06 ± 0.149 µg CO_2/g/h) and co-composted BC (1.08 ± 0.042 µg CO_2/g/h) exhibiting the highest values. This aligns with basal and glucose-induced respiration patterns, where microbial activity was highest in pre-conditioned biochar treatments. Fresh BC recorded a lower respiration rate but remained higher than the control (0.78 ± 0.214 µg CO_2/g/h). The enhanced respiration in biochar-amended soils suggests an increased microbial capacity to process complex organic nitrogen sources.

In the NPK-treated series, aged BC + NPK exhibited the highest respiration levels at both 6 hours (1.28 ± 0.059 µg CO_2/g/h) and 24 hours (1.51 ± 0.062 µg CO_2/g/h), significantly differing from the control + NPK and the lowest-performing co-composted BC + NPK (0.95 ± 0.158 µg CO_2/g/h).

This suggests that aged BC combined with NPK may enhance the microbial community specialized in metabolizing more complex substrates, such as chitin derivatives. The fresh BC + NPK treatment recorded an intermediate value, indicating that NPK influenced microbial utilization of nitrogen-containing substrates differently across biochar treatments. At 24 hours, respiration rates in biochar-amended treatments, both in NPK and non-NPK series, remained higher than the control, indicating sustained microbial utilization of N-acetylglucosamine. Unlike basal and glucose-induced respiration, where activity generally decreased, N-acetylglucosamine respiration either increased or remained stable, highlighting prolonged microbial engagement with nitrogen-rich compounds.

Statistical analysis showed that, in the non-NPK series at 6 hours, the control differed significantly from aged and co-composted BC, but not from fresh BC. In the NPK series, aged BC + NPK significantly differed from both control + NPK and co-composted BC + NPK, but not from fresh BC + NPK. When comparing corresponding variants between series, significant differences were observed between control and control + NPK, as well as between aged BC and aged BC + NPK, suggesting that NPK enhanced microbial activity in aged BC-amended soil. At 24 hours, the control soil significantly differed from all three biochar treatments in the non-NPK series, with no significant differences found among the biochar treatments themselves. In the NPK-treated series, control + NPK and aged BC + NPK differed significantly from both fresh BC + NPK and co-composted BC + NPK, with no significant differences observed between the latter two treatments. When comparing corresponding variants between the non-NPK and NPK series, significant differences were found between the control and control + NPK, as well as between aged BC and aged BC + NPK.

The observed trends suggest that biochar amendments influence microbial respiration in complex ways, depending on biochar processing, substrate composition and availability, as well as nutrient supplementation. Fresh BC almost consistently exhibited lower basal respiration but showed a notable stimulation in glucose-induced respiration when combined with NPK. This suggests that fresh BC may initially suppress microbial activity, which is later activated upon nutrient addition. In contrast, aged and co-composted BC generally promoted higher respiration across both substrates, indicating that microbial colonization and transformation of biochar over time enhance its role as a microbial habitat and promote nutrient cycling.

The addition of NPK had varying effects on microbial respiration, depending on the type of biochar. In some cases, such as with aged BC + NPK, NPK stimulated microbial respiration in both

basal and, notably, N-acetylglucosamine-induced respiration, highlighting its potential to enhance microbial activity. However, in other treatments, such as aged and co-composted BC in glucose-induced respiration, NPK seemed to suppress microbial activity. This differential response is likely due to nutrient availability influencing microbial community composition and metabolic strategies employed.

Substrate consumption varied over time, with respiration in response to D-glucose being high at 6 hours but significantly declining at 24 hours, indicating that microbes rapidly metabolize simple sugars and deplete available carbon sources. However, N-acetylglucosamine-induced respiration remained relatively stable, suggesting that microbial communities are capable of sustaining the breakdown of more complex nitrogenous compounds over a longer period, particularly in biochar-amended soils and with NPK addition.

The significant differences in respiration rates between corresponding variants with and without NPK highlight the interactive effects of biochar and fertilization. These interactions are likely influenced by biochar's surface properties, its ability to retain or release nutrients, and its impact on microbial community dynamics. The effects of NPK addition were most pronounced in fresh BC, which showed the highest increase in respiration rates, particularly in basal and glucose-induced respiration. On the other hand, aged BC exhibited a more complex response, with positive effects seen in basal and N-acetylglucosamine-induced respiration but a negative response in glucose-induced respiration. Co-composted BC showed a negative response to NPK across all respiration types, suggesting that the interaction between co-composted biochar and NPK may not be conducive to enhancing microbial activity. These findings highlight the role of biochar and fertilization in enhancing microbial activity, with the NPK addition stimulating microbial respiration to varying degrees depending on the biochar type and the specific substrate utilized.

2.2. Plant Parameters

NOTES:

– Due to the conditions described in the second note of the "Soil Characterization" chapter, the differences observed in the physiological and biochemical parameters of the plants in the tested variants cannot be attributed solely to the effects of different types of biochar or the addition of NPK; they must also be linked to the heat stress to which the plants were exposed. The first signs of wilting were detected in the aged BC + NPK and co-composted BC + NPK treatments, which were planted two weeks earlier than the other variants. This phenomenon was subsequently observed in the other variants as well, progressively

increasing until harvest (see **Photos 44 to 47**, first row). Consequently, the interpretation of the data was influenced by these factors, making it difficult to draw definitive conclusions;

– Despite using identical seeds, the plant of replicate 2 in the Aged BC + NPK variant differed from the others, likely being a wild lettuce (see **Photos 48 and 49**). As a result, although all parameters were measured for this plant, its data were excluded from the overall treatment calculations, which were based on the remaining two plants;
– The recorded weight of root biomass is potentially overestimated due to the difficulty in completely removing the soil from the roots at the time of harvesting, particularly in the control and control + NPK treatment variants. This limitation introduces a degree of uncertainty, which may affect the interpretation of the results related to the measured plant parameters, making it challenging to reach definitive conclusions;
– Statistical analysis of all results was performed using two-way ANOVA followed by a post-hoc Tukey test. A difference was considered statistically significant when $p < 0.05$. Different letters on the figures indicate statistically significant differences.

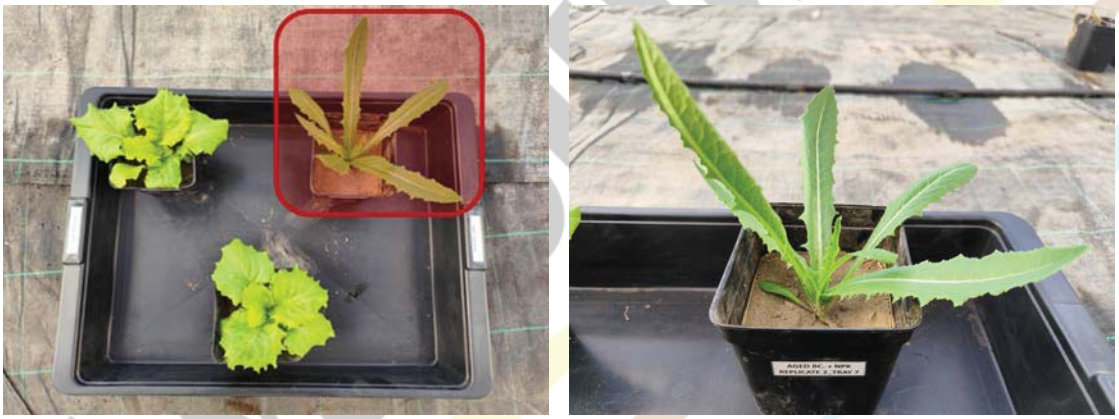

Photos 48 and 49. Wild lettuce plant in replicate 2 of aged BC + NPK variant

2.2.1. SPAD Index and Quantum Yield

The SPAD index and quantum yield values, measured during weeks 6, 7, and 8 of the vegetative stage after sowing (WAS), are shown in **Figure 10**. These values were obtained from measurements taken on each plant replicate (except for replicate 2 of the aged BC + NPK variant), with six measurements taken per plant for each WAS.

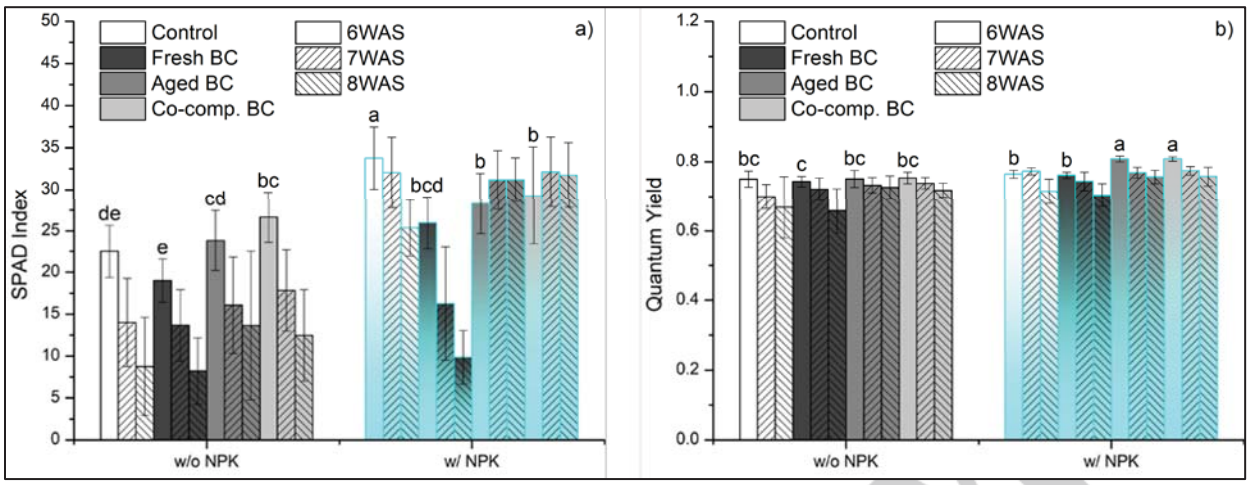

Figure 10. SPAD index (a) and quantum yield (b) measured at 6, 7, and 8 weeks after sowing

The SPAD index and quantum yield values across the variants reveal similar trends, with both parameters showing patterns of improvement or decline that correspond with the type of biochar used and the application of NPK fertilizer.

In the control variant, both the SPAD index and quantum yield declined over time. The SPAD index decreased from 22.51 ± 3.15 at 6 WAS to 8.77 ± 5.86 by 8 WAS, and the quantum yield dropped from 0.75 ± 0.02 to 0.67 ± 0.09 during the same period. This decline in both parameters indicates that plants were nutrient-limited, with the lack of biochar or NPK fertilizer contributing to reduced chlorophyll content and photosynthetic efficiency. Environmental stress, especially heat stress, played a significant role in exacerbating this decline. The fluctuating water availability also added to the stress, intensifying the effects on plant health (see **NOTES** in chapters: “Soil Characterization” and “Plant Parameters”).

The fresh BC treatment exhibited a comparable pattern of decline over time. The SPAD index decreased from 18.98 ± 2.58 at 6 WAS to 8.23 ± 3.96 by 8 WAS, while the quantum yield dropped from 0.74 ± 0.01 to 0.66 ± 0.06. While fresh BC likely improved soil aeration and water retention, its relatively limited impact on nutrient release meant that it could not fully support plant growth under the combined stress of heat and water fluctuation. This limited nutrient availability likely resulted in the observed reduction in both chlorophyll content and photosynthetic efficiency, particularly during periods of intense heat stress.

In contrast, both aged BC and co-composted BC treatments exhibited higher values for both the SPAD index and quantum yield, suggesting that these biochar types provided enhanced nutrient availability and better mitigated the impacts of environmental stress. Aged BC exhibited a SPAD

index of 23.85 ± 3.62 at 6 WAS, which declined to 13.64 ± 8.85 by 8 WAS, and its quantum yield of 0.75 ± 0.02 at 6 WAS only slightly decreased to 0.73 ± 0.03 by 8 WAS. Co-composted BC followed a similar trend, with SPAD values ranging from 26.66 ± 3.01 at 6 WAS to 12.46 ± 5.46 by 8 WAS, and quantum yield values ranging from 0.75 ± 0.02 at 6 WAS to 0.72 ± 0.02 by 8 WAS. These results suggest that both aged and co-composted BC helped alleviate some of the negative effects of heat and water stress. The organic matter in co-composted BC likely played a key role in supporting plant health, while aged BC enhanced nutrient retention capacity likely helped sustain chlorophyll levels and photosynthetic activity under stress.

The application of NPK fertilizer led to noticeable increase in both the SPAD index and quantum yield across all variants, with particularly strong improvements in the control + NPK variant. The SPAD index reached 33.76 ± 3.70 at 6 WAS and quantum yield increased to 0.76 ± 0.01, indicating a positive response to the added nutrients. Both the aged BC + NPK (31.16 ± 3.51 at 8 WAS, quantum yield of 0.81 ± 0.01) and co-composted BC + NPK (32.11 ± 4.19 at 8 WAS, quantum yield of 0.81 ± 0.01) treatments also showed high values, suggesting that these biochars, when combined with NPK, promoted optimal nutrient retention and photosynthetic efficiency (since these treatments were sown two weeks earlier, they experienced less heat stress, which may have contributed to their more favorable results). In contrast, the fresh BC + NPK treatment, while showing some improvement, had lower SPAD index and quantum yield values (9.86 ± 3.19 at 8 WAS for SPAD index and 0.70 ± 0.03 at 8 WAS for quantum yield). These lower values likely reflect the reduced interaction between fresh biochar and the NPK fertilizer, which, due to its lower cation exchange capacity and increased instability, did not effectively support nutrient availability under stress conditions.

To minimize the impact of environmental stress and highlight the effect of the applied biochar type or NPK addition, only data obtained from measurements at 6 WAS were used for statistical comparison.

The statistical analysis supports the observed trends in the SPAD index. In the group without NPK, the control significantly differs from co-composted BC, and fresh BC differs from both aged BC and co-composted BC, aligning with the observed lower SPAD values in the control and fresh BC variants. In the group with NPK, the control + NPK variant showed a significant improvement compared to all other variants, which is consistent with previously made observations. However, no significant differences were found between the aged BC + NPK, co-composted BC + NPK, and fresh BC + NPK treatments, suggesting that these biochar treatments, when combined with

NPK, produced similar results in SPAD index. A notable deviation from previously made observations is the lack of a statistically significant difference between co-composted BC and co-composted BC + NPK, which did not align with the assumption that NPK would significantly enhance the performance of co-composted BC. This could be due to the fact that the nutrient release from co-composted BC, when combined with NPK, may have already reached an optimal level, limiting the additional benefit of the fertilizer.

Concerning quantum yield in the non-NPK group, no significant differences were observed between the variants, which aligns with the similar quantum yield values seen across all variants at 6 WAS. In the group with NPK, both the control + NPK and fresh BC + NPK variants showed significant differences compared to the aged BC + NPK and co-composted BC + NPK treatments, indicating that the application of NPK enhanced the quantum yield in the aged BC and co-composted BC treatments more effectively. A notable deviation from previous assumptions is the lack of a statistically significant difference between the control and its corresponding treatment with NPK, suggesting that the expected improvement in quantum yield due to NPK addition was less pronounced than initially anticipated.

Overall, the results indicate that both aged BC and co-composted BC, particularly when combined with NPK fertilizer, had the most consistent positive effects on both chlorophyll content and photosynthetic efficiency. These treatments likely helped mitigate the adverse effects of environmental stress, particularly heat stress, by improving nutrient availability, enhancing nutrient retention, and supporting plant growth. However, it is important to note that the potential positive effects of biochar were overshadowed by severe environmental stressors in the later vegetative weeks, which may have confounded the impact of the treatments.

2.2.2. Biomass Distribution and Leaf Area

The biomass distribution, described by the weight of the shoot and root fractions, their ratio, and leaf area, of the plants for the tested variants is shown in **Figure 11**. These values were obtained from each plant replicate, except for replicate 2 in the aged BC + NPK variant.

The aerial biomass values indicate that in the non-NPK series, no significant differences were observed among the tested variants. The control recorded an aerial biomass of 13.06 ± 3.13 g, while biochar-treated variants ranged slightly higher, from 14.15 ± 1.63 g to 14.80 ± 2.05 g. These results suggest that biochar, in the absence of NPK, did not significantly enhance above-ground

growth, indicating that its potential benefits on soil structure and water retention did not translate into increased shoot biomass under these conditions.

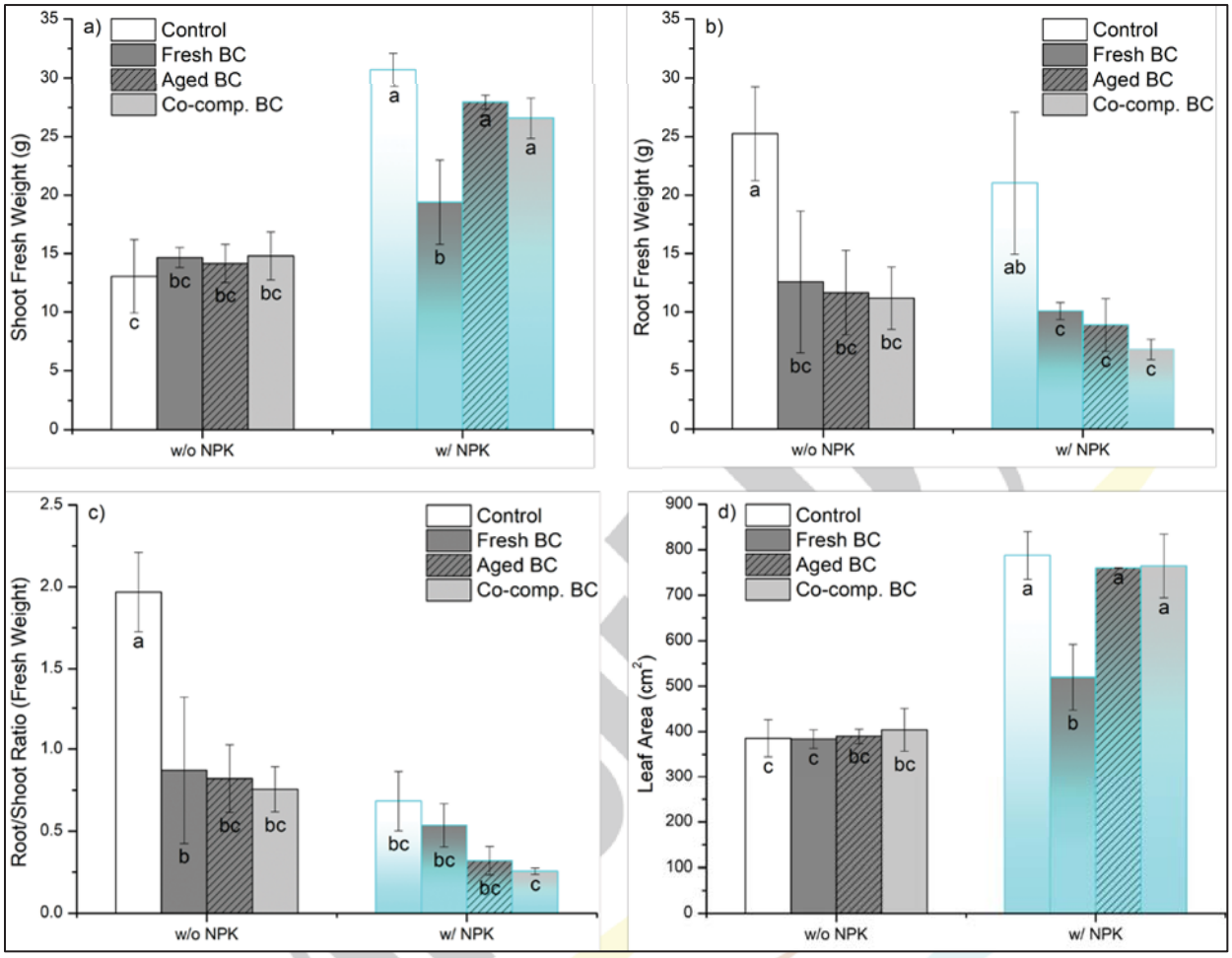

Figure 11. Shoot fresh weight (a), root fresh weight (b), root-to-shoot ratio (c), and leaf area (d) of plants for the tested variants

In the NPK-treated series, a notable increase in aerial biomass was observed across all variants. The control + NPK variant exhibited the highest biomass (30.70 ± 1.40 g), likely due to the optimal nutrient availability from the NPK fertilizer, with aged BC + NPK (27.96 ± 0.85 g) and co-composted BC + NPK (26.58 ± 1.73 g) showing slightly lower values. However, the fresh BC + NPK treatment had significantly lower aerial biomass (19.40 ± 3.60 g) compared to the other NPK-treated variants. This reduced biomass in the fresh BC + NPK treatment may be attributed to the nutrient immobilization properties of fresh BC, which can temporarily reduce nutrient availability to plants before gradually releasing them over time.

When comparing corresponding variants across both non-NPK and NPK series, a significant increase in aerial biomass was recorded in all cases except for the fresh BC treatment. This suggests that fresh BC did not enhance plant growth regardless of fertilization, whereas aged and co-composted BC provided greater benefits when combined with NPK.

The root biomass values exhibited a different trend compared to the aerial biomass. In the non-NPK series, the control showed the highest root biomass (25.25 ± 4.00 g), whereas biochar treatments led to a significant reduction in root biomass, with values ranging from 11.18 ± 2.66 g to 12.58 ± 6.06 g. The reduction in root biomass following biochar application could be attributed to improved soil water retention, reducing the plant's need for extensive root development to access water. Additionally, biochar may have altered soil aeration or microbial interactions, influencing root architecture.

In the NPK-treated series, a similar trend was observed, with the control + NPK treatment exhibiting the highest root biomass (21.03 ± 6.08 g), while biochar treatments resulted in lower values, ranging from 6.81 ± 0.87 g to 10.08 ± 0.73 g. These results indicate that biochar amendments consistently led to lower root biomass, regardless of fertilization. However, no statistically significant differences were found among fresh, aged, and co-composted BC treatments, suggesting that the type of biochar did not strongly influence root biomass once incorporated into the soil.

Unlike aerial biomass, root biomass did not show significant differences when comparing corresponding variants across NPK-treated and non-NPK series. This implies that while NPK increased shoot growth, it had a less pronounced effect on root development in biochar-amended soils. As already pointed out, a possible explanation is that biochar-amended soils altered nutrient and water distribution, potentially reducing the necessity for extensive root proliferation despite the immobilization of nutrients in some biochar treatments.

The root-to-shoot ratio provides insight into the plant’s resource allocation strategy under different soil conditions. In the non-NPK series, the control had the highest root-to-shoot ratio (1.97 ± 0.24), while all biochar treatments resulted in significantly lower values, ranging from 0.76 ± 0.14 to 0.87 ± 0.45. This suggests that biochar-amended soils promoted relatively higher aerial biomass accumulation while reducing root biomass investment, due to the phenomena explained earlier.

In the NPK series, the root-to-shoot ratio was further reduced across all treatments. The control + NPK variant showed a root-to-shoot ratio of 0.68 ± 0.18, while biochar-amended soils exhibited even lower values, ranging from 0.26 ± 0.02 to 0.54 ± 0.13. These results align with the expectation that nutrient-rich conditions lead to greater investment in aerial biomass rather than root

structures. However, the particularly low root-to-shoot ratios in the aged BC + NPK and co-composted BC + NPK treatments suggest that these biochar variants provided additional benefits in nutrient retention and plant water uptake efficiency, allowing plants to allocate more resources toward shoot development.

Statistical analysis revealed significant differences in the non-NPK series only between the control and the biochar treatments, while no significant differences were found among biochar treatments themselves. In the NPK series, no statistically significant differences were observed among any variants, suggesting that fertilization overshadowed the differences observed in the non-NPK series. When comparing corresponding treatments across NPK and non-NPK series, a significant difference was found only in the control variant, indicating that biochar presence had a more profound effect on root-to-shoot ratio than fertilization alone.

Leaf area analysis further supports the trends observed in aerial biomass accumulation. In the non-NPK series, no significant differences were recorded among the tested variants, reinforcing the notion that biochar alone did not substantially influence aerial biomass expansion. However, in the NPK-treated series, a statistically significant reduction in leaf area was observed in the fresh BC + NPK treatment (519.67 ± 72.26 cm^2) compared to the three other variants, which ranged from 760.06 ± 0.76 cm^2 to 787.63 ± 52.68 cm^2 This further supports the hypothesis that fresh biochar initially immobilized certain nutrients, leading to restricted aerial development despite NPK supplementation.

A significant increase in leaf area was recorded in all cases when comparing corresponding variants across the NPK and non-NPK series. This highlights the critical role of NPK fertilization in promoting aerial growth. As previously pointed out, the particularly low leaf area observed in the fresh BC + NPK treatment suggests that nutrient availability was temporarily limited in this variant, aligning with the lower aerial biomass observed in the same treatment.

The results indicate that biochar alone did not significantly enhance aerial biomass or leaf area, suggesting that its potential benefits on soil structure and moisture retention did not directly translate into increased aerial growth under the given conditions. However, when combined with NPK, aged and co-composted BC variants promoted aerial biomass and leaf area development similar to the control + NPK, whereas fresh BC + NPK resulted in lower values, likely due to nutrient immobilization.

Root biomass was consistently lower in biochar-treated soils, indicating that biochar-amended soils altered root development patterns, possibly by improving soil water retention and nutrient

distribution. The root-to-shoot ratio analysis further confirmed that biochar application led to a shift in biomass allocation toward aerial biomass rather than root biomass, particularly in NPK-fertilized soils.

Overall, the findings emphasize the importance of biochar type and processing in determining its agronomic benefits. Aged and co-composted BC provided greater advantages in combination with NPK, while fresh BC initially restricted nutrient availability, negatively affecting plant growth. It is important to highlight once again that the inability to fully separate soil from roots, along with environmental factors such as temperature fluctuations and the need for reseeding, influenced the observed trends and should be considered when interpreting the results (see **NOTES** in chapters: “Soil Characterization” and “Plant Parameters”).

2.2.3. Total Carbon (TC) and Total Nitrogen (TN)

The total carbon (TC) and TN content in the shoots and roots of the plants for the tested variants are shown in **Figure 12**. These values were obtained from each plant replicate, except for replicate 2 in the aged BC + NPK variant.

TC: As observed from the results, no significant differences were found in total carbon (TC) content in the aerial parts of the plants across the tested variants, both in the non-NPK and NPK series. In the non-NPK series, TC values ranged from 39.15 ± 0.75% to 40.62 ± 0.72%, while in the NPK series, they ranged from 36.97 ± 2.00% to 39.92 ± 0.68%. These findings suggest that biochar, regardless of type, did not significantly enhance carbon accumulation in the aerial parts of the plants, whether or not NPK was added. This implies that biochar’s effects on soil structure and water retention did not substantially influence carbon storage in the aerial plant tissues under the experimental conditions.

Moreover, when comparing corresponding variants across both series, no significant differences were observed, reinforcing the conclusion that biochar alone did not lead to significant increases in aerial carbon, regardless of the presence of NPK.

Regarding the roots, significant differences in TC content were observed between variants, particularly in the non-NPK and NPK series, with aged BC showing a marked influence on root carbon content. In the non-NPK series, a statistically significant difference was recorded exclusively between the control (2.95 ± 0.42%) and aged BC (10.47 ± 3.70%) variants, with aged BC resulting in the highest root carbon content.

In the NPK series, aged BC + NPK exhibited significantly higher root carbon (13.69 ± 3.41%) compared to control + NPK (4.26 ± 0.84%) and fresh BC + NPK (6.60 ± 1.40%). Co-composted BC + NPK showed a root carbon content of 10.05 ± 1.79%, which was significantly higher than control + NPK but not significantly different from the other biochar treatments.

When comparing the corresponding variants between the NPK and non-NPK series, no significant differences were observed in root carbon content, suggesting that the influence of biochar on root carbon accumulation was similar, regardless of fertilizer application.

These results indicate that aged BC, in particular, may enhance root carbon accumulation through improved soil structure, microbial activity, and nutrient availability, promoting higher carbon storage, even though the root weight is not as high as in the control variant.

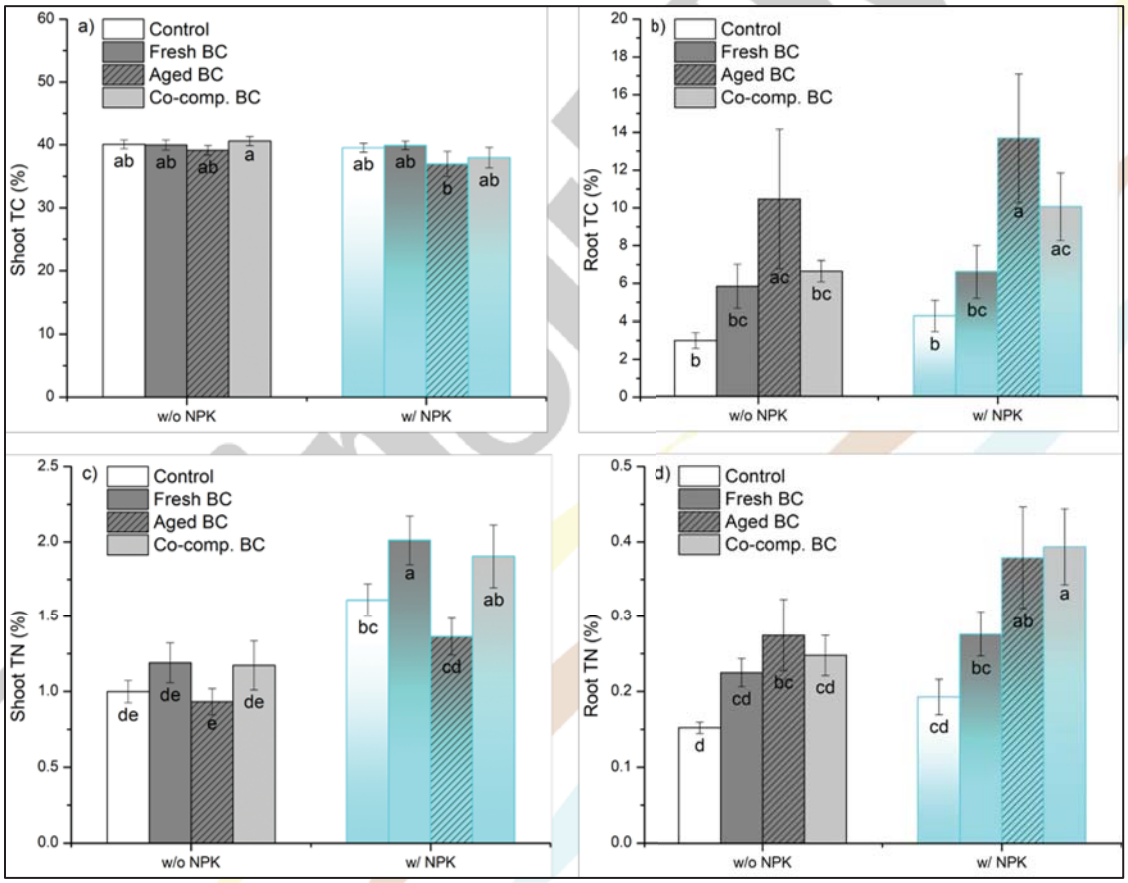

Figure 12. Total carbon (a and b) and total nitrogen (c and d) content in shoots and roots of plants for the tested variants.

TN: When considering TN, in the non-NPK series, no statistically significant differences were found in the aerial parts of the plants across the tested variants. The values of TN ranged from 0.93 ± 0.09% to 1.19 ± 0.13%, indicating that biochar application, regardless of type, did not

significantly affect nitrogen accumulation in the aerial plant tissues under unfertilized conditions. This suggests that biochar alone did not enhance nitrogen availability enough to influence plant uptake. A possible explanation is that biochar, particularly when freshly applied, may initially adsorb nitrogen, temporarily reducing its availability for plant uptake. Additionally, the soil's native nitrogen supply and mineralization rates may have been insufficient to create distinguishable differences between variants.

However, in the NPK series, TN content ranged from 1.36 ± 0.12% to 2.01 ± 0.16%, with notable differences among variants. Fresh BC + NPK resulted in the highest TN accumulation, significantly differing from both control + NPK and aged BC + NPK, although it did not differ from co-composted BC + NPK. Co-composted BC + NPK also showed significantly higher TN content compared to aged BC + NPK. Comparing corresponding variants between the NPK and non-NPK series, significant differences were found in all cases, highlighting the role of fertilization in nitrogen uptake. These results suggest that while biochar alone did not substantially influence nitrogen accumulation in aerial tissues, its combination with NPK – particularly in fresh and co-composted forms – appeared to enhance nitrogen retention and uptake efficiency. This can be explained by the fact that fresh BC, when combined with NPK, may improve nitrogen uptake by modifying soil nitrogen dynamics, likely through reduced nitrogen losses or enhanced microbial activity. The composting process likely further increased biochar's nutrient retention capacity, promoting more efficient nitrogen utilization. Co-composted biochar, in particular, could be effective in enhancing nitrogen retention in plant tissues due to the synergy between composting and biochar's nutrient retention properties.

In the case of root TN, clear differences were observed across variants in both the NPK and non-NPK series. In the non-NPK series, aged BC (0.28 ± 0.05%) resulted in significantly higher TN content compared to the control (0.15 ± 0.01%), while no other variants showed significant differences. This suggests that aged BC may have impacted nitrogen retention in the rhizosphere or affected microbial activity, leading to enhanced nitrogen accumulation in root tissues.

In the NPK-treated series, co-composted BC + NPK (0.39 ± 0.05%) showed significantly higher root TN content compared to control + NPK (0.19 ± 0.02%) and fresh BC + NPK (0.28 ± 0.03%), but did not differ significantly from aged BC + NPK (0.38 ± 0.07%). Furthermore, aged BC + NPK exhibited significantly higher TN content in roots compared to control + NPK. These results suggest that both co-composted and aged BC variants, when combined with NPK, promoted favorable conditions for nitrogen retention in root tissues. The relatively high nitrogen accumulation in

aged BC + NPK, despite having a lower impact on aerial nitrogen accumulation, highlights its role in enhancing root-associated nitrogen retention mechanisms.

When comparing corresponding treatments between the NPK and non-NPK series, a significant difference was observed only for co-composted BC, where the addition of NPK resulted in increased nitrogen accumulation in roots. This supports the hypothesis that co-composting biochar enhances its capacity to retain nitrogen and improves plant nutrient uptake, particularly under fertilized conditions. However, it is important to emphasize that the impact of environmental stress and biochar particle retention on the roots may have influenced both TC and TN accumulation levels, and this should be carefully considered when interpreting the findings (see **NOTES** in chapters: “Soil Characterization” and “Plant Parameters”).

2.2.4. Micro- and Macronutrient Content

The amounts of micro- and macronutrients in the shoots and roots, analyzed for each plant replicate of the tested variants, are presented as mean values in **Table 3**. The key trends identified are summarized and discussed in the following section.

As demonstrated by the results, biochar amendments influence nutrient uptake in plants, with notable differences observed across some of the key elements. The highest levels of Ca were exhibited by the co-composted BC treatment without NPK, likely due to its enhanced ability to improve nutrient exchange and availability in non-fertilized soils. The addition of NPK further enhanced Ca uptake in the aged BC treatment, which showed the highest concentration in shoots under fertilized conditions. This interaction implies that biochar aging increases its CEC, improving Ca retention and uptake, particularly when combined with fertilizer. In contrast, the fresh BC treatment consistently showed lower Ca levels in both NPK and non-NPK series, possibly due to its limited capacity for sustained nutrient release over time.

Levels of Fe in plant shoots were highest in the co-composted BC treatment, both with and without NPK. This suggests that co-composted biochar may enhance Fe mobility and its translocation to the shoots, potentially through improved microbial activity and nutrient cycling. Interestingly, fresh BC treatment showed the highest Fe concentration in roots under non-NPK conditions, indicating that the impact of biochar on Fe uptake varies depending on both the element and the plant organ.

Table 3. Amount of micro- and macronutrients in the shoots and roots of the tested variants

Variant [1]	Al	As	B	Ba	Ca	Cd	Co	Cr	Cu	Fe	K
	mg/kg										
V_1	148	1.44	24.9	4.21	1.16	0.39	0.35	11.9	3.05	213	3.08
	7285	20.0	3.17	34.7	0.15	0.14	2.67	89.4	6.49	8219	0.27
V_2	153	6.33	21.2	5.22	1.10	0.42	0.57	5.85	3.41	181	3.80
	8150	26.5	3.82	40.0	0.20	0.20	3.35	98.4	7.78	9749	0.39
V_3	166	8.82	25.2	5.47	1.17	0.28	0.58	6.09	3.22	187	4.75
	9485	15.3	5.57	47.3	0.32	0.18	2.40	87.0	7.85	8310	0.63
V_4	503	3.61	29.1	7.58	1.43	0.40	0.61	20.7	3.57	514	5.01
	8475	13.5	4.26	45.6	0.22	0.19	2.56	106	7.12	7634	0.38
V_1 + NPK	362	3.78	31.6	6.25	1.36	0.43	0.50	22.8	3.70	445	3.88
	7727	13.2	2.88	33.8	0.16	0.16	2.34	64.8	6.03	7632	0.30
V_2 + NPK	325	5.17	24.4	6.07	1.21	0.28	0.68	11.7	2.52	326	4.22
	8308	15.1	3.76	38.4	0.21	0.23	2.84	117	6.95	8012	0.46
V_3 + NPK	363	5.65	29.1	7.23	1.53	0.29	0.70	14.3	2.80	410	6.31
	9730	14.7	7.18	47.1	0.42	0.16	3.16	94.4	7.95	7982	1.01
V_4 + NPK	677	1.70	19.4	7.52	1.05	0.30	0.55	16.2	3.72	629	3.77
	9412	17.2	6.42	42.2	0.64	0.24	2.63	133	8.13	8444	0.65

Variant [1]	Li	Mg	Mn	Na	Ni	P	Pb	S	Sr	V	Zn
	mg/kg										
V_1	0.19	0.25	201	0.06	0.93	0.35	< 1.00	0.13	20.0	1.34	48.0
	9.04	0.09	347	0.01	6.25	0.06	14.2	0.03	11.0	38.4	27.1
V_2	0.21	0.24	294	0.06	1.26	0.33	< 1.00	0.17	21.1	1.22	55.2
	10.6	0.11	393	0.02	7.81	0.08	18.8	0.04	13.6	44.5	34.4
V_3	0.22	0.26	258	0.06	0.89	0.37	< 1.00	0.19	20.4	1.17	52.9
	10.9	0.12	419	0.01	7.52	0.10	14.7	0.04	18.1	42.3	33.9
V_4	0.46	0.27	190	0.05	1.00	0.39	< 1.00	0.15	24.9	2.57	57.4
	9.64	0.11	346	0.02	6.64	0.08	11.9	0.04	14.8	37.2	31.3
V_1 + NPK	0.38	0.28	244	0.05	1.42	0.43	< 1.00	0.13	23.1	1.90	67.3
	9.46	0.10	346	0.01	6.27	0.07	12.5	0.03	12.0	37.8	27.7
V_2 + NPK	0.32	0.22	126	0.04	1.21	0.37	< 1.00	0.11	19.1	1.79	44.2
	9.70	0.12	360	0.03	7.25	0.09	14.5	0.05	14.1	40.8	32.6
V_3 + NPK	0.34	0.28	135	0.05	1.35	0.41	< 1.00	0.15	24.8	2.01	56.7
	10.7	0.14	398	0.03	7.72	0.12	12.7	0.10	20.4	42.7	35.1
V_4 + NPK	0.66	0.23	251	0.06	1.09	0.38	< 1.00	0.18	20.4	3.03	50.8
	10.2	0.15	358	0.05	8.19	0.11	12.8	0.08	19.7	43.4	38.7

[1] V_1 - Control; V_2 - Fresh BC; V_3 - Aged BC; V_4 - Co-composted BC

[2] Each micro- and macronutrient's values are stacked: shoot on top, root below

The uptake of K was most enhanced with aged BC, particularly when combined with NPK. This highlights the importance of biochar aging in improving K retention and availability, a benefit that is amplified when paired with fertilizer. Co-composted BC also performed well, especially in the non-NPK series, further emphasizing its utility in nutrient-poor environments.

Levels of P were highest in co-composted BC treatment under non-NPK conditions, while aged BC showed the highest values among the biochar treatments when combined with NPK, although still lower than the control. This suggests that co-composted BC plays a significant role in improving P availability in nutrient-deficient soils, while aged BC becomes more efficient when paired with fertilizer.

The uptake of Zn in shoots was optimized with co-composted BC in the non-fertilized series, while the highest concentration in roots was found with aged BC under NPK application. This pattern indicates that co-composting enhances micronutrient availability for plant shoots, while aging biochar improves micronutrient retention in roots.

Overall, biochar amendments, particularly aged and co-composted variants, play an important role in improving nutrient availability and uptake in plants. When combined with NPK fertilizer, these effects are further amplified, suggesting that the combination of biochar treatments and conventional fertilizers can significantly enhance nutrient provision, supporting more sustainable agricultural practices. However, it is important to note again that environmental factors, particularly heat stress, may have influenced plant responses, introducing some uncertainty in identifying the best-performing variant (see **NOTES** in chapters: “Soil Characterization” and “Plant Parameters”).

Impact on your project

The six-month secondment at the CSIC Institute provided an excellent opportunity for knowledge exchange between the CSIC and UNSPMF research teams. The training focused on the design, setup, and execution of isotope-labeled pot experiments, as well as the application of both fundamental and advanced characterization techniques relevant to soil-plant system studies. These methodologies, with advanced techniques including nutrient profiling, microbial activity assays, isotope ratio analysis, and solid-state NMR, provided hands-on experience with approaches that are only partially represented within UNSPMF laboratories.

Through active participation in every stage of the experiment–from soil preparation to sowing, fertilization, isotope application, monitoring, sampling, and analysis–the UNSPMF researcher

developed strong practical competencies in experimental design and execution. Importantly, the techniques and methodologies learned during the secondment are highly relevant not only for the TwinSubDyn project but also for future research initiatives in the field of soil science at UNSPMF. The knowledge gained is directly transferable to upcoming projects, particularly those focused on understanding the interactions between soil organic amendments and nutrient cycling in sustainable agricultural systems.

Overall, the secondment not only enhanced the skills of the visiting researcher but also provided valuable knowledge and tools that will be shared with the wider UNSPMF team and the TwinSubDyn project network. This exchange will help strengthen research capabilities and create new opportunities for collaboration in soil-plant systems and sustainable soil management.

Subtask 1.2.5 (leader FZJ) 6-months secondment (PM20-PM26) for ESR/RR and 1-months secondment (PM24) for QR/RR at the FZJ at the FZJ.

MOBILITY REPORT – 6-months visit to Forschungszentrum Jülich, Jülich, Germany

Researcher: Dr. Slaven Tenodi, UNSPMF

Assigned supervisor: Dr. Lutz Weihermüller

Duration of the visit: 02.10.2024. - 28.03.2025.

Executive Summary

The purpose of the 6-month secondment to Forschungszentrum Jülich (FZJ), Agrosphere Institute (IBG-3), was to enhance collaborative research and technical capacity related to soil hydraulic modelling and the influence of organic amendments on water dynamics in sandy soils. The secondment formed part of an ongoing joint research effort between FZJ and the University of Novi Sad, focused on assessing and improving the water retention performance of degraded sandy soils through the application of biochar, compost, and sludge. The work was structured into complementary segments. Laboratory analysis was performed on soil mixtures previously used in a medium-term lysimeter experiment conducted in Novi Sad, Serbia, with additional characterization of untreated sandy soil. Key soil hydraulic properties such as saturated hydraulic conductivity (K_s), bulk density (BD), saturated soil water content (θ_s), field capacity (FC), and plant available water (PAW) were determined using standardized laboratory procedures. Parallel to laboratory work, extensive efforts were dedicated to processing and statistically analyzing the 441-day sensor and leachate dataset obtained from the lysimeter experiment. This included quality screening, structured formatting of soil moisture and temperature data, and derivation of drainage volumes from weight-based leachate measurements. Based on this dataset and newly compiled long-term climatic data for the Novi Sad region, hydrological modelling was initiated using the AgroC model. Soil-specific hydraulic parameters were incorporated into the model setup, with simulations aimed at evaluating long-term water fluxes under different amendment strategies. The secondment also included participation in field visits and advanced training at three major experimental platforms hosted by FZJ: the AgraSim controlled-environment system,

the TERENO Eifel observatory, and the Selhausen minirhizotron facility for root and rhizosphere monitoring. The secondment resulted in significant scientific outcomes. One manuscript is currently under review in the *Biochar* journal, and another—focused on AgroC-based modelling—is in the final stage of preparation. The collaboration reinforced knowledge exchange and provided critical modelling experience, contributing to long-term joint research development between the two institutions.

Introduction

Background

Sandy soils are widely distributed and are characterized by limited water-holding capacity, rapid drainage, and reduced nutrient retention. These properties make them particularly vulnerable to drought and inefficient water use, posing a challenge for sustainable agriculture in water-limited regions. Organic soil amendments such as biochar, compost, and municipal sludge have emerged as promising materials to improve hydraulic functioning in such soils. However, quantifying their influence under realistic field conditions remains essential.

A lysimeter experiment was established at the University of Novi Sad to assess how these amendments—individually and in combination—affect soil water balance, retention, and drainage in a sand substrate. The experiment utilized 18 gravity-driven lysimeters filled with treated sandy soil and monitored over 441 days. Each lysimeter was equipped with sensors for soil moisture and temperature at two depths (10 cm and 20 cm from the bottom), as well as a system for capturing and weighing leachate water. Six treatments (biochar, sludge, compost, and their combinations) were replicated three times. The experiment provided a valuable dataset for evaluating amendment impacts on field-scale water fluxes.

Building upon this dataset, further investigation was undertaken at FZJ to characterize the hydraulic properties of the soil mixtures and to use these data for long-term hydrological modelling. The AgroC model was selected for simulating soil water dynamics due to its physically based framework, ability to incorporate amendment-specific properties, and suitability for long-term climate data integration.

Scope of the secondment

The scope of the secondment was cantered on three core components:

- Laboratory Determination of Hydraulic Properties: Analysis of six soil-amendment mixtures and untreated sandy soil, measuring K_s, BD, and retention characteristics (θ_s, FC, PAW) following standardized protocols.

- Data Processing and Statistical Analysis: Cleaning, organizing, and statistically evaluating lysimeter data collected over 441 days, including the derivation of leachate volumes and screening of sensor-based soil water and temperature data.

- Hydrological Modeling with AgroC: Setting up and calibrating AgroC simulations using newly extracted climate data from the Republic Hydrometeorological Service of Serbia (2014–2023). Model parameterization was based on laboratory-determined soil properties.

In addition, the secondment included participation in field-oriented training and research infrastructure familiarization, enhancing methodological knowledge and exposure to integrated environmental monitoring platforms.

Despite a delayed start (originally planned for July 2024), the secondment was successfully executed from October 2, 2024, to March 28, 2025, achieving and exceeding all planned objectives.

Content

Lysimeter Experiment in Novi Sad (UNSPMF), Serbia

A medium-scale lysimeter experiment was set up at the University of Novi Sad, Faculty of Sciences, to assess the impact of organic amendments on the water balance of sandy soil. Conducted over 441 days (March 30, 2023 – June 14, 2024) in collaboration with FZJ, the experiment provided essential data for the modelling and lab work performed during the secondment.

Eighteen lysimeters, constructed from 35 cm-high PVC pipes (outer Ø 20 cm, inner Ø 18.28 cm), were used. Each had a 1 mm perforated plastic base and a 3 cm drainage layer of coarse sand. The lysimeters, randomly arranged, were filled with sandy soil mixed with various organic amendments (Treatments A–F). Soil water content (SWC) and temperature were monitored using 5TE and 5TM sensors at 10 and 20 cm depths, connected to EM50 or ZL6 data loggers. Data were downloaded weekly and checked for integrity.

Leachate was collected via hoses into 1 L pre-weighed, pre-cleaned glass bottles with PTFE/silicone septa. Drainage was weighed using a precision scale (0.01 g resolution, 3200 g max). Sampling occurred based on visual checks and weather forecasts. Drainage volume was then calculated from mass and converted to mm relative to lysimeter surface area.

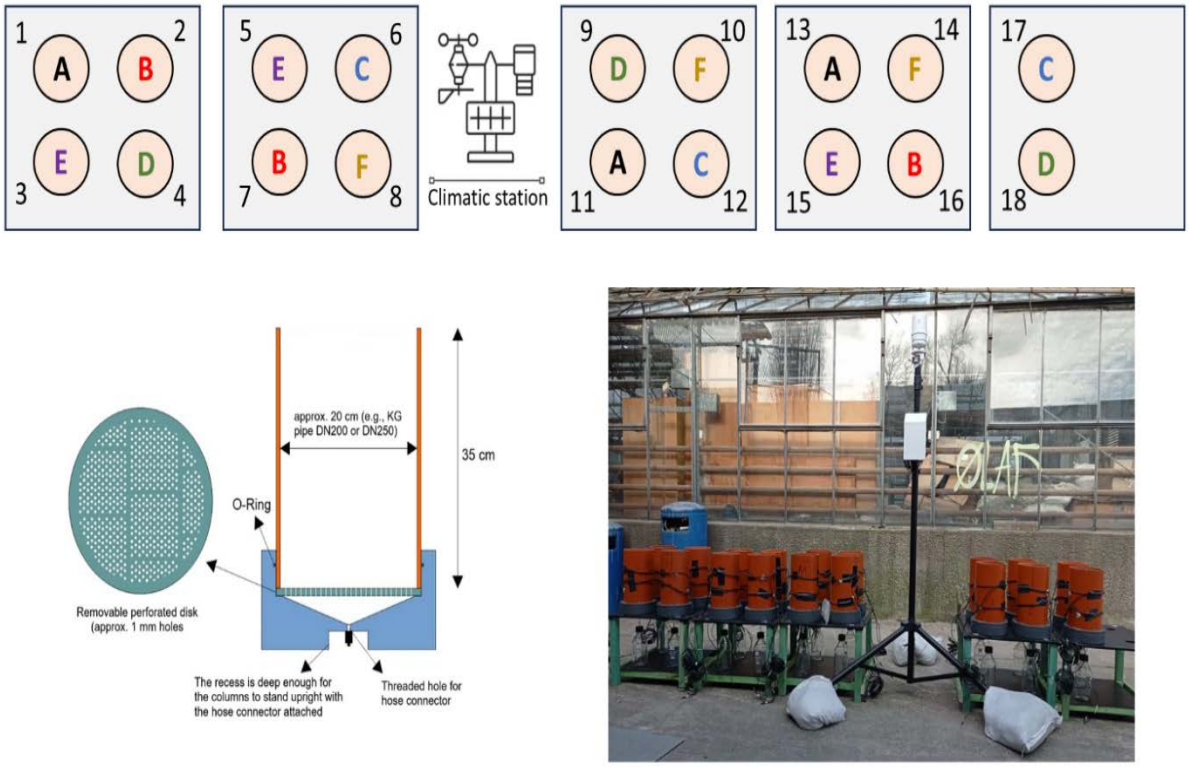

Figure 1. *Experimental setup for the lysimeter experiment. Top panel indicated the randomized setup of the individual treatments with treatment: sandy soil + biochar (treatment A), sandy soil + sludge (treatment B), sandy soil + compost (treatment C), sandy soil + biochar + sludge (treatment D), sandy soil + biochar + compost (treatment E), and sandy soil + biochar + sludge + compost (treatment F).*

Figure 2. *Mixing of materials, filling (and compacting) of lysimeters*

Figure 3. *Placing sensors and connecting to loggers*

The lysimeters were filled with marginal sandy soil collected near the Danube River at "Petrovaradinska ada" in Novi Sad, Serbia (45°15'39.89"N, 19°51'55.08"E). This soil contained 65 ± 4.6% sand, 16 ± 6.4% silt, 10 ± 3.6% clay, and had low organic carbon (C_{org}) content of 0.24 ± 0.05%.

To assess the effects of organic amendments on soil hydraulic properties, six treatments were created by mixing the sandy soil with biochar, compost, sludge, or their combinations. Each treatment was replicated three times (N = 3):

- A: +1% (w/w) biochar
- B: +20% (w/w) sludge
- C: +5% (w/w) compost
- D: +1% biochar + 20% sludge
- E: +1% biochar + 5% compost
- F: +1% biochar + 20% sludge + 5% compost

Treatment B (sludge only) served as a finer-textured reference soil, enhancing water retention relative to the original sand.

Biochar, produced from *Miscanthus* via slow pyrolysis at 550°C (RWTH Aachen), was 77.2% C and aimed to improve structure, nutrient retention, and reduce leaching. Its addition raised Corg to ~1.01% in mixtures. Sludge, sourced from the clay-rich Begej channel (Serbia), increased clay and silt content (to 14.3% and 14.5%, respectively) and raised C_{org} to 0.68%. Compost, derived from green waste in Novi Sad, was added in treatments C, E, and F. While its C_{org} was not quantified, compost is known to improve structure, nutrient availability, and water retention. Raw material properties are shown in Table 1.

All amendments (sludge, biochar, compost) were dried and thoroughly mixed with the dried sandy soil using a construction mixer (Figure 2). The mixtures were then filled into lysimeters with stepwise compaction to maintain a consistent bulk density (~1.4 g/cm^3) across all treatments. The setup was completed on March 31, 2023 (Figure 4), marking the start of the 441-day experiment. Throughout the period, soils were kept bare by regularly removing emerging vegetation.

Table 1. Physico-chemical properties of raw materials used in the experiment.

Materials and mixtures	Feedstock/Origin	Grain size distribution	C_{org} (%)
Sandy soil	Danube River bank, "Petrovaradinska ada" Novi Sad, Serbia	Sand: 65 ± 4.6% (2000 – 50 µm) Silt: 16 ± 6.4% Clay: 10 ± 3.6%	0.24 ± 0.05
Biochar	*Miscanthus* feedstock (pyrolysis at 550°C), Technical University Aachen (RWTH), Germany	-	77.2
Sludge	Sludge from Begej channel near Novi Sad, Serbia	Sand: 60.4 ± 6.22% (2000 – 50 µm) Silt: 8.3 ± 2.9% Clay: 31.3 ± 6.3%	2.45 ± 0.63
Compost	Green waste sourced from Novi Sad, Serbia	-	-

Hourly climate data (precipitation, humidity, wind speed, air temperature, solar radiation) were recorded using an ATMOS 41 weather station and stored via a ZL6 data logger (Meter Group, Munich, Germany). Data were downloaded weekly to ensure integrity. Potential evaporation (E_{pot}) was calculated per FAO56 and aggregated to daily values, consistent with soil water content (SWC) processing (Figure 5b).

***Figure 4**. Start of joint lysimeter experiment*

To maintain consistent drainage, especially during dry periods, all treatments received supplemental irrigation—126 events in total. Water was applied evenly using a perforated disk to avoid splashing, ponding, and infiltration bias. Irrigation was performed simultaneously across all

lysimeters using identical methods, ensuring uniform water distribution. Consequently, total water input (precipitation + irrigation) was equal for all lysimeters throughout the experiment. Cumulative water input is shown in Figure 5a.

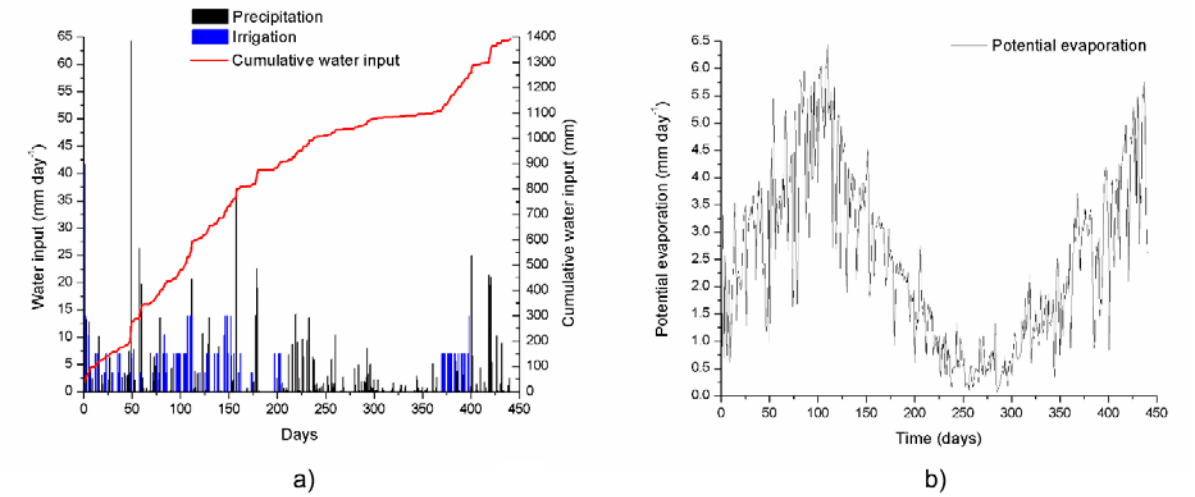

Figure 5. *a) Daily water input (mm day^{-1}) via precipitation and irrigation, alongside the cumulative water input (mm) the 441-day experimental period and b) potential evaporation (E_{pot}) (mm). In both plots the days of the experiment were shown, whereby the start of the experiment was on 31st of March 2023.*

Laboratory Work at FZJ – Soil Hydraulic Characterization

Upon arrival at Forschungszentrum Jülich, one of the initial tasks was the preparation and laboratory analysis of soil samples collected from the lysimeter experiment conducted in Novi Sad. The objective was to determine key hydraulic properties of each treatment mixture, as well as of the unamended sandy soil, in order to provide accurate parameterization inputs for the AgroC hydrological model. Each treatment mixture (A–F), along with the untreated sandy soil (denoted as S), was air-dried, homogenized, and sieved (<2 mm). The homogenized samples were prepared in three replicates per treatment, yielding a total of 21 subsamples for analysis. Before beginning the analysis, Slaven reviewed basic safety and working instructions (see Figure 6) with the soil physics collaborators. The following preparatory steps were performed:

- Drying of samples using laboratory oven (see Figure 7)
- Weighing and portioning of subsamples for each analysis (see Figure 8)
- Packing of samples into standardized measurement vessels (see Figure 9)

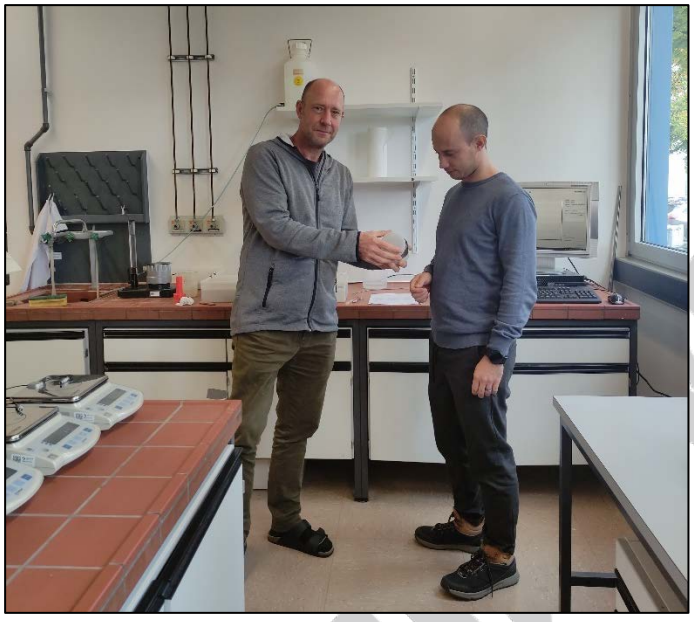

Figure 6. *Lutz Introducing Slaven to the soil physics lab at FZJ, and explaining the procedures for the upcoming soil analysis*

Figure 7. *Drying of soil samples in laboratory oven prior to hydraulic characterization*

Figure 8. *Determination and weighting of soil mixture samples based on corresponding bulk density*

Soil hydraulic properties were analyzed at the Institute of Bio- and Geosciences (Aerosphere, IBG-3), Forschungszentrum Jülich GmbH, using standardized laboratory methods. For this 250 cm^3 cylinders were filled with the soil-mixtures to the same BD as used in the lysimeters. After filling the cylinders, the soil was gradually saturated from the bottom to ensure complete saturation. The saturated hydraulic conductivity K_s was measured using a permeameter with the falling-head method (KSAT Device, Meter Group, Munich), whereby the same sample was measured three times and the arithmetic mean was calculated (see Figure 10).

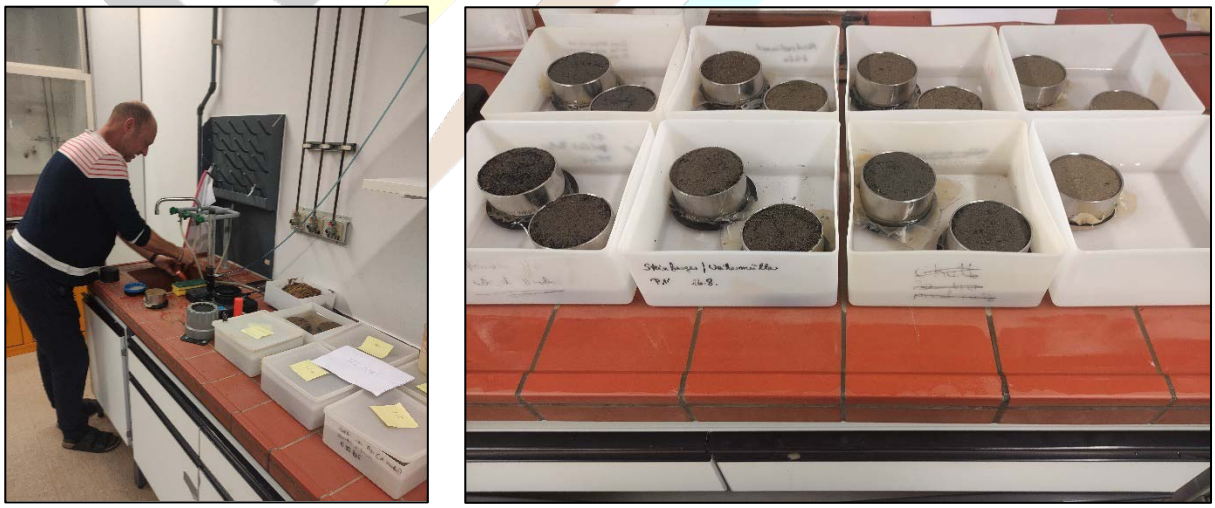

Figure 9. *Packing soil into cylinders and appearance of filled cylinders during the saturation process*

Figure 10. *Measuring saturated hydraulic conductivity of all soil (mixture) samples using the KSAT Device (Meter Group, Munich)*

Soil hydraulic characteristics (water retention and hydraulic conductivity characteristics) were determined by the evaporation method using the HYPROP® system (Meter Group, München, Germany) in combination with the WP4® Dewpoint Potentiometer (Decagon Devices, WA, USA). Two different soil hydraulic models describing the retention and hydraulic conductivity functions were fitted to the HYPROP® data, namely the unimodal van Genuchten model and second the dual-porosity Durner model using the HYPROP Fit software (Meter Group, Munich, Germany). The retention function for the dual-porosity Durner model can be written as:

$$\theta(h) = \theta_r + (\theta_s - \theta_r) \sum_{i=1}^{k} \omega_i Se_i \quad (1)$$

with

$$Se_i = [1 + |\alpha_i h|^{n_i}]^{-m_i}, \quad (2)$$

where θ_r and θ_s are the residual and the saturated water contents [$cm^3\ cm^{-3}$], respectively, k is the order of porosity in the soil system (here $k = 1$ for the unimodal (van Genuchten) and $k = 2$ for

dual-porosity model), *Se* is the effective saturation [-], ω_i is the weighting factor ($\sum\omega_i = 1$). α_i [cm^{-1}], n_i [-], and m_i [-] are empirical parameters, whereby α_i can be related to the inverse of the air entry values and n_i to the width of the pore size distribution, whereas m_i is classically related to n_i by $m_i = 1\text{-}1/n_i$. *h* is the pressure head [cm].

The relative soil hydraulic conductivity function *K(h)* is given by Priesack and Durner:

$$K(h) = K_s \sum_{i=1}^{k} \omega_i Se_i^{\lambda} \left[\frac{\sum_{i=1}^{k} \left(1 - \left(1 - Se_i^{1/m_i}\right)\right)^{m_i}}{\sum_{i=1}^{k} \omega_i \alpha_i} \right]^{r} \quad (3)$$

where K_s is the saturated hydraulic conductivity [cm day^{-1}], which was kept fixed during the fitting of the soil hydraulic model to the measured data.

Based on the knowledge of the retention characteristics the plant available water (PAW) was derived as the difference between field capacity (FC) and permanent wilting point (PWP). Therefore, water contents at different pressure heads (h = -100, -200, and -250 cm) were calculated and assigned to field capacity of FC @ -100, FC @ -200, and FC @ -250 cm, respectively. Water content as PWP was calculated at pF = 4.2 (h = -15849 cm) and the differences between the FC and PWP was assigned as PAW.

All methods followed standardized protocols used within the IBG-3 laboratory and were coordinated with FZJ staff to ensure consistency with modelling requirements.

Figure 11. *Determination of soil hydraulic properties (water retention and hydraulic conductivity) using the evaporation method with the HYPROP® system (Meter group, München, Germany) in combination with the WP4® Dewpoint potentiometer (Decagon devices, WA, USA)*

Data screening and lysimeter dataset structuring

An essential part of the secondment involved extensive processing and quality screening of the dataset obtained from the 441-day lysimeter experiment at the University of Novi Sad. The objective was to produce a clean, structured dataset suitable for statistical evaluation and hydrological modeling using the AgroC model. The lysimeter system continuously recorded the following variables:

- Soil water content (SWC) at 10 cm and 20 cm from the bottom
- Soil temperature at the same depths
- Precipitation
- Drainage measured as leachate mass using digital balances under sealed collection containers

Sensor data were recorded at either 15-minute or 1-hour intervals, depending on the sensor type and time segment of the experiment. Across the full period, this resulted in tens of thousands of datapoints per variable, per lysimeter.

A combined manual and script-based approach was used to detect and correct anomalies in the dataset:

- Interpolation or removal of sensor gaps and faulty readings
- Identification and correction of offset values due to power outages or calibration drifts
- Filtering out flat-line periods or sensor freezing during winter months
- Adjustment of leachate values to correct for container repositioning or erroneous weight shifts

Precipitation data (see Figure 5a) were verified against publicly available meteorological records and used to support interpretation of drainage trends and SWC fluctuations.

Drainage was calculated from cumulative leachate mass over time. Manual validation was performed to ensure accurate event detection, particularly in cases of minor changes below balance sensitivity thresholds. Cumulative drainage was then calculated per lysimeter and averaged across replicates.

Where needed, irrigation events were added to precipitation data to create a complete water input timeline, later used for modelling.

Statistical Methods

To evaluate the effects of different organic amendments on the soil hydraulic properties and drainage behaviour of sandy soil, statistical analyses were applied to both laboratory-derived parameters and lysimeter data. All analyses were conducted at a 95% confidence level ($p < 0.05$) using OriginPro 8.0. Box-plots for presenting SWC, drainage and evaporation data, as well as soil hydraulic properties, were made in OriginPro 8.0.

A one-way analysis of variance (ANOVA) was performed for each measured variable to test for statistically significant differences among the seven soil treatments:

- Untreated sandy soil (S)

- Treatments A–F (biochar, compost, sludge, and combinations)

Variables analyzed included:

- Laboratory-measured hydraulic properties:
  - Saturated hydraulic conductivity (K_s)
  - Bulk density (BD)
  - Saturated soil water content (θ_s)
  - Field capacity (FC)
  - Plant available water (PAW)
- Lysimeter-based parameters:
  - Cumulative drainage over 441 days
  - Soil water content at 10 cm and 20 cm depth
  - Evaporation over 441 days

Where ANOVA revealed statistically significant differences ($p < 0.05$), a Tukey's Honest Significant Difference (HSD) test was applied to identify specific group differences between treatments. This method controls for Type I error across multiple pairwise comparisons and enables a ranked interpretation of treatment effects.

Results of the ANOVA and Tukey HSD analyses are presented in summary table reporting F-values, p-values, and post-hoc comparisons

These analyses provided the statistical foundation for evaluating amendment effectiveness and informed the selection of input parameters for hydrological modeling in AgroC (Section 3e).

AgroC Hydrological Modeling

Hydrological modelling is a key tool for assessing how soil amendments affect water dynamics. Models like HYDRUS-1D, AgroC, and SWAT simulate processes such as infiltration, storage, and drainage, and help evaluate amendment impacts on hydraulic properties under varying

conditions. When calibrated with field data, they provide valuable insights into amendment performance over time, supporting informed agricultural and environmental decisions.

During the secondment, AgroC was used to simulate water balance dynamics under different amendment treatments. This one-dimensional, process-based model captures water, heat, and carbon fluxes in the soil-plant-atmosphere system and is well-suited for modelling unsaturated flow and amendment-specific effects.

AgroC was chosen for its physically based structure, using the Richards equation and van Genuchten functions to simulate soil water capacity and unsaturated hydraulic conductivity (K(h)). This framework allows it to accurately reflect how different amendments influence water flow in marginal sandy soils. By integrating long-term field data, AgroC helps predict amendment performance under realistic environmental conditions, offering practical guidance for soil water management. The van Genuchten equation for soil water retention describes the relationship between soil water content (θ) and matric potential (h) as:

$$\theta(h) = \theta_r + \frac{\theta_s - \theta_r}{(1+|\alpha h|^n)^m} \quad (3)$$

where $\theta(h)$ is soil water content at a given matric potential, θ_s is saturated soil water content (cm^3 cm^{-3}), θ_r is the residual soil water content (cm^3 cm^{-3}), h is matric potential or soil water tension (negative pressure head), α, n, and m are empirical parameters, whereby $m = 1 - \frac{1}{n}$.

The hydraulic conductivity as function of pressure head $K(h)$ is given by:

$$K(h) = K_s \cdot S_e^{\lambda} \cdot \left[1 - \left(S_e^{\frac{1}{m}}\right)^m\right]^2 \quad (4)$$

where $K(h)$ is unsaturated hydraulic conductivity (cm d^{-1}), K_s is saturated hydraulic conductivity (cm d^{-1}), S_e is effective saturation (defined as $S_e = \frac{\theta(h) - \theta_r}{\theta_s - \theta_r}$), λ is pore connectivity parameter (often assumed to be 0.5 based on empirical findings).

The AgroC model was configured to match the experimental soil profile, with 310 vertical nodes (0.1 cm spacing) and a total depth reflecting the filled lysimeters. The lower boundary was set as a seepage face, and the upper as atmospheric, allowing ponding and delayed infiltration when

saturation exceeded capacity. Initial soil moisture was set using a pressure head of –1500 cm, and the critical switch point (hCrit) was –100,000 cm.

Model calibration involved estimating van Genuchten parameters using the Shuffled Complex Evolution (SCE-UA) global optimizer. The objective was to minimize the sum of squared residuals (SSR) between observed and simulated SWC and drainage. Optimization was done in steps: first on SWC, then drainage, and finally on combined results using normalized SSRs. Due to occasional gaps in SWC data, arithmetic means across replicates (n = 3) were used for calibration.

Winter wheat (*Triticum aestivum*) was selected as the simulated crop, reflecting its dominance (≈25%) in the Novi Sad region's crop rotation. Its well-documented phenology and local relevance make it an ideal reference for evaluating amendment effects on water use and yield.

Additional factors supporting this choice:

- Well-documented phenological stages and crop parameters
- Defined sowing period (mid-October to early November) and harvest (late June to mid-July)
- Typical sowing density of 180–220 kg/ha, and yields of 5–7 t/ha
- Standardized fertilization practices known for the region

Model parameterization was based on measured values obtained during the secondment:

- K_s, θ_s, FC, PAW
- Fitted van Genuchten parameters (α, n, θ_r, θ_s)
- Parameters were adjusted separately for each treatment (A–F, S)

A 10-year climatic dataset (2014–2023) for Novi Sad was extracted from the Republic Hydrometeorological Service of Serbia. The dataset included:

- Daily precipitation
- Minimum and maximum air temperature

- Global solar radiation (estimated where needed)
- Reference evapotranspiration (ET_0), calculated using the Penman–Monteith method

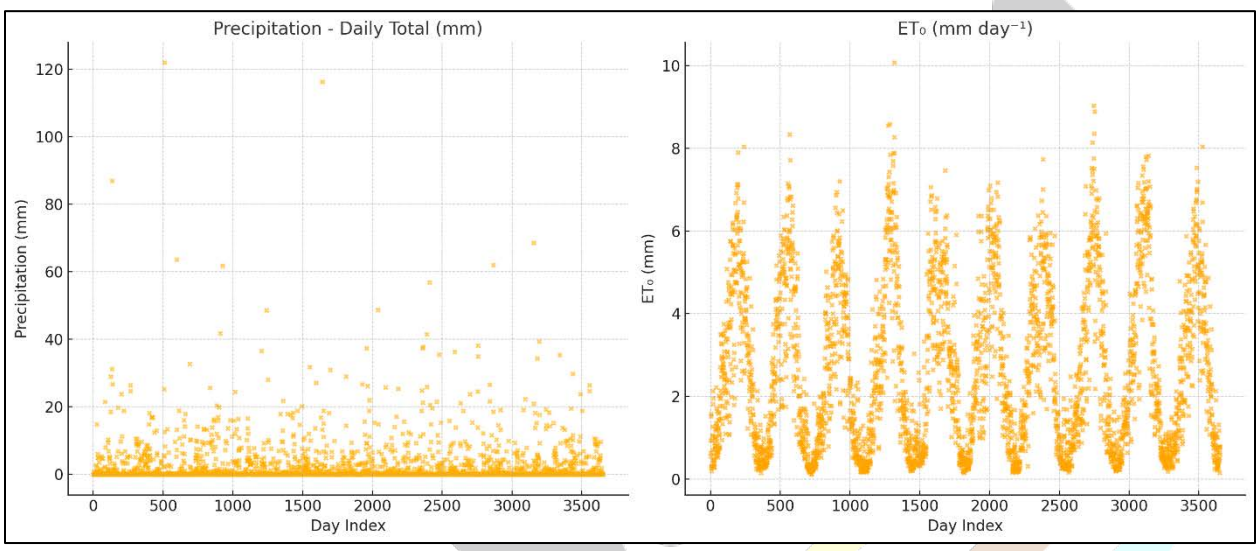

Figure 12. *Temporal Trends of Daily Precipitation and ET_0 in Novi Sad (2014–2023)*

Model Setup:

- Soil profile depth: 60 cm (matching lysimeter dimensions)
- Number of vertical nodes: 310 (Δz = 0.1 cm)
- Upper boundary: Atmospheric with dynamic ponding allowed
- Lower boundary: Free drainage (seepage face)
- Initial condition: Pressure head of -1500 cm (to simulate dry pre-planting conditions)
- hCrit (surface boundary switch): -100,000 cm

Model calibration focused on:

- Soil water content (SWC) dynamics at both depths
- Cumulative drainage data

Field Trainings and Research Platform Visits

During the second half of the secondment, three specialized research platforms affiliated with Forschungszentrum Jülich were visited. These excursions provided direct exposure to advanced infrastructure for monitoring soil-plant-atmosphere interactions across different spatial and temporal scales. The visits included presentations, guided tours, and in-field discussions with researchers, enabling participants to connect theoretical modelling with real-world applications.

AgraSim Platform (January 17, 2025)

The AgraSim facility is a state-of-the-art experimental platform at IBG-3 designed to simulate controlled environmental conditions and study soil–plant–atmosphere processes in a reproducible way. During the visit, the upper and lower components of the system were shown, including:

- Plant growth chambers and soil containers
- Sensors and control units located in the substructure
- Automated irrigation, climate regulation, and drainage control systems

The control room provided an overview of how the entire system is monitored and regulated. Presenters explained the original design philosophy behind AgraSim, highlighting its role in testing scenarios of future climate conditions, root-zone dynamics, and interactions between soil amendments and plant performance. In addition to the AgraSim facility, the group was also given a tour of the soil physics laboratory at IBG-3. The lab presented complementary methods and instrumentation used to analyze soil physical properties, including retention characteristics, porosity, and infiltration behaviour under controlled settings.

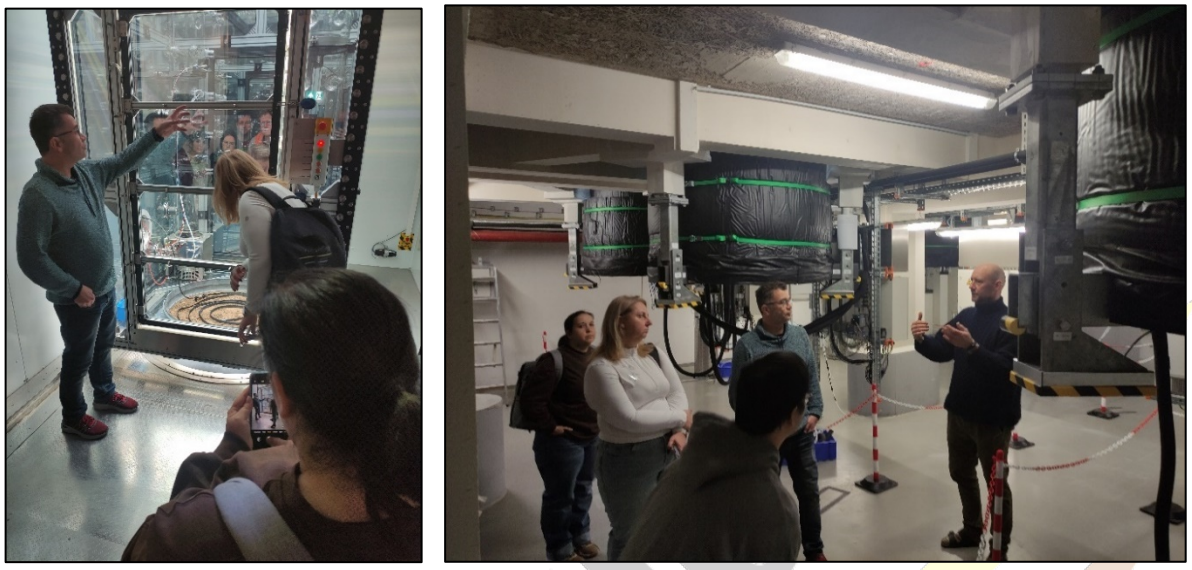

Figure 13. *AgraSim: plant growth chambers (left) and substructure control systems (right)*

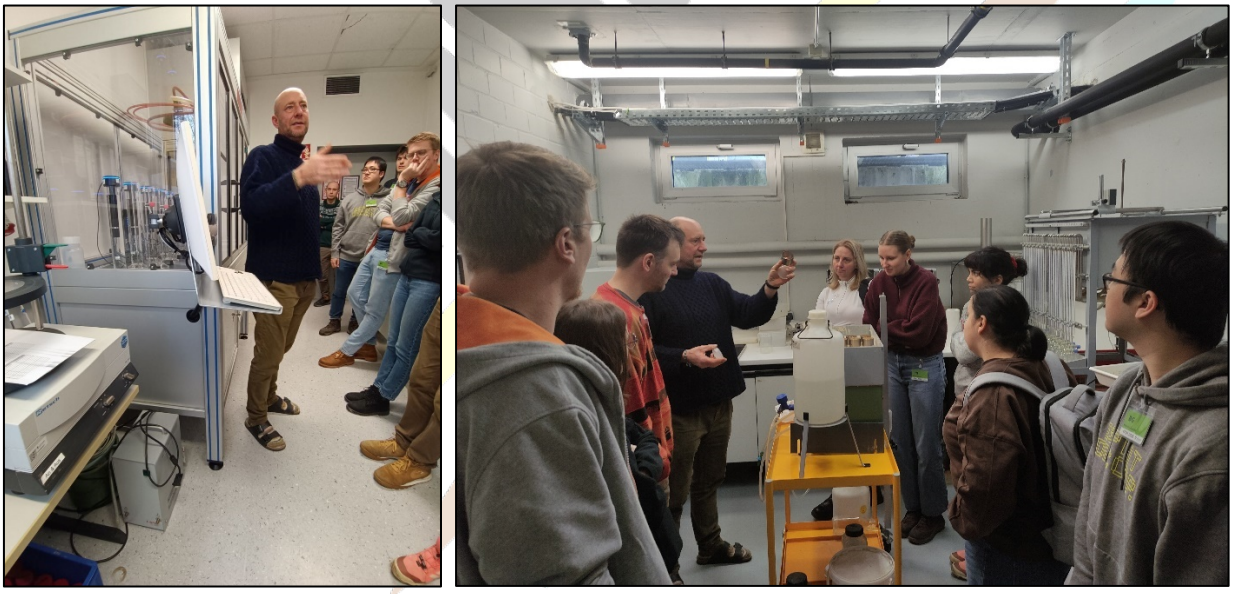

Figure 14. *Laboratories for sample preparation (right) and texture determination (left)*

Selhausen Minirhizotron Field and Lysimeter Station (January 17, 2025)

The Selhausen experimental field is part of the "CropSense" and "RhizoTraits" research initiatives, focusing on non-invasive monitoring of root system architecture and rhizosphere processes. The visit included a comprehensive tour of the minirhizotron facility, where underground imaging tubes and high-resolution cameras are used to track root growth dynamics

in real-time. Researchers explained how the data collected from root imaging is integrated with crop development models and environmental parameters. Interdisciplinary collaboration with plant physiologists, remote sensing experts, and modelers was emphasized as a key aspect of the platform.

Following the minirhizotron demonstration, the group visited the lysimeter station and multi-system weather station, also located at the site. This portion included:

- Inspection of large-scale lysimeters from inside and outside
- Explanation of leachate sampling, soil moisture tracking, and boundary conditions
- Overview of weather station components (rain, wind, radiation, temperature sensors)

The Selhausen setup provided a valuable bridge between process-level modeling and large-scale field monitoring.

Figure 15. *Minirhizotron field at Selhausen: Real-time root imaging*

***Figure 16**. Lysimeter systems and climate monitoring at Selhausen*

TERENO Eifel-Lower Rhine Observatory (January 23, 2025)

The final site visit took place at the TERENO (TERrestrial ENvironmental Observatories) station in the Eifel region, a key component of Germany's long-term environmental monitoring network. Led by Dr. Lutz Weihermüller, the visit focused on multi-scale hydrological and biogeochemical measurements.

The first part of the tour included:

- A lysimeter station for long-term observation of water balance and nutrient leaching
- Detailed explanation of the network's role in climate impact research

Next, the team was shown a canal water monitoring station used for analyzing dissolved organic matter (DOM) and nutrient transport through surface waters.

The final segment included a walk to an atmospheric monitoring station, where air quality and carbon cycle parameters (e.g., CO_2 fluxes) are tracked. Although not all systems could be observed in full operation, the diversity of instrumentation illustrated the breadth of the platform's integrative approach.

Figure 17. *Environmental monitoring at TERENO Eifel: Canal water analysis (left) and atmospheric tracking of air quality & carbon cycle (right)*

RESULTS

This section presents the main outcomes of the laboratory analyses, lysimeter dataset evaluation, and hydrological modelling performed during the secondment.

Soil Hydraulic Properties

To characterize the water retention behavior of the sandy soil and its amended variants, two commonly applied hydraulic models were considered: the unimodal van Genuchten (1980) model and the bimodal formulation proposed by Durner (1994). Both models were fit to measured water retention data derived from the HYPROP® evaporation method and extended with WP4® measurements for the dry-end range. Model selection was based on minimization of the AIC, which penalizes overfitting while accounting for model complexity.

Across all treatments, the Durner model consistently provided a superior fit to the measured retention data, particularly in the mid-range of pressure heads (–100 to –1000 cm), where the presence of amendment-induced secondary pore systems resulted in inflection points not

adequately captured by the unimodal van Genuchten function. This dual-porosity behavior was especially evident in treatments involving compost and sludge, suggesting that organic amendments enhanced the heterogeneity of the pore size distribution — a finding in agreement with other recent work on organic matter–enriched soils. During model fitting, the K_s was not estimated simultaneously but rather held constant at the value determined independently using the falling-head permeameter method. This approach ensured consistency between the hydraulic conductivity measurement and the subsequent parameterization of the retention model, as recommended when coupling empirical K_s values with HYPROP-derived retention curves. The fitted Durner parameters, along with measured K_s, were used as inputs for the AgroC simulations to reflect the water retention characteristics of each treatment.

The amendment of sandy soil with organic materials resulted in distinct and measurable shifts in key soil hydraulic properties across treatments. Figures 1 and 2 illustrate the variability among the seven soil types based on five replicated measurements per treatment.

The box plot (Figure 18a) provides a visual overview of how amendments influence K_s, revealing substantial differences across treatments. The untreated sandy soil (S) exhibited an intermediate K_s (~730 cm day^{-1}), reflecting a relatively loose structure with moderate permeability. Compost-amended treatments, particularly C (compost only) and E (biochar + compost), exhibited the highest K_s values (>1300 cm day^{-1}), suggesting compost's role in increasing pore connectivity and promoting rapid water infiltration. Treatment C showed the most consistent K_s values, indicating reliable improvement across replicates. Treatment E exhibited slightly more variability, likely due to interactions between biochar particle size and compost matrix.

451

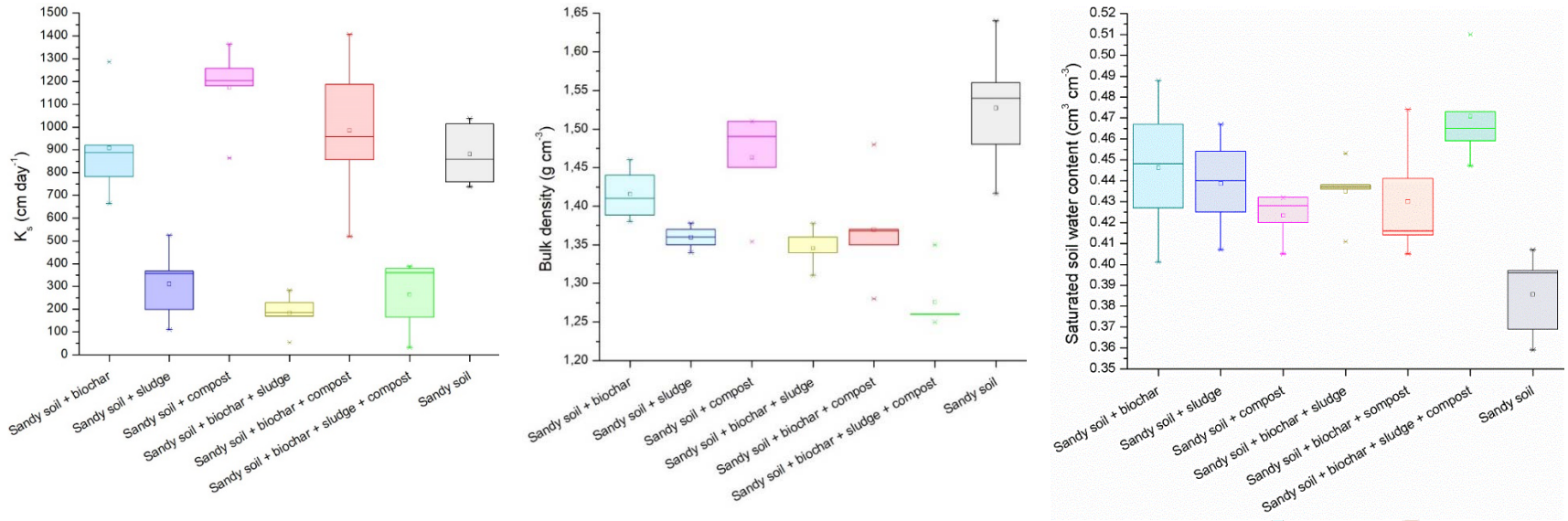

a) b) c)

452 ***Figure 18.*** *Distribution of measured values for (a) saturated hydraulic conductivity (K_s), (b) bulk density (BD), and (c) saturated water*
453 *content (θ_s) across sandy soil and six amended treatments, presented as box plots based on five replicates per treatment (n = 5).*

Biochar-amended soil (A) showed moderate saturated hydraulic conductivity (K_s ~800 cm day^{-1}), with high variability, indicating improved permeability but less consistency. Sludge significantly reduced K_s—treatments B (sludge only) and D (biochar + sludge) recorded the lowest values (<200 cm day^{-1}), likely due to pore clogging by fine particles. Treatment F (biochar + compost + sludge) had intermediate K_s, suggesting compost and biochar partially mitigated sludge's restrictive effects.

BD patterns (Figure 1b) highlighted structural changes: sandy soil (S) had low BD (~1.34 g cm^{-3}), while compost-only (C) reached the highest (~1.48 g cm^{-3}), indicating pore space reduction. In contrast, treatment E (biochar + compost) had the lowest BD (~1.36 g cm^{-3}), pointing to a beneficial interaction. Treatments A and B had intermediate BD (~1.40–1.41 g cm^{-3}), while biochar addition in D and F slightly reduced the compaction seen with sludge alone.

θ_s (Figure 1c) was lowest in untreated sand (~0.386 cm^3 cm^{-3}), reflecting its limited microporosity. Treatment F had the highest θ_s (~0.471 cm^3 cm^{-3}), showing a synergistic effect of all three amendments, enhancing pore complexity and retention. Treatments A, B, and D showed intermediate θ_s (~0.42–0.44 cm^3 cm^{-3}), suggesting individual or binary amendments improve retention, though less effectively than the triple combination. Compost alone (C) yielded lower θ_s (~0.423 cm^3 cm^{-3}), indicating limited capacity to enhance saturation when applied in isolation.

FC, measured at pressure heads of –100, –200, and –250 cm, showed clear and statistically significant differences across treatments (Figures 2a–c), confirming that amendment type and combination strongly affect moisture retention. At –100 cm, treatment F (biochar + sludge + compost) had the highest FC (~0.23 cm^3 cm^{-3}), followed by treatment D (biochar + sludge). The control sandy soil had the lowest FC (~0.062 cm^3 cm^{-3}), highlighting its poor retention capacity. Sludge-only (B) and compost-only (C) treatments performed moderately, while biochar (A) and biochar + compost (E) had the lowest retention among amended soils. This trend remained consistent across all pressure heads, with treatment F consistently outperforming others—demonstrating the synergistic effect of combining amendments with different structural properties.

PAW, calculated as FC minus the permanent wilting point (–15848 cm), also varied significantly across treatments and suction levels (Figures 2d–f). Treatment F consistently showed the highest PAW (~0.16 cm^3 cm^{-3} at –100 cm), indicating optimal conditions for water storage and release. Its performance reflects the combined benefits of biochar's porosity, compost's organic matter, and sludge's fine texture. Treatment D (biochar + sludge) also showed strong performance, especially

at –100 and –200 cm, due to sludge-enhanced microporosity. In contrast, treatment C (compost only) had the lowest PAW across all pressure heads, suggesting limited impact when used alone. Biochar-only (A) and sludge-only (B) treatments showed moderate, consistent PAW, while treatment E (biochar + compost) produced mixed results—improving slightly on compost alone but not matching sludge-containing mixes. This suggests that compost and biochar, without sludge, may lack the necessary synergy to significantly enhance water availability under unsaturated conditions.

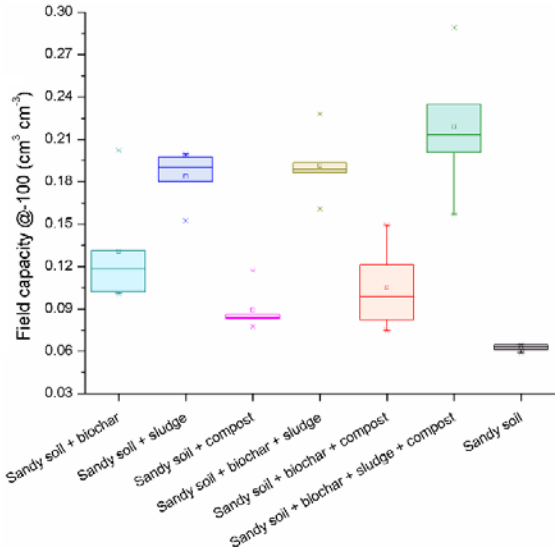

a)

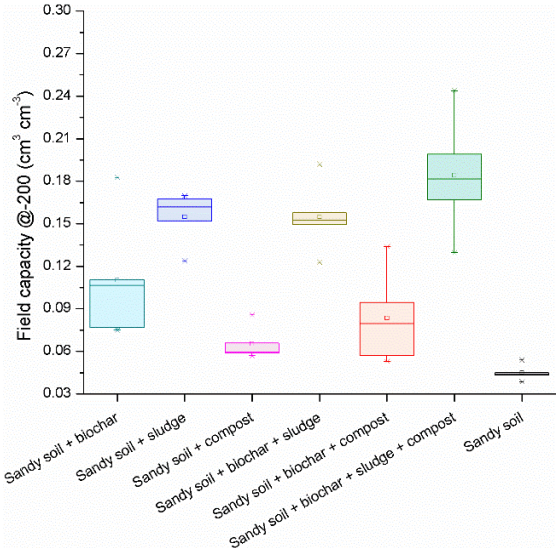

b)

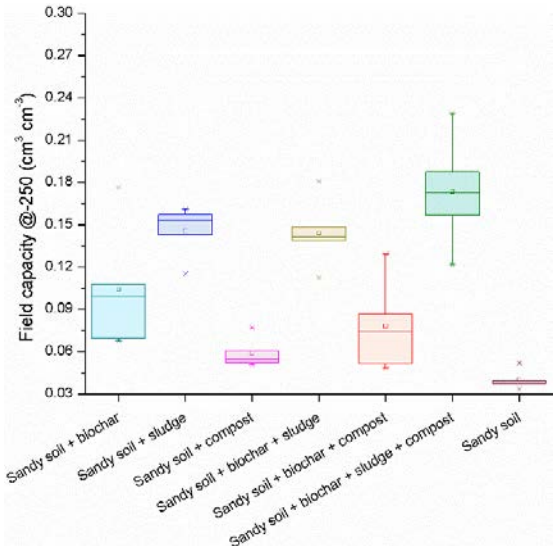

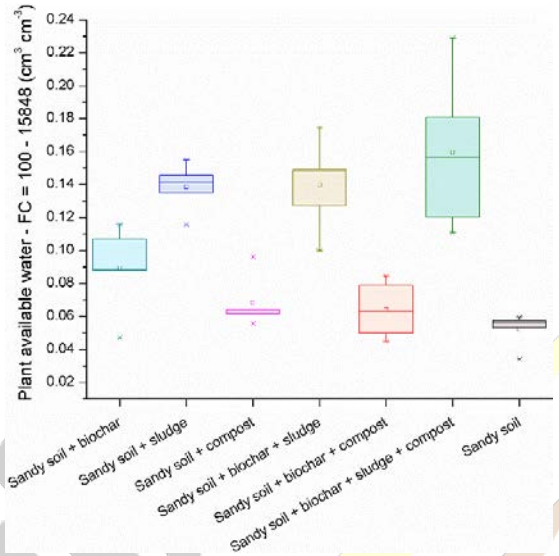

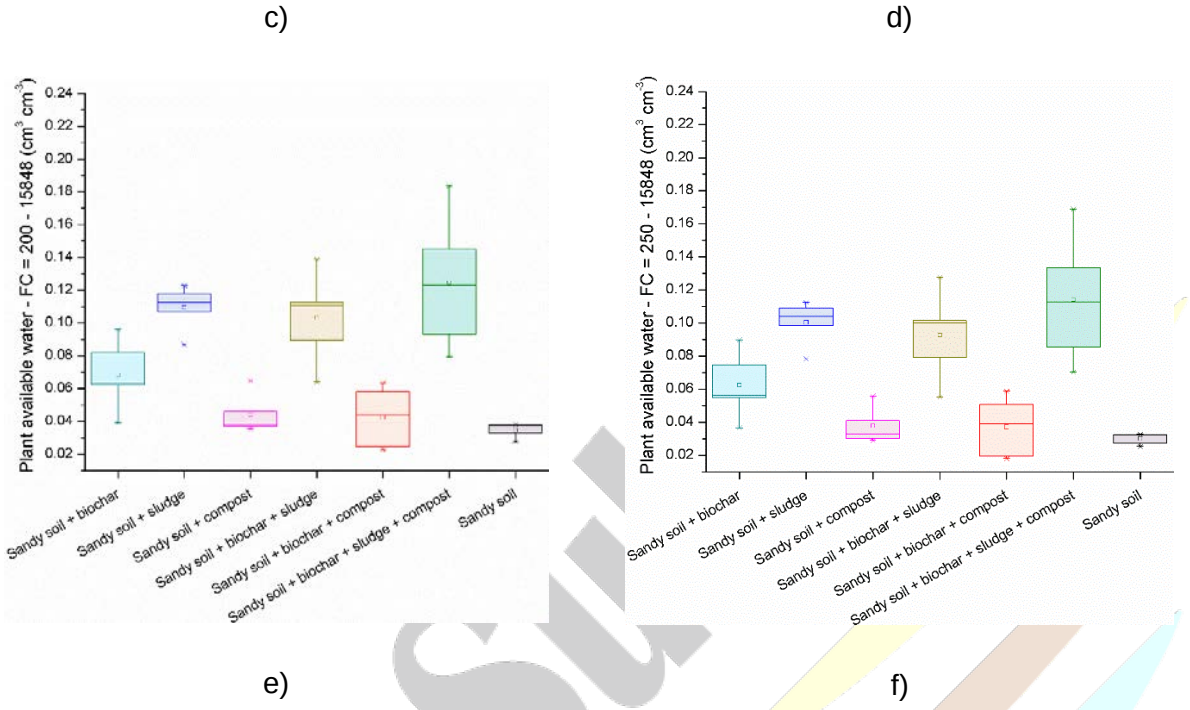

Figure 19. *Distribution of (a–c) field capacity and (d–f) plant-available water (PAW) at pressure heads of –100 cm, –200 cm, and –250 cm, respectively, across sandy soil and six amended treatments. Values are presented as box plots based on five replicates per treatment (n = 5).*

Table 2 provides a concise overview of the most relevant outcomes from the ANOVA and Tukey HSD tests, emphasizing statistically significant treatment differences. Statistical analysis revealed that soil amendment type significantly influenced all examined hydraulic properties, with *p*-values < 0.0001 for nearly every parameter tested (Table 2). Treatments containing sludge and compost, particularly when combined with biochar (F), produced statistically distinct effects on K_s, BD, θ_s, FC, and PAW at all evaluated pressure heads.

K_s varied substantially among treatments (F = 11.97, $p < 0.0001$). Treatments C (compost-only) and E (biochar + compost) showed significantly higher K_s than all sludge-containing treatments (B, D, F), suggesting that sludge additions reduced pore connectivity, possibly through partial blockage of larger pores. In contrast, compost promoted high K_s, likely due to improved macrostructure and reduced compaction resistance.

BD exhibited a clear inverse trend relative to θ_s and PAW, with the lowest BD observed in treatment F, which also had the highest θ_s. The trend was statistically significant (F = 5.46, p =

0.0023), and aligns with the notion that organic matter inputs reduce bulk density, particularly when sludge and compost are co-applied.

For θ_s, treatment F again stood out with the highest values, while pure sand had the lowest. Although the differences were moderate, ANOVA confirmed significant effects (F = 6.06, p = 0.0004), and Tukey tests highlighted significant pairwise differences involving treatment F.

FC increased across all suctions in treatments containing compost and sludge. The effect was most pronounced at –100 cm (F = 19.37, p < 0.0001), where treatment F significantly outperformed nearly all others. As suction increased, differences persisted (FC@200: F = 16.21; FC@250: F = 15.33; both p < 0.0001), indicating that treatment effects extend beyond near-saturation zones, enhancing retention deeper into the pore size spectrum.

PAW showed the strongest treatment responses. Across –100, –200, and –250 cm field capacities, ANOVA results yielded F-values of 14.16, 12.84, and 12.48, respectively (all p < 0.0001). The triple-amended soil (F) consistently showed significantly higher PAW than most other treatments. Interestingly, compost-only (C) treatment, despite having relatively high K_s and moderate FC, exhibited the lowest PAW due to elevated PWP values. This underscores that increases in θ_s or FC alone do not guarantee improved plant water availability — pore size distribution and water retention at PWP play decisive roles.

Table 2. Summary of ANOVA and Tukey HSD results for key soil hydraulic properties across all treatments (n = 5 replicates per treatment), highlighting statistically significant differences (p < 0.05).

Parameter	F-value	p-value	Significant pairwise comparisons (Tukey HSD, p < 0.05)
BD	11.97	<0.0001	A–F, B–C, B–E, B–F, C–D, C–F
K_s	5.46	0.0023	A–F, B–F, C–F
θ_s	6.87	0.0005	A–F, B–C, B–F, C–F
FC @ 100	11.39	<0.0001	A–F, B–E, B–F, C–F, D–F, E–F
FC @ 200	9.42	<0.0001	A–F, B–C, B–F, C–F, D–F, E–F
FC @ 250	8.33	<0.0001	A–F, B–C, B–F, C–F, D–F, E–F
PAW 100 - 15848	14.79	<0.0001	A–F, B–C, B–F, C–F, D–F, E–F
PAW 200 - 15848	11.86	<0.0001	A–F, B–C, B–F, C–F, D–F, E–F
PAW 250 - 15848	9.54	<0.0001	A–F, B–C, B–F, C–F, D–F, E–F

Lysimeter dataset evaluation

Since single-point measurements alone can't fully describe post-amendment soil functioning, a 441-day lysimeter experiment was conducted to assess how biochar, sludge, and compost affect hydraulic responses in amended sandy soil. Continuous monitoring of SWC, soil temperature, and drainage, combined with climatic data, provided a detailed, real-world picture of soil water dynamics.

Water input and potential evaporation

Figure 5a shows daily water input, distinguishing precipitation (black bars) and irrigation (blue bars), alongside cumulative input (red line) over the 441-day experiment. Precipitation was irregular, with several intense events (>20 mm) on days 49, 58, 112, 136, 179, and 421. Total rainfall reached 790 mm. To ensure adequate drainage across treatments, 126 irrigation events were applied (up to 14 mm/day; 42 mm on the first day for dry soil), adding 604 mm. Combined, total water input reached 1394 mm.

Figure 5b presents daily potential evaporation (E_{pot}), which followed a clear seasonal trend—peaking in late spring and summer (up to 5.5 mm/day), and dropping in colder months. Over the full period, E_{pot} totaled 1090 mm, indicating a net positive water balance (input > evaporative demand).

Soil water content dynamics across treatments

Figures 20 and 21 display SWC across treatments, showing clear differences based on amendment type and combination. Some sensor data gaps occurred due to logger or sensor malfunctions; loggers were promptly replaced, though buried sensors could not be accessed.

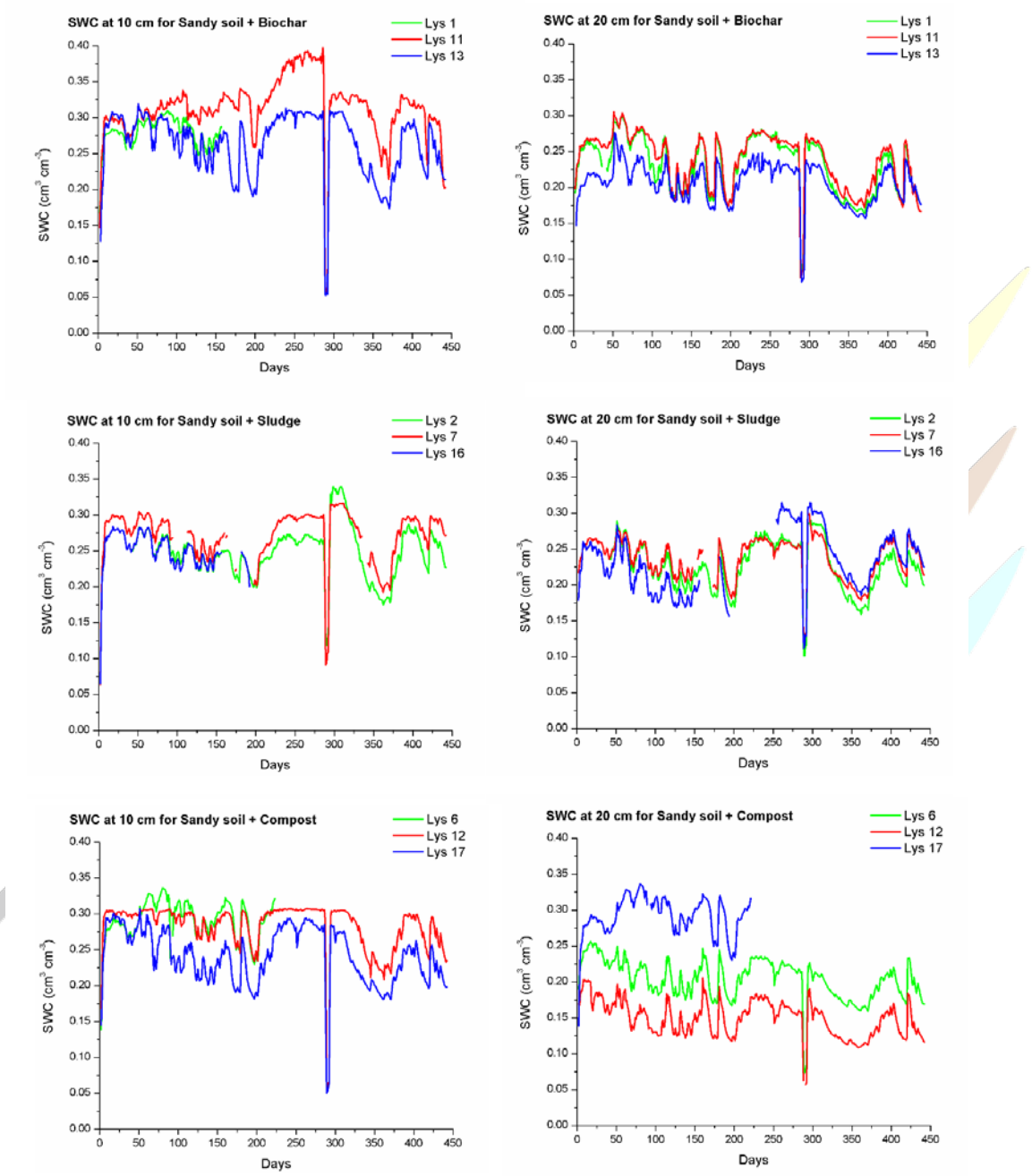

Figure 20. *Soil water content (SWC) (cm^3 cm^{-3}) over the experimental period of 441 days for different soil treatments: sandy soil + biochar (treatment A), sandy soil + sludge (treatment B), and sandy soil + compost (treatment C), at two depths (10 and 20 cm from the bottom of the lysimeters) for the 3 replicated lysimeters. Days of the experiment were shown, whereby the start of the experiment was at 31st of March 2023.*

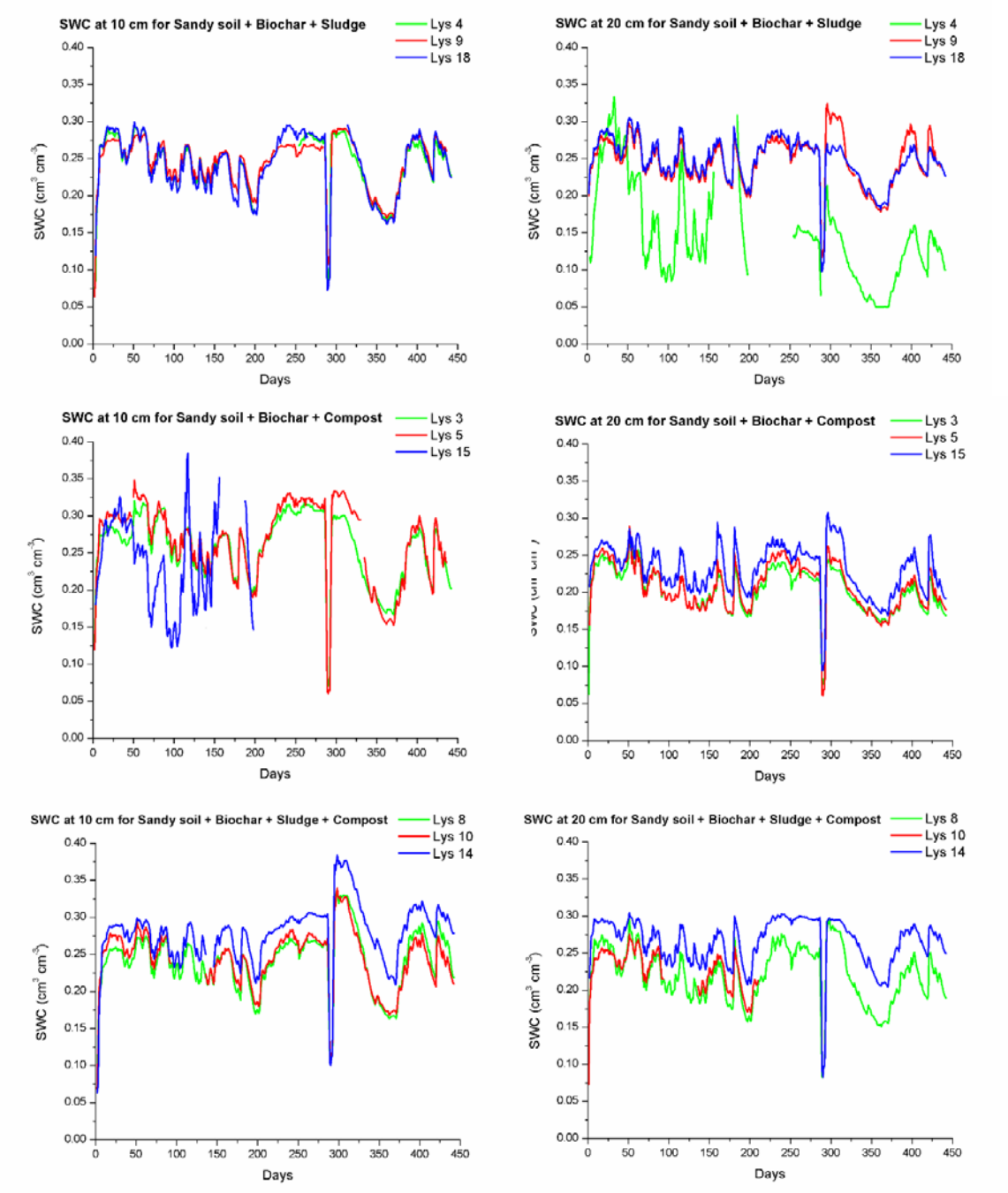

Figure 21. *Soil water content (SWC) (cm^3 cm^{-3}) over the experimental period of 441 days for different soil treatments: sandy soil + biochar + sludge (treatment D), sandy soil + biochar + compost (treatment E), and sandy soil + biochar + sludge + compost (treatment F), at two depths (10 and 20 cm from the bottom of the lysimeters) for the 3 replicated lysimeters. Days of the experiment were shown, whereby the start of the experiment was at 31st of March 2023.*

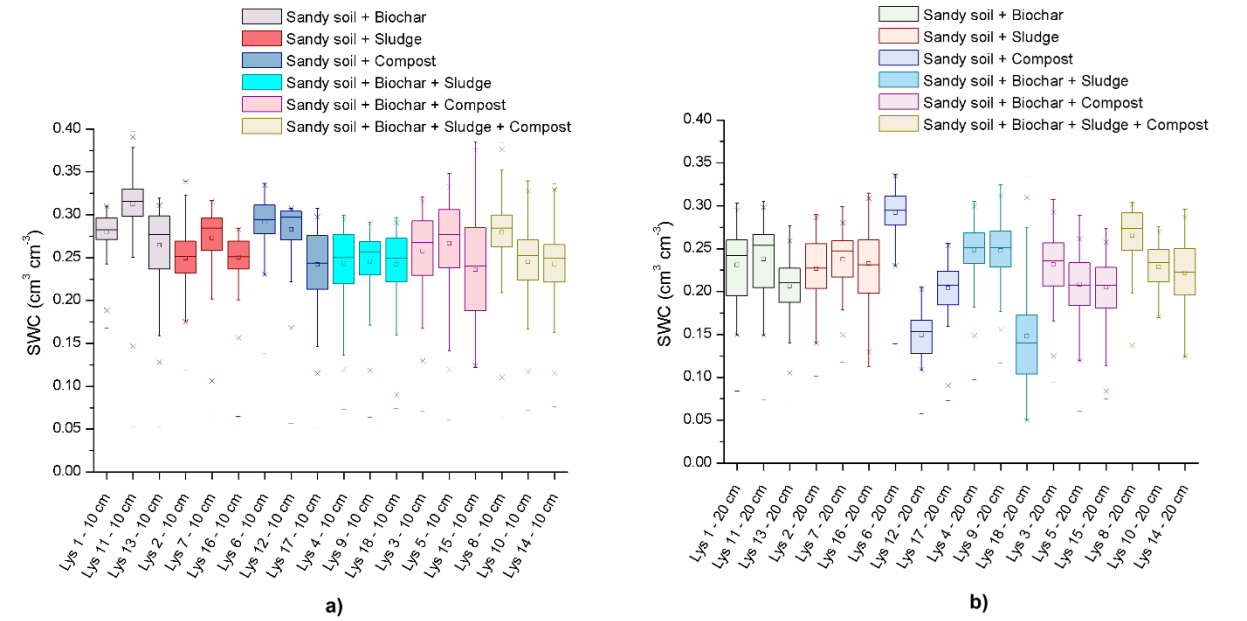

Figure 22. *Box plots for soil water content (SWC) for the different treatments over the 441-day experimental period for: a) measurements at 10 cm from the bottom and b) measurements at the 20 cm from the bottom of the lysimeters.*

Biochar alone (treatment A) showed higher initial SWC than sludge-only (B), confirming its role in enhancing porosity and reducing BD. Combined treatments—biochar + sludge and biochar + compost—generally maintained higher and more stable SWC, likely due to complementary effects of biochar's structure and the organic content of compost and sludge. These amendments enhanced soil structure and water retention under fluctuating conditions.

The triple amendment (F) had the highest and most stable SWC over time, demonstrating a cumulative benefit for water retention and irrigation efficiency in sandy soils. In contrast, biochar-only treatments (A and D) showed more SWC variability, especially at shallow depths, indicating that biochar's benefits are enhanced when used with other amendments. These findings align with previous studies showing compost's improved performance when co-applied with biochar.

Figure 22 presents SWC variability across treatments as box plots. Median values (box lines) show central water retention, while box heights and whiskers reflect variability. Clear differences emerged between measurements at 10 cm and 20 cm depths.

At 10 cm (Figure 22a), SWC values were generally higher and more stable across treatments, likely due to gravitational water accumulation. Combined treatments—especially D (biochar + sludge) and E (biochar + compost)—showed higher and more consistent SWC, indicating effective water retention in the lower lysimeter zones, beneficial during dry periods.

At 20 cm (Figure 22b), SWC values were lower and more variable. Biochar-only treatments showed wider interquartile ranges, suggesting that while biochar improves retention, it may also introduce variability when applied alone.

Treatment F (biochar + sludge + compost) showed the most consistent and stable SWC across both depths, with narrow IQRs and high medians. This reflects a cumulative effect, where biochar's porosity, sludge's fine particles, and compost's organic matter create a well-balanced structure with uniform water retention. Such stability supports deeper root growth and reduces irrigation needs.

Impact of amendments on drainage

Figure 23 shows the total measured drainage sampled at the bottom of the lysimeters. The data show that biochar, sludge, and compost had differing impacts on total drainage. Treatments involving biochar (A, D, E, and F) tend to reduce cumulative drainage, as indicated by the downward shift (blue dashed line), suggesting enhanced water retention and also higher water return to the atmosphere (higher actual evaporation) in sandy soils.

The "sludge effect" (red dashed line) showed reduced drainage and implied higher actual evaporation, especially when combined with biochar (treatment D). The "compost effect" (green dashed line) also reduced drainage moderately, though results varied with combination (treatments E and F). These patterns highlight how specific amendments influence not only hydraulic properties but also broader soil functioning—key for optimizing water storage and evaporation in sandy soils.

Figure 24 confirms that treatments with biochar—especially when combined with sludge and compost (D, E, F)—consistently reduced cumulative drainage compared to sludge- or compost-only treatments. The triple mix (F) showed the lowest drainage, demonstrating the additive benefits of combining amendments. In contrast, treatments B (sludge only) and C (compost only) showed higher drainage, underscoring their limited retention capacity when used alone.

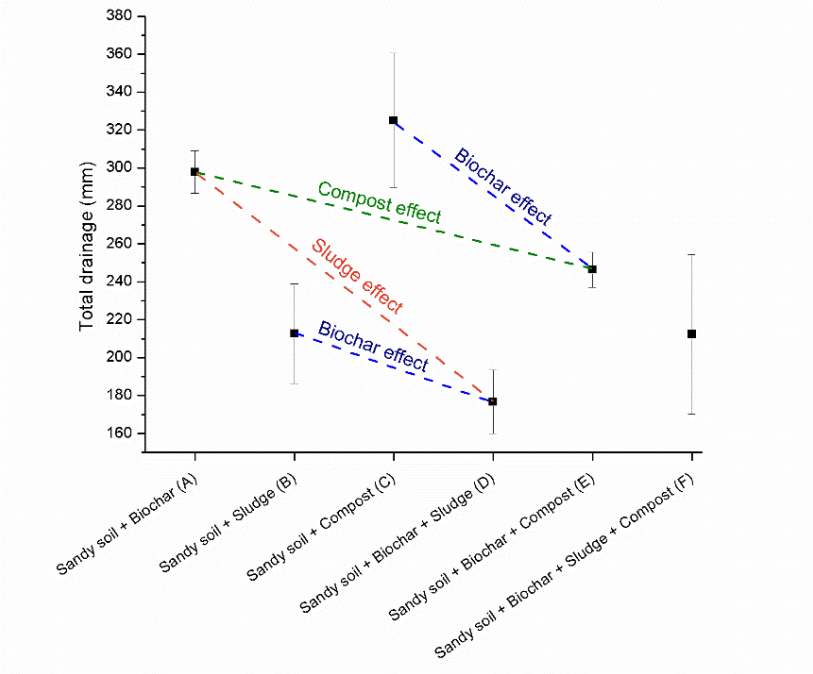

Figure 23. *Cumulative measured drainage (mm) after 441 days of the experimental period for the different soil treatments (n = 3 for each treatment)*

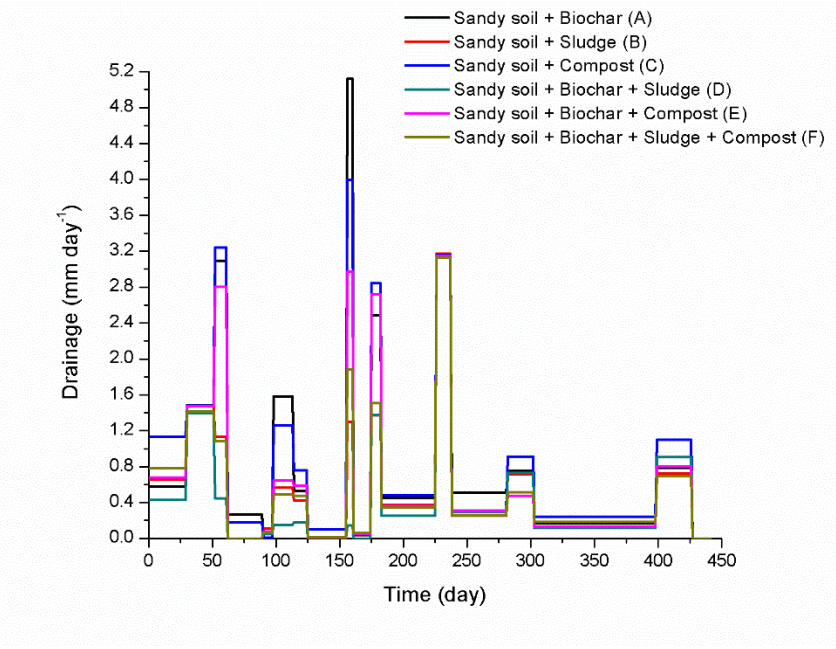

Figure 24. *Average daily drainage (mm day^{-1}) of the different sampling periods for the different soil treatments (n = 3 for soil treatments).*

Biochar's ability to improve pore connectivity and reduce bulk density likely contributed to its role in lowering drainage. When combined with sludge—rich in clay—water retention further stabilized, as seen in treatments D and F. Compost alone had moderate drainage-reducing effects, enhanced when co-applied with biochar and sludge. These complementary effects were strongest in treatment F, which showed the lowest drainage and most consistent water retention, emphasizing the benefits of combining amendments in sandy soils. These results also highlight trade-offs: compost improves structure and buffers SWC, while biochar offers long-term porosity and drainage control. Their combined use enhances soil resilience and should be tailored to specific water management goals.

Drainage spikes on days 49 and 179—coinciding with intense rainfall (Figure 5a)—suggest minor overflow in sampling bottles, though efforts minimized this risk. Any overflow was negligible and does not affect the overall validity of the results, which clearly show amendment-driven improvements in soil water retention under variable conditions.

Water balance

Next, water balance was calculated for each lysimeter using input (precipitation + irrigation), drainage, and soil water storage (from SWC data). Actual evaporation was derived as the residual in the balance. Figure 25 illustrates how amendments influenced infiltration, drainage, storage, and evaporation.

Table 4. Results of ANOVA and Tukey HSD tests showing significant pairwise comparisons for drainage, storage, and actual evaporation.

Variable	ANOVA *F*-statistic	ANOVA *p*-value	Significant pairwise comparison (Tukey HSD)	Mean difference (range)	*p*-value (adjusted)
Drainage	13.18	0.0002	A vs C, A vs E, B vs D, B vs E, D vs F	-126.84 – 98.59	0.0005 – 1.0000
Storage	2.31	0.1086	-	-10.75 – 10.73	0.3070 – 1.0000
Actual evaporation	10.50	0.0005	A vs C, A vs E, B vs D, B vs F, C vs E, D vs E, D vs F, E vs F	-88.74 – 126.94	0.0009 – 1.0000

ANOVA and Tukey HSD were applied to identify statistically significant differences in these components. While storage showed no significant variation, drainage and actual evaporation

differed notably across treatments (Table 4). ANOVA confirmed significant variation in drainage ($F = 13.18$, $p = 0.0002$), with Tukey HSD highlighting reductions in biochar-amended treatments—especially when combined with sludge or compost—underscoring their effect on water movement through the soil.

Treatment F (biochar + sludge + compost) consistently showed the lowest cumulative drainage, confirming the synergistic effect of combining amendments to reduce water loss. Compared to treatments A (biochar only) and C (compost only), the combined approach proved significantly more effective, reflecting biochar's hydraulic properties and the structural benefits of sludge and compost.

The storage term (SWC), shown as a negative value in Figure 8 to indicate retained water, varied among treatments but was not statistically significant ($F = 2.31$, $p = 0.1086$). However, trends from Tukey HSD suggest treatments D, E, and F supported greater storage stability—consistent with observed improvements in pore connectivity and organic content.

Cumulative actual evaporation differed significantly among treatments ($F = 10.50$, $p = 0.0004$). Tukey HSD showed that treatments with combined amendments, especially F, had moderate evaporation levels, effectively balancing retention and atmospheric loss. This highlights the value of integrating biochar with other organics to optimize soil water use while minimizing evaporation.

Treatment B (sludge only), used as a reference for assessing biochar and compost effects, showed intermediate drainage and storage, validating sludge's contribution to water retention. Treatments without sludge (A, C, E) had higher drainage, despite slight storage increases, indicating lower retention efficiency. Biochar's role was evident in reduced drainage in treatments B vs. D and C vs. E. Since water storage varied only slightly, higher actual evaporation in non-biochar treatments likely reflects less effective retention.

These findings align with known biochar properties—enhancing porosity and water retention by increasing microporosity and improving pore size distribution. Sludge and compost complement biochar: sludge adds structure via its semi-clay content, while compost buffers SWC fluctuations and helps reduce evaporation through surface insulation. This explains why treatment F (biochar + sludge + compost) showed lower evaporation than treatment D (biochar + sludge).

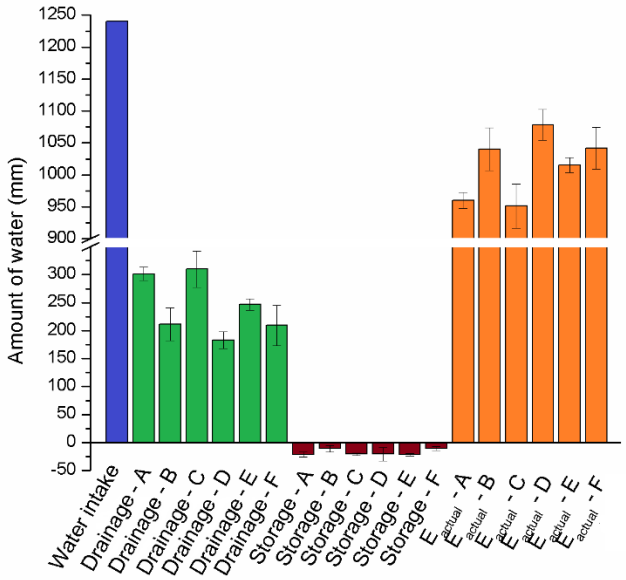

Figure 25. *Water balance components (infiltration (water intake), drainage, storage, and actual evaporation) for the different soil treatments (sandy soil + biochar (A), sandy soil + sludge (B), sandy soil + compost (C), sandy soil + biochar + sludge (D), sandy soil + biochar + compost (E), and sandy soil + biochar + sludge + compost (F)).*

Water balance results highlight biochar's role in reducing drainage and evaporation when added to sludge-amended soil, as seen when comparing treatments B and D. Strong correlations were observed between soil hydraulic properties and drainage: K_s (R^2 = 0.92), FC at –100 cm (R^2 = 0.66), and PAW (R^2 = 0.83), confirming that parameters like K_s, FC, and PAW are effective indicators of soil hydrological performance. Overall, combining biochar with other organic amendments offers a promising strategy to address the hydraulic limitations of sandy soils, improve water management, and support sustainable agriculture—especially in water-scarce regions.

AgroC Simulation Outputs

The AgroC model simulations provided a comprehensive perspective on how different organic soil amendments affect the water balance and productivity of sandy soil under field-relevant conditions. Simulations were carried out for one full winter wheat growing season, incorporating

all measured soil hydraulic properties (see Figures 21, 22, 23 and 24) and 10 years of local climate data (see Figure 12). Output of AgroC simulation is presented as plots on Figure 26. The model was run under the assumption of no nutrient stress, allowing isolated assessment of hydrological influences.

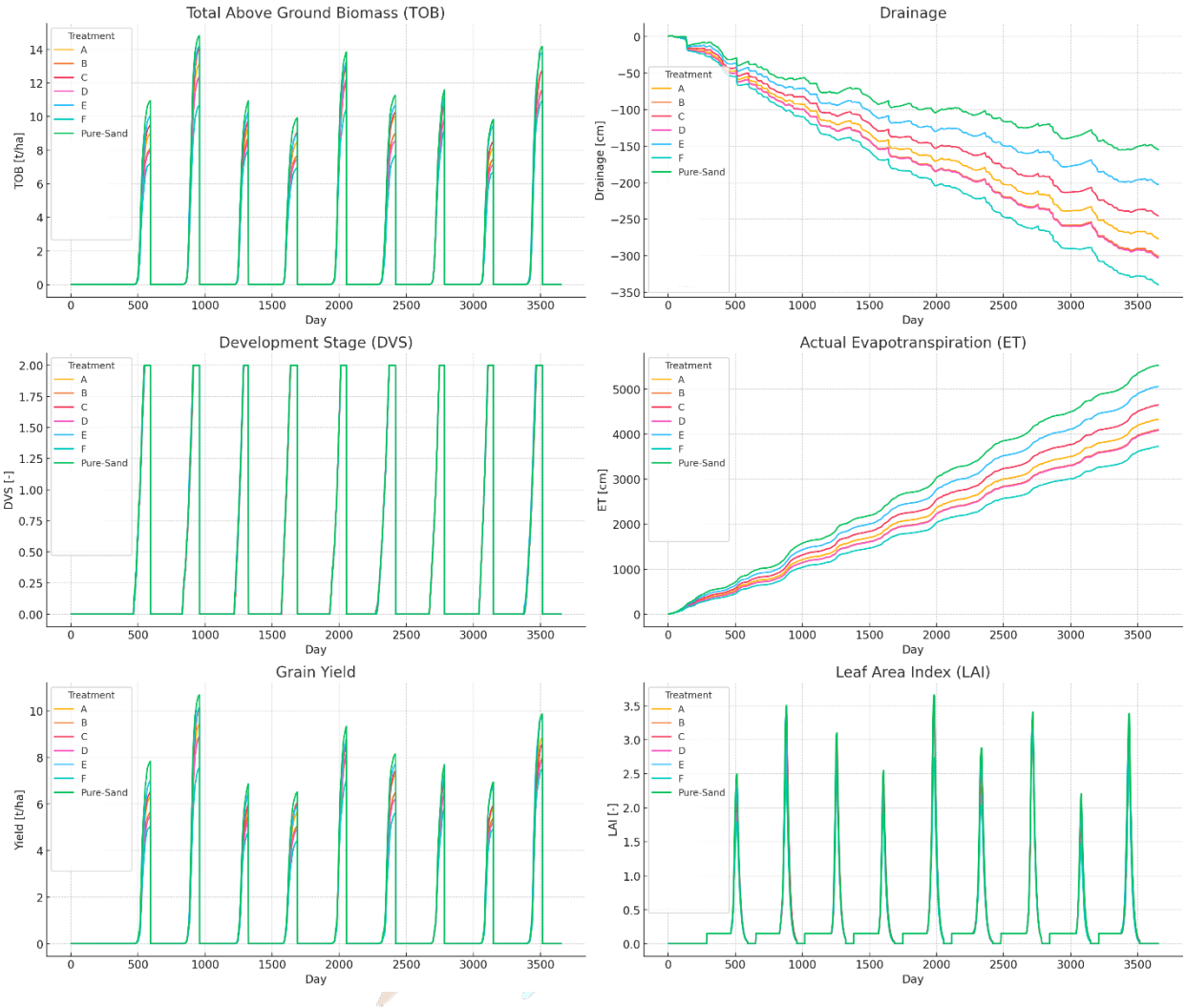

Figure 26. *AgroC-simulated crop and water dynamics in sandy soil and amended treatments over 10 years (no nutrient limitation scenario)*

The analysis focused on several key outputs:

- Grain yield
- Drainage
- Actual transpiration (T_{act}) and evaporation (E_{act})

- Water stress duration
- Leaf area index LAI

Drainage and Actual Evapotranspiration

Over the 10-year simulation, cumulative drainage varied clearly across treatments. Pure sand had the highest drainage due to its coarse texture and low water-holding capacity. All amended soils significantly reduced drainage, with the greatest reductions in treatments C, E, and F—those containing compost. These results align with lab-measured increases in θ_s and PAW. However, in highly retentive soils like F, reduced drainage may have led to poor aeration or slower drying, affecting crop performance. Actual evapotranspiration (ET_{act}) increased over time across all treatments. Surprisingly, pure sand had the highest ET_{act}, likely due to rapid drainage and frequent but short-lived water availability supporting root activity. Treatments F and D showed the lowest ET_{act}, suggesting reduced water use—possibly from waterlogging or limited root development. Treatments B and C showed moderate ET_{act}, indicating more favorable water balance. These results highlight that while retention is beneficial, excess moisture can limit plant uptake in the absence of nutrient stress.

Grain Yield and LAI

Grain yield was the most telling model output. Surprisingly, pure sand produced the highest yields (5.2–8.0 t/ha), due to the simulation's nutrient-stress-free conditions—despite the soil's poor natural fertility. Among amended soils, treatment E (biochar + compost) had the best yields, followed by C (compost only). Treatment F (biochar + compost + sludge), despite its high water retention, showed the lowest yields (3.5–4.1 t/ha), likely due to reduced root oxygen availability and limited transpiration under excessive moisture. These findings underline the importance of coupling water and nutrient dynamics—high retention alone doesn't ensure high productivity.

Leaf area index (LAI) trends mirrored yield and biomass results. Pure sand showed the highest peak LAI (>3.0), indicating rapid canopy growth. Treatments C and E had strong LAI responses, while F consistently lagged, suggesting suppressed photosynthesis due to wet conditions or poor aeration. Lower LAI directly limited light capture and grain production, consistent with observed yield patterns.

Water Stress Duration Across Treatments

Water stress duration, as expressed through the mean water stress coefficient (α-average) over the simulation period, provides critical insight into the availability of extractable water in the root zone. In the AgroC simulations, this indicator effectively captured how each soil mixture modulated plant-available water under long-term climatic forcing and hydrological response.

The pure sand treatment, despite its low retention capacity, showed relatively low average water stress values, suggesting that water was frequently replenished and rapidly accessible to plants. Its high drainage rate prevented prolonged saturation while maintaining a dynamic equilibrium between infiltration and root uptake. As a result, even though water passed quickly through the profile, it aligned well with the crop's uptake rhythm, leading to minimal water stress accumulation. In contrast, treatments with higher retention (especially F and D) experienced longer cumulative periods of water stress, despite their larger storage potential. This counterintuitive result is likely linked to reduced root water uptake under high moisture conditions due to limited oxygen diffusion, and possibly slower drying cycles in the soil profile. The retained water may not have been physiologically available when needed, especially during critical crop stages such as heading and grain filling. The combination of biochar, compost, and sludge in treatment F resulted in the highest and most persistent water stress, which aligns with its poor performance in yield and transpiration.

These findings highlight a nuanced interplay: water retention alone is not sufficient—the timing and physiological availability of water are key. High PAW values do not guarantee low stress if hydraulic conductivity, aeration, or drying dynamics restrict timely root uptake. Additionally, because AgroC was run under no nutrient limitation, this water stress signal can be considered isolated from competing nutrient-induced effects.

MOBILITY REPORT – 3 week visit to Forschungszentrum Jülich, Jülich, Germany

Researchers: Prof. Dr. Snežana Maletić, Dr. Tamara Apostolović, UNSPMF

Assigned supervisors: Prof. Dr. Lutz Weihermüller, Prof. Dr. Roland Bol, FZJ

Duration of the visit: 13.01.2025. - 31.01.2025.

Executive Summary

The main purpose of the visit to Forschungszentrum Jülich was to acquire new knowledge and skills regarding sophisticated techniques used for soil characterization and soil organic matter dynamics and element cycles. Part of the training was specifically focused on the analytical methods for the detailed characterization soils layers using state-of-the-art instrumental techniques. These techniques included the use of advanced instruments such as inductively coupled plasma mass spectrometry (ICP-MS) and multi-collector inductively coupled plasma mass spectrometry (MC-ICP-MS), as well as techniques such as are such as flow field fractionation (AF4, SPLITT). The second part of the training was focused on acquiring knowledge and skills in designing and carrying out large-scale lysimeter experiments, by visiting several experimental sites.

Introduction

Background

Soil organic matter (SOM) dynamics encompass the processes through which organic materials are introduced, decomposed, and transformed within soil systems. SOM is vital for maintaining soil fertility, regulating nutrient cycling, and enhancing carbon sequestration. Soil microorganisms, including bacteria and fungi, decompose organic inputs, facilitating the release of essential nutrients such as nitrogen, phosphorus, and sulfur, which subsequently become available to plants. Key research objectives related to SOM and nutrient cycling include: (i) Gaining insights into the origin, residence time, cycling, and priming effects of organic matter and nutrients (e.g., N, P, K, Ca, Si, Fe) within the soil-plant system and their potential movement into surface and groundwater; (ii) Enhancing understanding of complex carbon and nutrient biogeochemical

processes and interactions at both field and laboratory scales; (iii) Applying innovative technologies to assess the effects of natural and anthropogenic factors on biogeochemical cycles; (iv) Collecting field and laboratory data to support sustainable system management, by integrating findings into a holistic systems biogeochemistry framework. The focus of the visit was learning about sophisticated techniques to study soils. This involves techniques such as ICP-MS and MC-ICP-MS, along with field flow fractionation methods like AF4 and SPLITT.

Lysimeter experiments are a cornerstone of soil science research, providing valuable data on water and solute movement through soil profiles under natural or controlled conditions. They allow researchers to directly measure leachate volumes and analyze nutrient and contaminant fluxes, which is essential for understanding nutrient cycling, pollutant transport, and the environmental impact of agricultural practices. By replicating realistic field scenarios, lysimeters help validate models and inform sustainable soil and water management strategies.

Scope of the secondment

The visit to Forschungszentrum Jülich aimed to enhance expertise in advanced techniques for soil characterization, with a particular focus on soil organic matter dynamics and elemental cycling. The training involved hands-on experience with cutting-edge analytical tools, including ICP-MS, MC-ICP-MS, and field flow fractionation methods (AF4, SPLITT), for in-depth analysis of soil layers. Additionally, the visit provided valuable insights into the design and implementation of large-scale lysimeter experiments through site visits and practical demonstrations. Overall, the visit supported capacity building in both laboratory and field-based approaches essential for studying complex soil processes and supporting sustainable land management.

Content

PART I: Laboratory training

Field flow fractionation (FFF) – (AF4, Postnova Analytics, Landsberg, Germany)

Colloidal organo–mineral associations play a key role in the preservation of soil organic matter (OM) and typically exist in two forms: (i) as water-dispersible, potentially mobile particles (free colloids) and (ii) as structural components within soil microaggregates (occluded colloids). These free and occluded colloids can be size-separated using asymmetric flow field-flow fractionation (AF4). AF4, when coupled online with various detectors—including inductively coupled plasma

mass spectrometry (ICP-MS), organic carbon detector (OCD), ultraviolet (UV) detector, and dynamic light scattering (DLS)—enables detailed characterization of natural colloidal particles. The separation in AF4 is based on particle size or molar mass, following the principles of asymmetrical flow field-flow fractionation. This process takes place in a thin, ribbon-shaped channel formed by clamping a spacer between a porous and a nonporous plate, as illustrated in Figure 1.

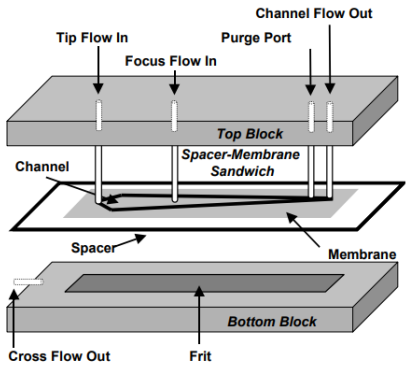

Figure 1. Schematic of the asymmetrical flow FFF channel

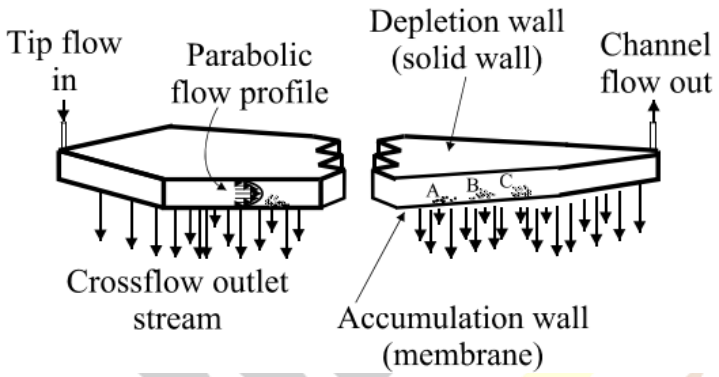

Figure 2. Separation mechanism of asymmetrical flow FFF

In asymmetric flow field-flow fractionation (AF4), the carrier liquid entering the channel splits into two flows: a longitudinal channel flow and a perpendicular crossflow. The parabolic channel flow moves the sample down the channel, while the crossflow, directed through a porous membrane (the accumulation wall), pushes particles toward this wall. Once at the wall, particles establish equilibrium layers based on their size and diffusivity. Smaller or more diffusive particles extend further into the faster flow regions and elute earlier, while larger particles remain near the wall, moving slower and eluting later. This differential movement enables the separation of components. As illustrated in Figure 2, components A, B, and C are separated based on their proximity to the accumulation wall and corresponding flow velocities.

Analysis preparation

- Prepare fresh FFF eluent (25 |M NaCI; 1.461 g NaCI/L) and if necessary, OCD solution (K2S208 2.5 g/5 L; concentrated H3PO4: 20 mL/5 L; do not change/refill during measurement) using MiliQ water
- Clean channel and use new membrane
- Change all filters (check eluent flow direction)
- Correct 'Loop' for your method installed?

- Reboot the computer before a new measuring campaign (help to prevent software bugs)

Detectors

UV

- Switch on lamp at least 30 min before measurement o
- func. -> enter -> func. -> func. -> lamp: 1

OCD

- Switch on about 3-4 h before measurement -> baseline should be stable
- Make sure that there is enough solution for acidification of the OCD (do not refill during measurement)
- Connect to FFF onlv shortly before measurement
- Please always disconnect FFF from OCD after measurement and insert plug

Figure 3. FFF-UV-OCD

Software

New sequence

Open 'Basic Run' -> Load 'Method' that was previously created

- Determine number of samples -> Set 'End Position' to the number of samples
- Then press 'Create

(For single samples if you just want to use an existing sequence as a basis):

- File -> new -> sequence
- In the 'Sequence' window -> click on empty 'run' field - 'Open run' -> load run file
- Press 'Show run' -> Check 'Auto'
- then change the name of the sample -> if you press 'next' (bottom left) you get to the next sample and can change the name here
  When you are finished press 'Save/Exit'
- Then save the entire sequence
- To change the autosampler position of the sample press 'Vial'

- Before starting the measurements, the settings of the flows of the used method should be pre-set -› 'Run' -> show run -> In the 'Method' window -> 'preset flows' (center left
- If you want to change the method of all samples again you should create a new method and reload it under 'basic Run'
- If you only want to change something for single samples you can click on Method in the list and then change the method for single samples
- Before each measurement the settings of the autosampler should be checked again (e.g., does the used tray match the settings etc.).
- You can cool the autosampler -> useful for long measurements

Troubleshooting:

1. back pressure is too low: can be increased by the length of the red capillary - the longer the higher the pressure (pressure becomes even higher after coupling with detectors, e.g., ICP-MS or OCD)
2. reset the pumps: Press the button at the bottom right and then turn the wheel at the bottom right to the left until it stops, then press the button at the top. You also must reset in the software -› Tools -› Interface -> K hloen Pumps -> Reset
3. strange signs on the pump display: everything must be restarted
   a. Turn off ALL devices at the back of the switch
   b. Close software
   c. Switch on the devices at the back of the switch
   d. Restarting the software
4. pressure is unstable -> check valves of pump heads (tip and focus pump) in ultrasonic bath (approx. 5 min in 2 % EtOH) -> see FFF manual

Preparation of separation channel/filter/loop

Channel (figure 4):

- Unscrew channel from AF4 - › Pump flow all to 0 mL/min

- Loosen screws: Loosen the screws from the outside to the inside

- Tighten screws: Tighten the screws from inside to outside (with a torque wrench)

Figure 4. Preparation of the membrane of the separation channel/filter/loop

- Cut the membrane (to size (29.5 x 3.4 cm) -> Cut slightly larger than the frit, but must not protrude over the seal
- Place the membrane in Milli-Q overnight or rinse the instrument for 2-3 hours (at 0.5, 0.5, 0.5)
- Assembly: aluminium top plate with screws - top plate - spacer - membrane (shiny side up) - frit - bottom plate with sealing ring - metal plate with screw thread
- Rinse everything with Milli-Q and then screw it back together again -› Caution Frit may fall out

-Vent the channel: 1. screw in Out port for detector, 2. screw in Focus Port and purge with Focus pump (press buttons ^ and < simultaneously) until there is no more air in the channel, 3. turn Purge Port, 4. fill the channel with Focus "Purge" until there is no more air in the channel and then turn Tip Port and Cross Flow Port in

Filter:

- Open with 23" wrench - Pay attention to the direction of the running medium
- Structure: screw - metal nut with "-›" - membrane - frit – screw
- Both screws should be in the middle of the metal nut (do not tighten one first and then the other, but both at the same time and then tighten)
- To purge the two filters press "Purge" without entering the system (or simply rinse the system 2-3 hours before measurement at 0.5, 0.5, 0.5)
- Filter holders should be cleaned in an ultrasonic bath from time to time -> 2 % EtOH for 5 min

Loop:

- Pay attention to correct loop
- Purge new loop by purging the tip pump -> Flow rate of the pump must be 0 mL/min (or simply run the system for 2-3 hours at 0.5, 0.5, 0.5)
- Test if the loop is vented: Tools -> Interface -> Autosampler -> 'manual washing' until the loop is filled - test if there is still air in the loop by switching 'injection valve' between 'inject and 'load' -> if the pressure drop is > 1 bar then there is still air in the loop

Leakage test:

- Tip, Focus, & Cross: 0.5 ml/L -> run for 10 min -> the purge valve must be closed
    - back pressure should be between 6-9 bar
- Then test method pressures -› Preset flows

Rinse system -> Open purge valve

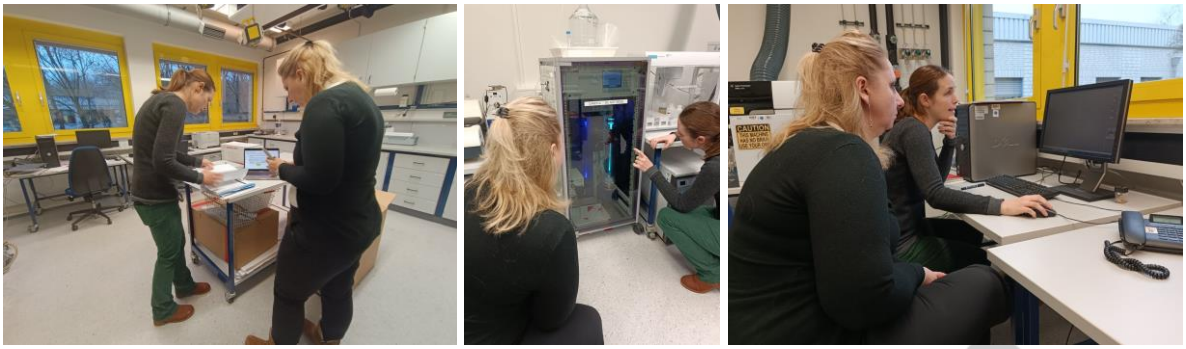

Figure 5. Sample analysis with FFF

FFF-DLS

Dynamic Light Scattering (DLS, figure 6) detectors provides detailed, quantitative size distributions and structural information, sampled over large ensembles, for good statistical robustness. It is based on the Brownian motion of particles - this states that smaller particles move faster, while larger ones move slower in a liquid. The light scattered by particles contains information on the diffusion speed and thus on the size distribution. Dynamic light scattering enables the analysis of particles in a size range from 0.3 nm to 10000 nm.

Figure 6. FFF-DLS

Standard Operation Procedure FFF-DLS coupling

- Use the flow cuvettes
    - Connect the flow cuvette with the tube coming from the UV-detector
    - Be careful with the inlet and outlet - inlet right side, outlet left side o 1 tube into waste (the long tube)

    - insert the cuvette into the DLS (arrow on cuvette should be located right hand side on the front) - the cuvette tubing should exit at the side
- start the UV detector
- start the DLS
- Only 1 sample at the time can be measured > label the sample manually within the DLS software, as there is no communication between the DLS and the FFF software
- Prepare FFF and us the method that was also used for normal FFF measurements
- only 1 sample in the sequence
- Open Zetasizer software
    - Select -> flow cuvette
      Browse for SOP (use existing one or create new one)
    - Example SOP for small natural colloids:
    - Measurement type: flow
    - Material: clay_smaller_022
    - Temperature: 19 °C
    - Cell: flow cell
    - "Measurement: change time - must be if the time of method
    - Safe SOP
- Browse for SOP -> open SOP
- Measurement -> start online window
- In the FFF software start the run
  When the FFF injection starts start DLS measurement in the Zetasizer software

ICP-MS

ICP-MS (inductively coupled plasma-mass-spectrometry, figure 7) is a technique to determine low-concentrations (range: ppb = parts per billion = µg/l) and ultra-low-concentrations of elements (range: ptt = parts per trillion = ng/l). Atomic elements are lead through a plasma source where they become ionized. Then, these ions are sorted on account of their mass. The advantages of the ICP-MS technique above AAS (Atomic Absorption Spectroscopy) or ICP-OES (inductively coupled plasma optical emission spectrometry) are: (i) Extremely low detection limits; (ii) A large linear range and (iii) Possibilities to detect isotope composition of elements.

Figure 7. ICP-MS

Particle Size analyzer LA960, Horiba

The principle of laser diffraction is the relationship that exists between light scattering (its angle and intensity) and particle size (figure 8). The larger the particle, the smaller the angle and the higher the intensity of the scattering. The device does not directly measure the size of the particle but the angle and intensity of light scattering from the particles. This data is entered into an algorithm that uses the Mie scattering theory to yield information about the particle size from the data on light scattering. Size measurement can only be reliable if the data on light scattering is good. The analyzer is therefore designed to acquire the best data from what is available, which is then sent to the algorithm that makes use of it to produce a particle size distribution.

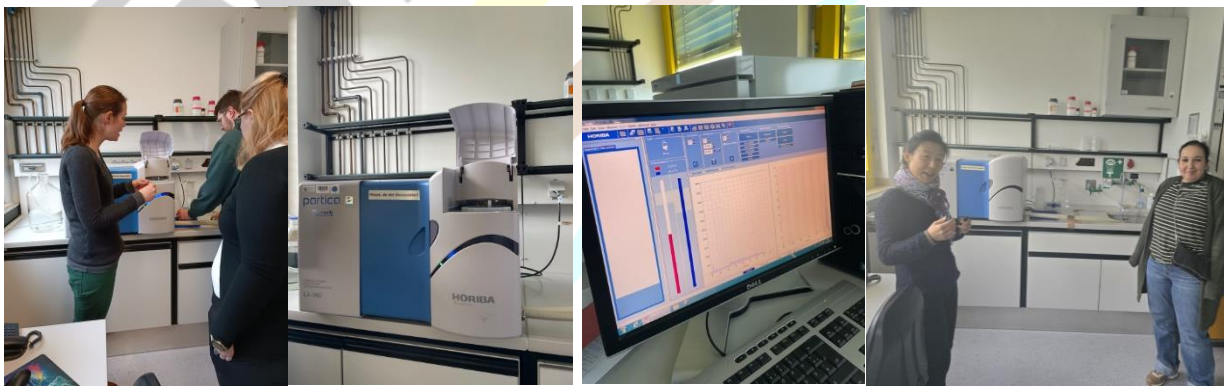

Figure 8. Particle size analyzer LA960, Horiba

MC-ICP-MS

Multicollector Inductively Coupled Plasma Mass Spectrometry (MC-ICP-MS, Figure 9) is an advanced analytical technique widely used for high-precision and high-accuracy isotopic analysis across a broad range of elements. It integrates two key components: an inductively coupled plasma (ICP) source for ionization and a multicollector mass spectrometer for simultaneous isotope ratio measurements. The sample, usually in liquid form, is introduced into the ICP, which generates a high-temperature plasma that vaporizes and ionizes the sample, producing positively charged ions. These ions are then directed into the mass spectrometer, where they are separated based on their mass-to-charge ratio (m/z). Unlike conventional ICP-MS systems that typically rely on a single detector, MC-ICP-MS uses multiple detectors (collectors) to measure different isotopes simultaneously. This capability enables highly precise isotope ratio determinations, making the technique particularly valuable in fields such as geochronology, geochemistry, and environmental science. A major advantage of MC-ICP-MS is its ability to analyze elements with high ionization potentials—elements that are often challenging to measure using Thermal Ionization Mass Spectrometry (TIMS). Furthermore, the ICP source allows for flexible sample introduction methods, accommodating both aspirated solutions and aerosols generated by laser ablation.

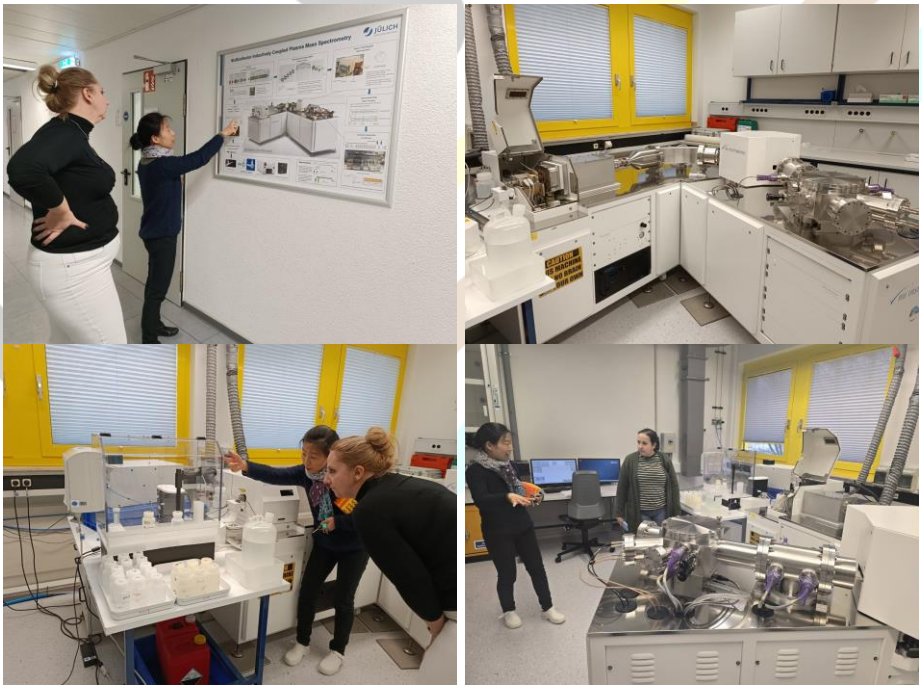

Figure 9. MS-ICP-MS

Fundamental Principles of MC-ICP-MS: As a hybrid mass spectrometer, the MC-ICP-MS integrates an ICP ion source, an energy filter, a magnetic sector mass analyzer, and an array of collectors for ion detection. When the sample is introduced into the plasma, electrons are stripped from the atoms, creating positive ions. These ions are then accelerated across an electric potential of up to 10 kV and focused into a coherent ion beam using electrostatic lenses and slits. This ion beam passes through an energy filter, ensuring a consistent energy profile, before entering a magnetic field where the ions are separated according to their mass-to-charge ratios. The resulting mass-separated ion beams are directed into individual collectors, where the ions are converted into voltages. Isotope ratios are determined by comparing the voltages recorded by each collector. To achieve the high level of precision (often in the range of 0.01–0.001%), the instrument's electronic systems must operate with extremely tight tolerances. Additionally, a high vacuum is maintained along the ion beam path to prevent ion scattering due to collisions with air molecules.*Data Collection, Results and Presentation.* Measured isotope ratios must be properly corrected for all instrumental biases, including mass fractionation. Once corrected, these ratios are suitable for plotting in any diagrams requiring atomic ratios (e.g., isochron, concordia, etc.).

PART II: Visiting FZJ experimental sites

During the second half of the secondment, three specialized research platforms affiliated with Forschungszentrum Jülich were visited. These excursions provided direct exposure to advanced infrastructure for monitoring soil-plant-atmosphere interactions across different spatial and temporal scales. The visits included presentations, guided tours, and in-field discussions with researchers, enabling participants to connect theoretical modeling with real-world applications.

AgraSim Platform (January 17, 2025)

The AgraSim facility is a state-of-the-art experimental platform at IBG-3 designed to simulate controlled environmental conditions and study soil–plant–atmosphere processes in a reproducible way. During the visit, the upper and lower components of the system were shown (Figure 10), including:

- Plant growth chambers and soil containers
- Sensors and control units located in the substructure
- Automated irrigation, climate regulation, and drainage control systems

Figure 10. AgraSim: plant growth chambers (left) and substructure control systems (right)

The control room provided an overview of how the entire system is monitored and regulated. Presenters explained the original design philosophy behind AgraSim, highlighting its role in testing scenarios of future climate conditions, root-zone dynamics, and interactions between soil amendments and plant performance.

In addition to the AgraSim facility, the group was also given a tour of the soil physics laboratory at IBG-3 (Figure 11). While not directly tied to AgraSim, the lab presented complementary methods and instrumentation used to analyze soil physical properties, including retention characteristics, porosity, and infiltration behavior under controlled settings.

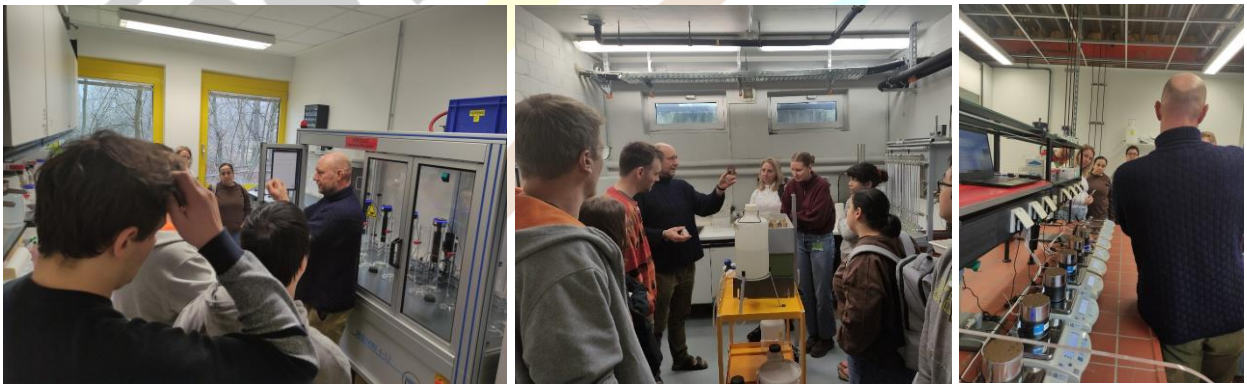

Figure 11. Laboratories for sample preparation and texture determination

Selhausen Minirhizotron Field and Lysimeter Station (January 17, 2025)

The Selhausen experimental field is part of the "CropSense" and "RhizoTraits" research initiatives, focusing on non-invasive monitoring of root system architecture and rhizosphere processes (Figure 12). The visit included a comprehensive tour of the minirhizotron facility, where underground imaging tubes and high-resolution cameras are used to track root growth dynamics in real-time. Researchers explained how the data collected from root imaging is integrated with crop development models and environmental parameters. Interdisciplinary collaboration with plant physiologists, remote sensing experts, and modelers was emphasized as a key aspect of the platform.

Following the minirhizotron demonstration, the group visited the lysimeter station and multi-system weather station, also located at the site. This portion included:

- Inspection of large-scale lysimeters from inside and outside
- Explanation of leachate sampling, soil moisture tracking, and boundary conditions
- Overview of weather station components (rain, wind, radiation, temperature sensors)

Figure 12. Lysimeter systems and climate monitoring at Selhausen

The Selhausen setup provided a valuable bridge between process-level modeling and large-scale field monitoring.

TERENO Eifel-Lower Rhine Observatory (January 23, 2025)

The final site visit took place at the TERENO (TERrestrial ENvironmental Observatories) station in the Eifel region, a key component of Germany's long-term environmental monitoring network (Figure 13). Led by Dr. Lutz Weihermüller, the visit focused on multi-scale hydrological and biogeochemical measurements.

The first part of the tour included:

- A lysimeter station for long-term observation of water balance and nutrient leaching
- Detailed explanation of the network's role in climate impact research

Next, the team was shown a canal water monitoring station used for analyzing dissolved organic matter (DOM) and nutrient transport through surface waters.

The final segment included a walk to an atmospheric monitoring station, where air quality and carbon cycle parameters (e.g., CO_2 fluxes) are tracked. Although not all systems could be observed in full operation, the diversity of instrumentation illustrated the breadth of the platform's integrative approach.

Figure 13. Environmental monitoring at TERENO Eifel: Canal water analysis and atmospheric tracking of air quality & carbon cycle

Impact on your project

The three-week research visit to Forschungszentrum Jülich (FZJ) had a significant and multifaceted impact on the ongoing project, particularly in the domains of knowledge transfer and the adoption of advanced soil analysis techniques and experimental designs. This mobility facilitated training for the visiting researchers from UNSPMF in state-of-the-art analytical methods that are central to the study of soil organic matter (SOM) dynamics and elemental cycling. The hands-on experience with advanced instrumentation - including inductively coupled plasma mass spectrometry (ICP-MS), multicollector ICP-MS (MC-ICP-MS), and asymmetric flow field-flow fractionation (AF4) - equipped the team with sophisticated tools for characterizing soil layers and colloidal fractions. These techniques not only improve analytical resolution but also allow for more accurate quantification and isotopic fingerprinting of elements associated with organic and mineral soil fractions, which is particularly valuable in tracing element pathways and transformations in soil systems.

Equally impactful was the exposure to large-scale experimental designs through site visits to FZJ's research platforms, such as AgraSim, Selhausen, and the TERENO Eifel observatory. These visits introduced the researchers to cutting-edge facilities for lysimeter-based experiments and rhizosphere monitoring, offering deep insight into the experimental infrastructure required to assess soil-plant-atmosphere interactions under both controlled and natural field conditions. Observing the functioning of automated irrigation systems, leachate collection setups, and weather stations helped clarify the practical aspects of maintaining experimental accuracy and consistency over time. The interdisciplinary context in which these platforms operate - integrating soil physics, plant physiology, and environmental modeling - also provided valuable perspectives on collaborative project design.

The knowledge gained during the visit will be transferred into current and planned activities at UNSPMF. New analytical protocols can be adapted and validated, to establish a comparable analytical pipeline for colloid and isotope analysis. Additionally, experimental planning for future lysimeter studies is now grounded in a stronger methodological framework, with clearer guidelines for instrumentation, site setup, and data acquisition. This visit not only enhanced the technical expertise of the visiting team but also contributed to strategic project planning, capacity building, and international collaboration, all of which will have long-term benefits for the research group and the broader scientific objectives of the project.

Subtask 1.2.3 (leader MLU) 6-months secondment (PM20-PM26) for ESR/RR, and two 1-months secondments (PM20, PM25) for a QR/RR at MLU.

MOBILITY REPORT – 1-month secondment at MLU

Researcher: Dr. Snežana Maletić, UNSPMF

Assigned supervisor: Prof. Dr. Bruno Glaser, MLU

Duration of the visit: 01.07.2024. - 28.07.2024.

Executive Summary

The secondment at Martin Luther University Halle-Wittenberg (MLU) focused on scientific training and knowledge transfer in the areas of soil science, spectroscopy, and carbon-based soil amendments. Key activities included training in the use of field spectroscopy techniques for real-time analysis of natural surfaces, and participation in a field trip to Schesslitz that provided students with practical experience in soil description, classification, and landscape interpretation. Knowledge exchange on biochar transport and carbon flow in soils was facilitated through a Master's course presentation and laboratory training on the analysis of black carbon molecular markers (BPCAs) from lysimeter experiment samples. Further skills were acquired through theoretical and practical training in isotope ratio mass spectrometry (IR-MS), including participation in method development for lignin compound analysis, laboratory maintenance, and cleaning procedures. The researcher also attended the Soil Science Colloquium in Halle, including a lecture by Prof. Susan Trumbore, and participated in the EcoLig project meeting focused on carbon sequestration. Additionally, method development for the analysis of pesticide metabolites (cypermethrin and cyprodinil) in soil amended with various organic materials was conducted.

Introduction

Background

The secondment was carried out within the framework of collaborative research focused on sustainable soil management, particularly the application of organic soil amendments (OSAs) such as biochar, compost, and aquatic sediments. These materials are central to current efforts to improve soil health, carbon sequestration, and pollutant retention. As part of this research, lysimeter experiments conducted at UNSPMF provided valuable data for studying the effects of

OSAs on soil processes. The mobility at Martin Luther University Halle-Wittenberg (MLU) was designed to enhance technical competencies and support knowledge transfer in several key areas: field spectroscopy, soil classification, biochar dynamics, molecular marker analysis (BPCAs), and advanced techniques such as isotope ratio mass spectrometry (IR-MS). Participation in the Soil Science Colloquium in Halle and the EcoLig project meeting also deepened the understanding of carbon cycling and linked the research to broader international scientific networks. The impact of different OSA on pesticide transport and biodegradation was also investigated through metabolite method development (cypermethrin and cyprodinil).

Biochar is a carbon-rich material produced through the pyrolysis of organic matter and is widely used as a soil amendment due to its ability to improve soil structure, enhance nutrient retention, and sequester carbon. When biochar is applied to soil, its mobility and interaction with soil particles depend on factors such as soil texture, biochar particle size, and the presence of other organic amendments. In sandy soils, biochar is more likely to move vertically due to the soil's larger pore spaces and high permeability. The transport of biochar in the soil profile can be influenced by its particle size, with finer particles having a greater potential for vertical movement. Over time, biochar undergoes aging effects that can alter its physical and chemical properties, potentially affecting its retention and stability in the soil. The addition of organic soil amendments (OSA), such as compost or sludge, can alter the dynamics of biochar in soil. These amendments improve soil aggregation, which can reduce the vertical movement of biochar by stabilizing it in the upper layers. Sludge, rich in organic matter, can enhance biochar retention by promoting the formation of stable biochar-organic matter complexes, while compost helps further structure the soil, making biochar less prone to leaching. The use of black carbon (BC) as a molecular marker enables the tracking of biochar's movement and degradation in soil. By analyzing BC content and its associated molecular markers, such as benzene carboxylic acids (BPCAs), researchers can gain insights into biochar's transport and stability, as well as its long-term role in carbon cycling and soil health.

Isotope Ratio Mass Spectrometry (IRMS) for bulk carbon-13 (^{13}C) analysis is a powerful technique used to measure the isotopic composition of carbon in soil samples, providing insights into carbon sources, cycling, and sequestration. In IRMS, the ratio of stable isotopes ^{13}C to ^{12}C is determined by measuring the mass difference between these isotopes. This analysis can differentiate between organic matter derived from different sources, such as plant material, biochar, or soil microorganisms, by identifying unique isotopic signatures. ^{13}C analysis is particularly useful for

tracing the movement and fate of carbon in soil, allowing researchers to assess the stability of organic amendments like biochar and monitor long-term changes in soil carbon pools. By providing detailed information on the origin and turnover of carbon, IRMS contributes to a better understanding of carbon sequestration processes and the impact of soil management practices on soil health and climate mitigation.

The contamination of soils and water bodies with pesticide residues, such as cypermethrin and cyprodinil, is a significant environmental issue due to their widespread use in agriculture. Cypermethrin, a synthetic pyrethroid insecticide, is highly hydrophobic, leading to strong adsorption to soil particles and potential long-term accumulation in sediments. In contrast, cyprodinil, a systemic fungicide, is moderately persistent and tends to bind to soil organic matter. These compounds, along with their metabolites, can persist in the environment, posing risks to soil health and aquatic ecosystems. To mitigate these risks, organic soil amendments (OSAs) such as biochar, compost, and sewage sludge are being explored due to their ability to influence pesticide sorption, degradation, and mobility in soils. The addition of OSAs can enhance the microbial degradation of pesticides, reduce their vertical migration, and improve the overall environmental health of contaminated soils. By studying the dynamics of pesticide transformation and the vertical migration of metabolites, researchers can better understand how different soil amendments affect pesticide behavior, paving the way for more effective remediation strategies.

Scope of the secondment

The scope of the secondment included the following:

1. Training related to the application of field spectroscopy which involves using portable spectrometers to measure the reflectance, absorbance, or emission of light from natural surfaces (like soil, vegetation, or water) in the field, without needing to collect samples.
2. Knowledge transfer involving participation in the field trip at Schesslitz to provide students with hands-on experience in soil science through the observation, description, and classification of various soil types and landscapes. It also aimed to deepen understanding of soil genesis, hydromorphology, and the influence of land use and geology on soil formation.
3. Knowledge transfer focused on biochar transport and carbon flow in soils was conducted through (1) Participation in a Master's course final presentation. The session covered the vertical and horizontal movement of biochar in soils, based on findings from three different

field studies. (2) Training on soil sample preparation and the analysis of molecular markers—specifically, black carbon (BC)-derived benzene polycarboxylic acids (BPCAs). The soil used in the analysis originated from a lysimeter experiment carried out at UNSPMF, where different organic soil amendments (OSAs), including biochar, were applied. Further methodological details are provided in Deliverable D3.1.

4. Acquisition of fundamental knowledge and skills in utilizing IR-MS techniques. Trough theoretical training at MLU laboratory, participation in developing the method for compound specific IR-MS method for analyzing lignin products, participation in IR-MS cleaning and maintenance in MLU lab, participation in Soil Science Colloquium – Halle, presented by Prof. Susan Trumbore, participation in project meeting EcoLig dealing with carbon sequestration.
5. Developing method for pesticide metabolite (cypermethrin and cyprodinil) analysis from soil from the lysimeter experiment was conducted at the UNSPMF, amended with different OSA including biochar, compost, and aquatic sediment which is explained in detail in deliverable D3.1.

In the following chapters, a detailed description of the methodologies applied within this secondment, along with the results obtained through their application, will be provided.

Content

1. Training in Field Spectroscopy (Fig 2.): The training was focused on the application of field spectroscopy, a powerful, non-invasive technique that involves the use of portable spectrometers to measure the reflectance, absorbance, or emission of light from natural surfaces such as soil, vegetation, or water bodies directly in the field. This method allows for rapid and in-situ data collection without the need for destructive sampling or laboratory processing, making it ideal for environmental monitoring and precision agriculture. Participants were introduced to the theoretical background of spectroscopy, including how different wavelengths of light interact with surface materials and what spectral signatures can reveal about physical and chemical properties. Practical sessions involved hands-on use of field spectrometers, calibration procedures, and data acquisition techniques under varying environmental conditions. The training also covered the interpretation of spectral data, data preprocessing, and potential applications such as soil moisture estimation, vegetation health assessment, and mapping of land cover types. Overall, the training

aimed to equip students with both conceptual understanding and practical skills for integrating field spectroscopy into environmental and soil science research.

Figure 1. Training - application of field spectroscopy using portable spectrometers

2. Knowledge transfer involving participation in the field trip at Schesslitz to provide students with hands-on experience in soil science through the observation, description, and classification of various soil types and landscapes was performed from 14-15th of July. It also aimed to deepen understanding of soil genesis, hydromorphology, and the influence of land use and geology on soil formation. Tasks per Day (Fig. 3):

   Day 1 – Schesslitz Area (Buntsandstein Region): Together with students we visited different mineral soil profiles, where they described soil horizons, recorded horizon boundaries, determined soil color using the Munsell scale, and measured soil pH. They also interpreted parent material, soil processes (like clay illuviation and stagnogleying), and classified the soils (e.g., Parabraunerde, Pseudogley, Podzol).

   Day 2 – Bischofsgrün and Raised Bog (Hochmoor): The focus shifted to hydromorphic and organic soils. A core part of the training include participating in field measurements and sampling activities. Together with students we took part in tasks such as collecting soil samples (10 from defined locations), measuring pH values, identifying soil colors using the Munsell scale, and noting the thickness of soil horizons. These activities were conducted at various stations, including mineral soil profiles near Schesslitz and organic soil layers in the raised bog (Hochmoor). Through these exercises, students gained hands-on experience with methods used in soil classification and environmental assessment. These methodes ranged from soil genesis and classification to hydromorphic characteristics and the influence of land use on soil development. Students described the

structure and composition of soils in a raised bog, assessed peat formation and degradation, and discussed soil water dynamics and land use impacts. They practiced identifying gleyic features and the degree of peat decomposition (using von Post's scale).

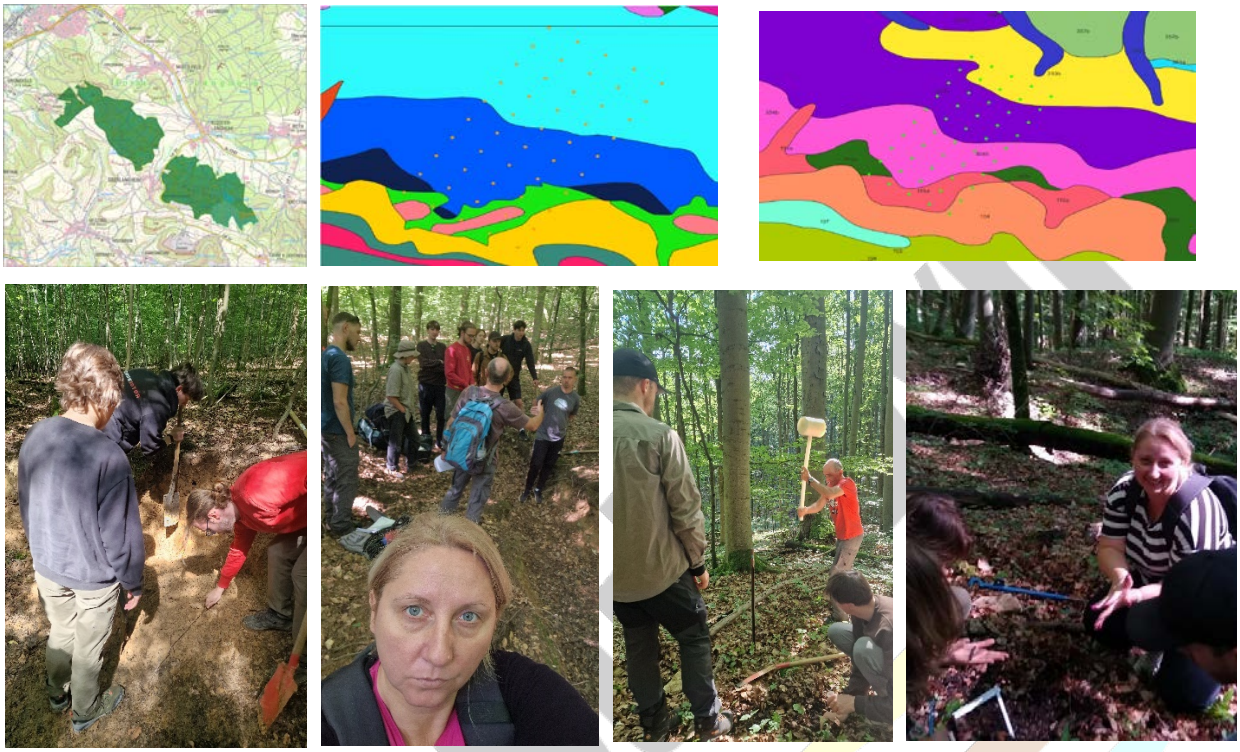

Figure 3. Environmental Monitoring and Soil Analysis Training, upper photos represent description of the training fields, bottom figures representing students and us performing assigned tasks

3. Knowledge transfer focused on biochar transport and carbon flow in soils:

(1) Participation in a Master's course final presentation (Fig. 4) provided valuable insights into the dynamics of biochar transport in soils. The session focused on the vertical and horizontal movement of biochar, drawing on results from three distinct field studies conducted near Bayreuth and Halle. Students presented their experimental findings, including measurements that demonstrated biochar mobility within the soil profile. Their work

Figure 4. Presentations of Master students

involved the statistical processing of collected data and a comparative analysis with existing literature, offering evidence-based conclusions on the extent and influencing factors of biochar transport under different field conditions. The presentation emphasized the relevance of such studies for understanding long-term carbon stability and distribution in amended soils.

(2) Learning about the vertical biochar transport and carbon flow in sandy soil. For this purpose, the lysimeter was filled with sandy soil and mixed with different OSA material, including sludge, compost and biochar. The objective was to measure the black carbon content, which we used as a molecular marker for biochar, in different lysimeter depth increments, at each 5 cm, after 441 days to retrace the vertical biochar movement, and to analyze, whether the addition of pristine biochar and biochar mixed with other OSA showed different dynamics, and which biochar-OSA combination revealed the lowest biochar and SOC dissipation rates. The black carbon content was analyzed following the method of Glaser et al. (1998)[1], with modifications by Brodowski et al. (2005)[2]. Summary of the Method (Fig 5.): The method for determining black carbon (BC) in soil is based on the chemical degradation of its highly aromatic structure into identifiable molecular markers—benzene carboxylic acids (BPCAs). The process begins with acid hydrolysis, where approximately 500 mg of soil is treated with 4 M trifluoroacetic acid (TFA) to remove polyvalent metal cations (notably Fe^{3+} and Al^{3+}) that may interfere with subsequent reactions. After filtration and drying, the residue undergoes oxidation with 65% nitric acid in a high-pressure digestion system at 170 °C for 8 hours. This converts BC into a suite of

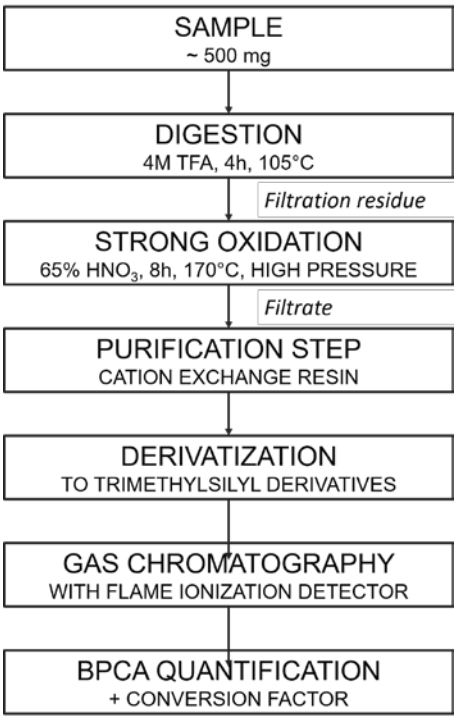

Figure 5. Scheme of BPCAs analysis method

[1] https://doi.org/10.1016/S0146-6380(98)00194-6
[2] https://doi.org/10.1016/j.orggeochem.2005.03.011

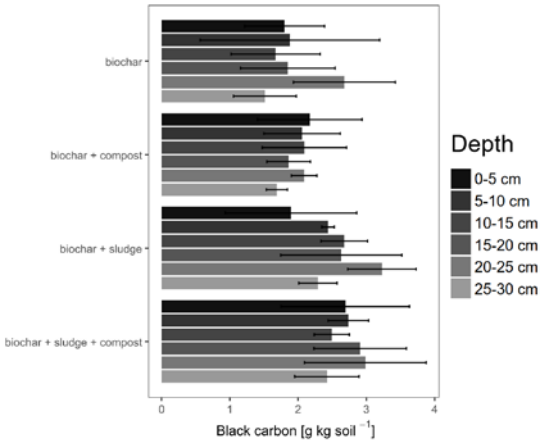

Figure 6: Total organic carbon content of six different organic soil amendment treatments in six different depths of the lysimeters

BCAs. The oxidized solution is then purified using a Dowex 50W×8 cation exchange resin to remove remaining impurities. After freeze-drying the eluate, the sample is subjected to derivatization, converting BPCAs into volatile trimethylsilyl derivatives by treatment with N,O-bis(trimethylsilyl)-trifluoroacetamide (BSTFA) and N-trimethylsilylimidazole (TSIM). This step ensures compatibility with gas chromatography. For analysis, capillary gas chromatography with flame ionization detection (GC-FID) is used, providing sensitive and precise quantification of BPCAs. Internal standards (phthalic acid and biphenylen-2,2-dicarboxylic acid) and a series of external BPCA standards ensure accurate identification and calibration. The aromaticity of the samples was assessed by calculating the relative contributions of hemimellitic, trimellitic, and trimesic acids (B3CA); pyromellitic, melophanic, and prehnitic acids (B4CA); benzene pentacarboxylic acid (B5CA); and mellitic acid (B6CA). The sum of all individual BPCA amounts were multiplied with 2.27, to convert them into black carbon equivalents. This method provides a reliable and reproducible approach to trace the presence and quantify the content of BC in soil samples, making it particularly valuable for studies on carbon cycling and soil amendment effects. First obtained results is given on the Fig 6., but detail explanation and further data processing will be presented in Deliverable 3.2. Black carbon (BC) levels varied across treatments and depths, not only appearing in biochar treatments but also in sludge and compost, which were subtracted to normalize the biochar data. The highest BC content was observed in the combined biochar + sludge + compost treatment, followed by biochar + sludge, indicating that sludge enhances BC retention. Vertical BC transport was notable in treatments with biochar alone and in combination with sludge or compost, especially with accumulation in the 20–25 cm layer. However, the lowest BC levels were generally found in the deepest layer (25–30 cm). Biochar mobility is influenced by

particle size, soil texture (e.g., sandy soils promote movement), and aging effects. Co-application with compost and OSA improves soil structure and reduces BC transport, making these combinations effective for stabilizing biochar in soil.

(3) In addition to the above, during the student field trip, a visit was made to a local biochar production facility (Fig. 7). The production process was presented, including feedstock selection, pyrolysis conditions, and post-processing steps. The staff explained technical aspects of biochar production, such as temperature control, emission management, and quality assurance. This hands-on experience provided valuable practical insight into real-world biochar production and complemented the theoretical knowledge from lectures and laboratory work.

Figure 7. Visit to biochar production facility

4. Obtaining fundamental skills in utilizing stable isotope ratio mass spectrometry techniques (IR-MS).

(1) For bulk sample measurements, this activity began with a theoretical introduction to the operation principles of isotope ratio mass spectrometry (IR-MS). Participants gained insight into how the instrument separates and detects isotopes, as well as its applications in environmental and soil science. In the case of compound-specific isotope analysis, the training was more advanced and included both theoretical and practical components. This involved the development of an analytical method for quantifying ^13C in lignin, which required configuring and calibrating a gas chromatography (GC) system for compound separation prior to IR-MS detection.A key part of the training also focused on system maintenance and troubleshooting. Preventive maintenance tasks—such as the cleaning of the ion source and replacement of consumables—were demonstrated, deepening the understanding of the inner workings of the IR-MS and the importance of system care for ensuring reliable data quality. These hands-on exercises enhanced operational competence

and contributed to a broader understanding of stable isotope techniques in environmental research (Fig. 8).

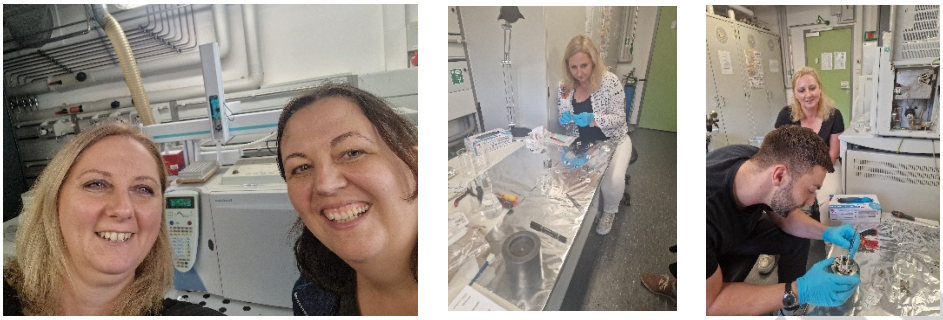

Figure 8. Introduction to the operation principles of isotope ratio mass spectrometry (IR-MS)

(2) Participation in the Soil Science Colloquium in Halle took place on July 11th, 2024 (Fig 9), featuring a keynote presentation by Prof. Susan Trumbore titled *"Radiocarbon Constraints on the Terrestrial Carbon Cycle."* The lecture addressed one of the critical uncertainties in terrestrial carbon cycle models: the residence time of carbon fixed by plants before it returns to the atmosphere via respiration and decomposition.

Figure 9. Soil Science Colloquium in Halle

Prof. Trumbore highlighted how the atmospheric release of 'bomb' ^{14}C during nuclear weapons testing in the 1960s created a distinct radiocarbon signature. This signature allows researchers to trace the "transit time" of carbon—i.e., the time elapsed between carbon fixation through photosynthesis and its subsequent release as CO_2. By measuring the ^14C content of respired CO_2 from different ecosystem components, this method offers powerful constraints for understanding and modeling carbon cycling dynamics. The presentation was followed by an in-depth discussion, allowing participants to explore methodological challenges and implications for improving carbon cycle models. The session provided valuable insights into the application of radiocarbon techniques in ecosystem studies and their relevance to climate change research.

(3) Participation in the EcoLig project meeting, held from July 18–19, 2024 (Fig 10), in Raum Bärenstein, focused on advancing the understanding of carbon sequestration processes under increasing forest disturbances such as drought, storms, and bark beetle outbreaks. These disturbances lead to canopy loss and shifts in the forest microclimate, yet the implications for litter decomposition and long-term carbon storage remain uncertain.The central objective of the EcoLig project is to investigate whether abiotic degradation of lignin is a key driver of canopy cover-regulated litter transformation and subsequent carbon sequestration following such disturbances. A particular focus of the meeting was the application of stable isotope techniques—especially compound-specific ^13C measurements—to trace lignin-derived carbon through different stages of decomposition. Isotope-based methods are being employed to quantify the relative contributions of biotic and abiotic processes in lignin breakdown and to better constrain the fate of carbon in forest floor systems. During the meeting, project partners presented updates on current progress, including initial field and laboratory results, site-specific observations, and preliminary isotopic data. Attendees included project members, scientific partners, and invited experts from the National Park authorities, as well as researchers from Freiburg, Halle, and various forest research institutes, fostering interdisciplinary collaboration and planning for the next project phase.

Figure 10. Participation in the EcoLig project meeting

5. Development of a Method for Pesticide Metabolite Detection (Cypermethrin and Cyprodinil) (Fig. 11)The contamination of agricultural soils and water bodies by pesticide residues has become a growing environmental concern due to the extensive use of chemical pesticides in modern agriculture. Among the widely applied compounds,

cypermethrin, a synthetic pyrethroid insecticide, and cyprodinil, a systemic fungicide, are frequently used to manage insect pests and fungal diseases, respectively.

Cyprodinil is moderately persistent in soils and exhibits a strong tendency to bind to organic matter, while cypermethrin, being highly hydrophobic, strongly adsorbs to soil particles, often leading to long-term accumulation in soil and sediment layers. Addressing the environmental risks posed by such compounds requires sustainable remediation strategies. One promising approach involves the use of organic soil amendments (OSA)—such as biochar, compost, and sewage sludge—which are rich in carbon and functional groups capable of influencing the sorption, degradation, and mobility of pesticides in soil environments.

Figure 11. Developing method for pesticide metabolite analysis

To investigate the interaction between OSAs and pesticide metabolites, a lysimeter experiment was established (29th of March 2024). The lysimeter was filled with sandy soil and amended with different OSAs, including biochar, compost, and sludge, either individually or in combination. On June 20th, cypermethrin and cyprodinil were applied to the soil surface. The study aimed to measure the concentration of key pesticide metabolites in soil layers after 441 days, using 5 cm depth increments. This setup enabled the assessment of both vertical biochar movement and the dynamics of pesticide transformation and transport in amended soils.

Key objectives included: Evaluating the retention and vertical migration of pesticide metabolites; Assessing the influence of OSAs on pesticide biodegradation and metabolite mobility; Developing a sensitive method for quantifying major metabolites of cypermethrin and cyprodinil.

Metabolite Estimates: Cypermethrin was applied at a rate of 0.2 mg per 12 kg of soil, equating to approximately 0.05 mg/kg in the upper 10 cm of soil. In a 5 g soil sample, this corresponds to 0.25 µg of cypermethrin. Assuming 10% conversion to metabolite 3-phenoxybenzoic acid (3-PBA), ~13 ng would be expected. Assuming 47.4% conversion

to DCCA, also ~13 ng would be present [3]. Cyprodinil was applied at a rate of 1.125 mg per 12 kg of soil, equating to 0.28 mg/kg in the top 10 cm. In 5 g of soil, this results in 1.4 µg of cyprodinil. Assuming 1% conversion to its main metabolite CGA30407, the estimated concentration is ~15 ng. This method development and subsequent analysis are essential for understanding the environmental behavior of pesticides under different soil management practices, and for designing effective mitigation strategies using OSAs. GA30407 ≈ 15 ng[4].

Table 1. Pesticide and its metabolite (cypermethrin and cyprodinil)

Pesticide	Metabolite
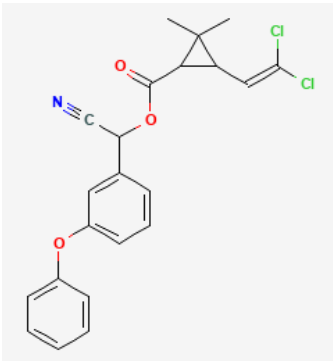 Insecticide - Grupe Pyrethroide	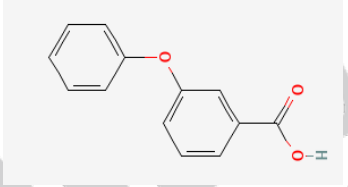 3-Phenoxybenzoic acid (3PBA)
	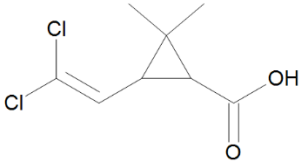 3-(2,2-dichlorovinyl)-2,2-dimethylcyclopropanecarboxylic acid - DCCA
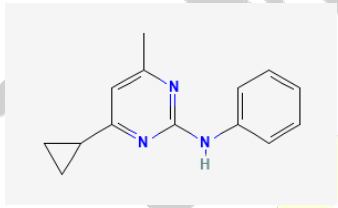 Cyprodinil -fungicide	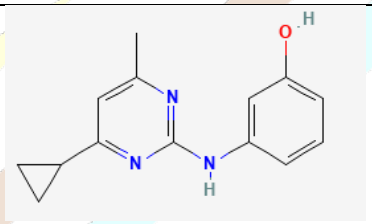 3-(4-cyclopropyl-6-methylpyrimidin-2-ylamino)phenol (Ref: CGA 275535)
	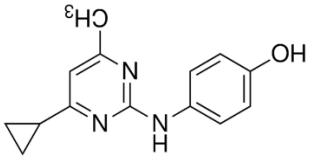 4-(4-cyclopropyl-6-methyl-pyrimidin-2-yl-amino)-phenol (Ref: CGA 304075) - only this metabolite was available for purchasing

[3] https://sitem.herts.ac.uk/aeru/ppdb/en/Reports/197.htm
[4] https://sitem.herts.ac.uk/aeru/ppdb/en/Reports/197.htm

For method development 5 trials have been tested for recovery and detection limit. Trials have been described below:

TRIAL1 - *Method according to Mudiam et al. (2013)*

3-Phenoxybenzoic acid (3-PBA) and CGA 304075

Extraction - 1 g of soil sample place to a 50-mL centrifuge tube and do extraction with 30 mL of ammonium acetate 100 mM. The mixture should be shacked 10 min for 170 o/min, ultrasonicated for 10 min at room temperature**,** and centrifuged at 4500 rpm for 5 min. Supernatant is than filtrated, and then, 15 mL of the upper layer of the soil extract was passed through C18- SPE cartridges (3 mL / 500 mg).

SPE cleanup procedure – Conditioning with 5 ml of Methanol, equilibrate with 5 ml of ammonium acetate, add 15ml of soil extract, wash with 5 ml 30% of Methanol in water, dry 1hour in full vacuum, eluate with 4 ml 2%formic acid in methanol.

Derivatization – 4 ml of SPE extract evaporate to dryness. Re-dissolve residue in derivatization agents, 100 µl of pyridine and 200 µl of BSTFA (bis-(trimethlysilyl)-triflouroacetamide), mix with vortex shaker, transfer samples to amber GC-Vials with insert, and the leave solution in the dark for 2 h at room temperature.

GCMS analysis – GC-MS – conditions - operated in the electron impact ionization at 70 eV, using a high-resolution DB-5 MS UI column (30 m length, 0.25 mm diameter, 0.25 µm film thickness; Agilent, Santa Clara, USA). A volume of 1 µL was injected. The ion source temperature and the MS transfer temperature were at 200 °C. Operating in the splitless mode, the helium was used as carrier gas at a constant flow rate of 1.78 mL min^{-1}. The injector was maintained at 250 °C. Oven temperature was programmed as follows: initial temperature 40 °C (held for 1 min), increased by 15 °C/min to 250 °C (held for 10 min), and finally increased by 30 °C/min to 300 °C (held for 7 min). In Table 2. Target and Qualifier ions for quantification is given.

Table 2. Target and Qualifier ions for quantification

Selected ions Compound	Target	Qualifier 1	Qualifier 2
3PBA	271	197	286
CGA30407	313	149	298

Results Test-1

Standard preparation

- Stock - 3PBA 25 mg dissolved in 25 ml of Methanol + 1 mg/ml, 10 mg of CGA dissolved in 10 ml of Methanol = 1 mg/ml

- WS1 1 ml of stock solution diluted up to 100 ml in methanol = 10 µg/ml
- WS2 – 5 ml of WS1 dissolved in 50 ml of Methanol = 1 µg/ml

Table 3. Calibration concentration range: 25–2500 ng

3PBA /CGA (ng)	Volume of WS2 µl	Area-3PBA	Area -CGA
25	25	14732	4777
50	50	22102	7518
100	100	37716	19405
250	250	94373	74908
500	500	218438	206380
1000	1000	417435	406104
2500	2500	1415675	1959063

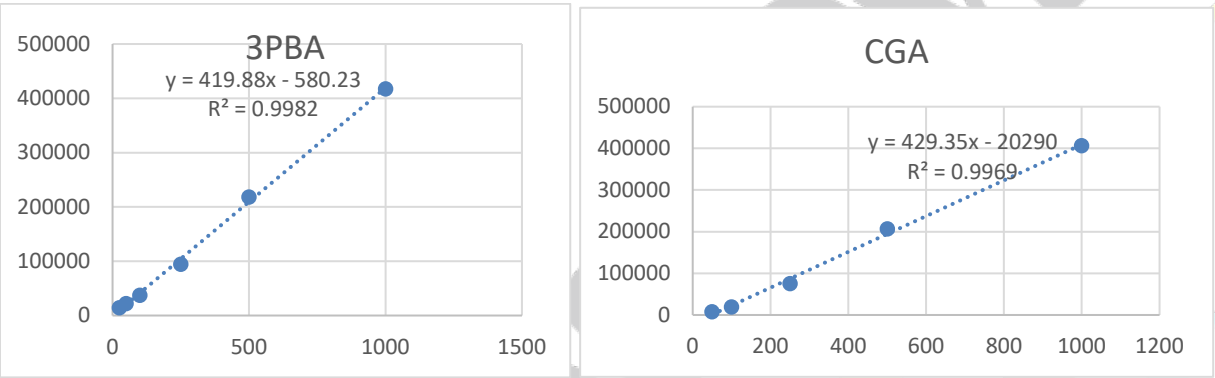

Figure 12. Calibration curve for PBA and CGA

Spiking of sample 0.5 ml of 10 µg/ml = 5000 ng, of 3PBA and CGA in methanol solutions, extracted with 30 ml, of which only 15 was used in further procedure, expected amount=2500 ng, results are given in Table 4.

Table 4. Recovery of the 3PBA and CGA

					Calculation with 2500 ng		Recovery %		Stdev	
	3PBA	CGA	3PBA (ng)	CGA (ng)	3PBA	CGA	3PBA	CGA	3PBA	CGA
AA_304075_soil_1	17880	22305	44.0	99.2	31.58	28.46	1.26	1.14	11.4	4.4
AA_304075_soil_2	3060	16144	8.7	84.9	5.40	20.60	0.22	0.82		
AA_304075_soil_2	5858	24157	15.3	103.5	10.34	30.83	0.41	1.23		
AA_Seasand_1	2866	874574	8.2	2084.2	5.06	1116.06	0.20	44.64	0.9	237.9
AA_Seasand_2	2018	703823	6.2	1686.5	3.56	898.16	0.14	35.93		
AA_Seasand_3	3172	1155927	8.9	2739.5	5.60	1475.10	0.22	59.00		

TRIAL 2 - *Extraction method according to Hedges and Ertel (1982) with modifications by Goñi and Hedges (1992) without cupric oxidation*

Extraction - 1 g of soil sample place to a 50-mL centrifuge tube; extraction with 30 mL of 2M NaOH by shaking for 1 hour at 170 o/min; centrifuged at 4500 rpm for 15 min. Supernatant is then transferred to a new centrifuge tube and acidified with 6M HCl to pH 1.8-2.2, left in the dark for 1 h hour for precipitation of humic acids, and finally centrifuged again for 25 min at 4500 rpm. The entire supernatant was passed through pre-conditioned C18- SPE cartridges (3 mL / 500 mg).

SPE cleanup procedure – Activate columns with 3 mL ethylacetate, methanol and finally water, never letting columns run dry. Mount the glass rinsing funnel over the column and pass 10 mL water. Pass the sample through the column and rinse column with 3 mL water. Dry up columns under a stream of nitrogen gas (ca. 1.3 bar for 30 minutes). Elute SPE columns with 8 portions of 500 µL ethylacetate, collecting the eluate in 5-mL pointed flasks.

Derivatization – Remove ethylacetate by rotary evaportation (maximum water bath temperature of 40˚C, vacuum of ca. 180 mbar). Re-dissolve residue in derivatization agents, 100 µl of pyridine and 200 µl of BSTFA (bis-(trimethlysilyl)-triflouroacetamide), mix with vortex shaker, transfer samples to amber GC-Vials with insert, and the leave solution in the dark for 2 h at room temperature.

GCMS analysis – GC-MS – conditions - operated in the electron impact ionization at 70 eV, using a high-resolution DB-5 MS UI column (30 m length, 0.25 mm diameter, 0.25 µm film thickness; Agilent, Santa Clara, USA). A volume of 1 µL was injected. The ion source temperature and the MS transfer temperature were at 200 °C. Operating in the splitless mode, the helium was used as carrier gas at a constant flow rate of 1.78 mL min^{-1}. The injector was maintained at 250 °C. Oven temperature was programmed as follows: initial temperature 40 °C (held for 1 min), increased by 15 °C/min to 250 °C (held for 10 min), and finally increased by 30 °C/min to 300 °C (held for 7 min). In Table 2. Target and Qualifier ions for quantification is given.

Results Test-2

Table 5. Recovery of the 3PBA and CGA

					Calculation with 2500 ng		Recovery		Stdev	
	3PBA	CGA	3PBA (ng)	CGA (ng)	3PBA	CGA	3PBA	CGA	3PBA	CGA
NaOH-Sand1	2872938	11231	6843.7	73.4	5073.44	14.33	101.47	0.29		
NaOH-Sand2	2811545	9993	6697.4	70.5	4965.03	12.75	99.30	0.26		
NaOH-Sand2	357247	3735	852.2	56.0	630.88	4.77	12.62	0.10	2069	4.2
NaOH_304075_soil_1	1403015	567914	3342.8	1370.0	2477.64	724.73	49.55	14.49		
NaOH_304075_soil_2	2446695	474370	5828.5	1152.1	4320.72	605.35	86.41	12.11		

NaOH_304075_soil_2	1310	1334	4.5	50.4	2.31	1.70	0.05	0.03	1769.3	316.5

Conclusion – Good recovery for 3PBA for sand, some issue with soil – due to high amount of spiked compounds. CGA method extraction or SPE cleanup not adequate low recovery.

TRIAL3 - Test -3 SPE check

100 µl of 10 µg/ml 3PBA and CGA (1000 ng each) was added to nine reactivials and dried under nitrogen. For the first set of three replicates, the standards were then re-disolved in 4 ml ammonium acetate (100 mM). For the second and third set of three replicates each, the standards were re-disolved in 4ml of 1 M HCl solution.

Solution was applied to the C18- SPE cartridges (3 mL / 500 mg), tested procedures for SPE:

1. Conditioning with 5 ml of Methanol, equilibrate with 5 ml of ammonium acetate, add 15ml of soil extract. Dry up columns under a stream of nitrogen gas (ca. 1.3 bar for 30 minutes). wash with 5 ml 30% of Methanol in water, dry 1hour in full vacuum, eluate with 4 ml 2%formic acid in methanol. Evaporate in rotavapor at 40ºC, and then derivatized.
2. Activate columns with 3 mL ethylacetate, methanol and finally water, never letting columns run dry. Mount the glass rinsing funnel over the column and pass 10 mL water. Pass the sample through the column and rinse column with 3 mL water. Dry up columns under a stream of nitrogen gas (ca. 1.3 bar for 30 minutes). Elute SPE columns with 8 portions of 500 µL ethylacetate, collecting the eluate in 5-mL pointed flasks. Evaporate in rotavapor at 40ºC, and then derivatized.
3. Activate columns with 3 mL ethylacetate, methanol and finally water, never letting columns run dry. Mount the glass rinsing funnel over the column and pass 10 mL water. Pass the sample through the column and rinse column with 3 mL water. Dry up columns under a stream of nitrogen gas (ca. 1.3 bar for 30 minutes). Elute SPE columns with 8 portions of 500 µL ethylacetate, collecting the eluate in 5-mL pointed flasks, than elute with 2% formic acid in methanol. Evaporate in rotavapor at 40ºC, and then derivatized.

Results Test-3

Table 6. Recovery of the 3PBA and CGA

	3PBA	CGA	3PBA (ng)	CGA (ng)	3PBA	CGA	3PBA	CGA
1-1	3989	848	10.9	49.2	1.09	4.92		
1-2	3450	480	9.6	48.4	0.96	4.84		

1-3	5375	524	14.2	48.5	1.42	4.85	1.9	0.4
2-1	487598	1087	1162.7	49.8	116.27	4.98		
2-2	532648	457	1270.0	48.3	127.00	4.83		
2-3	546385	726	1302.7	48.9	130.27	4.89	59.8	0.6
3-1	523670	612	1248.6	48.7	124.86	4.87		
3-2	400424	1203	955.0	50.1	95.50	5.01		
3-3	595797	384	1420.4	48.2	142.04	4.82	192.1	0.8

Conclusion – Good recovery for 3PBA. CGA method SPE- not clear weather the extraction or cleanup is causing low recovery.

TRIAL 4 - Further validation steps for 3PBA and DCCA analysis, Testing the lysimeter samples for 3PBA analysis

Table 7. Optimization of method for lysimeter soil samples - spiking 3PBA for recovery determination

Sample	Mass	Mix	Spike	Replicates
36773	2.5 g	36773+36774	no spike	2
36774	2.5 g			
36773	2.5 g	36773+36774	100 ul, (1000 ng)	1
36774	2.5 g			
36695	2.5 g	36695+36996	no spike	2
36696	2.5 g			
36695	2.5 g	36995+36696	100 ul, (1000 ng)	1
36696	2.5 g			
Chernozem soil sample	5g	-	no spike	2

Internal standard 1 (IS1) – Ethyl Vanillin (EV) stock solution (2.5 mg PAA/100 ml methanol, preparation: dissolve 50,01 mg PAA in 100 methanol, dilute an aliquot of 5 ml with 95 ml of methanol.

Internal standard 2 (IS2) – phenyl acetic acid (PAA) stock solution (2.5 mg PAA/100 ml methanol, preparation: dissolve 49,93 mg PAA in 100 methanol, dilute an aliquot of 5 ml with 95 ml of methanol.

Extraction – *5* g of soil sample place to a 50-mL centrifuge tube; 500 µl of IS1 (Ethyl vanillin, corresponds to 12.500 ng) was added to each sample to estimate recovery; extraction with 30 mL of 2M NaOH by shaking for 1 hour at 170 o/min; centrifuged at 4500 rpm for 15 min. Supernatant is then transferred to a new centrifuge tube and acidified with 6M HCl to pH 1.8-2.2, left in the dark for 1 h hour for precipitation of humic acids, and finally centrifuged again for 25 min

at 4500 rpm. The entire supernatant was passed through pre-conditioned C18- SPE cartridges (3 mL / 500 mg).

SPE cleanup procedure – Activate columns with 3 mL ethylacetate, methanol and finally water, never letting columns run dry. Mount the glass rinsing funnel over the column and pass 10 mL water. Pass the sample through the column and rinse column with 3 mL water. Dry up columns under a stream of nitrogen gas (ca. 1.3 bar for 30 minutes). Elute SPE columns with 8 portions of 500 µL ethylacetate, collecting the eluate in 5-mL pointed flasks. 500 µl of IS2 (PAA, corresponds to 12.500 ng) was added. Remove ethylacetate by rotary evaporator (maximum water bath temperature of 40˚C, vacuum of ca. 180 mbar).

Derivatization – **Re-dissolve residue in derivatization agents, 50 µl of pyridine and 100 µl of BSTFA**, mix with vortex shaker, transfer samples to amber GC-Vials with insert, and the leave solution in the dark for 2 h at room temperature.

GCMS analysis – GC-MS – conditions - operated in the electron impact ionization at 70 eV, using a high-resolution DB-5 MS UI column (30 m length, 0.25 mm diameter, 0.25 µm film thickness; Agilent, Santa Clara, USA). A volume of 1 µL was injected. The ion source temperature and the MS transfer temperature were at 200 °C. Operating in the splitless mode, the helium was used as carrier gas at a constant flow rate of 1.78 mL min^{-1}. The injector was maintained at 250 °C. Oven temperature was programmed as follows: initial temperature 40 °C (held for 1 min), increased by 15 °C/min to 250 °C (held for 10 min), and finally increased by 30 °C/min to 300 °C (held for 7 min). In the Table 8. Target and Qualifier ions for quantification.

Table 8. Target and Qualifier ions for quantification

Selected ions Compound	RT, min	Target	Qualifier 1	Qualifier 2
3PBA		271	197	286
CGA30407		313	149	298
DCCA	10.510 and 10.685	128	265	---
PAA		164	193	(73)
EV (Ethyl Vanillin)		167	195	238

DCCA (3-(2,2-Dichlorovinyl)-2,2-dimethyl-1-Cyclopropane) carboxylic acid

100 µg/mL in Acetonitrile, 1.2 ml

Detection of target and qualifier ions

Transfer 5 µl of the stock solution (500 ng), evaporate. Re-dissolve residue in derivatization agents, 50 µl of pyridine and 100 µl of BSTFA, mix with vortex shaker, transfer samples to amber GC-Vials with insert, and the leave solution in the dark for 2 h at room temperature.

Standard preparation

Stock - 3PBA 25 mg dissolved in 25 ml of Methanol = 1 mg/ml, 10 mg of CGA dissolved in 10 ml of Methanol = 1 mg/ml –(this is already prepared it is in the fridge)

WS1 1 ml of stock solution diluted up to 100 ml in methanol = 10 µg/ml –(this is already prepared it is in the fridge)

WS2 – 1 ml of WS1 and 100 µl of DCCA stock dissolved in 10 ml of Methanol = 1 µg/ml

Table 9. Calibration concentration range: 10–1000 ng for 3PBA, CGA and DCCA

3PBA /CGA (ng)	Volume of WS2 µl	PAA (IS2) µl	EV (IS1) µl
5	5	500	25
10	10	500	50
25	25	500	100
50	50	500	200
100	100	500	300
250	250	500	400
500	500	500	500
1000	1000	500	600

Evaporate under N_2, at max 40°C. **Re-dissolve residue in derivatization agents, 50 µl of pyridine and 100 µl of BSTFA**, mix with vortex shaker, transfer samples to amber GC-Vials with insert, and the leave solution in the dark for 2 h at room temperature.

Table 10. Results – Internal calibration

Ethyl-Vanillin (IS1)	3-PBA	CGA 304075	amount (ng)	Ax/AIS2 DCCA	Ax/AIS2 3PBA	Ax/AIS2 CGA	amount (ng)	EV
27311	5576	2743	5	0.0000000	0.0015276	0.0007515	625	0.007482
75118	11424	7545	10	0.0000000	0.0046460	0.0030685	1250	0.030550
401775	28320	25283	25	0.0024850	0.0100838	0.0090024	2500	0.143059
474790	58241	51525	50	0.0044441	0.0265356	0.0234757	5000	0.216322
669864	118303	122492	100	0.0074551	0.0222320	0.0230192	7500	0.125883
1995047	308496	376092	250	0.0167998	0.0671347	0.0818449	10000	0.434161
3518796	688726	875604	500	0.0336399	0.1091116	0.1387178	12500	0.557466
13297986	1162664	1539871	1000	0.0632424	0.1653284	0.2189665	15000	1.890946
Sample Name	PAA (IS2)	Ethyl-Vanillin (IS1)	3-PBA	DCCA - 1st peak	Ax/AIS2	DCCA	3PBA	CGA

73+74A	12621661	14673067	56702	22868	73+74A	0.001812	0.004492	0.000000
73+74B	13264710	16956006	67624	25824	73+74B	0.001947	0.005098	0.000000
73+74S	13961273	17308847	1951208		73+74S	0.002196	0.139759	0.000000
95+96A	12977652	16424263	18720		95+96A	0.000000	0.001442	0.000000
95+96B	13362138	17509277	15731		95+96B	0.000000	0.001177	0.000000
95+96S	13029331	16728857	1342523		95+96S	0.000000	0.103039	0.000000
LBS1	13501368	17328942	28407		LBS1	0.000000	0.002104	0.000000
LBS2	14243282	19114273	16783		LBS2	0.000000	0.001178	0.000000

Table 11. Recovery of pesticide metabolite

amount in sample (ng)	DCCA	3PBA	CGA	EV	EV-recovery (%)
73+74A	28.2	24.8	0.0	15759.0	126%
73+74B	30.3	28.1	0.0	17328.1	139%
73+74S	34.1	770.3	0.0	16806.1	134%
95+96A	0.0	8.0	0.0	17155.9	137%
95+96B	0.0	6.5	0.0	17763.0	142%
95+96S	0.0	567.9	0.0	17404.8	139%
LBS1	0.0	11.6	0.0	17398.8	139%
LBS2	0.0	6.5	0.0	18191.6	146%

Conclusion: IS high amount 12500 ng per sample; IS higher response for the same amount in samples vs cal. Std; Not possible to calculate recovery by using IS

Table 12 Results – External calibration

amount in sample (ng)	DCCA	3PBA	CGA	Rec%
73+74A	276.3	48.6	nd	
73+74B	168.9	53.0	nd	
73+74S	403.3	1431.0	nd	137.8
95+96A	nd	14.7	nd	
95+96B	nd	17.1	nd	
95+96S	135.1	1009.0	nd	99.2
LBS1	157.8	23.5		
LBS2	157.8	23.5		

Conclusion – Good recovery using only external calibration

TRIAL 5 - Further validation steps for 3PBA analysis: Testing the lysimeter samples for 3PBA and DCCA analysis

Table 13. Optimization of method for lysimeter soil samples - spiking 3PBA for recovery determination

Sample	Mass	Mix	Spike
36775	2.4708 g	36775+36776	no spike
36776	2.2457 g		
36775	2.4195 g	36775+36776	250 ul, WS2 (250 ng)
36776	2.3694 g		
36775	2.5172 g	36775+36776	250 ul, WS2 (250 ng)
36776	2.6687 g		
36797	2.8085 g	36797+36798	no spike
36798	2.7585 g		
36797	2.6210 g	36797+36798	250 ul, WS2 (250 ng)
36798	2.5214 g		
36777	2.5754 g	36777+36778	no spike
36778	2.5944 g		
36799	2.5490 g	36799+36800	no spike
36800	2.5601 g		

Internal standard 1 (IS1) – Ethyl Vanillin (EV) stock solution (2.5 mg PAA/100 ml methanol, preparation: dissolve 50,01 mg PAA in 100 methanol (0.5001 mg/ml), dilute an aliquot of 5 ml with 95 ml of methanol (25.005 µg/ml)-WS1, dilute 5 ml WS1 with 45 ml of methanol (2.5005 µg/ml).
Internal standard 2 (IS2) – phenyl acetic acid (PAA) stock solution (2.5 mg PAA/100 ml methanol, preparation: dissolve 49,93 mg PAA in 100 methanol (0.4993 mg/ml), dilute an aliquot of 5 ml with 95 ml of methanol (24.965 µg/ml)-WS1, dilute 5 ml WS1 with 45 ml of methanol (2.4965 µg/ml).
Extraction – *5* g of soil sample place to a 50-mL centrifuge tube; 500 µl of IS1 (Ethyl vanillin, corresponds to 12.500 ng) was added to each sample to estimate recovery; extraction with 30 mL of 2M NaOH by shaking for 1 hour at 170 o/min; centrifuged at 4500 rpm for 15 min. Supernatant is then transferred to a new centrifuge tube and acidified with 6M HCl to pH 1.8-2.2, left in the dark for 1 h hour for precipitation of humic acids, and finally centrifuged again for 25 min at 4500 rpm. The entire supernatant was passed through pre-conditioned C18- SPE cartridges (3 mL / 500 mg).
SPE cleanup procedure – Activate columns with 3 mL ethylacetate, methanol and finally water, never letting columns run dry. Mount the glass rinsing funnel over the column and pass 10 mL water. Pass the sample through the column and rinse column with 3 mL water. Dry up columns under a stream of nitrogen gas (ca. 1.3 bar for 30 minutes). Elute SPE columns with 8 portions of 500 µL ethylacetate, collecting the eluate in 5-mL pointed flasks. 500 µl of IS2 (PAA, corresponds

to 12.500 ng) was added. Remove ethylacetate by rotary evaporator (maximum water bath temperature of 40˚C, vacuum of ca. 180 mbar).

Derivatization – **Re-dissolve residue in derivatization agents, 50 µl of pyridine and 100 µl of BSTFA**, mix with vortex shaker, transfer samples to amber GC-Vials with insert, and the leave solution in the dark for 2 h at room temperature.

GCMS analysis – GC-MS – conditions - operated in the electron impact ionization at 70 eV, using a high-resolution DB-5 MS UI column (30 m length, 0.25 mm diameter, 0.25 µm film thickness; Agilent, Santa Clara, USA). A volume of 1 µL was injected. The ion source temperature and the MS transfer temperature were at 200 °C. Operating in the splitless mode, the helium was used as carrier gas at a constant flow rate of 1.78 mL min^{-1}. The injector was maintained at 250 °C. Oven temperature was programmed as follows: initial temperature 40 °C (held for 1 min), increased by 15 °C/min to 250 °C (held for 10 min), and finally increased by 30 °C/min to 300 °C (held for 7 min). In the table 14.Target and Qualifier ions for quantification.

Table 14. Target and Qualifier ions for quantification

Selected ions Compound	RT, min	Target	Qualifier 1	Qualifier 2
3PBA		271	197	286
CGA304075		313	149	298
DCCA	10.510 and 10.685	128	265	---
PAA		164	193	(73)
EV (Ethyl Vanillin)		167	195	238

Standard preparation

Stock - 3PBA 25.56 mg dissolved in 25 ml of Methanol = 1.0224 mg/ml, 10 mg of CGA dissolved in 10 ml of Methanol = 1 mg/ml –(this is already prepared it is in the fridge)

WS1 1 ml of stock solution diluted up to 100 ml in methanol = 10.224 µg/ml of 3PBA and 10 µg/ml CGA

WS2 – 1 ml of WS1 and 100 µl of DCCA stock dissolved in 10 ml of Methanol = 1.0224 µg/ml of 3PBA and 1 µg/ml of CGA

Table 15. Calibration concentration range: 10–1000 ng for 3PBA, CGA and DCCA

3PBA (ng)	CGA (ng)	Volume of WS2 µl	PAA (IS2) µl of WS2	EV (IS1) µl of WS2
5.112	5	5	250	250
10.224	10	10	250	250
25.56	25	25	250	250
51.12	50	50	250	250

102.24	100	100	250	250
255.6	250	250	250	250
511.2	500	500	250	250
1022.4	1000	1000	250	250

Evaporate under N_2, at max 40°C. Re-dissolve residue in derivatization agents, 50 µl of pyridine and 100 µl of BSTFA, mix with vortex shaker, transfer samples to amber GC-Vials with insert, and the leave solution in the dark for 2 h at room temperature.

Results - Internal calibration

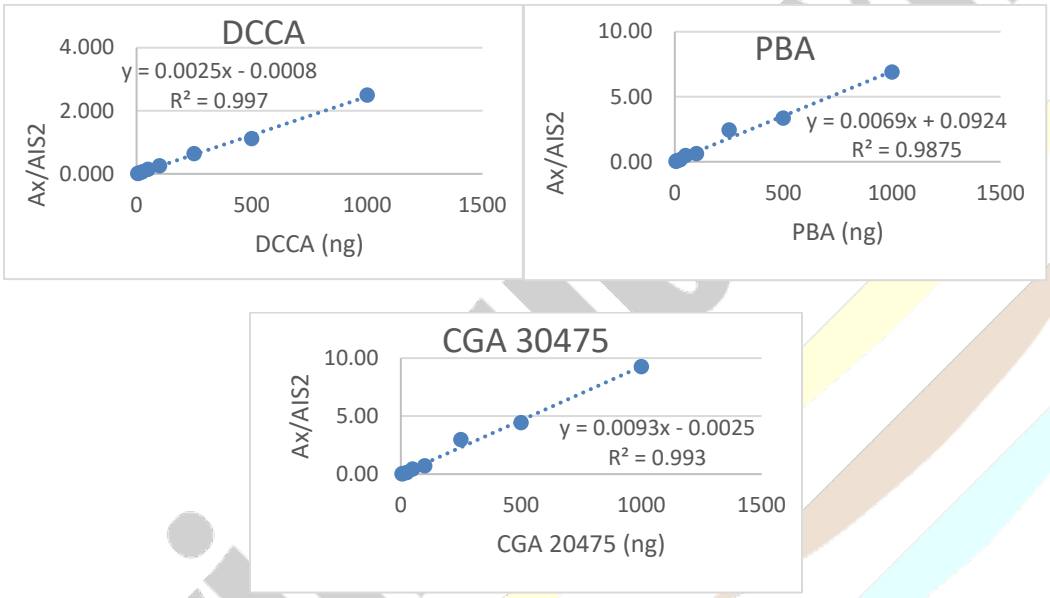

Figure 13. Results - Internal calibration

Table 16. Results of the calibration and spiked sample measurements

Sample Name	PAA (IS2)	DCCA - 1st peak	DCCa - 2nd peak	Ethyl-Vanillin (IS1)	3-PBA	CGA 304075	amount (ng)	A/AIS2 - DCCA	A/AIS2 - 3PBA	A/AIS2 - CGA	
Ex5	188935	1464	1143	122779	4341	2712	5	0.014	0.02	0.01	
Ex10	149537	1160	2525	134538	11313	8607	10	0.02	0.08	0.06	
Ex25	163343	2999	6457	147290	24441	22105	25	0.06	0.15	0.14	
Ex50	121123	4724	13189	79027	58602	52730	50	0.15	0.49	0.44	
Ex100	200334	15868	34383	160209	123452	142039	100	0.25	0.62	0.71	
Ex250	136903	23556	64429	54826	335870	405174	250	0.68	2.58	3.11	
Ex500	215430	72665	168032	55007	722831	953354	500	1.12	3.36	4.43	
Ex1000	224111	178698	380645	92596	1545596	2073725	1000	2.50	6.90	9.25	
Sample Name	PAA (IS2)	DCCA - 1st peak	DCCa - 2nd peak	Ethyl-Vanillin (IS1)	3-PBA	CGA 304075	Ax/AIS2	DCCA	3PBA	CGA	EV

75+76-1	1403849	12052	6523	395322	27172	3351	75+76-1	0.013231	0.019355	0.002387	0.281599
75+76-2	1387458	62637	115781	439206	443398	1911	75+76-2	0.128593	0.319576	0.001377	0.316554
75+76-3	1359350	55894	119943	372309	439238	3162	75+76-3	0.129354	0.323124	0.002326	0.273888
97+98-1	349458	6935	14632	292390	10078	832	97+98-1	0.061716	0.028839	0.002381	0.836696
97+98-2	358403	89087	115626	292168	256586	481	97+98-2	0.571181	0.715915	0.001342	0.815194
97+98-3	371931	61597	113956	274202	281932	636	97+98-3	0.472004	0.758022	0.001710	0.737239
77+78	1417880	7173	5501	391041	18958	721	77+78	0.008939	0.013371	0.000509	0.275793
99+00	432219	3950	5248	399071	6764	567	99+00	0.021281	0.015649	0.001312	0.923307

Table 17. Recovery of pesticide metabolite

amount in sample (ng)	DCCA	3PBA	CGA
75+76-1	18.3	6.3	nd
75+76-2	64.5	49.8	nd
75+76-3	64.8	50.3	nd
97+98-1	37.7	7.6	nd
97+98-2	241.5	107.2	nd
97+98-3	201.8	113.3	nd
77+78	16.6	5.4	nd
99+00	21.6	5.7	nd

Conclusion: IS1-EV higher response for the same amount in samples vs cal. Std. Not possible to calculate recovery by using IS2. IS2 not consistent in samples and cal std

Results – external calibration

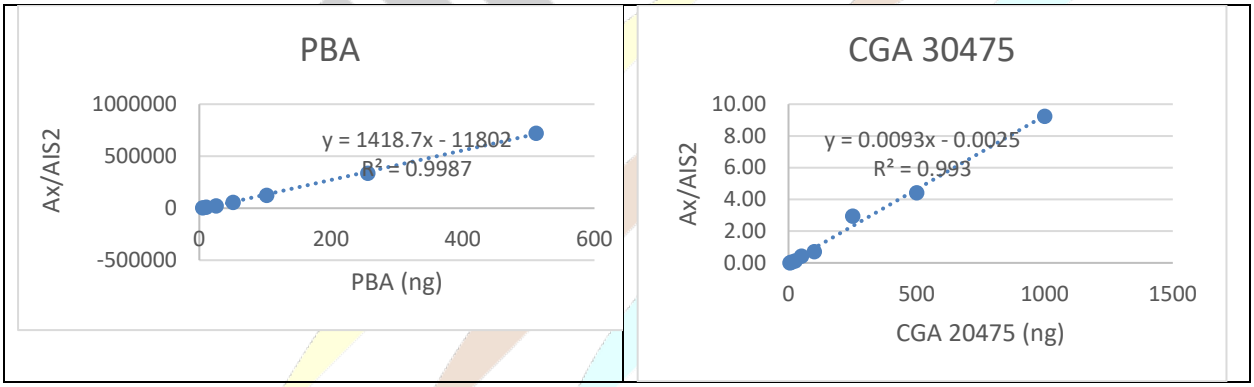

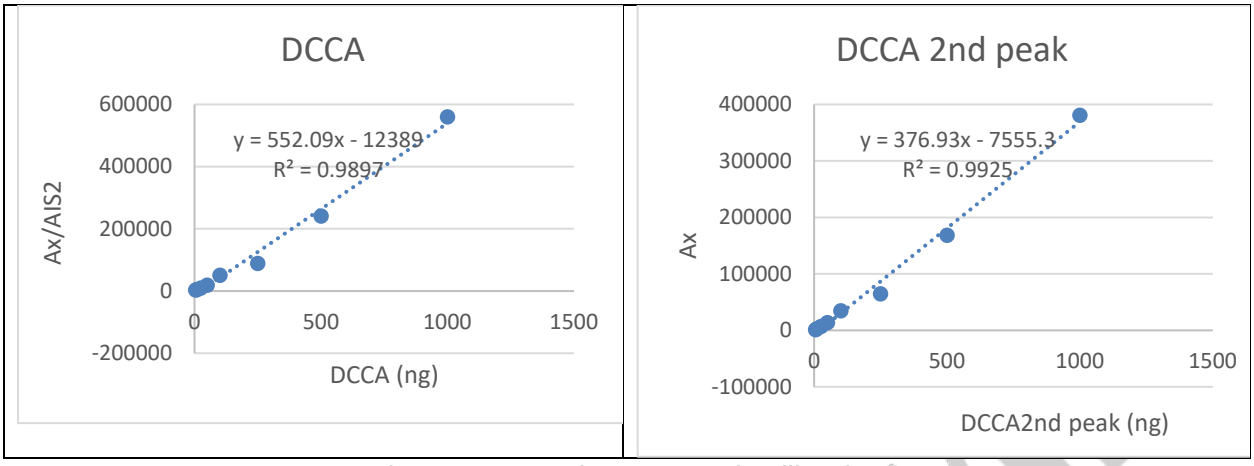

Figure 14. Results - External calibration

Table 18. Recovery of pesticide metabolite

	amount in sample (ng)				Recovery%		
	DCCA	3PBA	CGA	DCCA 2nd peak	DCCA	DCCA 2nd peak	PBA
75+76-1	56.1	26.9	nd	37.3			
75+76-2	345.6	313.8	nd	327.2	115.8	108.4	116.9
75+76-3	340.9	311.0	nd	338.3	113.9	112.9	115.7
97+98-1	61.5	15.1	nd	58.9			
97+98-2	393.2	185.0	nd	326.8	132.7	106.1	66.5
97+98-3	340.4	202.5	nd	322.4	111.6	104.3	73.3
77+78	45.4	21.2	nd	34.6			
99+00	39.1	12.8	nd	34.0			

Conclusion – Good recovery using only external calibration

DL and PQL – STD 5 ng - Based on the firs cal. point DL and PQL can be lower than 5 ng.

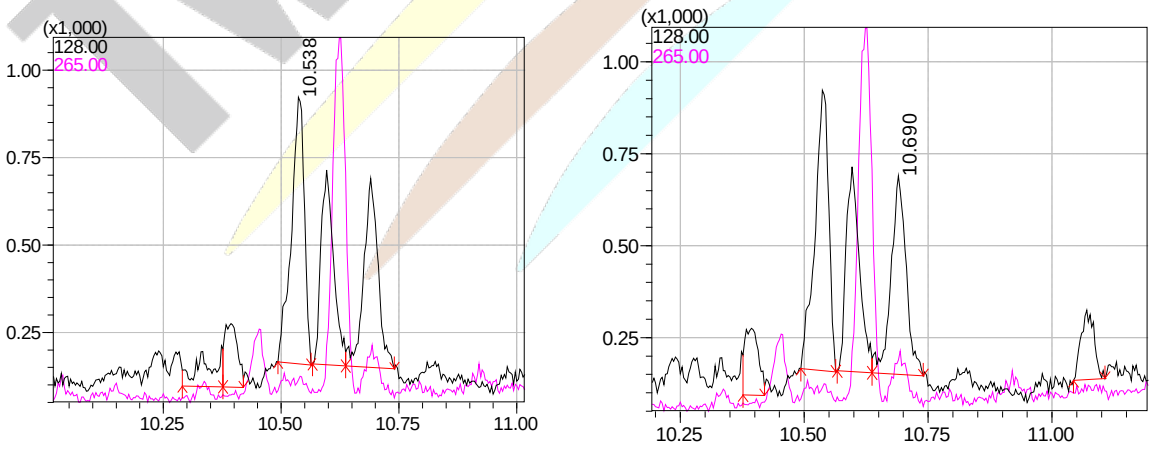

DCCA 1st

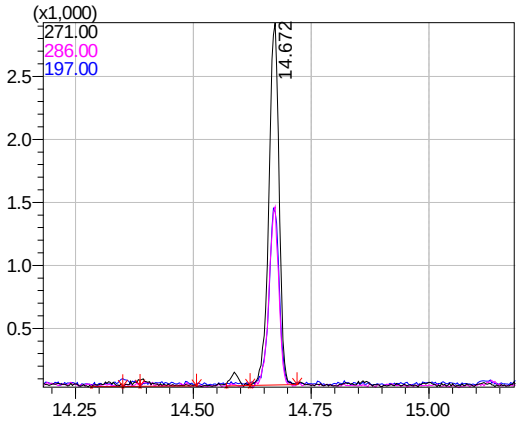

DCCA 2nd

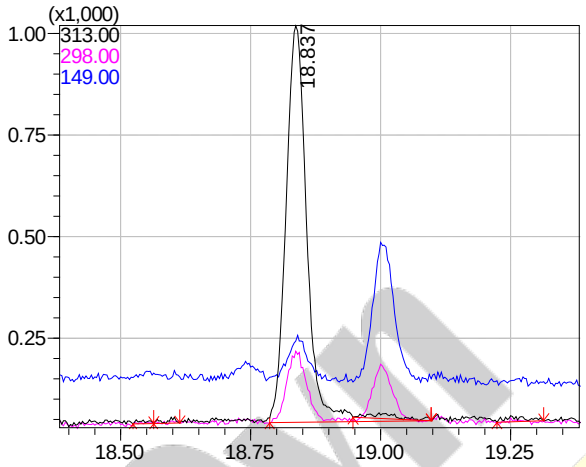

3PBA

CGA

Figure 16. DL and PQL determination

CONCLUSION - *Method for DCCA and 3PBA - final*

QA/QC – spike one sample (5g of soil) in batch with 50 ng of DCCA and 3PBA. (Based on the tested method Recovery for 3 PBA is 66-117%, and for DCCA 104-113%, PQL is 1 ng/g).

Extraction – *5* g of soil sample place to a 50-mL centrifuge tube; extraction with 30 mL of 2M NaOH by shaking for 1 hour at 170 o/min; centrifuged at 4500 rpm for 15 min. Supernatant is then transferred to a new centrifuge tube and acidified with 6M HCl to pH 1.8-2.2, left in the dark for 1 h hour for precipitation of humic acids, and finally centrifuged again for 25 min at 4500 rpm. The entire supernatant was passed through pre-conditioned C18- SPE cartridges (3 mL / 500 mg).

SPE cleanup procedure – Activate columns with 3 mL ethyl acetate, methanol and finally water, never letting columns run dry. Mount the glass rinsing funnel over the column and pass 10 mL water. Pass the sample through the column and rinse the column with 3 mL water. Dry up columns under a stream of nitrogen gas (ca. 1.3 bar for 30 minutes). Elute SPE columns with 8 portions of 500 µL ethyl acetate, collecting the eluate in 5-mL pointed flasks. Remove ethyl acetate by rotary evaporator (maximum water bath temperature of 40˚C, vacuum of ca. 180 mbar).

Derivatization – Re-dissolve residue in derivatization agents, 50 µl of pyridine and 100 µl of BSTFA, mix with vortex shaker, transfer samples to amber GC-Vials with insert, and the leave solution in the dark for 2 h at room temperature.

GCMS analysis GC-MS – conditions - operated in the electron impact ionization at 70 eV, using a high-resolution DB-5 MS UI column (30 m length, 0.25 mm diameter, 0.25 µm film thickness; Agilent, Santa Clara, USA). A volume of 1 µL was injected. The ion source temperature and the

MS transfer temperature were at 200 °C. Operating in the splitless mode, the helium was used as carrier gas at a constant flow rate of 1.78 mL min^{-1}. The injector was maintained at 250 °C. Oven temperature was programmed as follows: initial temperature 40 °C (held for 1 min), increased by 15 °C/min to 250 °C (held for 10 min), and finally increased by 30 °C/min to 300 °C (held for 7 min). In table 19 Target and Qualifier ions for quantification.

Table 19. Target and Qualifier ions for quantification

Selected ions Compound	RT, min	Target	Qualifier 1	Qualifier 2
3PBA	14.671	271	197	286
DCCA	10.510 and 10.685	128	265	---

Standard preparation:

Stock - 3PBA 25 mg dissolve in 25 ml of Methanol = 1 mg/ml.

WS1 1 ml of stock solution dilute up to 100 ml in methanol = 10 µg/ml of 3PBA

WS2 – 1 ml of WS1 and 100 µl of DCCA stock dissolve in 10 ml of Methanol = 1 µg/ml of 3PBA and DCCA.

WS3 - 1 ml of WS2 dissolve in 10 ml of Methanol = 0.1 µg/ml of 3PBA and DCCA.

Table 20. Calibration concentration range: 2.5–250 ng for 3PBA, CGA and DCCA

DCCA and 3PBA (ng)	Working solution	Volume of WS2 µl
2.5	WS3	2.5
5	WS3	50
10	WS3	100
25	WS3	250
50	WS2	50
75	WS2	75
100	WS2	100
250	WS2	250

Evaporate under N_2, at max 40°C. Re-dissolve residue in derivatization agents, 50 µl of pyridine and 100 µl of BSTFA, mix with vortex shaker, transfer samples to amber GC-Vials with insert, and the leave solution in the dark for 2 h at room temperature.

Impact on your project

The secondment had a direct and significant impact on the ongoing research activities of the visiting scientist. Training in field spectroscopy and soil classification enhanced methodological capabilities relevant for in situ soil monitoring and interpretation. The hands-on knowledge gained from BPCA analysis and IR-MS method development contributes to improved understanding of biochar transformation and lignin compound tracing in soils. These skills are directly applicable to the lysimeter experiment at UNSPMF, especially in evaluating the fate of carbon and pesticide residues in soils amended with different OSAs. Attendance at the Soil Science Colloquium and participation in the EcoLig project meeting expanded professional networks and fostered future collaboration opportunities. Overall, the secondment supported the development of Deliverable D3.2 and strengthened the scientific foundation for ongoing and future research in soil carbon dynamics and pollutant behavior.

Subtask 1.2.7 (leader UNIVIE) 6-months secondment (PM20-PM25) for ESR/RR and two 1-months secondments for QR/RR (PM30) at UNVIE.

MOBILITY REPORT - 1-month secondment at University of Vienna, Austria

Researcher: Dr. Marijana Kragulj Isakovski, UNSPMF

Assigned supervisor: Dr. Thorsten Hüffer, UNIVIE

Duration of the visit: 07.07.2024. - 27.07.2024.

Executive Summary

The one-month visit to the **University of Vienna (UNIVIE)** had two main focuses: **(1) characterization of colloidal particles in agricultural soils** and **(2) advanced training in LC/MS/MS for organic pollutant analysis**. These activities aimed to enhance analytical capabilities and improve understanding of soil properties and contaminant behavior in environmental systems.

As part of the **soil characterization**, 15 soil samples, including **Chernozem from Vojvodina, Serbia, and sewage sludge-treated soils** from **POT experiments with sorghum, alfalfa, and hemp**, were analyzed. The focus was on **particle size distribution and zeta potential measurements**, which provided valuable insights into **soil colloidal stability, aggregation tendencies, and pollutant mobility**. The results showed that **Chernozem soils exhibited higher negative zeta potential values, indicating better colloidal stability, whereas sewage sludge-treated soils had near-zero zeta potential, suggesting increased aggregation and altered dispersion properties**. These findings are essential for assessing soil amendments' impact on **soil structure, transport mechanisms, and potential environmental risks**.

In addition, a **two-week intensive training on LC/MS/MS analysis** was conducted, covering the **entire workflow of organic pollutant detection**. This included **solid-phase extraction (SPE) for sample preparation, chromatographic separation principles, tandem mass spectrometry operation, method optimization, instrument calibration, and data analysis**. The training strengthened expertise in **high-precision contaminant detection**, ensuring improved reliability in environmental monitoring studies.

Overall, the secondment at UNIVIE significantly advanced the project by **enhancing methodological skills, refining analytical techniques, and deepening knowledge of soil and water contamination processes**. The acquired expertise will be directly applied to future research, contributing to more effective environmental assessments and sustainable agricultural practices.

Introduction

Background

The one-month secondment at the **University of Vienna (UNIVIE)** focused on advanced methodologies for the **characterization of particulate contaminants** and the **analysis of organic pollutants**. The primary objectives were to evaluate **colloidal particle behavior in soil samples** and to develop expertise in **liquid chromatography-tandem mass spectrometry (LC/MS/MS) techniques** for detecting organic contaminants in environmental samples.

For this purpose, typical **agricultural soil samples**, including **Chernozem from Vojvodina, Serbia, and soil treated with sewage sludge**, were analyzed. These soils were collected from **POT experiments** with **sorghum, alfalfa, and hemp**, and a total of **15 soil samples** were delivered to UNIVIE for detailed examination.

The characterization phase involved measuring **particle size distribution and zeta potential** to assess the **presence, stability, and aggregation behavior of colloidal particles in soil suspensions**. These parameters are critical for understanding **soil-water interactions, pollutant mobility, and potential environmental impacts**.

Additionally, a **two-week specialized course** on **LC/MS/MS analysis of organic pollutants** was conducted. The training covered **solid-phase extraction (SPE) for sample preparation, chromatographic separation, mass spectrometric detection, instrument calibration, data processing, and interpretation of analytical results**. This knowledge will contribute to enhancing the project's analytical capabilities, particularly in assessing **organic contaminant presence in environmental and agricultural systems.**

Theoretical background:

Dynamic light scattering (DLS). The Litesizer 500 (Anton Paar) uses dynamic (DLS) and electrophoretic light scattering (ELS) for measuring particle size distributions and zeta potentials of finely dispersed suspensions and emulsions. It can also determine the transmittance and refractive index of liquid samples. DLS measures the Brownian motion of particles in a liquid. This motion causes fluctuations in the intensity of scattered light when a laser is shone on the sample. By analyzing these fluctuations, the DLS technique can determine the hydrodynamic diameter of the particles, which is the size of the particle along with the layer of solvent molecules attached

to it. A key step of sample preparation for DLS analysis is ensuring the sample is well-dispersed in the solvent, as large aggregates or air bubbles may interfere with measurements. Samples are measured after entering all input parameters into the software. The sample is placed into an appropriate cuvette (sample volume should be between 0.85 and 3 ml), and the cuvette is inserted into the sample holder of the instrument. During measurement, the laser beam is directed at the sample, and the light scattered by the particles is collected by the detector. The correlator measures the fluctuations in the intensity of scattered light over time, which reflects the movement of particles. The correlation function is created by comparing the intensity of the scattered light at different time points. This function provides insights into how fast the particles are diffusing in the solvent. The Litesizer software uses the measured diffusion coefficient (related to Brownian motion) to calculate the hydrodynamic diameter (D_h) of particles using the Stokes-Einstein equation:

$$D_h = \frac{k_B T}{3\pi\eta D}$$

where:

- k_B is the Boltzmann constant,
- T is the absolute temperature,
- η is the viscosity of the solvent, and
- D is the diffusion coefficient of the particles.

Also, the DLS method outputs a particle size distribution, which shows the relative frequency of particles of different sizes in the sample.

Zeta potential is a key indicator of the stability of colloidal dispersions and refers to the electric potential at the slipping plane surrounding a particle in a liquid. It arises due to the adsorption of ions onto the particle surface, creating an electrical double layer. The magnitude of the zeta potential determines whether particles repel or attract each other; high absolute values (positive or negative) indicate strong repulsion, leading to stable dispersions, while low values promote aggregation or flocculation. Zeta potential is widely used in soil to assess suspension stability, and control interactions.

Sample preparation for DLS analysis and zeta potential analysis

Soil samples are provided from POT experiments (each in triplicate) conducted at UNSPMF and delivered at UNIVIE. The total number of samples was 15 and used abbreviations are given in Table 1 below. Soil from conducted POT experiments is collected and try types of crops are used in POT experiments: Sorghum, Hemp and Alfaalfa on type types of soil Chernozem and soil treated with sewage sludge.

Table 1. Soil sample use for training purpose at UNIVIE

No	POT experiments	Abbreviation
1	Sorghum – Chernozem soil 1	S/D/C 1
2	Sorghum – Chernozem soil 2	S/D/C 2
3	Sorghum – Chernozem soil 3	S/D/C 3
4	Hemp – Chernozem soil 1	H/D/C 1
5	Hemp – Chernozem soil 2	H/D/C 2
6	Hemp – Chernozem soil 3	H/D/C 3
7	Alfaalfa – Chernozem soil 1	A/D/C 1
8	Alfaalfa – Chernozem soil 2	A/D/C 2
9	Alfaalfa – Chernozem soil 3	A/D/C 3
10	Sorghum – sewage sludge treated soil 1	S/S/C 1 sludge treatment
11	Sorghum – sewage sludge treated soil 2	S/S/C 2
12	Sorghum – sewage sludge treated soil 3	S/S/C 3
13	Hemp – sewage sludge treated soil 1	H/S/C 1
14	Hemp – sewage sludge treated soil 2	H/S/C 2
15	Hemp – sewage sludge treated soil 3	H/S/C 3

Solid:water ratio 1:10 - weigh 2 g of solid sample (dried, ground) into a 50 ml centrifuge tube

Water extraction

- Add 20 ml MiliQ water
- Shake for 24 h at 125 rpm in the dark (wrap the tubes in aluminum foil)

Centrifuge

- Place the tubes into the centrifuge
- Centrifuge for 1 h at 10xg

Decant supernatant into a glass vial, keep in the fridge in the dark. If necessary, it could be resuspended using an ultrasound bath. NOTE: if centrifuge does not separate larger particles with smaller density (e.g. biochar), samples could be filtered through 1 µm filter or water phase separated using a needle and syringe.

Zeta potential and DLS measurements procedures:

- On the start-up screen, click on the "+" icon to select a new measurement. Select "Zeta potential" or "Particle size distribution"
- Input parameters: Input parameters can be entered on the left side of the display. A detailed description of all input parameters can be found in the Litesizer Reference Guide.
- One crucial parameter for zeta potential measurement is the Henry factor. Refer to the Litesizer reference Guide for a detailed explanation of how to choose an appropriate approximation, or how to calculate an experiment-specific Henry factor.

.

Figure 1. DLS and zeta potential training: Marijana Kragulj Isakovski (UNSPMF) and Frank Von Der Kammer at UNIVIE

- Starting a measurement: Once the input parameters are complete, the “Start” icon in the bottom right corner of the screen will be activated and can be clicked to start the measurement.
- Following temperature adjustment, equilibrium and optical adjustment, the measurement will be displayed on the screen in real-time.
- Once the measurement is finished, all the measured and calculated values appear in the grey boxes to the right of the graphs, with the zeta potential result appearing in green.
- Please note: When using the “zeta potential” measurement mode, only single measurements are performed. If you are planning to measure your sample several times (e.g., triplicates), you have to use the “zeta potential series” measurement mode.

The training conducted at UNIVIE on particle size distribution and zeta potential using the Litesizer 500 instrument is shown in Figure 1

Results

Particle size distribution for all 15 samples is presented in Figure 2. The particle size distribution data presented in the table suggests variations in soil particle sizes across different treatments and plant types. The distinction between Chernozem and sewage sludge-treated soils indicates potential differences in aggregation behavior, dispersion, and colloidal stability. The variation in hydrodynamic diameters among the samples implies that factors such as organic matter content, soil texture, and amendments (e.g., sewage sludge) influence particle size distribution.

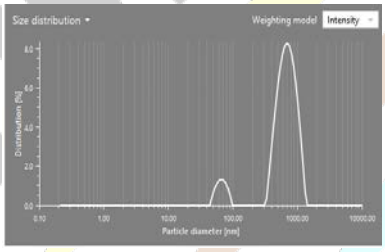

Sorghum – Chernozem 1

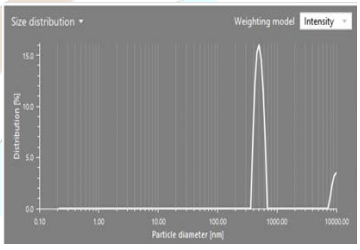

Sorghum – Chernozem 2

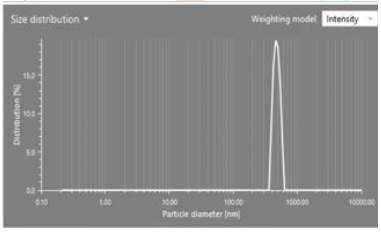

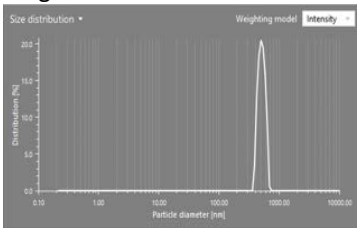

Sorghum – Chernozem 3

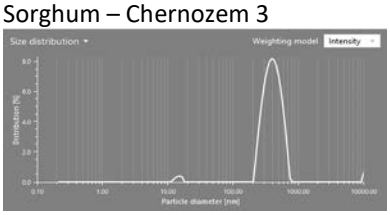

Hemp – Chernozem 1

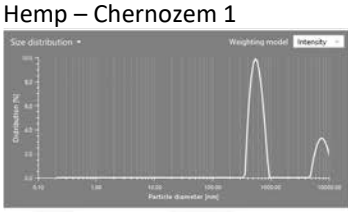

Hemp – Chernozem 2

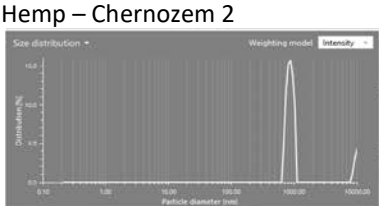

Hemp – Chernozem 3

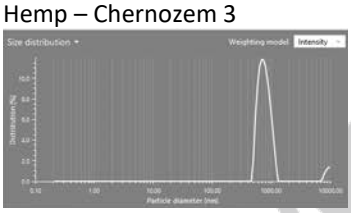

Alfaalfa–Chernozem 1

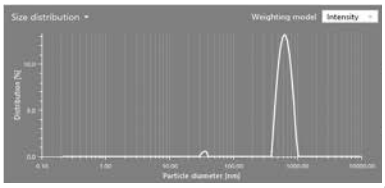

Alfaalfa–Chernozem 2

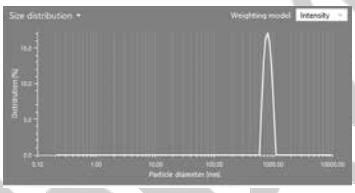

Alfaalfa–Chernozem 3

Sorghum – soil treated sewage sludge 1

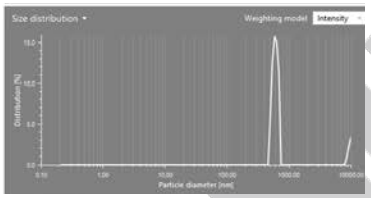

Sorghum – soil treated sewage sludge 2

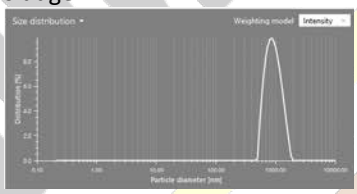

Sorghum – soil treated sewage sludge 3

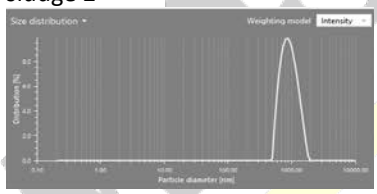

Hemp – soil treated sewage sludge 1

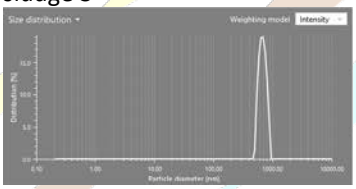

Hemp – soil treated sewage sludge 2

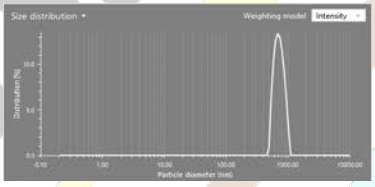

Hemp 3 – soil treated sewage sludge 3

Figure 2. Particle size distribution for all soil samples

From the data, we can conclude that soils treated with sewage sludge may exhibit different aggregation properties compared to Chernozem soils (TOC 1.615%), potentially due to increased organic matter (TOC 2.221%) or altered physicochemical interactions. If certain samples show larger hydrodynamic diameters, this may suggest enhanced particle aggregation, whereas smaller diameters may indicate better dispersion. Further analysis, such as polydispersity index or zeta potential, could provide deeper insights into the stability and interaction of soil particles in suspension.

Hydrodynamic diameters for each soil sample were calculated and are presented in Figure 3. The hydrodynamic diameters were determined as the mean values from triplicate samples, with corresponding standard deviations (SD). The measured hydrodynamic diameters ranged from 775 to 1338 nm across all soil types, while the SD values varied between 138 and 303 nm.

It is important to note that particle size distribution and hydrodynamic diameter are related but distinct parameters. The hydrodynamic diameter represents the apparent size of a particle in suspension, taking into account not only the core particle but also its hydration shell and interactions with the surrounding medium. In contrast, particle size distribution refers to the range and frequency of different particle sizes within a sample. While hydrodynamic diameter is often used to describe particle size in colloidal suspensions, it does not fully define the entire particle size distribution, which may include multimodal or polydisperse characteristics.

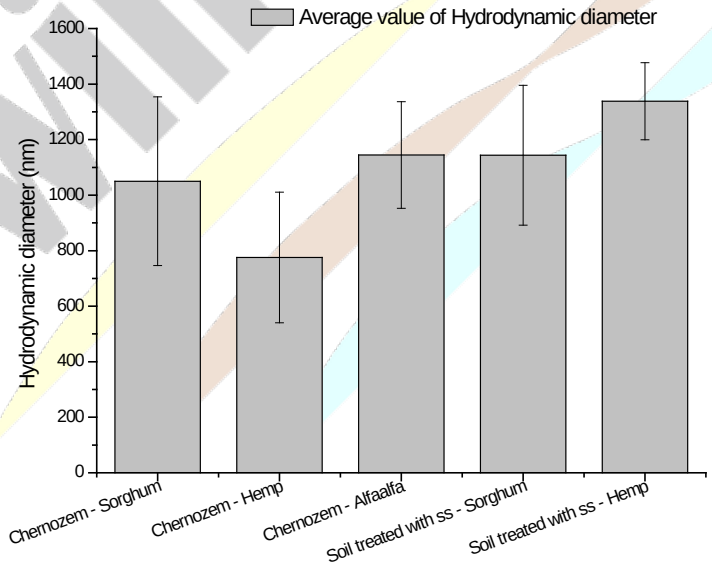

Figure 3. Average values of hydrodynamic diameter with corresponding SD for all types of soils

The range of hydrodynamic diameters (775–1338 nm) indicates a noticeable variation in particle sizes across different soil types. This suggests that soil composition, aggregation, or treatment (e.g., sewage sludge treated soil) may influence particle size in suspension.

The relatively high SD values (138–303 nm) suggest a broad particle size distribution, meaning the soil samples exhibit polydispersity. This could indicate the presence of both fine and coarse particles rather than a uniform particle size.

If different treatments were applied (e.g., biochar addition), comparing the hydrodynamic diameters and SD values between treated and untreated samples may provide insights into how the treatment affects soil particle aggregation or dispersion.

Larger hydrodynamic diameters might indicate stronger particle aggregation, potentially affecting soil water retention and transport properties. If the goal is to assess soil colloidal behavior, further analysis (e.g., polydispersity index) may be needed.

Mean values of Zeta potential measurements for triplicates samples with corresponding SD are presented in Figure 4. The zeta potential values presented for the different soil samples indicate significant differences in surface charge characteristics between Chernozem soils and sewage sludge-treated soils. Zeta potential is a key parameter in assessing the **stability of colloidal suspensions**, as it reflects the electrostatic repulsion between particles. Higher absolute values suggest greater repulsion and, consequently, a more stable dispersion, whereas values closer to zero indicate a tendency for aggregation due to lower repulsive forces.

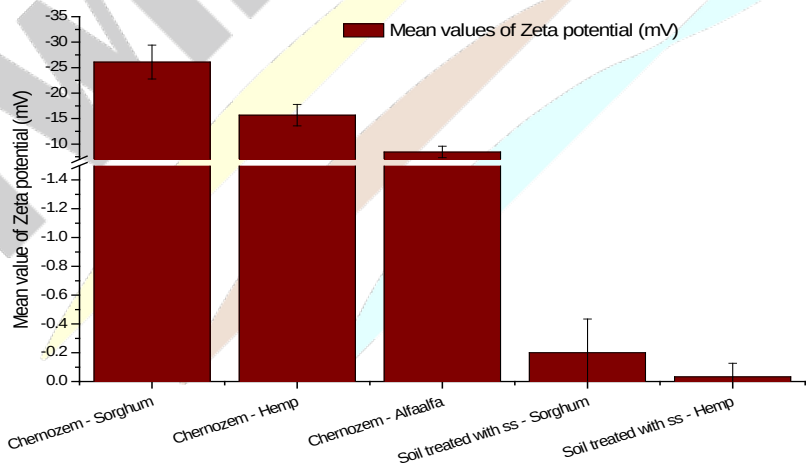

Figure 4. Mean values of zeta potential for Chernozem soil and soil treated with sewage sludge

Chernozem Soils showed negative high zeta potential. The Chernozem-based samples (Sorghum, Hemp, Alfalfa) exhibit highly negative zeta potential values (-26.09 mV, -15.69 mV, and -8.45 mV, respectively). This suggests **strong electrostatic repulsion**, meaning these soils likely have more stable particle dispersions and lower tendencies to aggregate. The decreasing magnitude of zeta potential (Sorghum > Hemp > Alfalfa) suggests a potential variation in organic matter content, surface charge, or soil composition that influences colloidal stability.

0**ewage Sludge-Treated Soils showed near zero zeta potential.** The zeta potential values for sewage sludge-treated samples (Sorghum: -0.20 mV, Hemp: -0.03 mV) are very close to zero. This implies that these particles have little to no electrostatic repulsion, making them **highly prone to aggregation and settling** in suspension. The presence of organic matter from sewage sludge might have neutralized surface charges, leading to reduced colloidal stability.

Higher Negative Zeta Potential & Smaller Particle Sizes: Chernozem soils exhibit **stronger repulsion**, which helps maintain smaller dispersed particles in suspension, leading to lower hydrodynamic diameters and a more uniform particle size distribution.

Lower Zeta Potential & Larger Aggregates: In sewage sludge-treated soils, weak electrostatic repulsion allows particles to **aggregate**, leading to **larger hydrodynamic diameters** and broader particle size distributions due to flocculation.

The zeta potential data supports the idea that **soil treatment significantly alters colloidal stability**. Chernozem soils maintain well-dispersed particles due to their higher negative surface charge, whereas sewage sludge treatment **reduces electrostatic repulsion**, encouraging aggregation and potential changes in soil texture and water retention. Understanding these interactions is essential for predicting soil behavior in agricultural and environmental applications.

LC/MS/MS training

A two-week training program was conducted on water sample preparation techniques, specifically **solid-phase extraction (SPE)**, followed by **LC/MS/MS analysis** of organic compounds (Figure 5). After completing the measurements, participants attended a short course on **data analysis**.

The training covered the entire analytical workflow, including **sample preparation, chromatographic separation, mass spectrometric detection, instrument operation, data processing, and interpretation of results**. The main topics included:

- **Sample Preparation: Solid-Phase Extraction (SPE)**
  - Introduction to **SPE principles**: selective retention and elution of analytes.
  - Selection of appropriate **SPE cartridges** based on analyte properties.
  - Optimization of **loading, washing, and elution** steps to improve extraction efficiency.
  - Sample **concentration and reconstitution** for LC/MS/MS analysis.
  - Quality control measures to minimize contamination and matrix effects.
- **LC/MS/MS Analysis of Organic Compounds**
  - **Liquid Chromatography (LC) Process:**
  - **Chromatographic separation**: Fundamentals of reversed-phase LC and column selection.
  - **Mobile phase composition**: Effect of solvent gradients and buffers on retention times.
  - **Injection parameters**: Sample volume, flow rate, and temperature optimization.
  - **Retention time stability**: Importance of calibration standards and system suitability tests.
  - **Tandem Mass Spectrometry (MS/MS) System:**
  - **Ionization techniques (ESI, APCI)** for detecting organic compounds in water.
  - **Mass filtering and fragmentation**: Quadrupole operation and product ion scanning.
  - **Optimization of MS parameters**: Collision energy, precursor-to-product ion transitions.
  - **Identification and quantification**: Standard curve generation and limit of detection (LOD/LOQ).
- **Software and Data Analysis**

- **Instrument control software**: Method development, acquisition setup, and troubleshooting.
- **Data processing workflows**: Peak integration, background subtraction, and spectral interpretation.
- **Quantification methods**: Internal standards, calibration curves, and matrix effects correction.
- **Quality control procedures**: Repeatability, reproducibility, and reporting of analytical results.

This comprehensive training equipped participants with hands-on experience in **water sample preparation, LC/MS/MS analysis, and advanced data interpretation**. The knowledge gained is essential for detecting and quantifying organic pollutants, pharmaceuticals, and contaminants in environmental water samples. Training materials are given below.

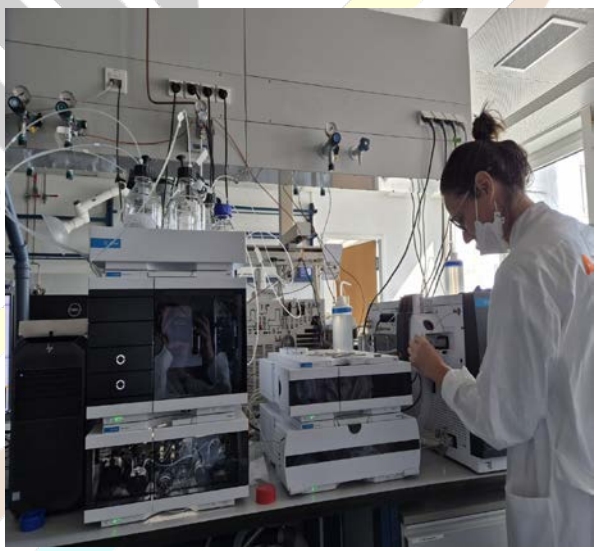


Figure 5. illustrates different aspects of the training:

- **Solid-phase extraction training** (Marijana Kragulj Isakovski, top left).
- **LC/MS/MS training** (Marijana Kragulj Isakovski, top right, with Anya Sherman, bottom left, and Valentin Göldner, bottom right).

Impact on your project

The one-month visit to the **University of Vienna** significantly advanced the project by providing **comprehensive insights into water sample preparation, analytical techniques, and soil characterization methods**. This visit enabled hands-on experience with state-of-the-art instruments and methodologies essential for environmental analysis.

A key aspect of the visit was the **determination of particle size distribution and zeta potential**, which allowed for a deeper understanding of **soil colloidal stability and aggregation behavior**. The findings highlighted the distinct differences between **Chernozem and sewage sludge-treated soils**, where **higher negative zeta potential values in Chernozem soils indicated better colloidal stability**, while **near-zero values in sewage sludge-treated soils suggested increased aggregation tendencies**. These insights are crucial for evaluating soil amendments and their influence on **soil structure and transport properties**.

Additionally, **training on LC/MS/MS analysis** provided an in-depth understanding of **solid-phase extraction (SPE), chromatographic separation, and tandem mass spectrometry detection** for analyzing organic contaminants in water samples. The training covered **sample preparation optimization, method development, instrument calibration, and data interpretation**,

ensuring high analytical accuracy. The acquired knowledge will be applied in the project to assess the presence of organic pollutants and evaluate their environmental impact.

Overall, the visit enhanced methodological expertise and analytical capabilities, contributing significantly to the project's objectives and improving the reliability of experimental resul

ANNEX III

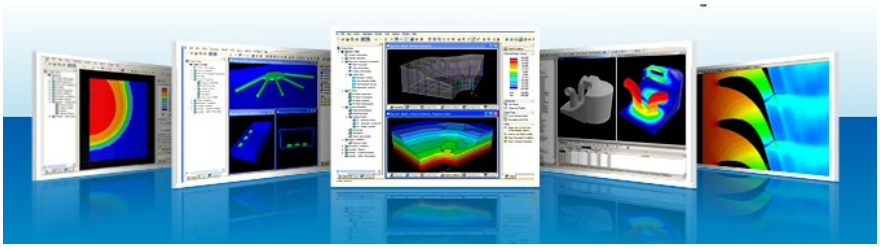

Short Course on Soil Hydrology Modelling

Lecturer

Lutz Weihermüller

Agrosphere Institute IBG-3, Forschungszentrum Jülich GmbH

Dates

26.06.2024 11:00 – 13:00 CEST Online

09.09.2024 – 13.09.2024 On-site, University Novi Sad, Serbia

Content

26.06.2024 Online

Introduction to the Short Course and Feedback from Questionnaire to students

09.09 to 13.09.2024 On-site

Principles of water content measurements

Soil hydraulic characterization

Soil hydraulic functions and parameters

Capillarity and water potential

Water movement in the saturated and unsaturated zone

Principles of solute transport in the unsaturated zone

Application to a real world scenario

The course will contain theory and practice on computers

No prior knowledge in soil hydraulics mandatory

AGENDA

Short Course on Soil Hydrology Modelling

Twinning excellence on organic soil amendments effect on nutrient and contaminant dynamics in the subsurface – TwinSubDyn (Grant agreement no 101059546)

DAY 1.	**09.09.2024.**	
09:00 – 09:15	Agenda overview	UNSPMF (Snežana Maletić)
9:15 – 10:45	Principles of water content measurements	Lutz Weihermüller
10:45-11:00	Coffee break	
11:00-12:00	Principles of water content measurements	Lutz Weihermüller
12:00-13:00	Lunch break	
13:00-14:45	Soil hydraulic characterization	Lutz Weihermüller
14:45-15:00	Coffee break	
15:00-16:00	Discussion	All participants
DAY 2.	**10.09.2024.**	
09:00 – 09:15	Agenda overview	UNSPMF (Snežana Maletić)
9:15-10:45	Soil hydraulic functions and parameters	Lutz Weihermüller
10:45-11:00	Coffee break	
11:00-12:00	Soil hydraulic functions and parameters	Lutz Weihermüller
12:00-13:00	Lunch break	
13:00-14:45	Capillarity and water potential	Lutz Weihermüller
14:45-15:00	Coffee break	
15:00-16:00	Discussion	All participants
DAY 3.	**11.09.2024.**	
09:00 – 09:15	Agenda overview	UNSPMF (Snežana Maletić)
9:15-10:45	Water movement in the saturated and unsaturated zone	Lutz Weihermüller
10:45-11:00	Coffee break	
11:00-12:00	Water movement in the saturated and unsaturated zone	Lutz Weihermüller

Funded by the European Union. Views and opinions expressed are however those of the author(s) only and do not necessarily reflect those of the European Union or European Research Executive Agency (REA). Neither the European Union nor the granting authority can be held responsible for them. Grant agreement No. 101059546.

12:00-13:00	Lunch break	
13:00-14:45	Principles of solute transport in the unsaturated zone	Lutz Weihermüller
14:45-15:00	Coffee break	
15:00-16:00	Discussion	All participants
DAY 4.	**12.09.2024.**	
09:00 – 09:15	Agenda overview	UNSPMF (Snežana Maletić)
9:15-10:45	Application to a real-world scenario	Lutz Weihermüller
10:45-11:00	Coffee break	
11:00-12:00	Application to a real-world scenario	Lutz Weihermüller
12:00-13:00	Lunch break	
13:00-14:45	Application to a real-world scenario	All participants
14:45-15:00	Coffee break	
15:00-16:00	Discussion	All participants
DAY 5.	**13.09.2024.**	
09:00 – 09:15	Agenda overview	UNSPMF (Snežana Maletić)
9:15-10:45	Application to a real-world scenario	Lutz Weihermüller
10:45-11:00	Coffee break	
11:00-12:00	Application to a real-world scenario	Lutz Weihermüller
12:00-13:00	Lunch break	
13:00-14:45	Application to a real-world scenario	All participants
14:45-15:00	Coffee break	
15:00-16:00	Discussion	All participants

Link for online participation (MS Teams):

https://teams.microsoft.com/l/meetup-join/19%3ameeting_NmQ1Y2RlZGEtZDYxNy00MDZiLWFhZTAtNmIzNzBhMWY0Y2Ni%40thread.v2/0?context=%7b%22Tid%22%3a%22e7a31644-4c56-46ed-af60-8b0906c738c0%22%2c%22Oid%22%3a%225c753ce1-8943-4c10-9e28-cb51e72c6d55%22%7d

Funded by the European Union. Views and opinions expressed are however those of the author(s) only and do not necessarily reflect those of the European Union or European Research Executive Agency (REA). Neither the European Union nor the granting authority can be held responsible for them. Grant agreement No. 101059546.

ATTENDANCE LIST

Short Course on Soil Hydrology Modelling

09 September 2024.

Twinning excellence on organic soil amendments effect on nutrient and contaminant dynamics in the subsurface – TwinSubDyn (Grant agreement No 101059546)

No	Attendee name	Institution name	Position	e-mail	Signature
1	Slaven Jenouli	PMF UNS	TA	slaven.jenouli@dh.uns.ac.rs	
2	Nina Đukanović	PMF UNS	RA	nina.djukanovic@dh.uns.ac.rs	
3	IRINA JEVROSIMOV	PMF UNS	RA	irinaj@dh.uns.ac.rs	
4	MARIJANA KLIMKOVIĆ	UNS-PMF	Full professor	marijana.klimkovic@dh.uns.ac	
5	JELENA MILUNOVIĆ JAZIĆ	UNS-PMF	full professor	jelena.milunovic@dh.uns.ac.rs	
6	SRĐAN ROLOVIĆ	PMF-UNS	FULL PROFESSOR	srdjan.rolovic@dh.uns.ac.rs	
7	JELENA BEĆIN		ASSOCIATE PROFESSOR	jelena.becin@dh.uns.ac.rs	
8	TAMARA APOSTOLOVIĆ	PMF-UNS	TEACHING ASSISTANT	tamara.apostolovic@dh.uns.ac.rs	
9	DRAGANA TOMAŠEVIĆ	PMF-UNS	ASSOCIATED PROFESSOR	dragana.tomasevic@dh.uns.ac.rs	
10	PIŠODOVIĆ				
11	SNEŽANA MAKSIĆ	PMF-UNS	FULL PROFESSOR	snezana.maksic@dh.uns.ac.rs	
12	Weihermüller Lutz	FZJ	Scientist	l.weihermueller@fz-juelich.de	
13	Sanja Vasiljević	PMF UNS	RA	sanjav@dh.uns.ac.rs	
14					
15					
16					
17					
18					
19					
20					
21					

Funded by the European Union. Views and opinions expressed are however those of the author(s) only and do not necessarily reflect those of the European Union or European Research Executive Agency (REA). Neither the European Union nor the granting authority can be held responsible for them. Grant agreement No. 101059546.

ATTENDANCE LIST

Short Course on Soil Hydrology Modelling

10 September 2024.

Twinning excellence on organic soil amendments effect on nutrient and contaminant dynamics in the subsurface – TwinSubDyn (Grant agreement No 101059546)

No	Attendee name	Institution name	Position	e-mail	Signature
1	Slaven Tenodi	PMF UNS	TA	slaven.tenodi@dh.uns.ac.rs	
2	Nina Đukanović	PMF UNS	RA	nina.djukanovic@dh.uns.ac.rs	
3	Sanja Vasiljević	PMF UNS	RA	sanjav@dh.uns.ac.rs	SVasiljevic
4	IRINA JEVRASHEVA	PMF UNS	RA	irina@dh.uns.ac.rs	Jevrasheva
5	MARIJANA K. IKANOVIĆ	PMF UNS	FP	marijana.kuc@dh.uns.ac.rs	
6	JELENA [illegible] JARIĆ	PMF UNS	FP	jelena.holub@dh.uns.ac.rs	
7	JELENA BELJIN	PMF UNS	AP	jelena.beljin@dh.uns.ac.rs	
8	TAMARA APOSTOLOVIĆ	PMF UNS	~~FP~~ TA	tamara.apostolovic@dh.uns.ac.rs	
9	SNEŽANA MAĆEN	PMF UNS	FP	snezana.macen@dh.uns.ac.rs	
10	SRĐAN ROLEVIĆ	PMF UNS	FP	srdjan.rolevic@dh.uns.ac.rs	
11	Weilersmüller Luh	FZJ	Scientist	l.weilersmueller@fz-juelich.de	
12					
13					
14					
15					
16					
17					
18					
19					
20					
21					

Funded by the European Union. Views and opinions expressed are however those of the author(s) only and do not necessarily reflect those of the European Union or European Research Executive Agency (REA). Neither the European Union nor the granting authority can be held responsible for them. Grant agreement No. 101059546.

ATTENDANCE LIST

Short Course on Soil Hydrology Modelling

11 September 2024.

Twinning excellence on organic soil amendments effect on nutrient and contaminant dynamics in the subsurface – TwinSubDyn (Grant agreement No 101059546)

No	Attendee name	Institution name	Position	e-mail	Signature
1	IRINA JOKOVIĆ	PMF UNS	RA	irina@dh.uns.ac.rs	
2	Nina Dulanović	PMF UNS	RA	nina.dulanovic@dh.uns.ac.rs	
3	Slaven Tenodi	PMF UNS	TA	slaven.tenodi@dh.uns.rs	
4	Svetlana Maletić	PMF UNS	FP		
5	Tamara Apostolović	PMF UNS	TA	tamara.apostolovic@dh.uns.ac.rs	
6	JELENA BEGIN	PMF UNS	AP	jelena.begin@dh.uns.ac.rs	
7	SRĐAN RONČEVIĆ	PMF UNS	FP	srdjan.roncevic@dh.uns.ac.rs	
8	JELENA MILANOVIĆ JOKIĆ	PMF UNS	FP	jelena.milanovic@dh.uns.ac.rs	
9	MARIJANA MARKOV	PMF UNS	FP	marijana.markov@dh.uns.ac.rs	
10	Luk Weihermüller	FZJ	Scientist	l.weihermueller@fz-juelich.de	
11					
12					
13					
14					
15					
16					
17					
18					
19					
20					
21					

Funded by the European Union. Views and opinions expressed are however those of the author(s) only and do not necessarily reflect those of the European Union or European Research Executive Agency (REA). Neither the European Union nor the granting authority can be held responsible for them. Grant agreement No. 101059546.

TwinSubDyn

Funded by the European Union

ATTENDANCE LIST

Short Course on Soil Hydrology Modelling

12 September 2024.

Twinning excellence on organic soil amendments effect on nutrient and contaminant dynamics in the subsurface – TwinSubDyn (Grant agreement No 101059546)

No	Attendee name	Institution name	Position	e-mail	Signature
1	IRINA JEROSIMOV	PMF UNS	RA	irinaj@dh.uns.ac.rs	
2	Sloven Jenooli	PMF UNS	TA	sloven.jenooli@dh.uns.ac.rs	
3	SNEŽANA MARKOVIĆ	PMF UNS	PP	snezana.markovic@dh.uns.ac.rs	
4	JELENA BEGIN	PMF UNS	PP	jelena.begin@dh.uns.ac.rs	
5	SRĐAN ROKOBRATIĆ	PMF UNS	PP	srdjan.rokobratic@dh.uns.ac.rs	
6	JELENA MILUTIN MARIĆ	PMF UNS	PP	jelena.milutin@dh.uns.ac.rs	
7	MARIJANA KRSTIĆ	UNS PMF	RA	marijana.krstic@dh.uns.ac.rs	
8	Sanja Vasiljević	UNS PMF	RA	sanjav@dh.uns.ac.rs	
9	TAMARA APOSTOLOVIĆ	UNS PMF	TA	tamara.apostolovic@dh.uns.ac.rs	
10	Lutz Weihermüller	FZJ	Scientist	l.weihermueller@fz-juelich.de	
11					
12					
13					
14					
15					
16					
17					
18					
19					
20					
21					

Funded by the European Union. Views and opinions expressed are however those of the author(s) only and do not necessarily reflect those of the European Union or European Research Executive Agency (REA). Neither the European Union nor the granting authority can be held responsible for them. Grant agreement No. 101059546.

ATTENDANCE LIST

Short Course on Soil Hydrology Modelling

13 September 2024.

Twinning excellence on organic soil amendments effect on nutrient and contaminant dynamics in the subsurface – TwinSubDyn (Grant agreement No 101059546)

No	Attendee name	Institution name	Position	e-mail	Signature
1	IRINA JEVROSIMOV	PMF UNS	RA	irina@dh.uns.ac.rs	Irina Jevrosimov
2	Slaven Jenodi	PMF UNS	TA	slaven.jenodi@dh.uns.ac.rs	
3	SVETLANA MALETIĆ	PMF UNS	PP	SVETLANA.MALETIC@DH.UNS.AC.RS	S Maletić
4	TAMARA APOSTOLOVIĆ	PMF UNS	TA	tamara.apostolovic@dh.uns.ac.rs	
5	JELENA BEGIN	PMF UNS	AP	jelena.begin@dh.uns.ac.rs	J Begin
6	JORDAN RONČEVIĆ	UNS PMF	FP	srdjan.radicevic@dh.uns.ac.rs	
7	MARIJANA KISIĆ	UNS PMF	FP	marijana.kisic@dh.uns.ac.rs	
8	Sanja Vasiljević	UNS PMF	RA	sanjav@dh.uns.ac.rs	SVasiljević
9	Lutz Weihermüller	FZJ	Scientist	l.weihermueller@fz-juelich.de	
10					
11					
12					
13					
14					
15					
16					
17					
18					
19					
20					
21					

Funded by the European Union. Views and opinions expressed are however those of the author(s) only and do not necessarily reflect those of the European Union or European Research Executive Agency (REA). Neither the European Union nor the granting authority can be held responsible for them. Grant agreement No. 101059546.